JPSS VIIRS Session

Day 2 - Tuesday, August 9, 2016

Time	Presentations / Topics	Speaker	Affiliation
0830 - 1650	*Session 3: VIIRS SDR* *Auditorium*		
0830 - 1150	*Part 1: JPSS J1 VIIRS and Beyond* *Chairs: Changyong Cao and Jack Xiong*		
0830 - 0835	*Opening Remarks*	Changyong Cao	NESDIS/STAR
0835 - 0855	*VIIRS SDR Science Overview*	Changyong Cao	NESDIS/STAR
0855 - 0915	*VIIRS Prelaunch Test Update (J1-J4)*	Kurt Thome/Jim McCarthy	NASA
0915 - 0935	*J1 VIIRS Block2 System Verification*	Wenhui Wang	NESDIS/STAR
0935 - 0955	*J1 VIIRS Early Mission SDR Processing and LUT Updates*	Frank Deluccia	Aerospace
0955 - 1030	*Break*	---	---
1030 - 1050	*J1 VIIRS Pre-launch Radiometric Performance and Lessons Learned*	Hassan, Xiong, et al.	NASA/VCST
1050 - 1110	*Geospatial calibration for Suomi NPP, J1 and beyond*	Gary Lin, Robert Wolfe	NASA/VCST
1110 - 1130	*J1 VIIRS RSR final release, comparison with SNPP, and potential impacts*	Moeller; Blonski	U. Wisc.; STAR
1130 - 1150	*Water vapor band trade study*	Slawomir Blonski, Chris Moeller	NESDIS/STAR; U.Wisc.
1150-1200	*Q&A*	All	
1200 - 1315	*Lunch*		

1200 - 1315	***Lunch***		
1315 - 1650	***Part 2: VIIRS Cal/Val Improvements*** ***Chairs: Slawomir Blonski, Frank Deluccia***		
1315 - 1335	***VIIRS RSB Calibration for Ocean Color applications***	Junqiang Sun and Menghua Wang	NESDIS/STAR
1335 - 1355	***Suomi NPP VIIRS RSB calibration stability assessments***	Jason Choi, Sean Shao, Slawomir Blonski	NESDIS/STAR
1355 - 1415	***Suomi NPP VIIRS RSB calibration improvements in support of SDR/L1B reprocessing***	Jack Xiong, Ning Lei, Ben Wang	NASA/VCST
1415 - 1435	***VIIRS TEB calibration potential improvements***	Wenhui Wang	NESDIS/STAR
1435 - 1530	***Poster Session I***		
1530 - 1550	***Preparation for DNB recalibration***	Sirish Uprety and Yalong Gu	NESDIS/STAR
1550 - 1610	***VIIRS DNB SDR algorithm improvements***	Steve Mills	NESDIS/STAR
1610 - 1630	***Q&A***	All	
1630 - 1650	***Wrap up and actions***	Changyong Cao	NESDIS/STAR
1650	***Session Adjourn***		

Seed questions for discussion

1. Which J1 LUT(s) may become a potential risk for reaching provisional maturity at Launch + 90?

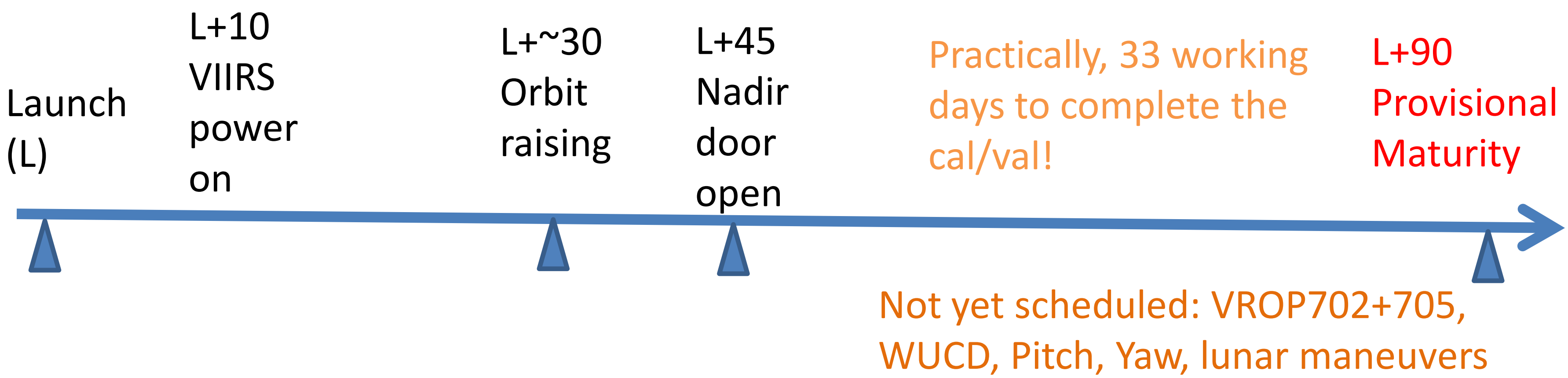

2. How to incorporate Ocean Color F-LUT into the operational and reprocessing system?

JPSS VIIRS SDR SCIENCE OVERVIEW

Changyong Cao
NOAA/NESDIS/STAR

Outline

- VIIRS SDR Cal/Val Science Team
- Sensor/Algorithm/Product Overview
- Top Ten Accomplishments
- JPSS-1 Readiness
    - J1/SNPP orbits and inter-calibration
- Calibration reanalysis
- Summary and Path Forward

VIIRS SDR Cal/Val Team Members

PI	Organization	Team Members	Roles and Responsibilities
C. Cao	STAR	-	Team lead
W. Wang/S. Blonski	STAR/ERT	J. Choi, Y. Gu, S. Mills (consultant)	VIIRS SDR calibration/validation for S-NPP, J1. (Prelaunch studies; software code changes and ADL tests; Postlaunch monitoring and LUT update)
C. Wallisch/F. DeLuccia	Aerospace	G. Moy, E. Haas, C. Fink, D. Moyer, P. Isaacson, and several others	VIIRS operational calibration update; RSB autocal; J1 LUT delivery;
J. Xiong	VCST	J. McIntire, G. Li, N. Lei, T. Schwarting	VIIRS TV data analysis; prelaunch characterization; LUT development
CICS	UMD/CICS	Y.Bai, Z. Wang, X. Shao (PT), B. Zhang(PT)	Geolocation validation, ADCS analysis, intercomparisons, solar diffuser calibration
CIMSS	U. Wisconsin	C. Moeller	VIIRS RSR, and Water Vapor band study
CIRA	CIRA	Sirish Uprety	Vicarious calibration, DNB calibration

VIIRS Instrument Overview

•VIIRS is a scanning imaging radiometer onbaord the Suomi NPP, and JPSS satellites in the afternoon orbits with a nominal altitude of 829km at the equator, and a swath width of ~3000km;

VIIRS has 22 types of SDRs:

- *•16 moderate resolution (750m), narrow spectral bands (11 Reflective Solar Bands (RSB); 5 Thermal Emissive Bands (TEB))*
- *•5 imaging resolution(375m), narrow spectral bands (3 RSB; 2 TEB)*
- *•1 Day Night Band (DNB) imaging (750m), broadband*

•VIIRS Onboard calibration relies on the solar diffuser (SD), solar diffuser stability monitor (SDSM), space view (SV), and the blackbody (BB);

•Vicarious calibration also used (lunar, dark ocean for DNB, and cal/val sites);

•Calibration is performed per band, per scan, per half angle mirror side (HAM), and per detector.

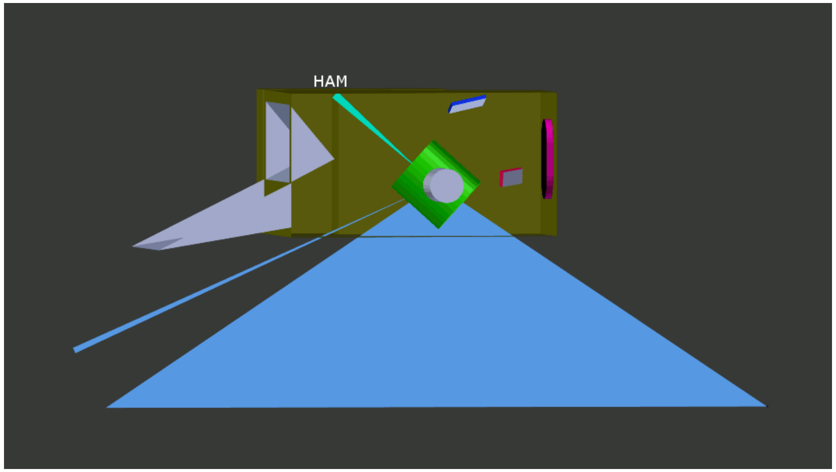

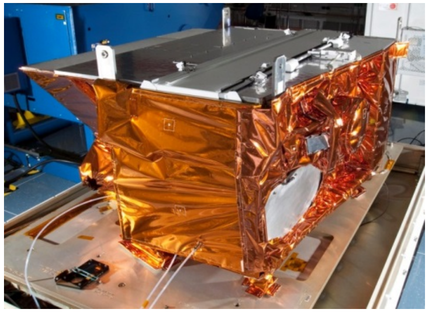

VIIRS instrument

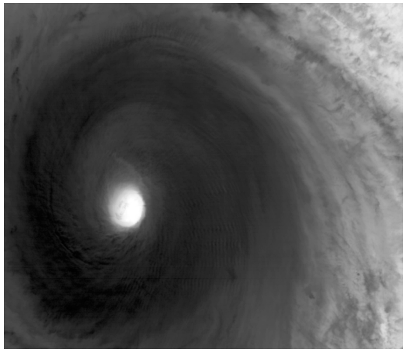

Super Typhoon Nepartak

VIIRS RDR to SDR Processing

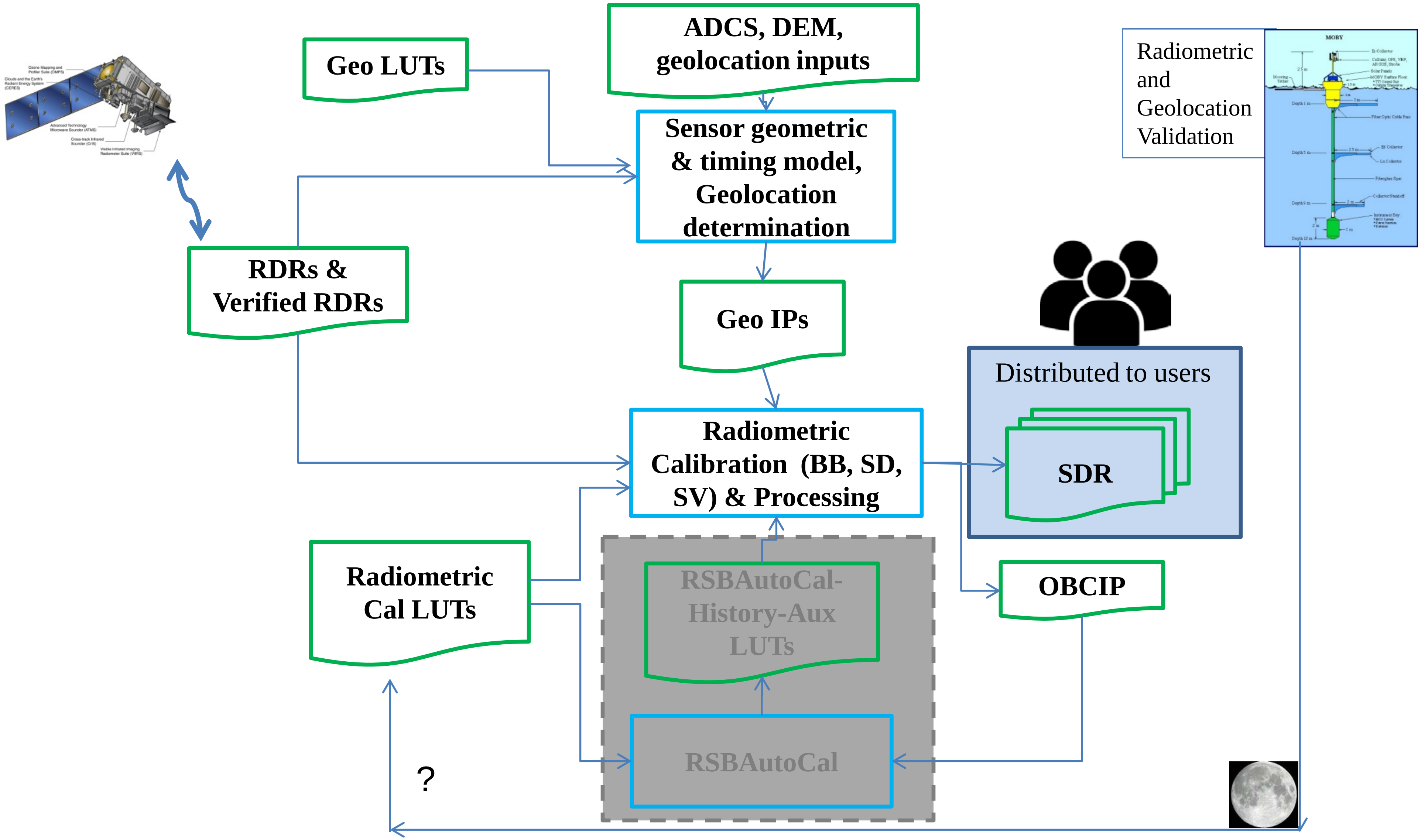

VIIRS Calibration Algorithm Overview (TEB/RSB)

Thermal Emissive Bands (TEB):

$$F = \frac{\mathrm{RVS}\ (\theta_{obc},\ B)\cdot\left[\overline{\epsilon_{obc}(\lambda)}\ \cdot\overline{L\ (T_{obc}\ (t)\ ,\ \lambda)}+\ \overline{L_{obc\_rfl}\ (T_{sh}\ (t)\ ,\ T_{cav}\ (t)\ ,T_{tele}\ (t)\ ,\lambda)}\right]}{\sum_{j=0}^{2} C_j dn_{obc}{}^{j}} + \frac{(\mathrm{RVS}\ (\theta_{obc}, B) -\ 1)\cdot\left(\frac{\left\{\left(1-\overline{\rho_{rta}(\lambda)}\right)\cdot\overline{L(T_{rta}\ (t),\ \lambda)}-\overline{L(T_{ham}\ (t),\ \lambda)}\right\}}{\overline{\rho_{rta}}(\lambda)}\right)}{\sum_{j=0}^{2} C_j dn_{obc}{}^{j}}$$

$$\overline{L_{ap}}\,(\theta_{ev}, B) = \frac{F\cdot\sum_{j=0}^{2} C_i\,(T_{det}, T_{ele})\ dn_{ev}{}^{j} + (1-\ \mathrm{RVS}\ (\theta_{ev}, B))\left(\frac{\left\{\left(1-\overline{\rho_{rta}(\lambda)}\right)\overline{L(T_{rta},\ \lambda)}-\overline{L(T_{ham},\ \lambda)}\right\}}{\overline{\rho_{rta}}(\lambda)}\right)}{\mathrm{RVS}\ (\theta_{ev},\ B)}$$

Reflective Solar Bands (RSB):

$$F = \frac{RVS\,(\theta_{sd}, B)\,.\cos(\theta_{inc})\,.\left[\overline{\tau_{sds}\ (\phi_h, \phi_v,\ \lambda,\ d)\,.\,E_{sun}\,(\lambda, d_{se})\,\mathrm{BRDF}\,(\phi_h, \phi_v,\ \lambda}\right])}{\sum_{i=0}^{2} c_i\ .\ dn_{sd}^{i}}$$

$$\overline{L_{ap}}\,(\theta, B) = \overline{L_{ap}\,(\theta, \lambda)} = \frac{\overline{\Delta L_{det}}\,(\theta, B)}{RVS\,(\theta, B)} = \frac{F\ .\ \sum_{i=0}^{2} C_i\ .\ dn^{i}}{RVS\ (\theta, B)}$$

VIIRS Calibration Algorithm Overview (DNB)

Day/Night Band (DNB):

$$L = RVS(n)A(m, N_{agg}, g)dn_{EV}(m,n)$$
$$dn_{EV}(m,n) = DN_{EV}(m,n) - DN_0(m,n,g)$$

$$A_{LGS} = \frac{\overline{L}_{SD}}{dn_{DNB}}$$
$$dn_{DNB} = DN_{SD\_DNB} - DN_{SV\_DNB}$$
$$\overline{L}_{SD} = RVS(\theta_{SD})\cos\theta_{inc} \int_{DNB} RSR_{DNB}(\lambda)E_{SUN}(\lambda)BRDF(\lambda)\tau_{SDS}(\lambda)H(\lambda)d\lambda$$

$$A_{MGS} = G_{LGS/MGS}A_{LGS}$$
$$A_{HGS} = G_{MGS/HGS}G_{LGS/MGS}A_{LGS}$$

VIIRS SDR Product Requirements from JPSS L1RD

Attribute	Threshold	Objective
Center Wavelength	412 to 12,013 nm	412 to 12,013 nm
Bandpass	15 to 1,900 nm	15 to 1,900 nm
Max. Polarization Sensitivity	2.5 to 3.0 %	2.5 to 3.0 %
Accuracy @ Ltyp	0.4 to 30 %	0.4 to 30 %
SNR @ Ltyp or NEdT @ 270 K	6 to 416 or 0.07 to 2.5 K	6 to 416 or 0.07 to 2.5 K
FOV @ Nadir	0.4 to 0.8 km	0.4 to 0.8 km
FOV @ Edge-of-Scan	0.8 to 1.6 km	0.8 to 1.6 km
Ltyp or Ttyp	0.12 to 155 $W \cdot m^{-2} \cdot sr^{-1} \cdot mm^{-1}$ or 210 to 380 K	0.12 to 155 $W \cdot m^{-2} \cdot sr^{-1} \cdot mm^{-1}$ or 210 to 380 K
Dynamic Range	0.12 to 702 $W \cdot m^{-2} \cdot sr^{-1} \cdot mm^{-1}$ or 190 to 634 K	0.12 to 702 $W \cdot m^{-2} \cdot sr^{-1} \cdot mm^{-1}$ or 190 to 634 K

VIIRS Noise Performance

(SNR/SNR$_{SPEC}$ > 1) or (NEdT/NEdT$_{SPEC}$ < 1): better performance

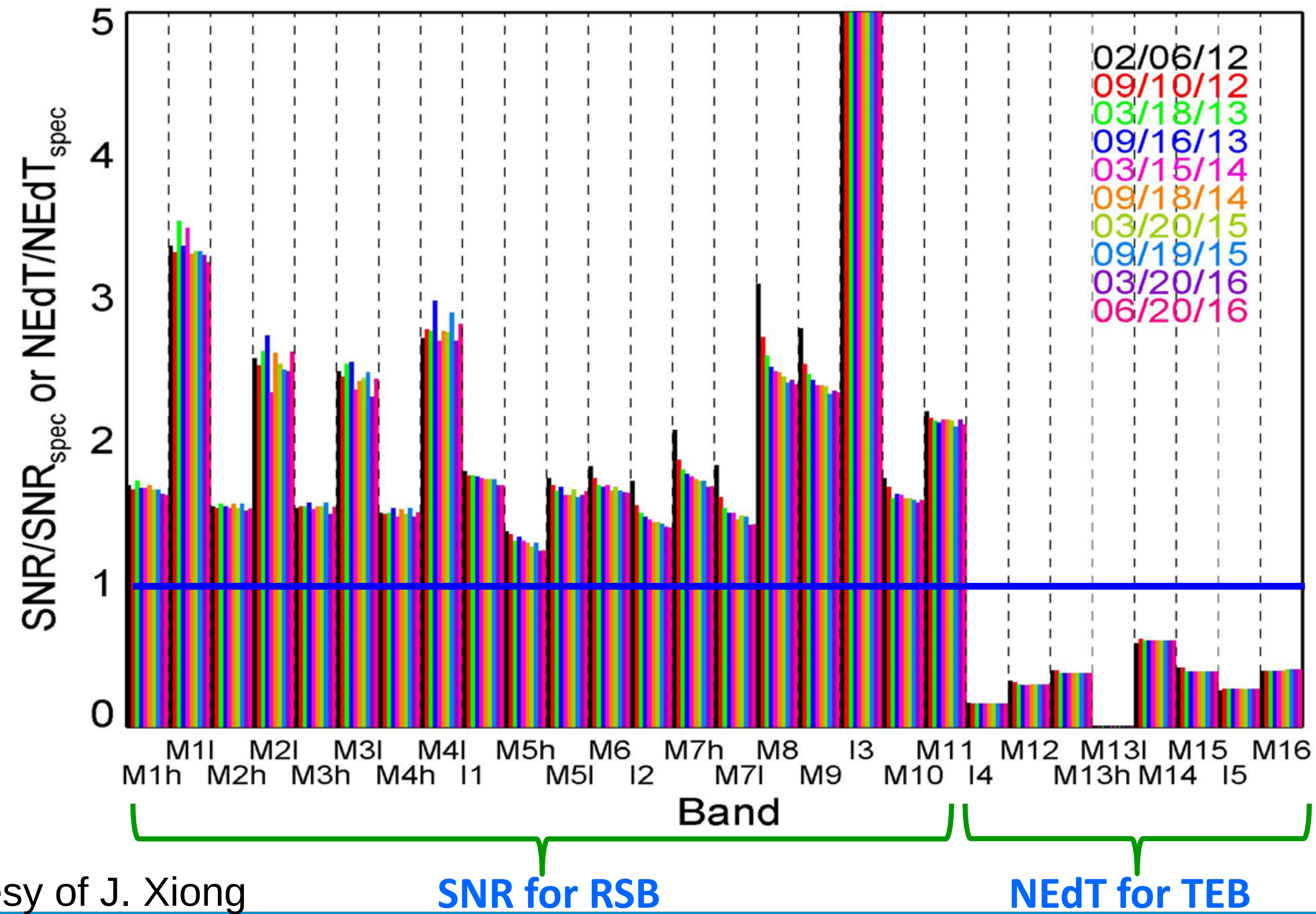

Courtesy of J. Xiong

VIIRS Responsivity Change since Launch

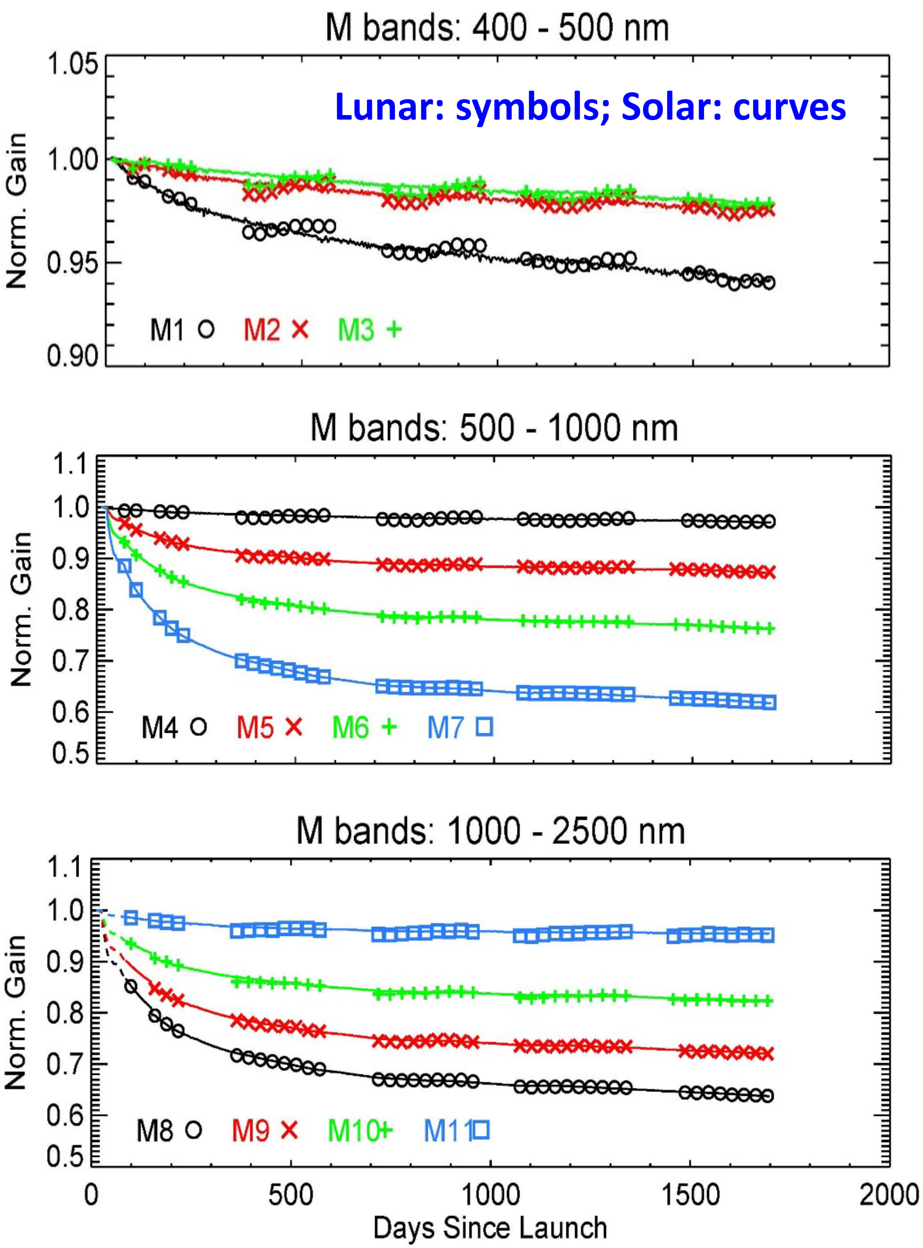

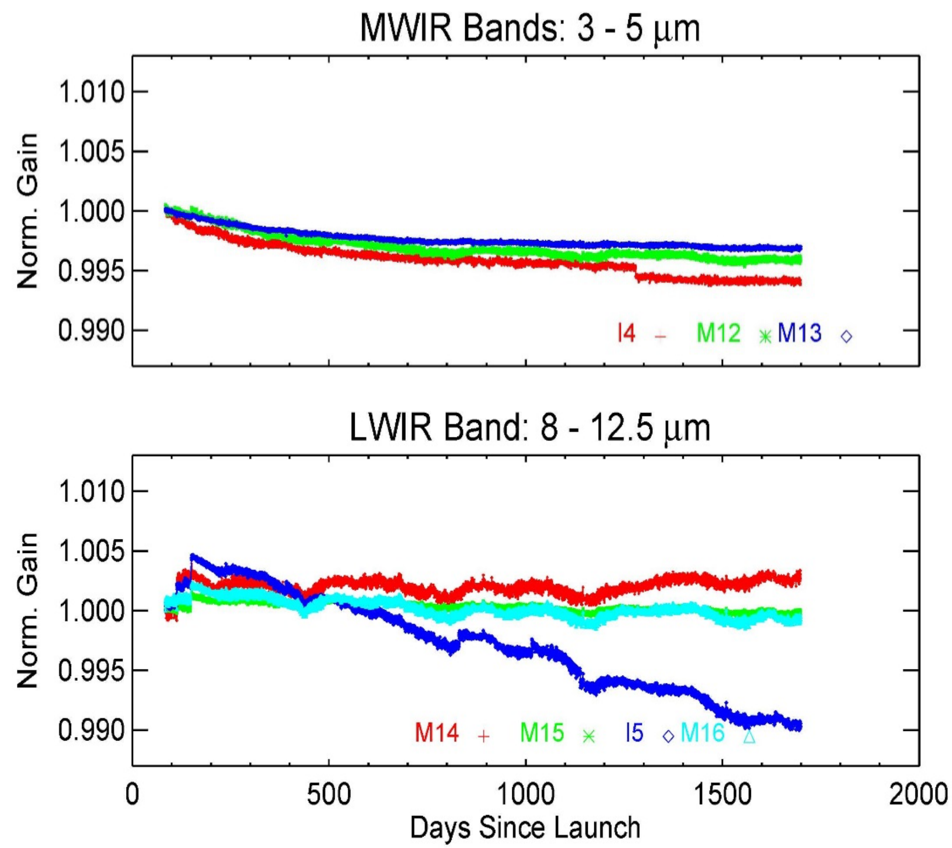

- Large changes in NIR and SWIR (due to mirror contamination)
- Small changes in VIS, MWIR, and LWIR

Courtesy of J. Xiong

VIIRS SDR Team Accomplishments (FY16)

1. J1 DNB Aggregation Mode code change
2. VIIRS Remote Sensing Journal Special issue (28 papers)
3. J1 LUT delivery
4. J1 waiver trade study
5. Water vapor band trade study
6. Geolocation CPM transition web and DBMS interface
7. DNB VROP (702 + 705) calibration reanalysis
8. Solar diffuser surface roughness induced degradation model
9. Testing F-LUT from OC group for operational and re-processing
10. Active nightlight for DNB SBIR project entering Phase II
11. Collaboration with GOES-R on UAS field campaign

- Monitoring Tools/Website
  - VIIRS SDR home page: http://ncc.nesdis.noaa.gov
  - ICVS: http://www.star.nesdis.noaa.gov/icvs/status_NPP_VIIRS.php

Geolocation monitoring on the web

- Transitioned NASA CPM capability
  - Landmark based geolocation monitoring
  - Landsat chips
  - Running on STAR servers
  - Results dynamically published on the web

- Enhanced the functionality:
  - Added web interface and dynamic plotting
  - Back-end DBMS support under testing

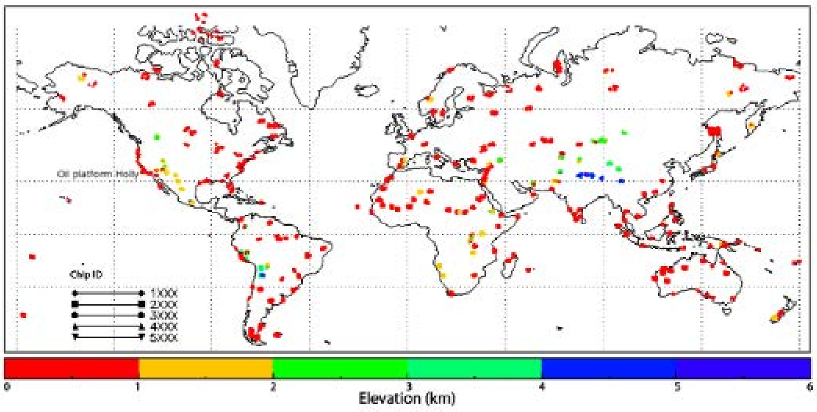

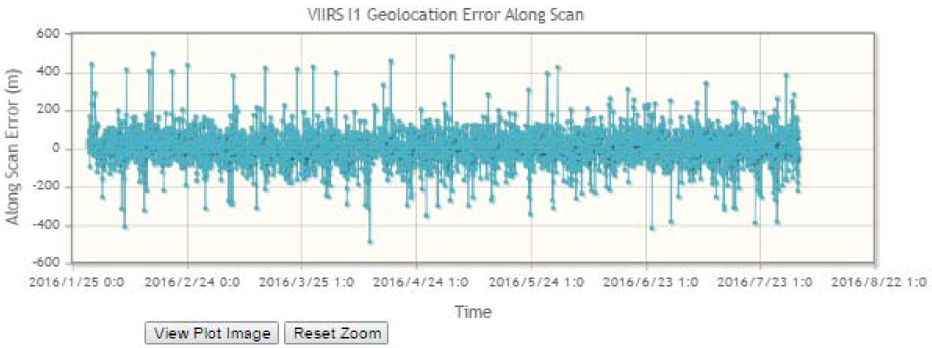

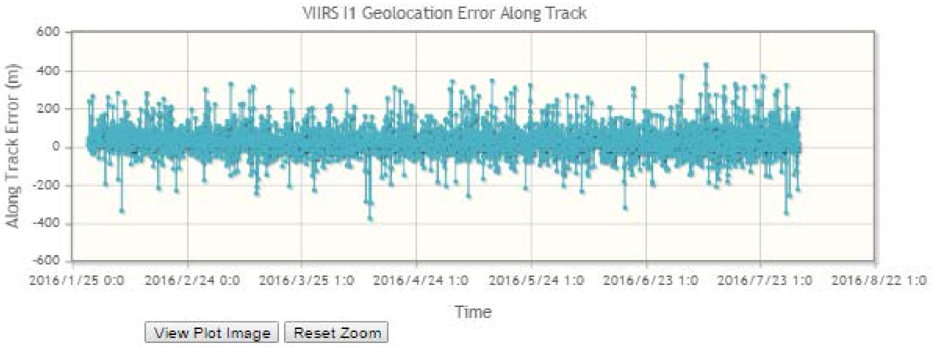

VIIRS intercalibration between J1 and SNPP

- Transfer orbit altitude is about 10km lower than final orbit
- SNO opportunities exist if instruments are turned on and **collecting earth view data before orbit raising**
- There will **be NO SNOs between SNPP and J1 after reaches final orbit**
- However, the current schedule shows VIIRS nadir door **will not be open till day 45,** which will miss the inter calibration opportunity

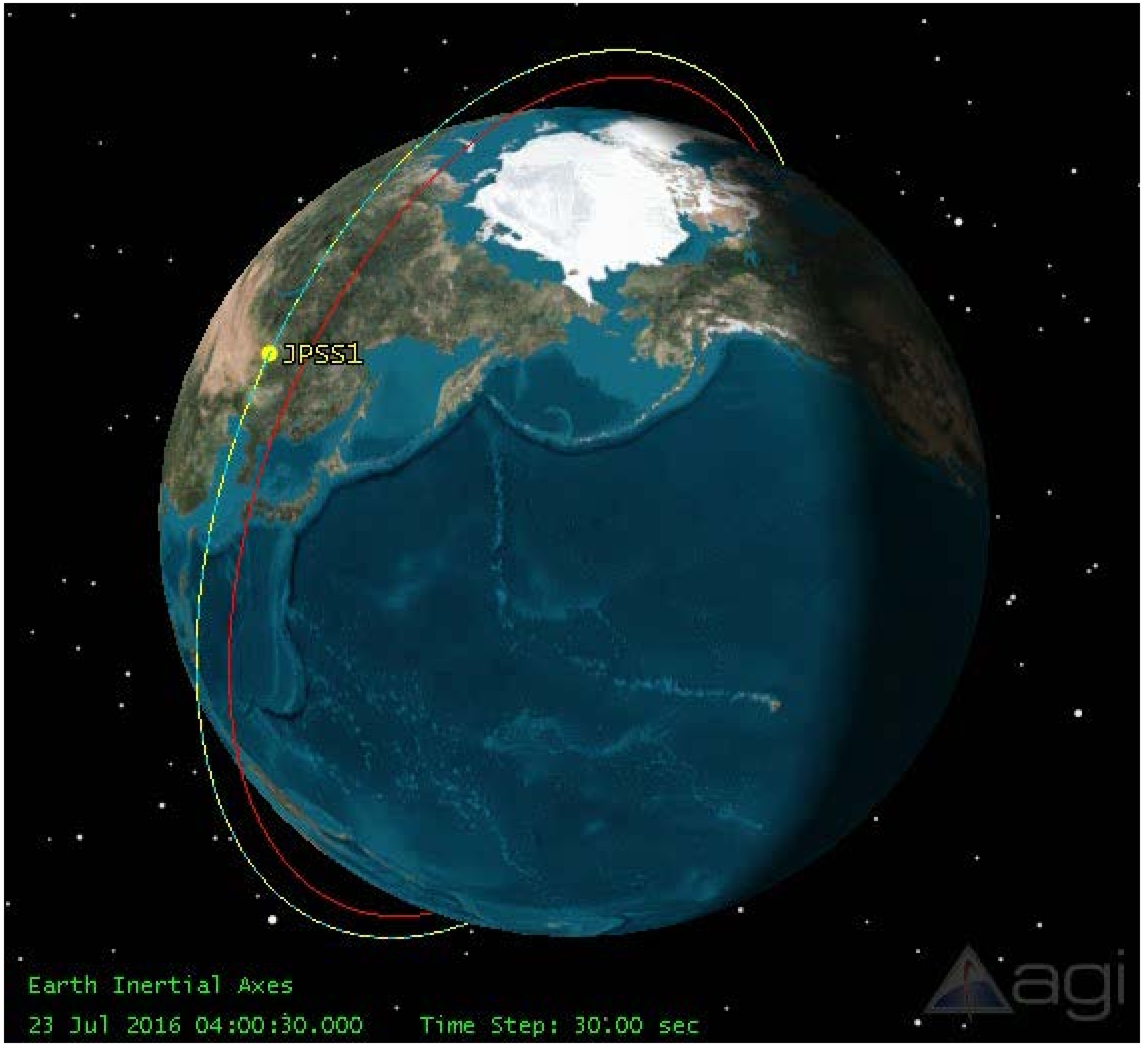

Intercalibration Opportunities between J1 and SNPP at Simultaneous Nadir Overpass (SNO)

- SNPP will be flying directly above J1 before the orbit raising
- Allows direct comparisons between SNPP and J1 earth view data (if nadir door opened)
- Support most waiver studies by comparing SNPP and J1 data (polarization, nonlinearity, data quality, consistency, etc…)

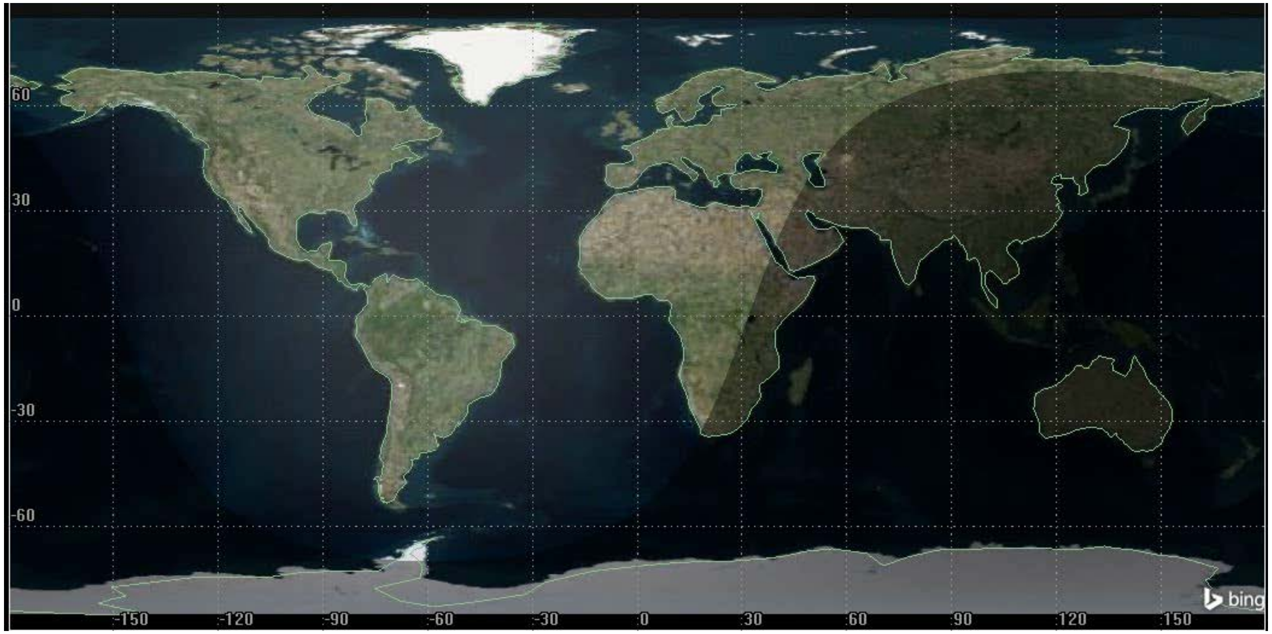

- Day 10: J1 reaches transfer orbit at ~814 km altitude with similar equator crossing as final orbit; VIIRS turn on
- Day 33: Orbit raising
- Day 45: J1 reaches final orbit: 50.75min separation from SNPP; same equator crossing as that of SNPP
- Day 45: VIIRS Nadir Door open; Cryocooler door open
    - Several maneuvers and tests are not yet scheduled:
        - Pitch/Yaw maneuvers, DNB VROP 702/705, WUCD, Lunar Maneuver

- Current schedule for provisional maturity (90 days) may be affected

J-1 VIIRS Instrument Waivers – Algorithm Updates

Waiver	VIIRS SDR Team Actions	Impact on Ground Processing System	Actions
Polarization sensitivity	Characterize the polalrization phenomena both pre and post launch	Post-launch code and LUT changes are likely	SDR team to develop methods to baseline and monitor on-orbit polarization changes; EDR teams to implement polarization corrections; Intercalibratin at SNOs with SNPP would help greatly. Unfortunately, currently no plan for SNO observations despite opportunity exist before orbit raising
DNB nonlinearity	Develop agg mode dependent calibration algorithm and test them in ADL	Aggregation Code and associated LUTs to work on aggregation modes 21 and 21/26 developed, tested, and delivered	Require extensive postlaunch validation of the new aggregation mode, and update of LUTs postlaunch; Intercalibratin at SNOs with SNPP would help greatly. Unfortunately, currently no plan for SNO observations despite opportunity exist before orbit raising.
Emissive band radiometric calibration	Investigate potential impacts on striping; may require algorithm enhancements	TBD postlaunch	Additional evaluation required postlaunch. Intercalibratin at SNOs with SNPP would help greatly. Unfortunately, currently no plan for SNO observations despite opportunity exist before orbit raising.
SWIR nonlinearty and uncertainty	Develop dual calibration to accommodate low radiance nonlinearity	Post-launch code and LUT changes are likely	Requires additional research to implement SWIR nonlinearity correction (low priority); Intercalibratin at SNOs with SNPP would help greatly.
Spatial Resolution DFOV & MTF	Monitor performance postlaunch	TBD	Impact on ground processing system is not expected unless postlauch test shows the need otherwise
Relative spectral response	Provide RSR on website	LUT updates in work	Final RSR is ready but waiting for official release ; Intercalibratin at SNOs with SNPP would help greatly.
Crosstalk	Monitor performance postlaunch	TBD	Impact on ground processing system is not expected unless postlauch test shows the need otherwise
Band to band registration	Monitor performance postlaunch	TBD	Impact on ground processing system is not expected unless postlauch test shows the need otherwise
M8/M9/I4 saturation (M6 rollover)/DNB	Post-launch code and LUT changes are likely	Post-launch code and LUT changes are likely	Currently under study; requires postlaunch validation; Intercalibratin at SNOs with SNPP would help greatly.
Near field scattering	Monitor performance postlaunch	TBD	Impact on ground processing system is not expected unless postlauch test shows the need otherwise
DNB straylight	Develop straylight correction for J1 VIIRS/DNB	Post-launch code and LUT changes are likely	Methodology used for S-NPP can be adapted for J1 to make corrections; requires the development of J1 LUT postlaunch; Intercalibratin at SNOs with SNPP would help greatly.
M1/M2 Absolute uncertainty	Monitor performance postlaunch	TBD	Requires improved calibration postlaunch such as lunar; Intercalibratin at SNOs with SNPP would help greatly.
M11 Uncertainty	Monitor performance postlaunch	TBD	Requires improved calibration postlaunch such as lunar; Intercalibratin at SNOs with SNPP would help greatly.

Red Font: Prelaunch code/LUT updates required **Green Font**: Mitigation prelaunch unnecessary

J1 vs. SNPP coverage

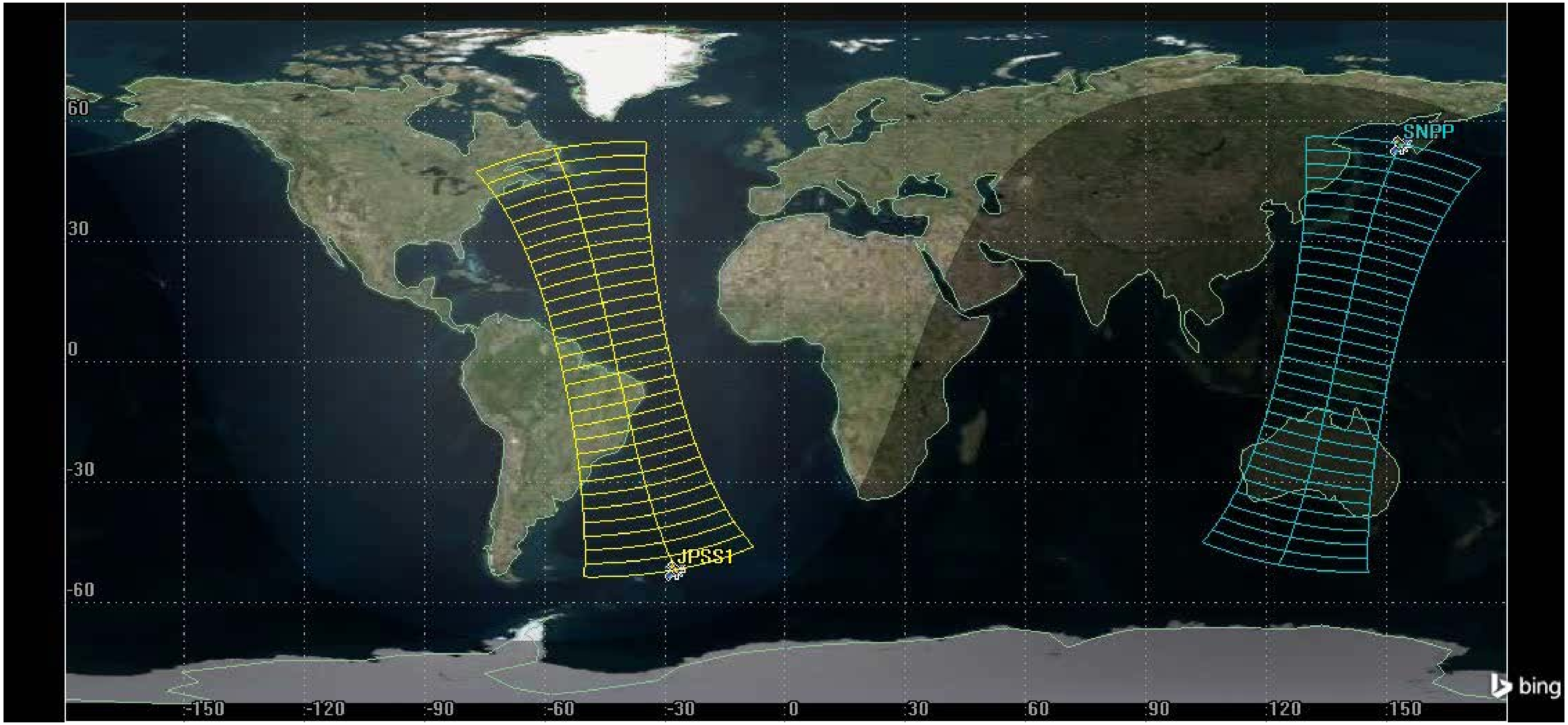

- Both on the same orbital plane
- Both have the same orbital equator crossing (LTAN)
- ~50.75 mins separation: one is observing in day while the other is at night
- Ground track repeating cycle is 16 days for each, and 8 days when combined
- Improved temporal coverage (~50 mins interval around 1:30pm)

Special issue of *Remote Sensing* (Guest Editor: Dr. Changyong Cao
"VIIRS Cal/Val and Applications" 28 papers published
(http://www.mdpi.com/journal/remotesensing/special_issues/VIIRS?view=default)

Chapter 1 Overview of Calibration/Validation		
Xiong, Xiaoxiong; Bu	Overview	Assessment of S-NPP VIIRS On-Orbit Radiometric Calibration and Performance
Sun, Junqiang; Wang	Overview	VIIRS Reflective Solar Bands Calibration Progress and Its Impact on Ocean Color Products
Datla, Raju; Shao, Xi	Overview	Comparison of the Calibration Algorithms and SI Traceability of MODIS, VIIRS, GOES, and GOES-R ABI Sensors
Zhou, Lihang; Divak	Overview	An Overview of the Joint Polar Satellite System (JPSS) Science Data Product Calibration and Validation
Hillger, Don; Kopp, T	Overview	User Validation of VIIRS Satellite Imagery
Chapter 2 Instrument Onboard Calibration and Prelaunch Characterization		
Blonski, Slawomir; C	OBC	Suomi NPP VIIRS Reflective Solar Bands Operational Calibration Reprocessing
Shao, Xi; Cao, Chang	OBC	Spectral Dependent Degradation of the Solar Diffuser on Suomi-NPP VIIRS Due to Surface Roughness-Induced Rayleigh Scattering
Lee, Shihyan; Cao, C	OBC	Soumi NPP VIIRS Day/Night Band Stray Light Characterization and Correction Using Calibration View Data
Wang, Zhuo; Cao, C	OBC	Assessing the Effects of Suomi NPP VIIRS M15/M16 Detector Radiometric Stability and Relative Spectral Response Variation on Striping
Oudrari, Hassan; Mc	Prelaunch	JPSS-1 VIIRS Radiometric Characterization and Calibration Based on Pre-Launch Testing
McIntire, Jeff; Moye	Prelaunch	Pre-Launch Radiometric Characterization of JPSS-1 VIIRS Thermal Emissive Bands
Moyer, David; McInt	Prelaunch	JPSS-1 VIIRS Pre-Launch Response Versus Scan Angle Testing and Performance

Special issue of *Remote Sensing* (Guest Editor: Dr. Changyong Cao
"VIIRS Cal/Val and Applications" 28 papers published
(http://www.mdpi.com/journal/remotesensing/special_issues/VIIRS?view=default)

Chapter 3 Sensor Data Record Intercomparisons and Monitoring

Li, Yonghong; Wu, Ais	SDR	Inter-Comparison of S-NPP VIIRS and Aqua MODIS Thermal Emissive Bands Using Hyperspectral Infrared Sounder Measurements as a Transfer Reference
Liang, Xingming; Igna	SDR	Preliminary Inter-Comparison between AHI, VIIRS and MODIS Clear-Sky Ocean Radiances for Accurate SST Retrievals
Yu, Fangfang; Wu, Xia	SDR	Radiometric Inter-Calibration between Himawari-8 AHI and S-NPP VIIRS for the Solar Reflective Bands
Wang, Likun; Trembla	SDR	Fast and Accurate Collocation of the Visible Infrared Imaging Radiometer Suite Measurements with Cross-Track Infrared Sounder
Wang, Zhipeng; Xiong	SDR	Improved Band-to-Band Registration Characterization for VIIRS Reflective Solar Bands Based on Lunar Observations
Choi, Taeyoung; Shao	SDR	Radiometric Stability Monitoring of the Suomi NPP Visible Infrared Imaging Radiometer Suite (VIIRS) Reflective Solar Bands Using the Moon
Wang, Wenhui; Cao,	SDR	Monitoring the NOAA Operational VIIRS RSB and DNB Calibration Stability Using Monthly and Semi-Monthly Deep Convective Clouds Time Series
Madhavan, Sriharsha	SDR	Evaluation of VIIRS and MODIS Thermal Emissive Band Calibration Stability Using Ground Target

Chapter 4 Environmental Data Record Product Calibration/Validation

Obata, Kenta; Miura,	EDR	Spectral Cross-Calibration of VIIRS Enhanced Vegetation Index with MODIS: A Case Study Using Year-Long Global Data
Liu, Yuling; Yu, Yunyu	EDR	Quality Assessment of S-NPP VIIRS Land Surface Temperature Product
Tu, Qianguang; Pan, D	EDR	Validation of S-NPP VIIRS Sea Surface Temperature Retrieved from NAVO
Brando, Vittorio; Lov	EDR	The Potential of Autonomous Ship-Borne Hyperspectral Radiometers for the Validation of Ocean Color Radiometry Data
Liu, Yinghui; Key, Jeff	EDR	Validation of the Suomi NPP VIIRS Ice Surface Temperature Environmental Data Record
Gao, Caixia; Zhao, Yo	EDR	An Investigation of a Novel Cross-Calibration Method of FY-3C/VIRR against NPP/VIIRS in the Dunhuang Test Site
Gladkova, Irina; Ignat	EDR	Improved VIIRS and MODIS SST Imagery
Jing, Xin; Shao, Xi; Ca	EDR	Comparison between the Suomi-NPP Day-Night Band and DMSP-OLS for Correlating Socio-Economic Variables at the Provincial Level in China

Calibration Reanalysis
Why? (Example of urban growth)

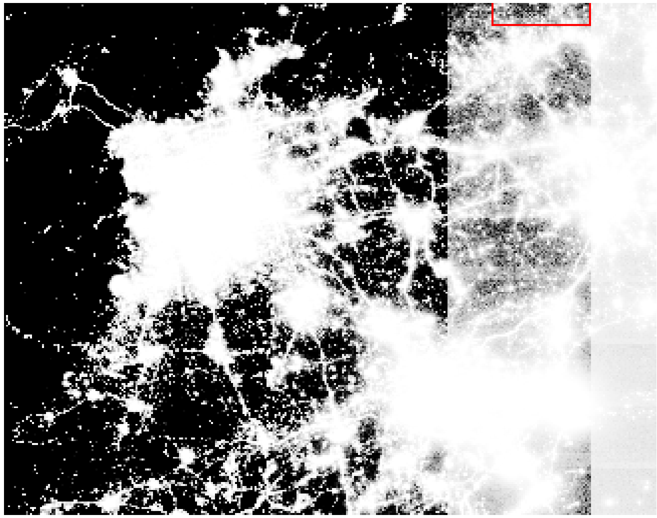

2012 original

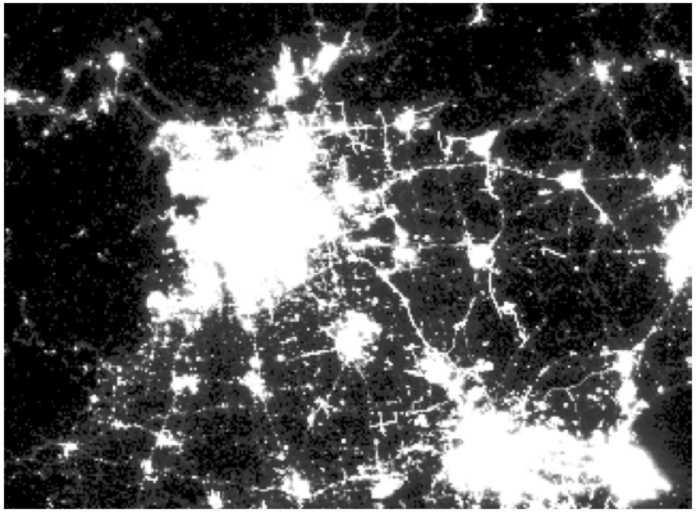

2016

2012 reprocessed

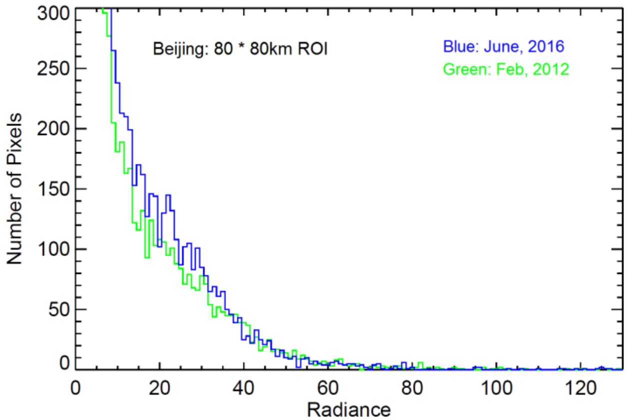

Quantitative comparisons of night light

Collaboration with GOES-R field campaign

- First test flight at UMD UAS test site in Bushwood, MD on Aug. 3, 2016 to demonstrate readiness for postlanch cal/val for GOES-R ABI and potentially VIIRS
- Provide 2D&3D imagery to NOAA National Estuary Research Reserve (NERR)
- Other sensors including both atmospheric and imaging will be tested later
- UAS is recognized by NOAA as one of the emerging technologies that can instill agility and infuse new technology in the NOAA observing system portofolio

UAS Test flight near Chesapeake Bay, MD

Collaboration with GOES-R field campaign – more to come…

Summary & Path Forward

The VIIRS SDR team has made great progress:

- Supported J1 VIIRS waiver studies
- Developed geolocation software code modifications for J1
- Developed and delivered at launch quality J1 VIIRS LUTs
- Transitioned and enhanced geolocation validation capabilities
- Water vapor band trade studies
- Documented research in peer reviewed publications (special issue)

Concerns:

- Time too short to reach provisional at L+90 (practically ~33 working days)
- Nadir door opens at L+day 45 significantly reduces the time required to update the on-orbit LUT, especially for VIIRS DNB, since both DNB offset and straylight LUT require VROPs that have yet to be scheduled (between L+50 and L+90?) which depends on the lunar cycle
- Missed SNO opportunity = extended effort in postlaunch cal/val

VIIRS Block 2.0 System Verification

Wenhui Wang, Slawomir Blonski, Bin Zhang,
Yalong Gu, Yan Bai, Zhuo Wang, and
Changyong Cao

NOAA/NESDIS/STAR

JPSS Annual Science Team Meeting (August 9, 2016)

Outline

- Background
- Verification of Block 2.0 system using SNPP data
  - Comparing Block 2.0/Block 1.2 GEO, SDR, and RDR products.
- Verification of Block 2.0 system using proxy J1 RDRs
  - J1 code change verification;
  - Verification of J1 SDR production.
- Summary

Background

- SNPP VIIRS SDRs is currently produced using Block 1.2 IDPS;
- JPSS-1 (J1) will be launched in 2017;
- Block 2.0 system that supports both SNPP and J1 SDR product generation is under extensive testing:
  - New code changes and SDR product improvements have been integrated to Block 2.0 for VIIRS SDRs
- SNPP ground processing will be switched to Block 2.0 IDPS
  - After Operational Readiness Review (ORR)
- Verification of Block 2.0 system test results is on going.

Purpose

To verify Block 2.0 system for VIIRS SDR production:

- Through Block 1.2/2.0 comparison, verify if SNPP VIIRS SDR products can be generated correctly using the Block 2.0 system

  In the Block 2.0 system, SNPP and J1 VIIRS share the same SDR science code, the SNPP comparison results will also apply to J1 VIIRS SDR products that are not changed.

- Using J1 proxy RDRs to verify if Block 2.0 can produce J1 VIIRS SDR products as expected.

Part 1 Block 1.2 and Block 2.0 Comparison

- **OBSAT (Operational Based Site Acceptance Test) test results verification (November 2015)**
  - Focused on # of VIIRS SDR product files

- **LG2 (L3AT/GPAT/GSAT) test results verification (June 2016)**
  - Block 2.0 and Block 1.2 SNPP VIIRS SDR products were compared in detail:
    - # of VIIRS SDR product files
    - I-bands, M-bands, DNB radiances
    - Geolocation
    - M11 at night
    - Sector rotation data

Part 1 Block 1.2 and Block 2.0 Comparison

- **OBSAT test results verification:** **issue of missing granules (esp. for M-band) in Block 2.0 was identified and the feedback sent to the program.**
- **LG2 test results verification:** **Small # of missing granules still exist, but significantly less than OBSAT.**

VIIRS SDR Products	20160408		20160409	
	BLK2	BLK1.2	BLK2	BLK1.2
I-bands SDR	1044	1013	986	1014
DNB	1044	1013	986	1014
M-bands SDR	1012	1013	939	1014
GIMGO/GITCO	1012	1013	939	1014
GDNBO	1012	1013	939	1014
GMODO/GMTCO	1012	1013	939	1014

Part 1 Block 1.2 and Block 2.0 Comparison

- **Block 2.0 I-bands, M-bands, DNB radiances are generally consistent with those produced by Block 1.2:**
  - RSB differences are less then 0.1% in worst cases (M2, I2);
  - DNB differences are less than 0.5%, and differences become smaller over time;
  - TEB radiances are consistent.

- **Geolocation:**
  - Block 2.0 and Block 1.2 are consistent in majority of data
  - NOVAS update in Block 2.0 causes small differences (not an issue);
  - **More TLE usages/gap interpolation were found in Block 2.0 →cause differences geolocation.**

- **Sector rotation data from Block 2.0 and Block 1.2 are consistent.**

- **M11 at night SDR from Block 2.0 are generally good.**

Comparing RSB F-factors (Block 2.0 versus Block 1.2)

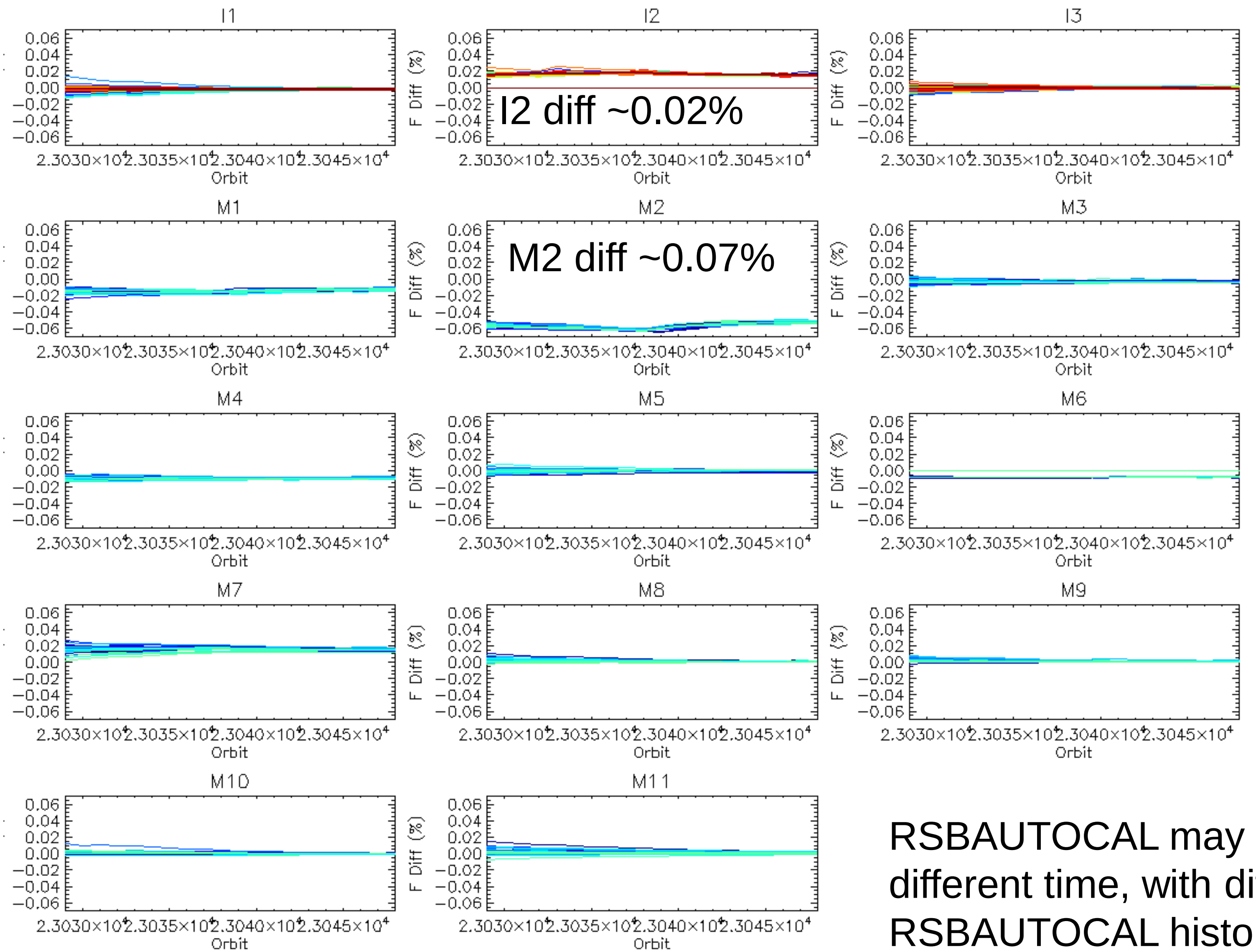

RSBAUTOCAL may started at a different time, with different RSBAUTOCAL history.

Comparing DNB LGS gain (Block 2 versus Block 1.2)

DNB LGS differences are less than 0.5%
Differences become smaller over time

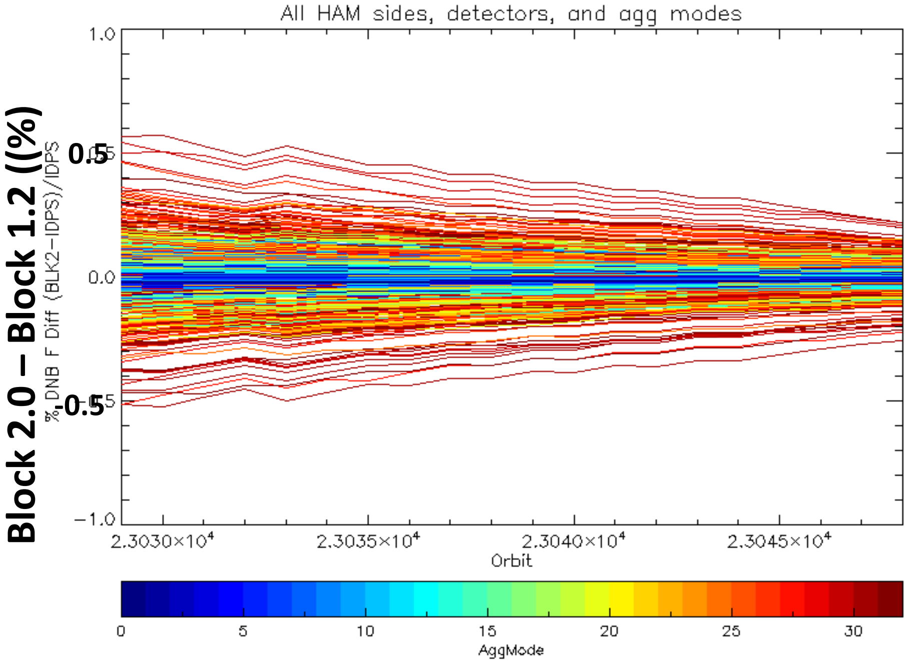

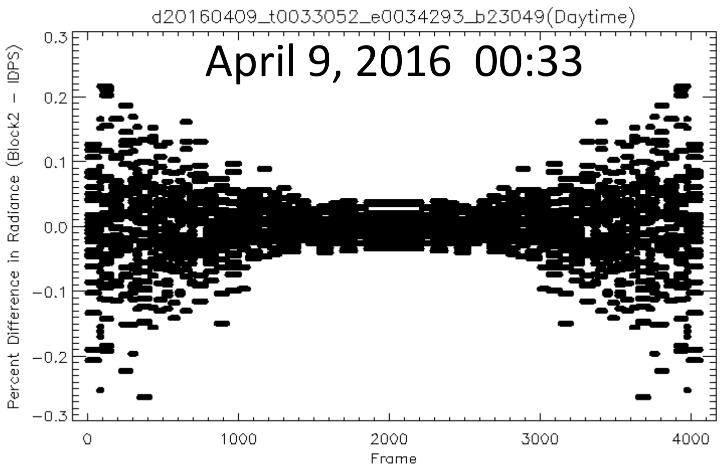

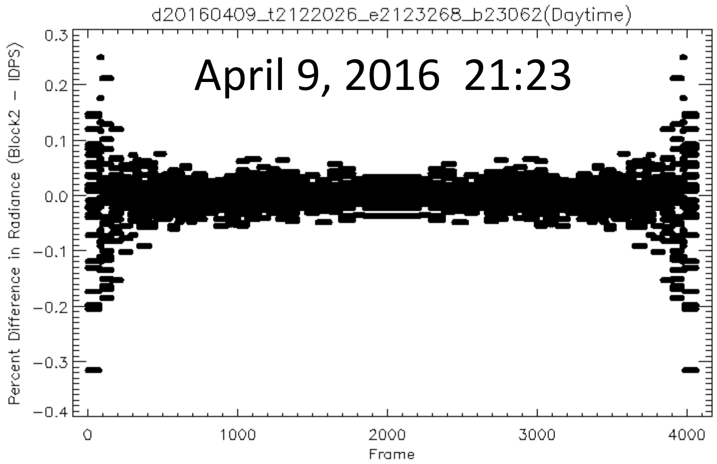

All other DNB calibration LUTs are consistent.

Geolocation (Non-Terrain Corrected)

April 8, 201616:19

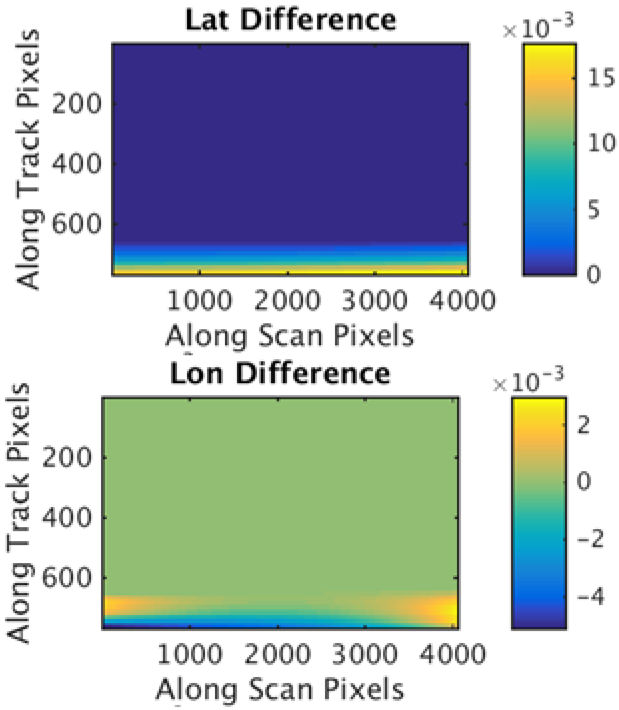

- **Large latitude differences (0.017 degree) at low latitude were observed;**
- The large differences are due to TLE usage or gap interpolation based on quality flags.

20160408	TLE Usage	GAP Interpolation
Block 2.0	4	57
Block 1.2	1	12

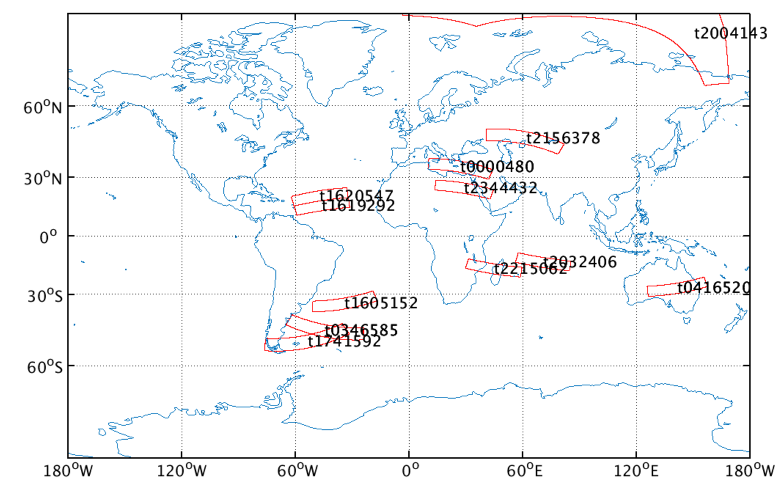

Sector Rotation Data Comparison

d20160417_t1136483_e1151018

M1 DNs

M15 DNs

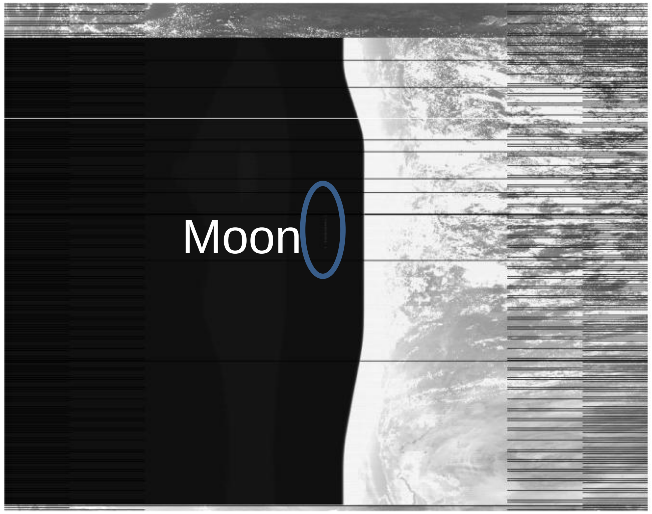

- Sector rotation data between Block 2.0 and Block 1.2 are consistent.

VIIRS M11 at Night

- Block 2.0 M11 nighttime radiances are generally good.
  - Block 1.2 does not support M11 nighttime data.

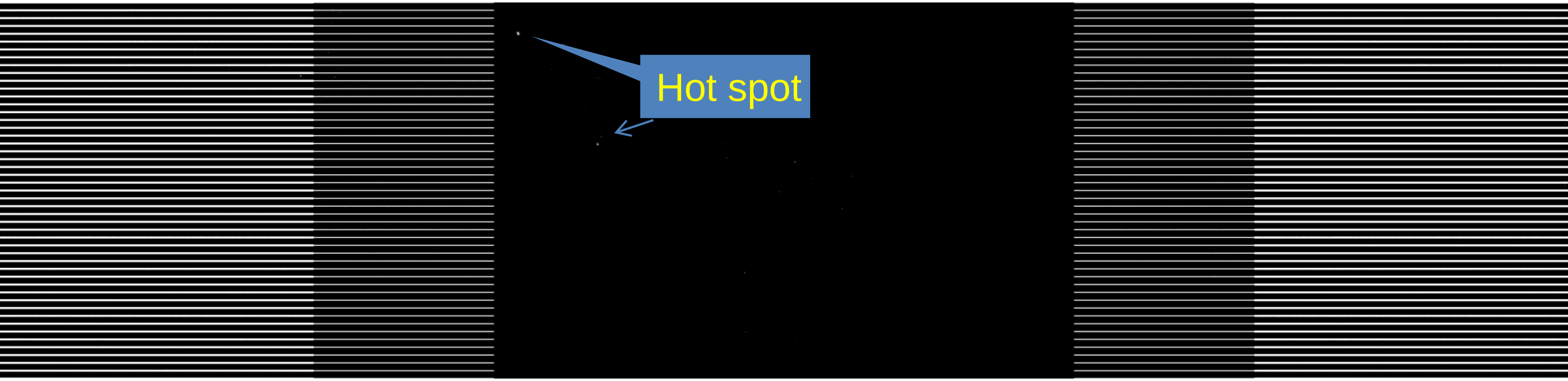

- Minor issues:
  - Block 2 M11 nighttime reflectance is a mixture of 0s and filling values, should be all fill values.
  - QF1 “reflectance out of range” bit should always be set to 1.

Part 2: Block 2.0 Verification Using Proxy J1 VIIRS RDRs

- Four proxy J1 RDRs were generated by the Raytheon Test Data Working Group;
- MDR_27, MDR_39, and MDR_47 were used for verification.

Name	Description	Note
MDR_28	Canned SNPP data	Cannot represent J1 conditions in some cases.
MDR_27	J1 Day-in-life, TVAC, cold/hot	Good for GEO testing and verification; HAM start enc not very stable in SCE Side-A; DNB CAL : good; RSB/TEB CAL: Tdet&Telec out of range.
MDR_39	J1 FP-X nadir alignment test, Ambient	Good for GEO testing and verification, esp. for DNB SCE Side-B RDR only HAM start enc is stable DNB: not good dp_dnb_dark_sub_eth disabled; RSB/TEB: Tdet out of range.
MDR_47	J1, Flight Operation (FOP), TAVC	Good for GEO testing and verification; Two granules that are good for CAL verification.

Note: S-NPP spacecraft ephemeris and attitude data were used in all 4 proxy J1 RDRs.

Verification of J1 GEO code changes

- Two J1 VIIRS GEO code changes have been developed and integrated to Block 2.0 to accommodate:
  - J1 DNB aggregation mode change (PSAT17)
  - Different TEL/HAM start encoder nominal, identify by Gary Lin from VCST (PSAT21)

- The GEO code changes were verified using:
  - ADL_5.3_PSAT21 ;
  - MDR 27, MDR_39, and MDR_47;
  - J1 prelaunch GEO PARAM LUTs.

- Both code changes perform as expected.

Verification of J1 GEO Code Change to Accommodate J1 DNB AggMode Change

MDR_39
DNB Op21 (baseline option for J1)

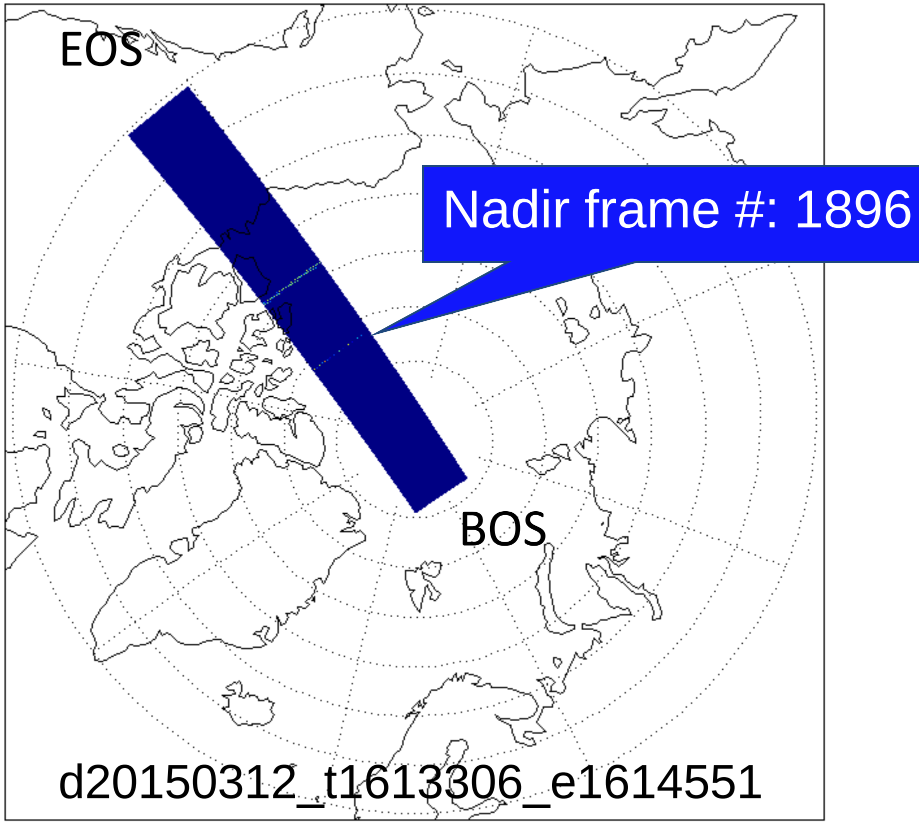

MDR_27
DNB Op32 (SNPP AggMode)

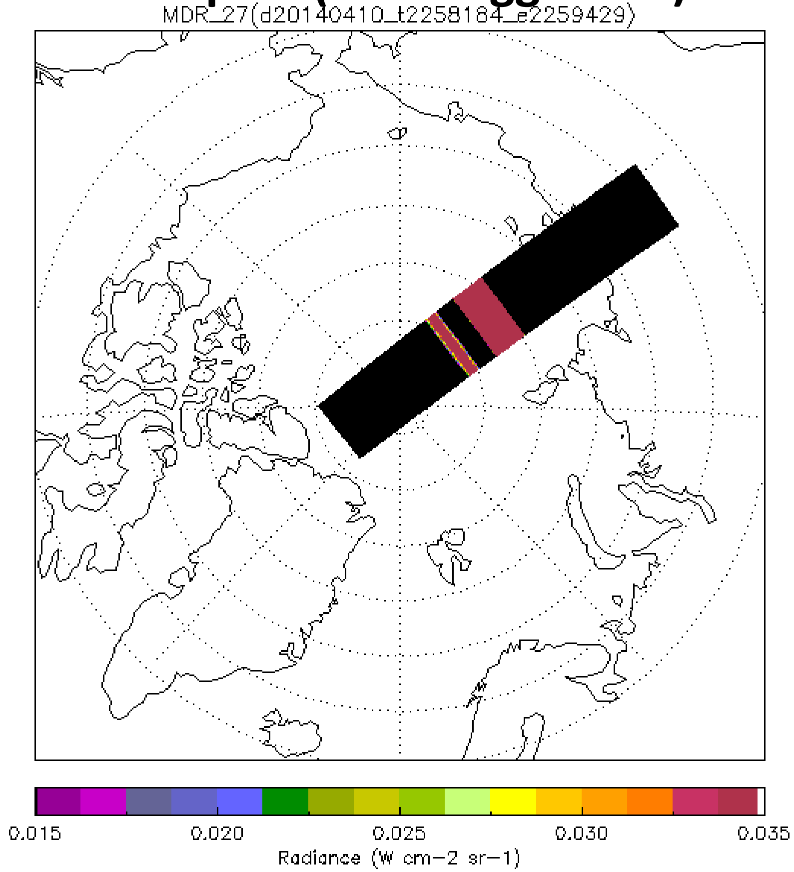

MDR_39 DNSs were used for plotting due to limitations in this proxy J1 RDR.

MDR_27 is good for GEO and DNB CAL verification.

Verification of J1 GEO Code Change

to Accommodate Different Start TEL/HAM Encoder Nominal

- Block 2 VIIRS SDR science code support both SNPP and J1 TEL/HAM start encoder nominal values.
  - J1 VIIRS geolocation products can be generated successfully using thress proxy J1 VIIRS RDRs that contain real J1 engineering data (MDR_27, MDR_39, MDR_47)

MDR 27

Side-A:

```
Check_Tel_Start_Not_Nominal: start value: 31002 sensorModel:3  SCEside:0 NOMINAL:31002
Check_Tel_Start_Not_Nominal: start value: 31002 sensorModel:3  SCEside:0 NOMINAL:31002
Check_Tel_Start_Not_Nominal: start value: 31002 sensorModel:3  SCEside:0 NOMINAL:31002
 Check_Ham_Start_Not_Nominal: start value: 10579 sensorModel:3 SCEside:0 NOMINAL:10579
 Check_Ham_Start_Not_Nominal: start value: 10579 sensorModel:3 SCEside:0 NOMINAL:10579
 Check_Ham_Start_Not_Nominal: start value: 10579 sensorModel:3 SCEside:0 NOMINAL:10579
 Check_Ham_Start_Not_Nominal: start value: 10579 sensorModel:3 SCEside:0 NOMINAL:10579
 Check_Ham_Start_Not_Nominal: start value: 10579 sensorModel:3 SCEside:0 NOMINAL:10579
 Check_Ham_Start_Not_Nominal: start value: 10579 sensorModel:3 SCEside:0 NOMINAL:10579
 Check_Ham_Start_Not_Nominal: start value: 10580 sensorModel:3 SCEside:0 NOMINAL:10579
 Check_Ham_Start_Not_Nominal: Non Nominal Value Detected
 Check_Ham_Start_Not_Nominal: start value: 10579 sensorModel:3 SCEside:0 NOMINAL:10579
```

Side-B:

```
Check_Tel_Start_Not_Nominal: start value: 30986 sensorModel:3  SCEside:1 NOMINAL:30986
Check_Tel_Start_Not_Nominal: start value: 30986 sensorModel:3  SCEside:1 NOMINAL:30986
Check_Tel_Start_Not_Nominal: start value: 30986 sensorModel:3  SCEside:1 NOMINAL:30986
: Check_Ham_Start_Not_Nominal: start value: 10579 sensorModel:3 SCEside:1 NOMINAL:10579
: Check_Ham_Start_Not_Nominal: start value: 10579 sensorModel:3 SCEside:1 NOMINAL:10579
: Check_Ham_Start_Not_Nominal: start value: 10579 sensorModel:3 SCEside:1 NOMINAL:10579
: Check_Ham_Start_Not_Nominal: start value: 10579 sensorModel:3 SCEside:1 NOMINAL:10579
: Check_Ham_Start_Not_Nominal: start value: 10579 sensorModel:3 SCEside:1 NOMINAL:10579
```

- The code change was backward compatible with SNPP (verified using SNPP RDRs).

Verification of J1 SDR Production

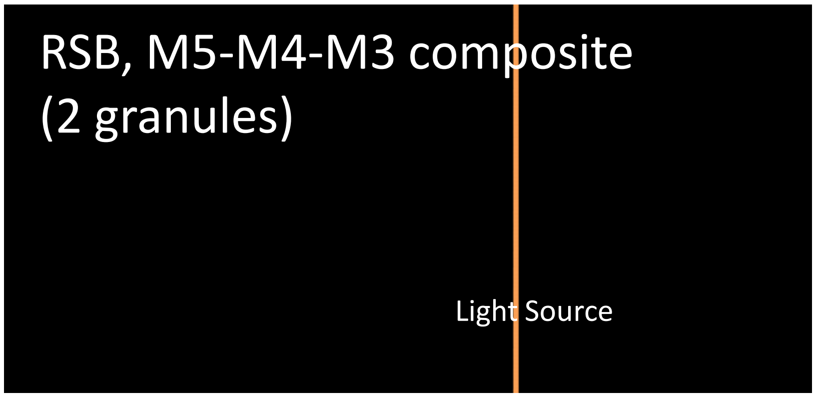

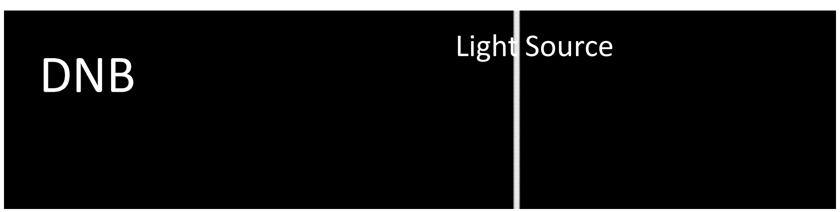

By Slawomir Blonski, STAR VIIRS SDR team

- GEO and RSB/DNB/TEB SDR products were generated successfully using:
  - ADL5.3_PSAT21
  - MDR_47 J1 VIIRS proxy RDRs:
  - Version 2 of J1 prelaunch calibration LUTs (recently delivered to the JPSS program on July 15, 2016)

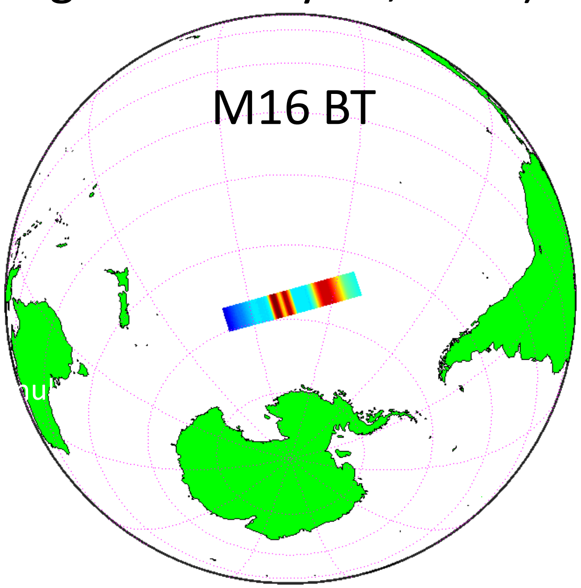

Verification of J1 SDR Production (Minor Issue with TEB QF)

- In MDR_47, cold FPA temperature was near the nominal value of 80.5 K;
- *Poor quality flag for all pixels were triggered due to non-nominal LWIR-FPA temperatures, occurs for all LWIR bands: M14-M16;*
- **Nominal LWIR-FPA temperatures are hardcoded, SNPP and J1 have different values but use the same addresses;**
- *Require code change.*

Nominal Cold FPA temperature settings :

- S-NPP (EDD154640-104_R_V8)

1.	78 K	0 0
2.	80 K	1 0
3.	82 K	0 1

FT_LW_80K_SETPT → first bit
FT_LW_82K_SETPT → second bit

- JPSS-1 (EDD154640-109D_v13)

1.	80.5 K	0 0
2.	82.0 K	1 0
3.	83.5 K	0 1

FT_LW_82_0K_SETPT → first bit
FT_LW_83_5K_SETPT → second bit

JPSS-1 vs. S-NPP: different names, but the same addresses (IDs)

By Slawomir Blonski, STAR VIIRS SDR team

Summary

- Block 2.0 system has been verified through:
  - Comprehensive comparisons of Block 2.0 and Block 1.2 SDR products for SNPP VIIRS using OBSAT and LG2 test data.
  - Using proxy J1 VIIRS RDRs.
- Block 2.0 system works well for SNPP/J1 SDR productions, with only some minor issues:
  - Small # of missing granules;
  - More TLE usage/gap interpolation;
  - Hard-coded nominal LWIR-FPA temperature.
- VIIRS SDR team will continue to support the program on further verification actives:
  - Post LG2 verification in September 2016;
  - When new J1 test data become available, J1 spacecraft TVAC data based RDRs will be very valuable for further Block 2.0 verification.

Summary of JPSS-1 VIIRS Pre-Launch Radiometric Performance

Hassan Oudrari[1] , Jeff McIntire[1], Xiaoxiong (Jack) Xiong[2], James Butler [2], Kurt Thome[2], Qiang Ji[1], Tom Schwarting[1], Jinan Zeng[3]

[1]NASA VIIRS Characterization & Support Team/SSAI, MD, 20706 USA
[2]NASA Goddard Space Flight Center, Greenbelt, MD, 20771 USA.
[3]NASA VIIRS Characterization & Support Team/Fibertek Inc., VA, 20171

Courtesy of NASA SNPP Land SIPS – S. Devadiga & P. Ma

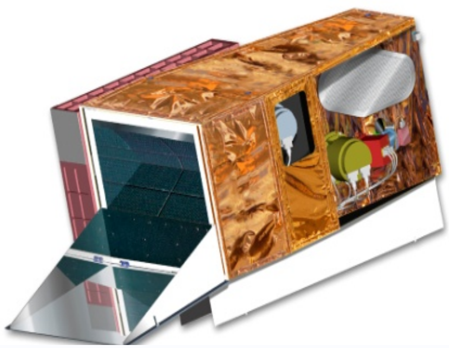

Courtesy of NASA SNPP Land SIPS – S. Devadiga & P. Ma

NOAA-STAR Annual Science Team Meeting
August 9th, 2016

Acknowledgements:

Government Data Analysis Working Group (DAWG), NASA VIIRS On-site Instrument Team

Content

- Background of VIIRS Sensor
- J1 VIIRS Pre-launch Testing
- J1 VIIRS Performance Assessment:
  - ✓ SNR/NEdT, Lmax, Polarization, NFR, RVS, RSR
- Status of J2 VIIRS Ambient Testing
- Summary/Conclusion

VIIRS Bands and Products

VIIRS 22 Bands:
16 M-Band, 5 I-Band and 1 DNB

	Band	λc(nm)	Δλ(nm)	Spatial Resolution (m)	MODIS Equivalent Band
VisNIR	DNB	700	400	750	
VisNIR	**M1**	**412**	**20**	**750**	B8
VisNIR	**M2**	**445**	**18**	**750**	B9
VisNIR	**M3**	**488**	**20**	**750**	B3-B10
VisNIR	**M4**	**555**	**20**	**750**	B4-B12
VisNIR	**M5**	**672**	**20**	**750**	B1
VisNIR	I1	640	80	375	B1
VisNIR	M6	746	15	750	B15
VisNIR	**M7**	**865**	**39**	**750**	B2
VisNIR	I2	865	39	375	B2
SMWIR	M8	1240	20	750	B5
SMWIR	M9	1378	15	750	B26
SMWIR	M10	1610	60	750	B6
SMWIR	I3	1610	60	375	B6
SMWIR	M11	2250	50	750	B7
SMWIR	I4	3740	380	375	B20
SMWIR	M12	3760	180	750	B20
SMWIR	**M13**	**4050**	**155**	**750**	B21-B22-B23
LWIR	M14	8550	300	750	B29
LWIR	M15	10763	1000	750	B31
LWIR	I5	11450	1900	375	B31-B32
LWIR	M16	12013	950	750	B32

Dual Gains

VIIRS 22 Environmental Data Products (EDRs)

Land

1- Active Fires
2- Snow Cover
3- Land Surface Albedo
4- Vegetation Index
5- Land Surface Temperature
6- Surface Type
7- Ice Surface Temperature
8- Net Heat Flux
9- Snow Ice Characterization

Ocean

1- Sea Surface Temperature
2- Ocean Color/Chlorophyll

Imagery and Clouds

1- Imagery and low light imaging
2- Cloud Top Height
3- Cloud Optical Thickness
4- Cloud Top Temperature
5- Cloud Effective Particle Size
6- Cloud Base Height
7- Cloud Top Pressure
8- Cloud Cover/Layers

Aerosol

1- Aerosol Optical Thickness
2- Aerosol Particle Size
3- Suspended Matter

- 14 reflective solar bands (RSB): 0.4-2.2 μm and 1 day night band (DNB)
- 7 thermal emissive bands (TEB): 3.7-12.0 μm
- Dual gain bands: M1-M5, M7, and M13

VIIRS Sensor & On-board Calibrators

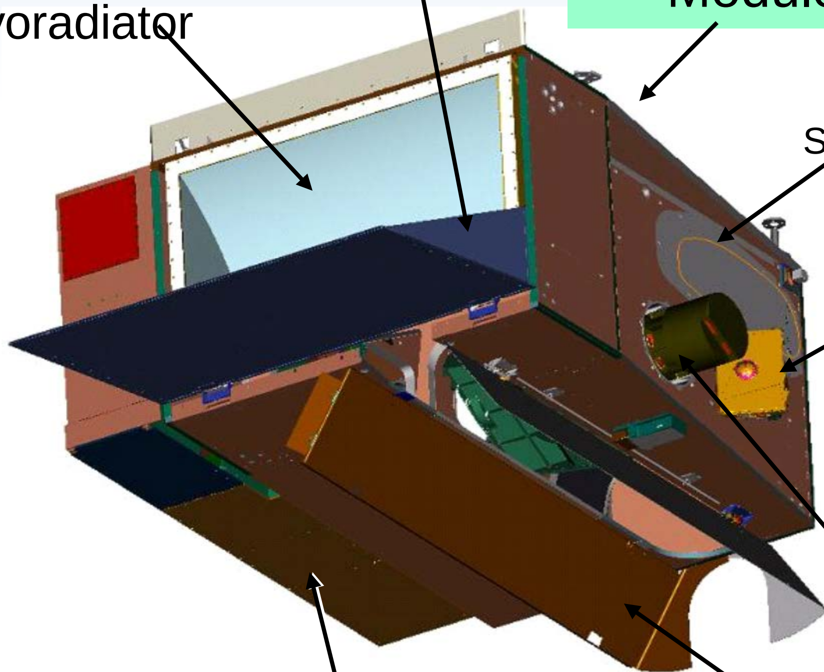

SDSM

Solar Diffuser

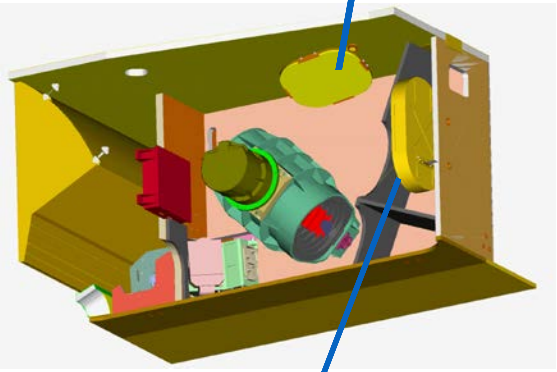

Blackbody (BB)

- *Proven design through SNPP mission*
- *Comprehensive pre-launch testing, and on-orbit predictions*

Pre-Launch Testing Objectives

- **Radiometric, Spectral and Spatial testing**
  - Ambient, TV (cold, nominal, hot), HAM sides, E-sides, detectors, etc.
- **Ensure sensor performance meets design requirements**
  - Compliance, Waivers
- **Capability to generate sensor performance parameters for on-orbit operation and calibration**
- **Support modeling and predictions to ensure overall science objectives are met**
- **Development and implementation of potential mitigation strategies to address artifacts and noncompliance issues**

Overview of J1 Pre-launch Testing

Performance Testing:

- Radiometric (SNR/NEdT, detector calibration, dynamic range)
- Spectral (IB and OOB RSR)
- Spatial and geometric (BBR, MTF, and pointing)
- Others
  - Polarization sensitivity
  - Response versus scan-angle
  - Stray light and Near-field response
  - BB/SD/SDSM characterization
- Thermal testing
- Vibration testing
- Electromagnetic interference
- Special testing (ETPs)

Testing Phases:

- **Component/Sub-system Testing**
- **Sensor Level Testing**
  - ✓ Ambient: *08/24/2013 - 01/19/2014*
  - ✓ TVAC: *07/16/2014 - 10/30/2014*
  - ✓ Sensor Delivery: *02/06/2015*
- **Observatory Level Testing:**
  - ✓ Sensor Integrated to J1: *02/20/2015*
  - ✓ Environmental Testing: *April-September 2016*
- **JPSS-1 Launch:**
  - ✓ Mid-March, 2017

Testing & Performance Teams

- **Test data independently analyzed and reviewed by**
  - Sensor Vendor (Raytheon)
  - Government Team
    - NASA
    - NOAA
    - Aerospace
    - U. of Wisconsin
- **Test results reviewed by**
  - Data Review Board (DRB): results primarily from sensor team
  - Data Analysis Working Group (DAWG): results primarily from gov. team
  - Technical Interchange Meetings (TIMs)
  - Regular briefings at NOAA-led VIIRS SDR meetings

General Agreement on the good quality of J1 VIIRS test data, and instrument performance

J1 Instrument Improvements

- RTA Mirrors Changed from Ni coated to VQ
  - Improved spatial stability with temperature
- Dichroic 2 Coatings Redesigned
  - Improved spatial performance between SMWIR & LWIR
- Eliminated Throughput Degradation Due to Tungsten
  - Improved radiometric sensitivity
- Enhanced VisNIR Integrated Filter Coating Change
  - Improved crosstalk, OOB, and RSR performances
  - Higher polarization sensitivity: Bands M1 – M4

Other changes were also included but not expected to make substantial change in the sensor performance

RSB Radiometric Performance

J1 SNR compliant with margin

I3 Det4 noisy

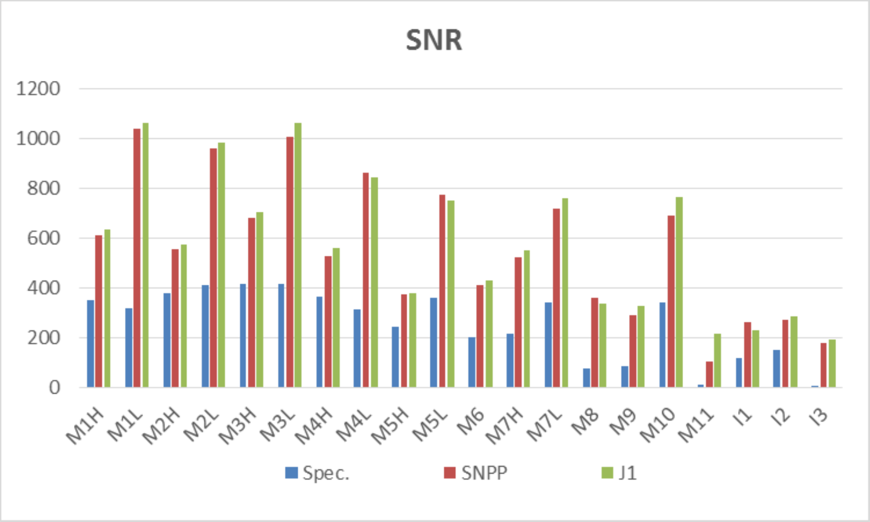

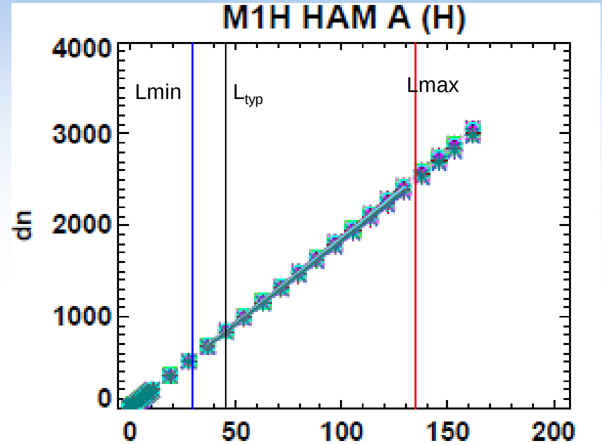

Minor Dynamic range non-compliance (M8, I3)

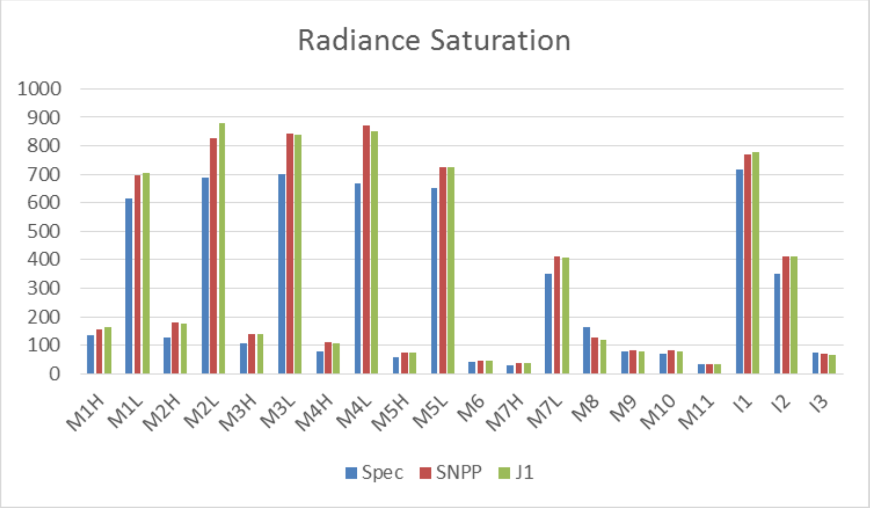

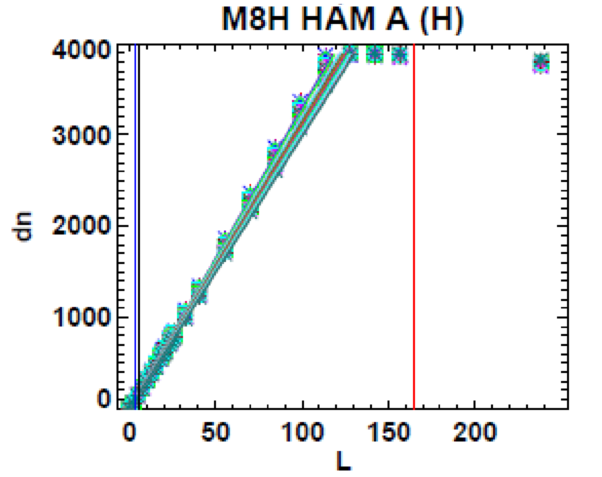

- **J1 Radiometric performance is quite similar to SNPP**
- **Higher than expected non-linearity seen in SWIR bands and DNB**

SWIR Radiometric Performance

SWIR Non-Linearity Issue (Low Radiance)

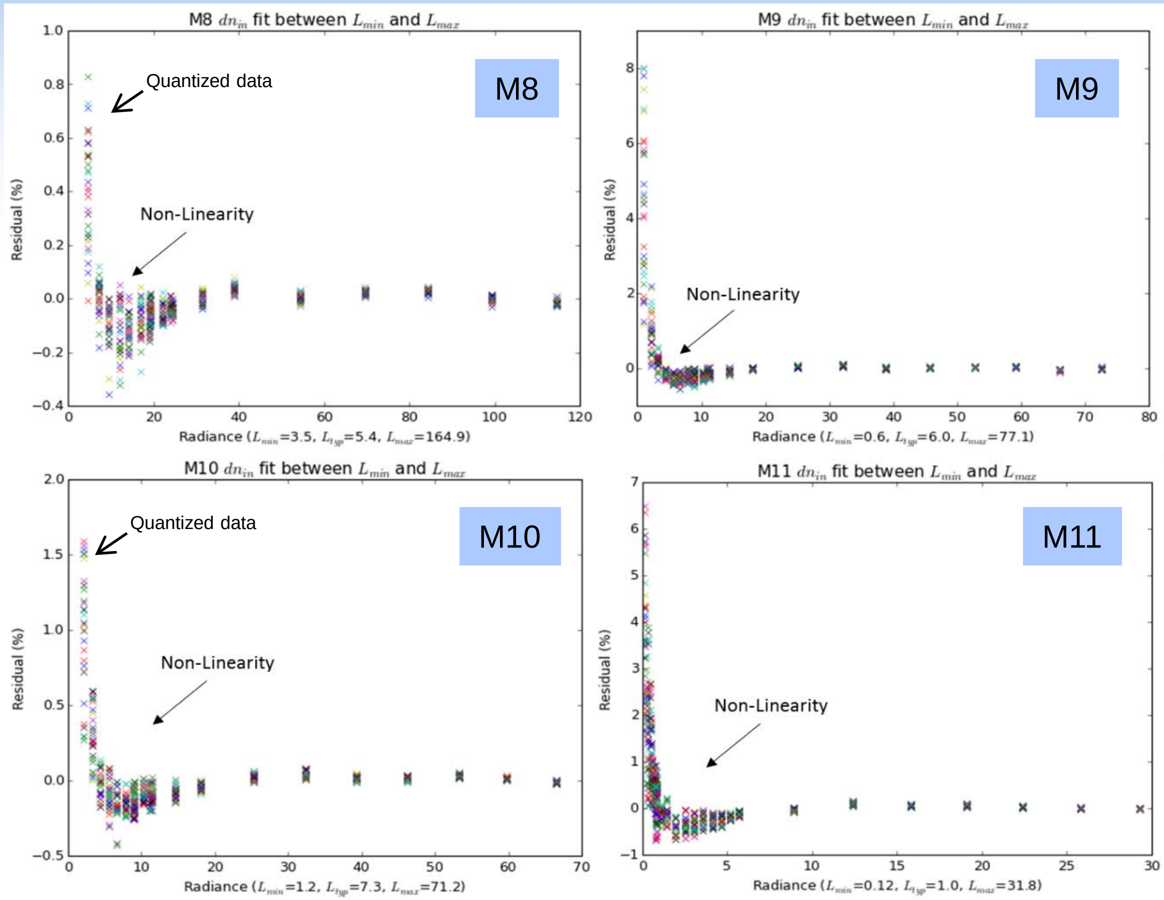

- **Issue characterized and root cause identified (electronics Voltage)**
- **Plan to mitigate in the SDR software (3rd degree equation, or other options)**

DNB Radiometric Performance

DNB Non-Linearity Issue (Low Radiance)

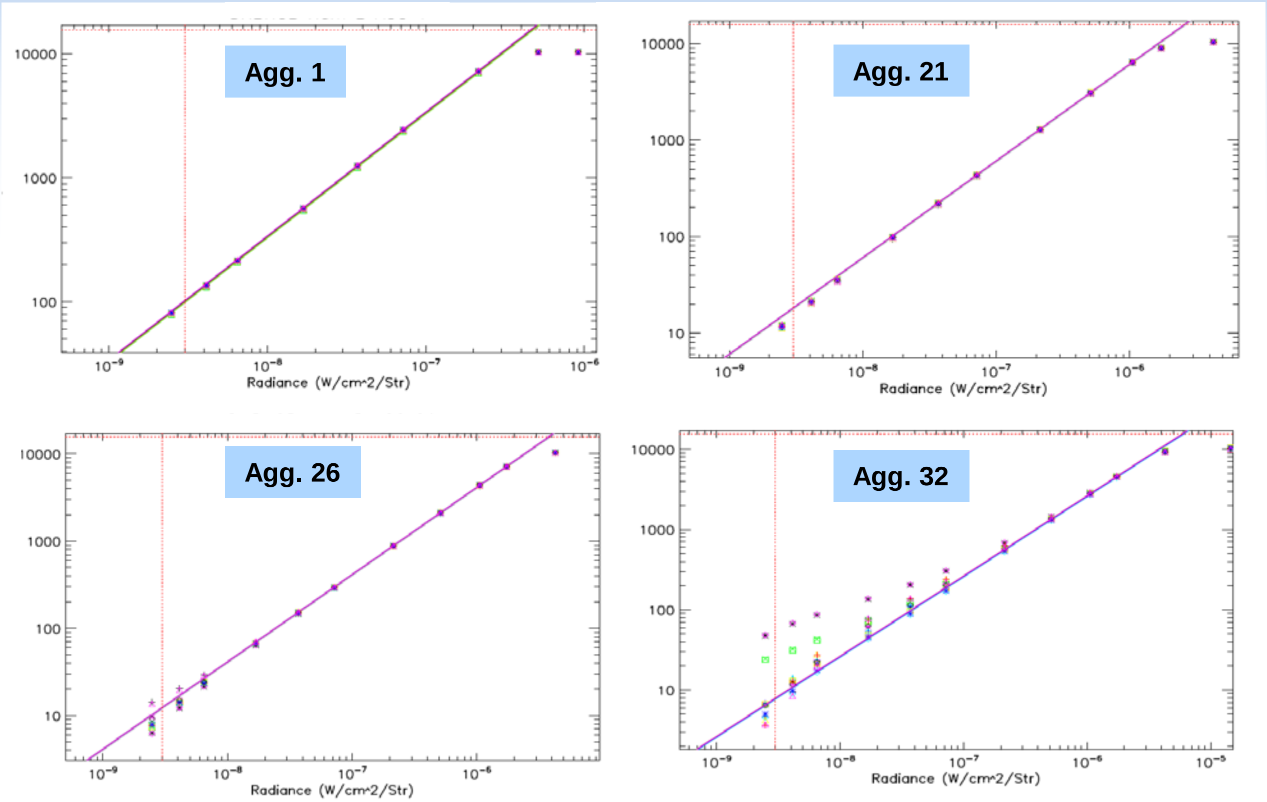

- Limited to agg. modes at the end of scan (22-32)
- Issue characterized and root cause identified (timing card setting)
- Resolved using Option21 approach at the expense of spatial resolution

TEB Radiometric Performance

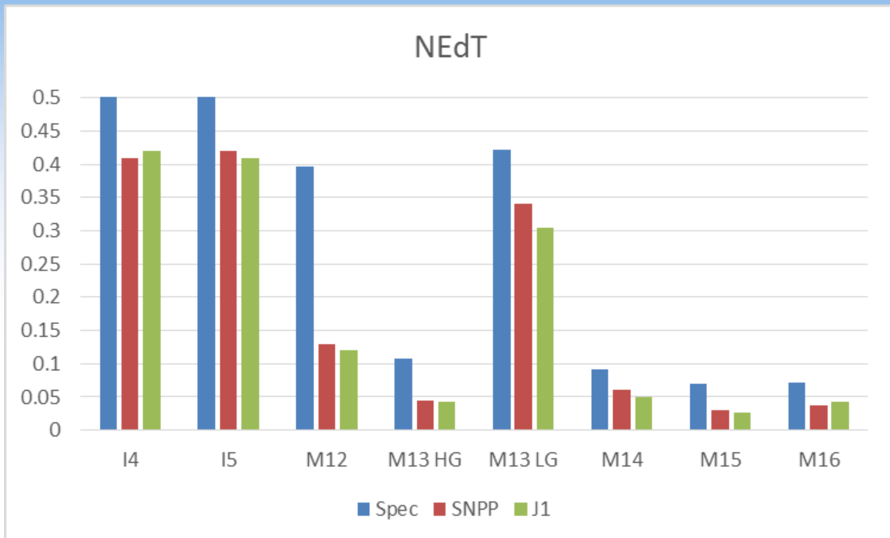

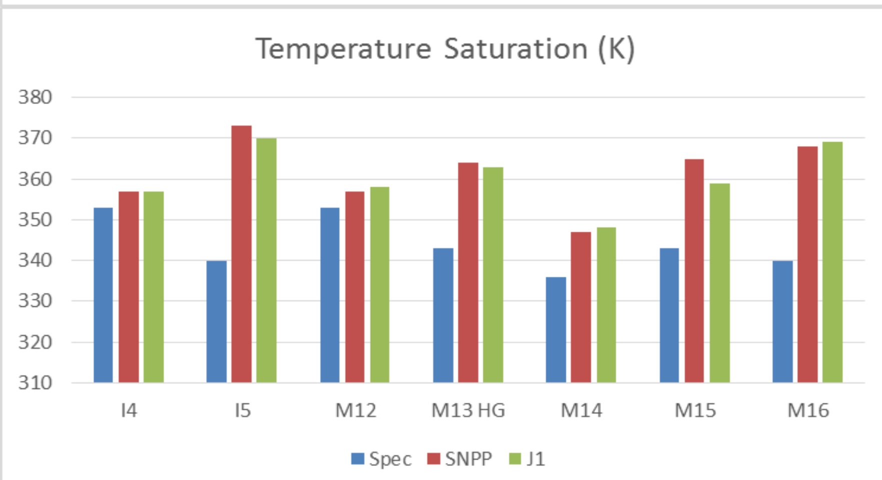

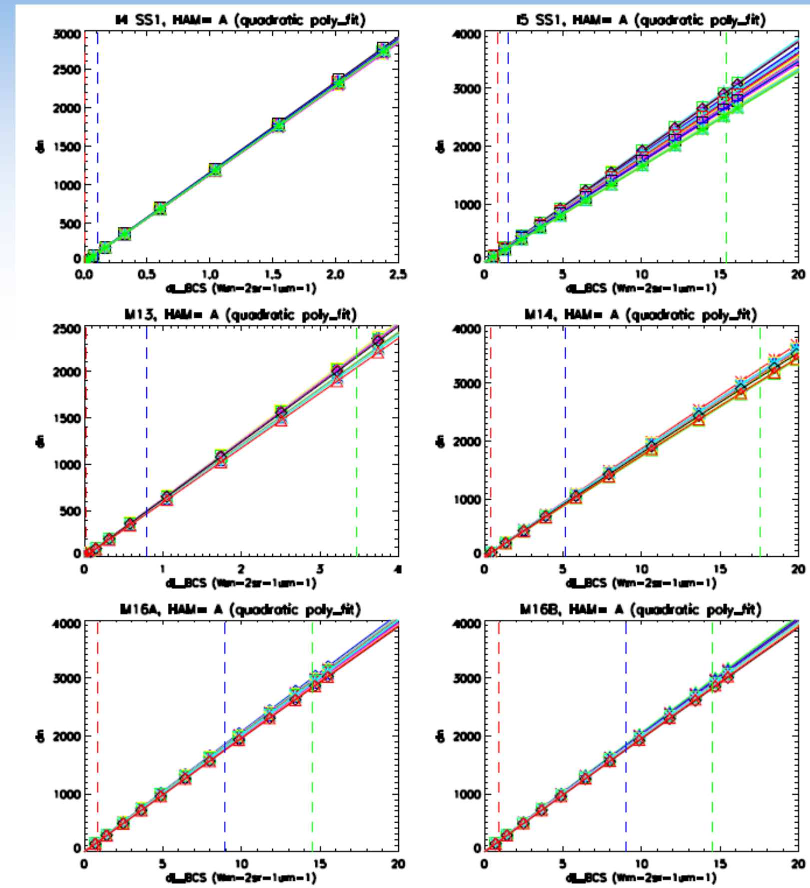

Radiance

- **J1 TEB calibration performance is very good, similar to SNPP performance.**
- **Minor non-compliances observed: T_{MIN} for I4 and M14; M13 gain transition radiance.**
  - **Impact to science is expected to be small.**

VisNIR Polarization Sensitivity

- **Bands M1–M4 were non-compliant with the polarization sensitivity requirements**
- **A series of telecons were held with NASA/NOAA SMEs**
  - Provided impact assessments for Ocean, Land , and Atmosphere disciplines
  - Correction methodologies available to enhance EDR products
- **Additional testing was requested after TVAC**
  - Additional scan angles were measured using a broadband source
  - Limited measurements performed with a laser source for model validation

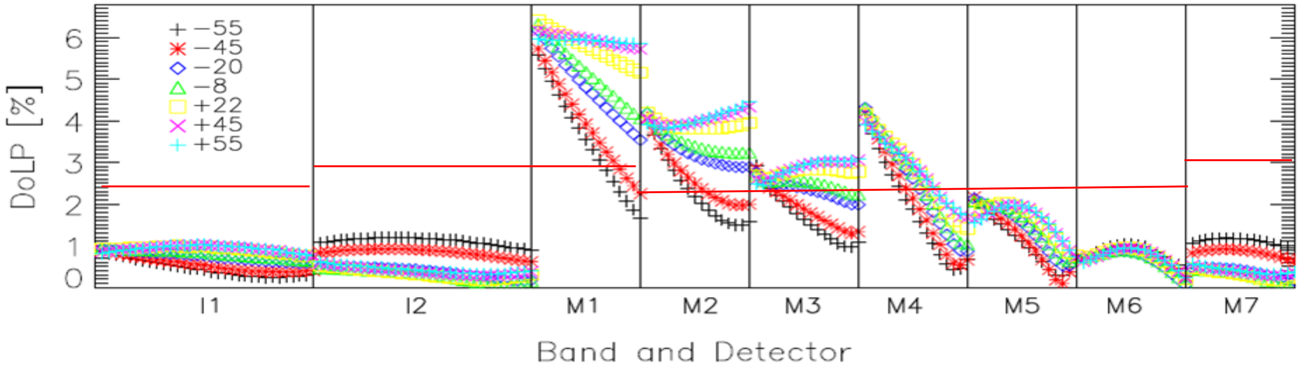

Successful and comprehensive J1 polarization testing was completed

- Uncertainty less than (0.4%), Repeatability within 0.13%

Near-Field Response (NFR) Performance

J1 NFR Performance at Beginning of Life (BOL)

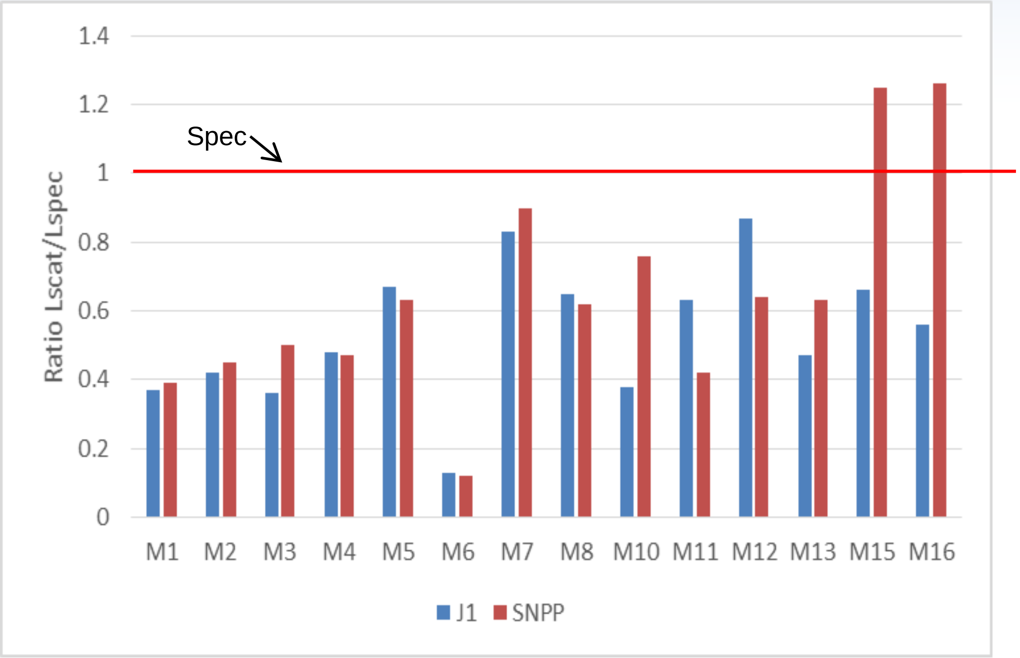

Band M5 (672 nm) detector 8

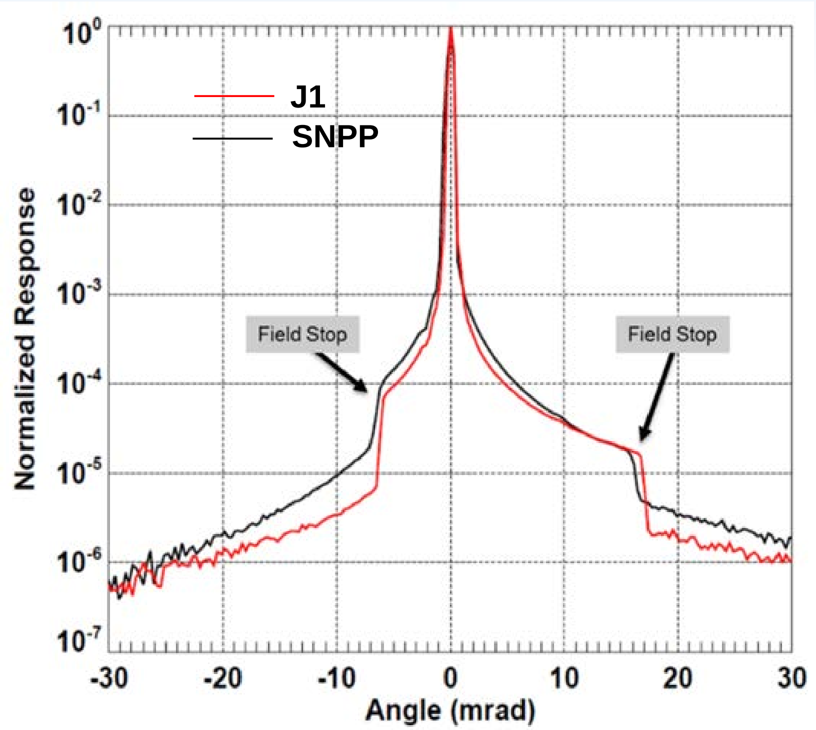

J1 NFR requirements are met for all bands

Response vs. Scan (RVS)

RVS is the HAM reflectance as a function of HAM Angle of incidence (AOI)

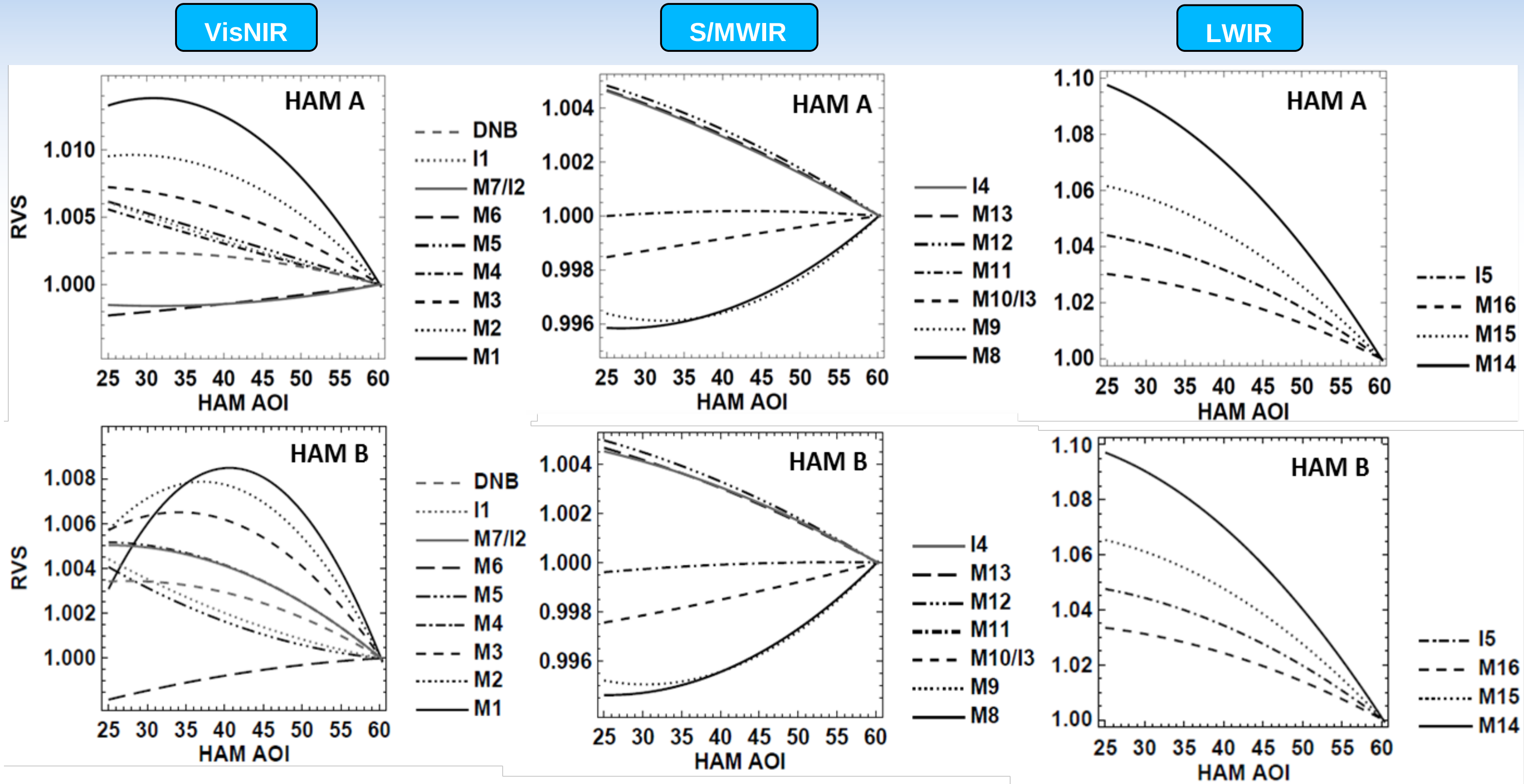

- **Excellent J1 RVS performance characterization, Similar to SNPP**
    - **RSB uncertainty under 0.06% (Spec 0.3)**
    - **TEB uncertainty under 0.15 % (Spec 0.2)**

Spectral Performance

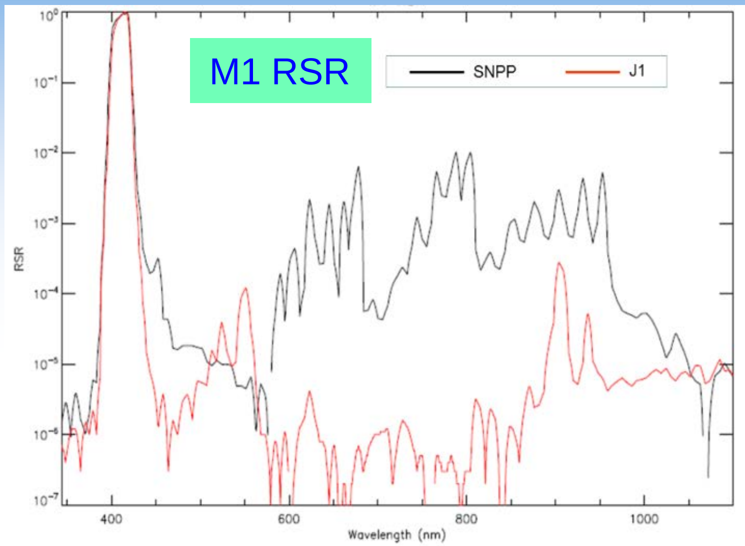

- J1 spectral performance testing was completed successfully for all bands
- Combination of best quality data from monochromator and laser is used for J1
- Overall spectral performance is expected to be better than SNPP.

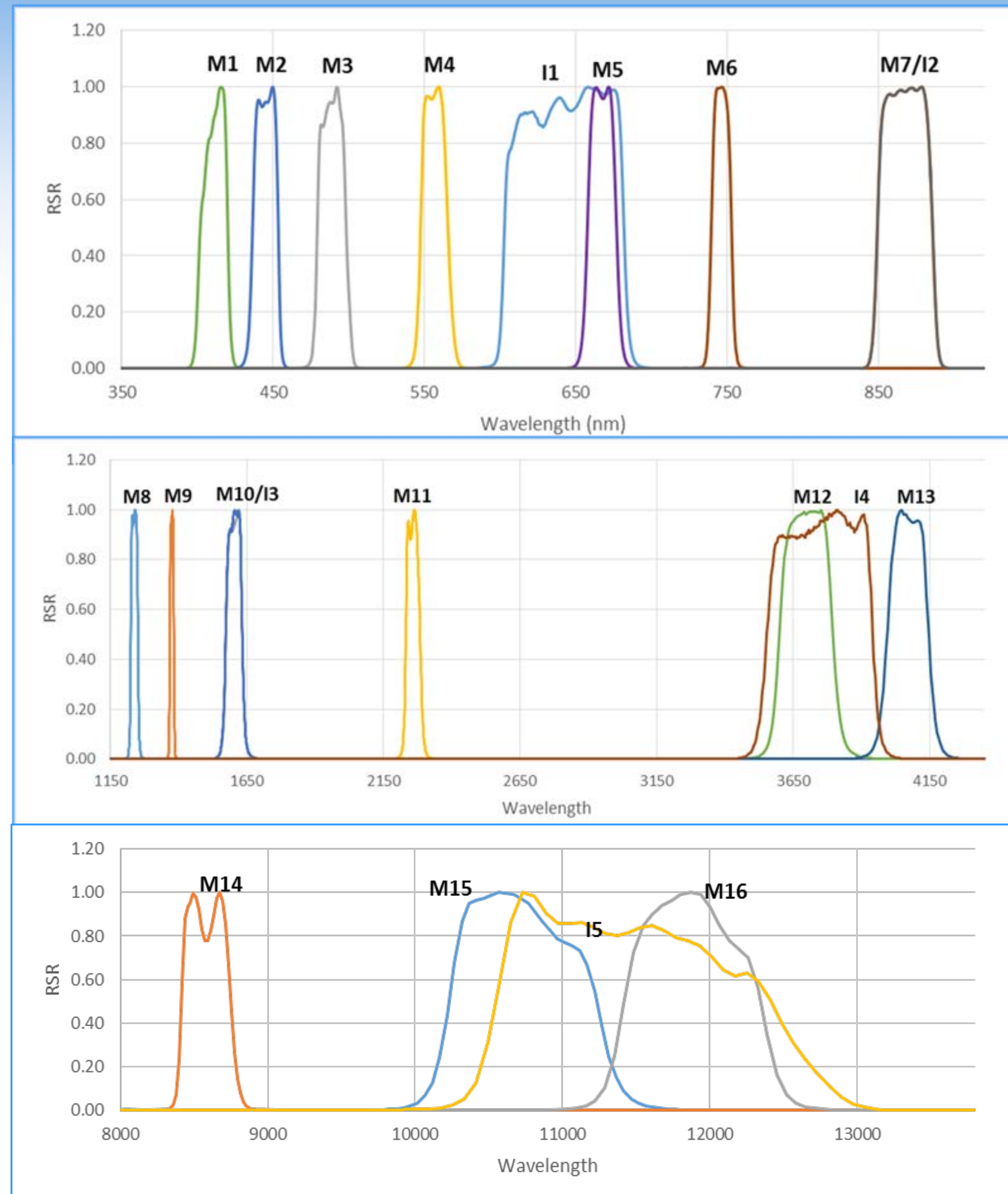

J1 VIIRS Performance Waivers

Raytheon Waiver #	Title	Status
RDW_148	J1 Relief against reflective band absolute radiometric calibration uncertainty requirements for bands M1-M3	Approved
RDW_149	J1 Relief against reflective band absolute radiometric calibration uncertainty requirements for band M11	Approved
RDW_150A	J1 Relief for DNB stray light in certain viewing geometries and related impacts on sensitivity and radiometric calibration	Approved
RDW_151	J1 relief against maximum radiance requirement for bands M8, I1 and possibly M1LG and I3.	Approved
RDW_166	J1 relief agains maximum polarization sensitivity requirement for bands M1 to M4.	Approved
RDW_153	J1 relief against electrical and optical crosstalk. Stringent requirements and testing artefacts are leading to non-compliances	Approved
RDW_150A	J1 relief against the sensor modulated transfer function (MTF)	Approved
RDW_161	J1 relief against the relative spectral response (RSR) requirements. Band center (M5, M16), Band width (M1,M8,M14,DNB), 1% limit (I5,DNB), IOOB (M16)	Approved
RDW_168	J1 relief against near field response (NFR). Non-compliance for (M7, M13, M16A and I3)	Approved
RDW_171	J1 relief from emissive relative radiometric reponse calibration uniformity (M12-M14 at high temp) and characterization uncertainty (I5 and M12).	Approved
RDW_172	J1 relief from reflective band characterization uncertainty (all bands non-compliant except M4HG and M5HG, and M7HG), and uniformity characterization (all bands non-compliant except M1-M7 high gain and M6)	Approved
RDW_173	J1 relief from band-to-band registration for I bands (non-compliance for I1-I3, I2-I3, I1-I4, I2-I4, I1-I5, I2-I5, I3-I5, I4-I5)	Approved
RDW_174	J1 relief from DNB SNR, uniformity and RCU.	Approved
RDW_175	J1 relief from spatial dynamic field of view (DFOV). All M bands and I5 not compliant	Approved
RDW_177	J1 DNB relief from dynamic range (LGS)	Approved

- **All 15 waivers were approved by NASA/NOAA review board**
- Completed a series of telecons (half-dozen) with NASA and NOAA SMEs to review each waiver
- Compliance is against end-of-life (EOL) performance
- All of non-compliances have mitigation plans, or will lead to acceptable impact.

JPSS VIIRS Future Enhancements

- **DNB On-orbit Stray light Issue Investigation**
  - Observed in SNPP on-orbit, but root-cause still to be identified.
- **Eliminate SWIR and DNB non-linearity at low radiance**
  - Both issues resolved for J2 VIIRS
- **Algorithm changes to reduce stripping effect due to sensor calibration artifacts (M15-M16, I3 Det4)**
- **Finalize List of J1 lessons learned, and Hardware/Software Improvements to be implemented for future builds (JPSS-2,3,4)**
  - Testing enhancements, adding a water vapor band, electronics noise, radiance roll-over, etc.

JPSS-2 VIIRS:

Initial Radiometric Performance

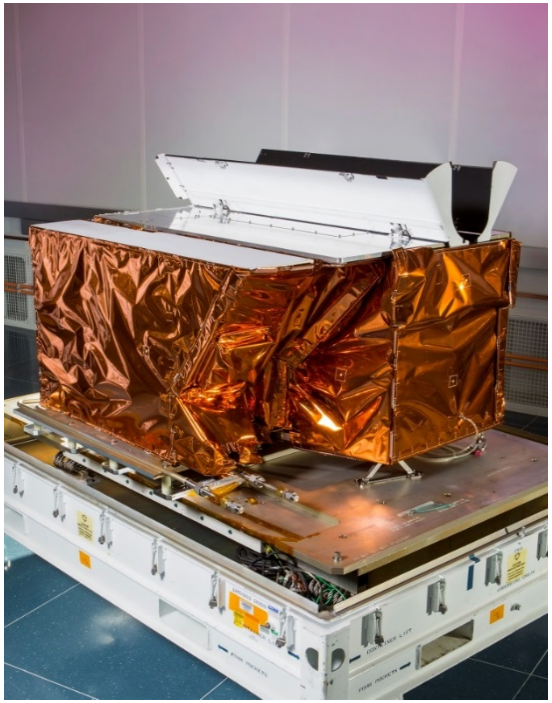

JPSS-2 VIIRS Status

- **JPSS-2 VIIRS is the 3rd unit of VIIRS sensors,**
  - **Ambient Phase**: April-August 2016
  - **Thermal Vacuum**: June-August 2017
  - **Expected Launch Date**: January, 2021

- **JPSS-2 VIIRS is similar to its two predecessors, with multiple performance enhancements, including:**
  - The redesign of the VisNIR IFA filter to reduce polarization sensitivity, and changes to the AOA fold mirror #2.
  - SWIR and DNB non-linearity issues seen in J1 were eliminated
  - JPSS-2 test program included numerous lessons-learned:
    - Better efficiency and cost reduction (e.g. enhanced stray light testing, shorter crosstalk testing, etc.)

J2 Radiometric Performance

Preliminary assessments based on Ambient testing

Polarization

JPSS-1

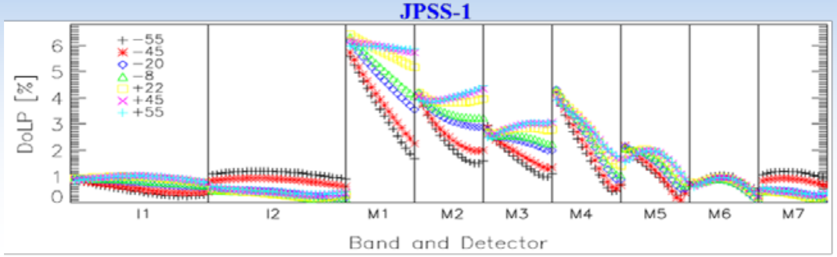

JPSS-2

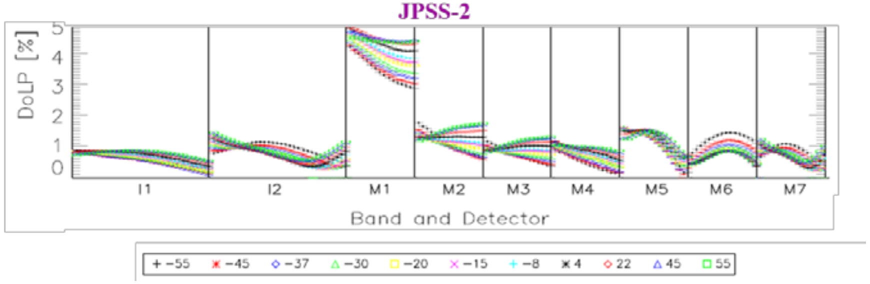

A-Side Elec.

Gain	Band	SNR spec	SNR		Lmax spec	Maximum radiance	
			HAM A	HAM B		HAM A	HAM B
HG	M1	352	732	752	135	164.8	164.8
	M2	380	702	701	127	169.5	169.1
	M3	416	861	851	107	126.1	126.0
	M4	362	683	672	78	98.9	98.9
	M5	242	359	359	59	81.0	81.0
	M6	199	567	571	41	53.4	53.4
	M7	215	654	658	29	37.5	37.4
	M8	74	302	292	164.9	158.2	158.1
	M9	83	177	176	77.1	131.9	131.9
	M10	342	767	749	71.2	99.1	99.0
	M11	90	237	235	31.8	33.1	33.0
	I1	119	208	204	718	969.2	969.1
	I2	150	372	372	349	455.6	455.1
	I3	6	200	199	72.5	100.7	100.7
LG	M1	316	1090	1099	615	508.7	508.7
	M2	409	1124	1128	687	844.3	841.9
	M3	414	1064	1065	702	894.4	894.7
	M4	315	819	851	667	775.2	774.7
	M5	360	665	660	651	949.5	949.4
	M7	340	1427	909	349	411.1	410.7

J2 radiometry is very good as expected

- SNR compliance with significant margin
- Lmax compliant except for M8 (95%)
- Better polarization performance than J1
- Near Field Response comparable to J1

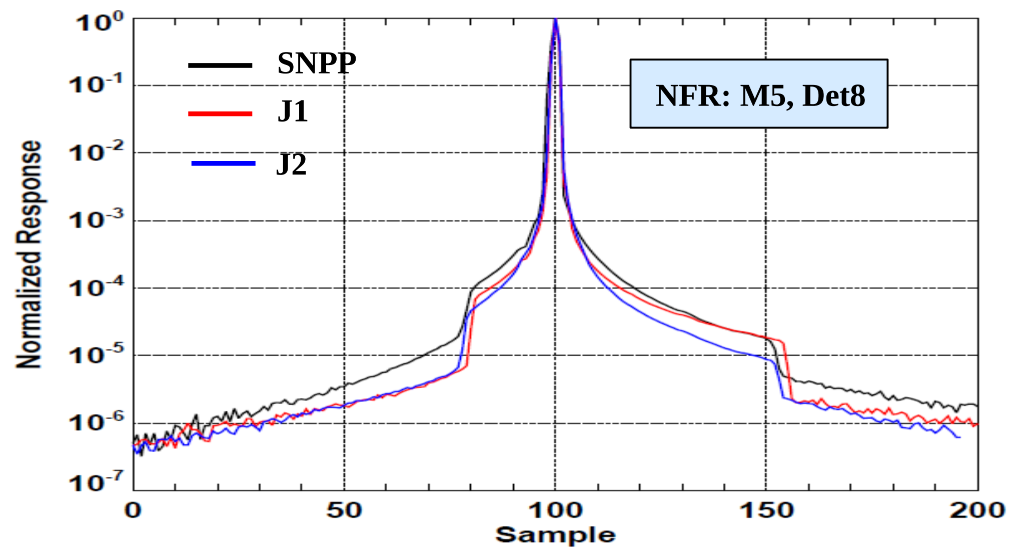

Summary & Conclusion

- **J1 VIIRS test program was completed successfully**
- **Provided an extensive amount of high quality data to assess sensor performance**
- **VIIRS performance exceeds requirements with few non-compliances**
  - Non-compliances have been reviewed, impacts have been assessed, and mitigation plans are being prepared for on-orbit processing
  - J1 VIIRS spacecraft testing is expected to be completed by September 2016
  - J1 LUTs needed for on-orbit calibration are being finalized.
  - J1 SDR software is ready, changes include DNB Option21 mitigation approach.
- **J2 VIIRS initial ambient testing has shown good performance**
  - Good initial radiometric and spatial performance (i.e. SNR, NFR, polarization, RVS and spatial)
  - J2 VIIRS TV testing will provide complete set of performances.
- **J3/J4 VIIRS contract complete and approved, and sensor parts are being selected from spares or in development,**
  - Taking advantage of lessons learned from previous sensors (i.e. SNPP, J1 and J2)

SNPP VIIRS Imagery

Eastern Seaboard

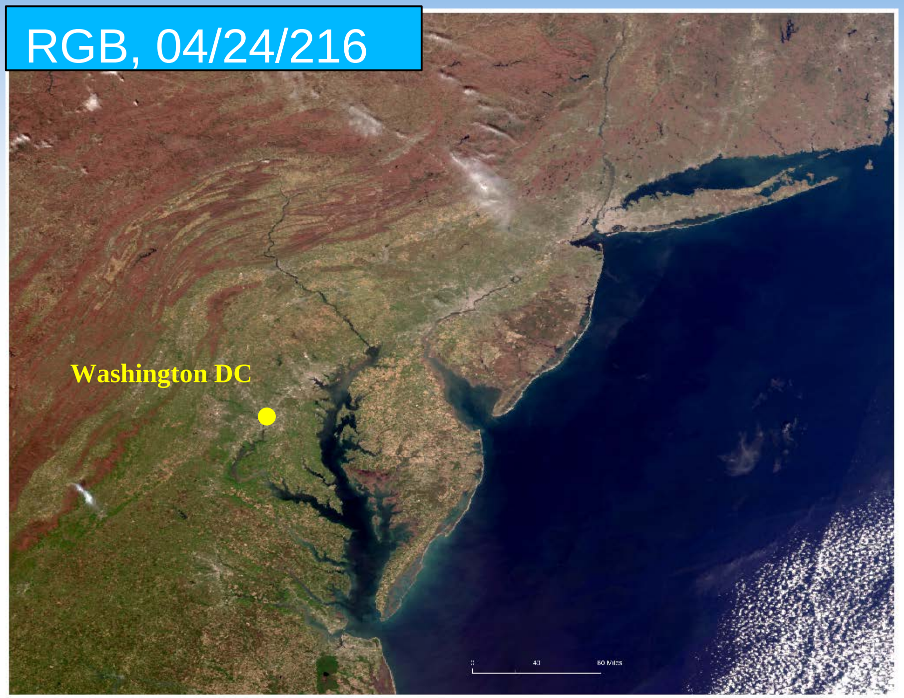

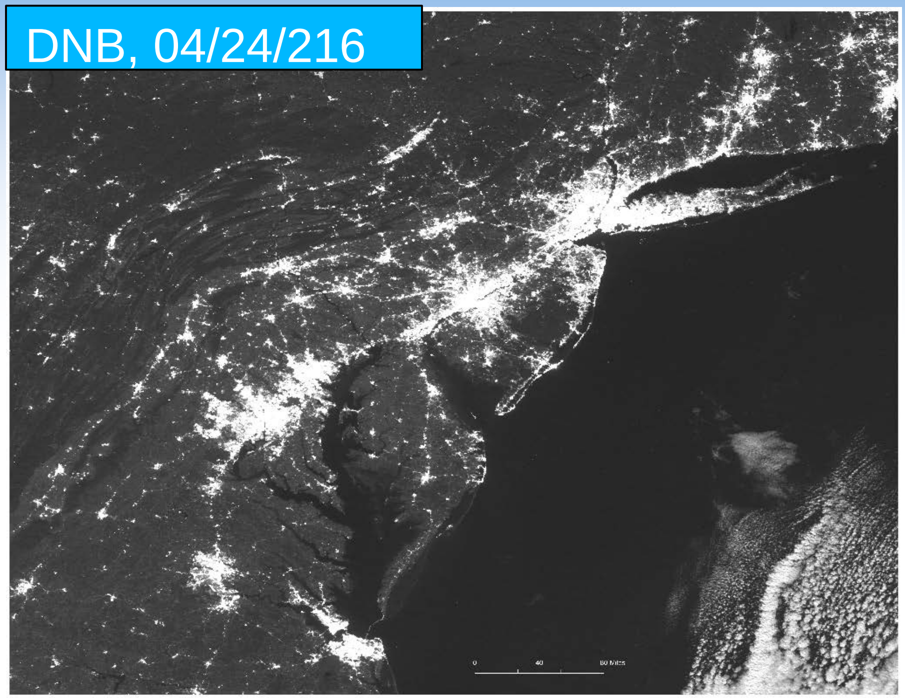

Courtesy of NASA SNPP Land SIPS – S. Devadiga & P. Ma

J1 VIIRS is also expected to deliver high quality radiance and environmental data products

Thanks!

Backup

J2 Scan Underlap Issue

- Underlap is defined as non-overlapping VIIRS swath projections on the ground in track extent
- Underlap will be seen on every other swath pair with current J2 as built tolerances
- **Combination of facts led to this Issue,**
  - **1) Requirement change from 833 to 828km,**
  - **2) HAM misalignment exceeded tolerance.**

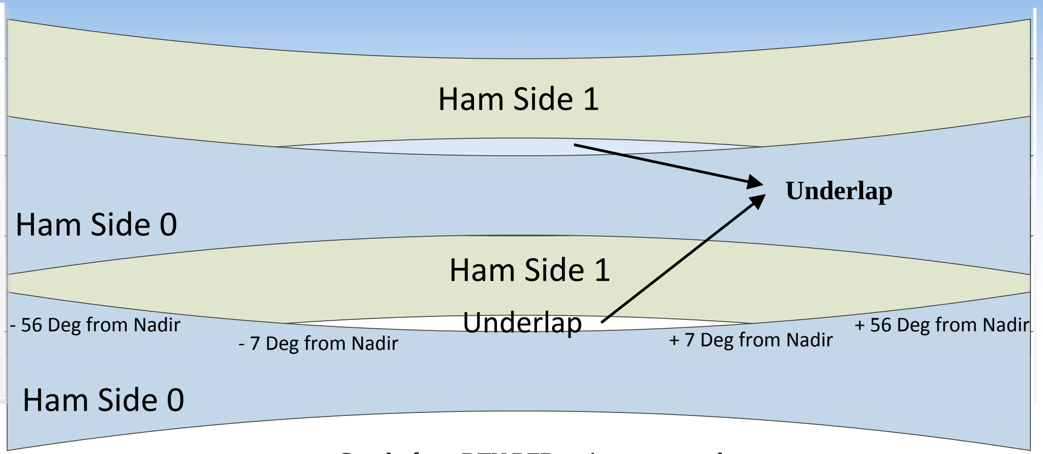

Graphs from RTN RFB review, not to scale

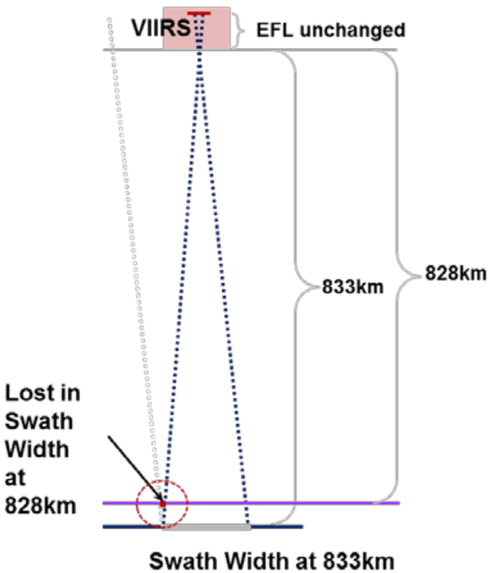

- Scan Overlap is driven by the following parameters:
  - **Altitude** – as altitude gets lower, projection on the ground gets smaller
  - **HAM Alignment** – alignment between A & B drives spacing between successive scans on the ground
  - **Scan Rate** – matched to EFL for BBR purposes, but drives the number of scans we get in one orbit
  - **Orbital velocity** – drives the number of scans we get in one orbit
  - **System EFL** – as EFL gets longer, projection on the ground gets smaller
  - **Spacecraft Jitter** – moves the LOS randomly between scans

The ongoing effort to adjust J2 HAM alignment is expected to eliminate this issue

J2 VIIRS Performance Testing

- **J2 VIIRS Ambient phased is planned for April to September 2016**
  - **Radiometric:** *SNR, NEdT, Lmax*
  - **Spatial:** *LSF/MTF*, *BBR*, *pointing*
  - **Spectral:** *RSRs using GLAMR (NASA)* *(In progress)*
  - **Special testing:** *polarization*, *RVS*, *NFR, Stray Light*, *Xtalk.*

Tests in Green means completed

J2 Ambient Preliminary Performance is as Expected

J1 Spectral Performance

SNPP

Band	Band center	Bandpass (FWHM)	Lower 1% point	Upper 1% point	MIOOB
'M1'	pass	pass	pass	pass	FAIL
'M2'	pass	FAIL	pass	pass	pass
'M3'	pass	pass	pass	pass	FAIL
'M4'	FAIL	pass	pass	pass	FAIL
'I1'	pass	pass	pass	pass	pass
'M5'	pass	pass	pass	pass	FAIL
'M6'	pass	pass	pass	pass	FAIL
'I2'	pass	pass	pass	pass	FAIL
'M7'	pass	pass	pass	pass	pass
'M8'	pass	FAIL	pass	pass	pass
'M9'	pass	pass	pass	pass	pass
'I3'	pass	pass	pass	pass	pass
'M10'	pass	pass	pass	pass	pass
'M11'	pass	pass	pass	pass	pass
'I4'	pass	pass	pass	pass	pass
'M12'	pass	pass	pass	pass	pass
'M13'	pass	pass	pass	pass	pass
'M14'	pass	FAIL	pass	pass	FAIL*
'M15'	pass	pass	pass	pass	FAIL*
'I5'	pass	pass	pass	FAIL	FAIL*
'M16A'	FAIL	pass	pass	pass	FAIL*
'M16B'	FAIL	pass	pass	pass	FAIL*
DNBLGS	pass	pass	pass	pass	pass

J1

Band	Band center	Bandpass (FWHM)	Lower 1% point	Upper 1% point	MIOOB
'M1'	pass	FAIL	pass	pass	pass
'M2'	pass	pass	pass	pass	pass
'M3'	pass	pass	pass	pass	pass
'M4'	pass	pass	pass	pass	pass
'I1'	pass	pass	Pass	pass	pass
'M5'	pass	pass	pass	pass	pass
'M6'	pass	pass	pass	pass	pass
'I2'	pass	pass	pass	pass	pass
'M7'	pass	pass	pass	pass	pass
'M8'	pass	FAIL	pass	pass	pass
'M9'	pass	pass	pass	pass	pass
'I3'	pass	pass	pass	pass	pass
'M10'	pass	pass	pass	pass	pass
'M11'	pass	pass	pass	pass	pass
'I4'	pass	pass	pass	pass	pass
'M12'	pass	pass	pass	pass	pass
'M13'	pass	pass	pass	pass	pass
'M14'	pass	FAIL	pass	pass	pass
'M15'	pass	pass	pass	pass	pass
'I5'	pass	pass	pass	FAIL	pass
'M16A'	FAIL	pass	pass	pass	pass
'M16B'	FAIL	pass	pass	pass	pass
DNBLGS	pass	pass	pass	pass	pass

- J1 RSR showing good performance as expected. Minor non-compliances are small risk
- J1 RSR version 2 (V2) was released to the science community in February, 2016

*High noise floor in LWIR out-of-band response test

Stray Light Response (SLR) Performance

J1 SLR performance is comparable to SNPP. The right hand side shows a couple of examples (out of 336) of simulated views from detectors.

All RSB detectors meet SLR specification at Beginning of Life (BOL) (plot below).

Bands M5 and M7 are predicted to fail Spec at the End of Life (EOL), while M6 will become marginal.

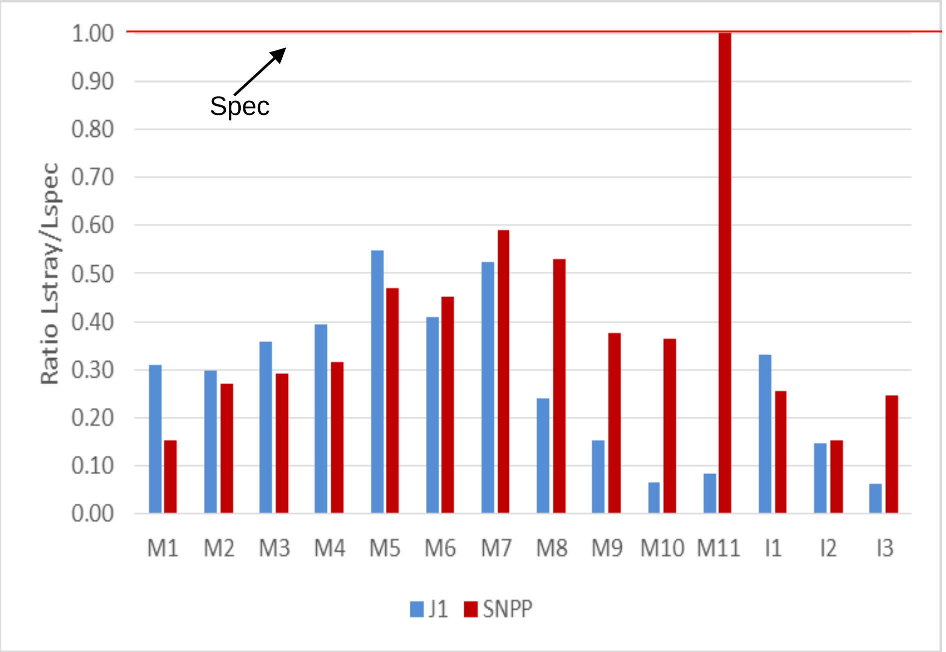

Lamp position chart

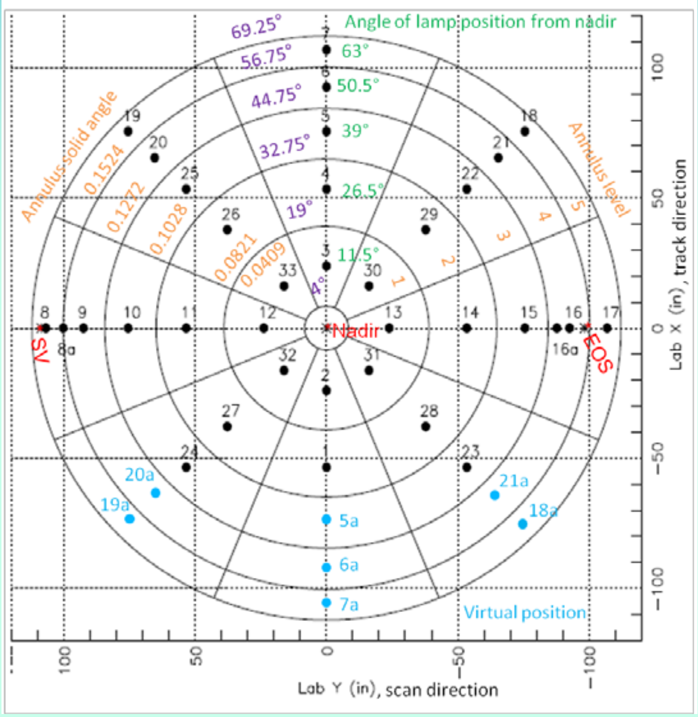

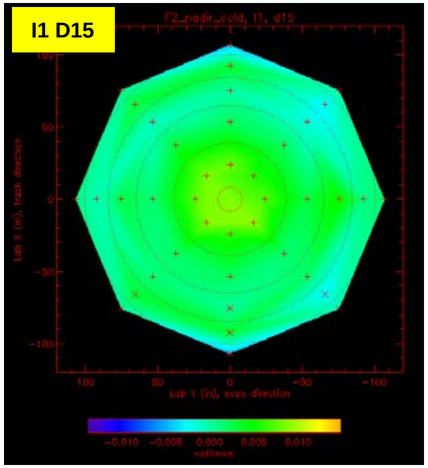

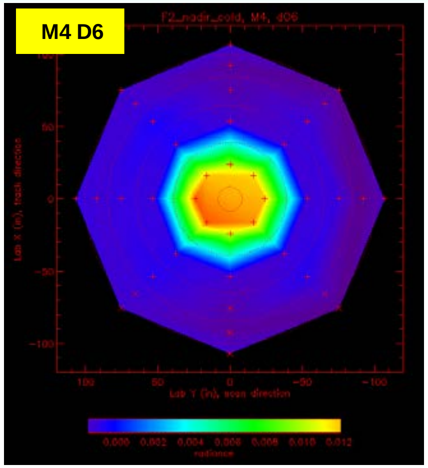

VIIRS Operation & Data Flow

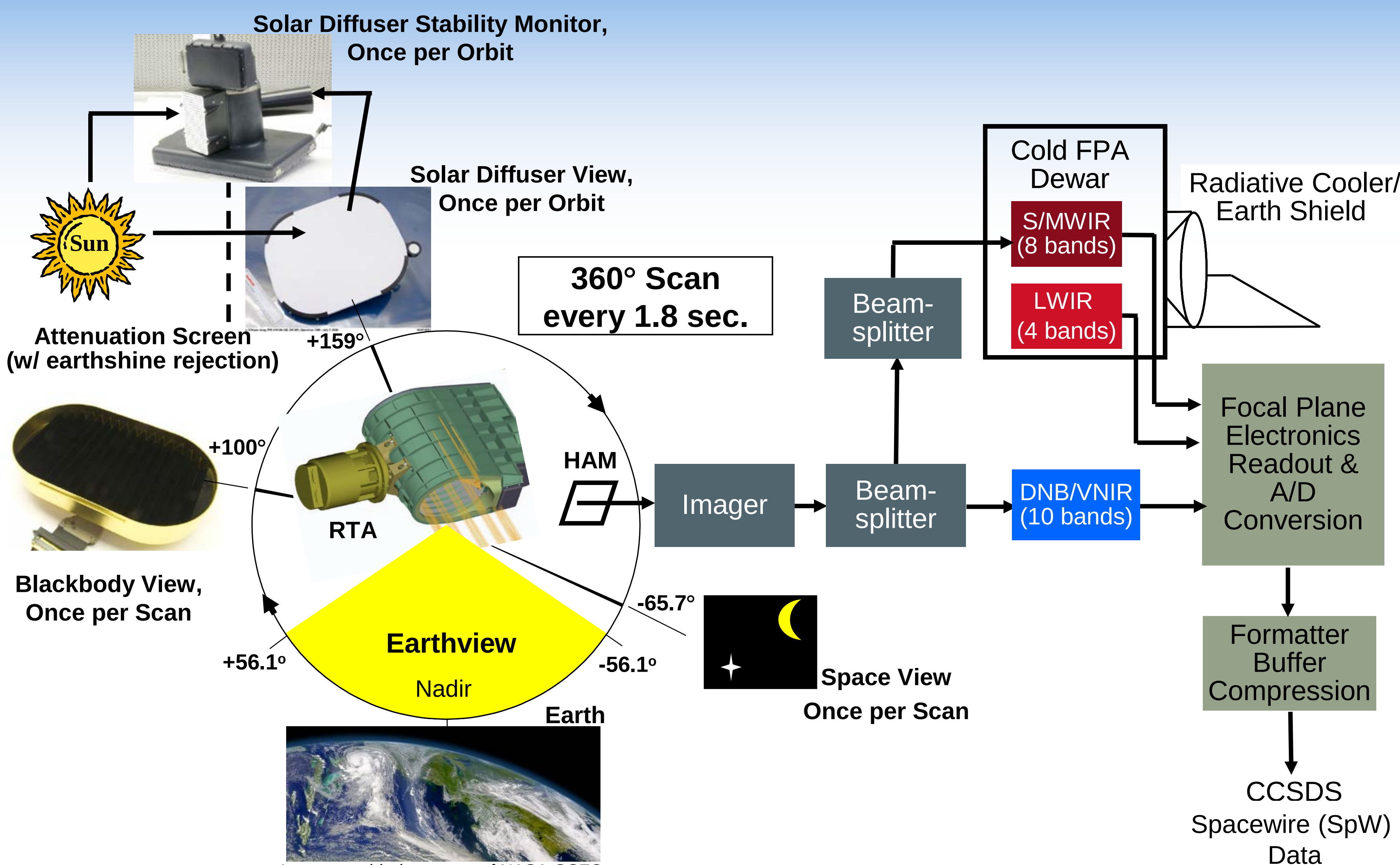

Image provided courtesy of NASA GSFC

J2 Polarization Performance

- **JPSS-1 has shown non-compliance for 4 bands, M1-M4**
  - Root cause understood, a combination of filter and Dichroic effect
- **JPSS-2 has shown non-compliance for one band: M1**
  - Filter redesigned, but improved performance for on M2-M4, not M1

JPSS-1

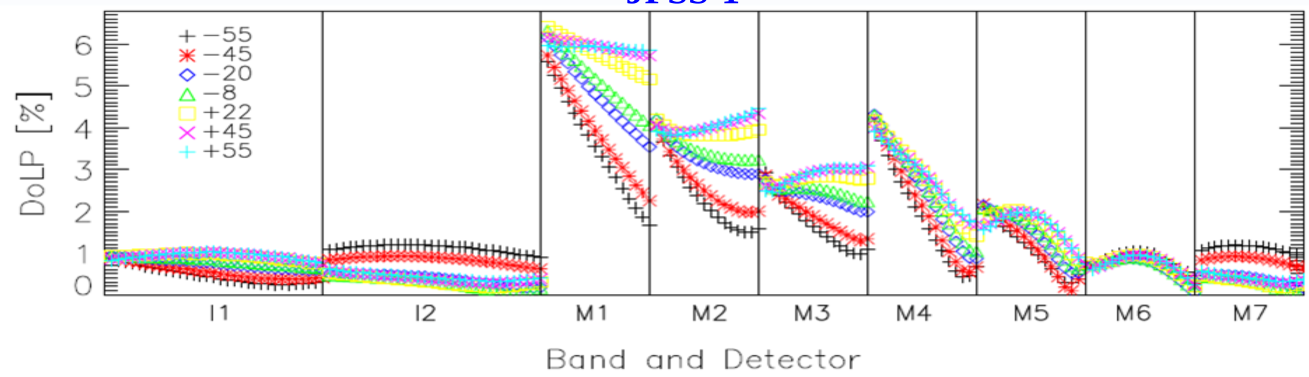

JPSS-2

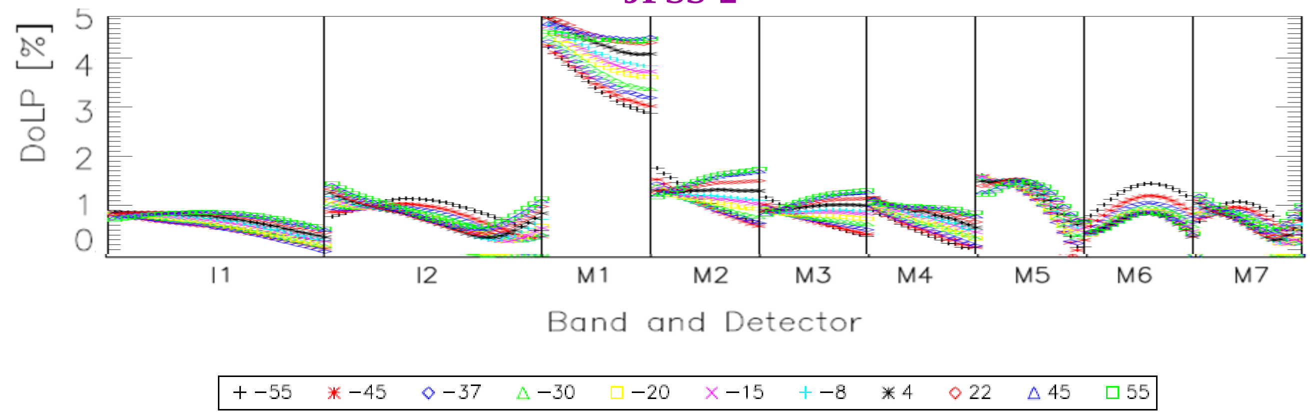

VIIRS Flight Units

- 1st Flight Unit (S-NPP) – On-Orbit
  - Integrated onto BATC Spacecraft
  - Sumoi NPP (S-NPP) Satellite Mission
  - Launched October 2011
  - Delta-2 Rocket from Vandenburg AFB
- 2nd Flight Unit (J1) – Integrated to Bus
  - JPSS-1 Satellite Mission
  - Launch Date January 2017
  - Delta-2 Rocket from Vandenburg AFB
- 3rd Flight Unit (J2) – Subassembly Integrat
  - Currently at Component/Sub-System build
  - JPSS-2 Satellite Mission
  - Spacecraft built by Orbital
  - Launch Vehicle TBD

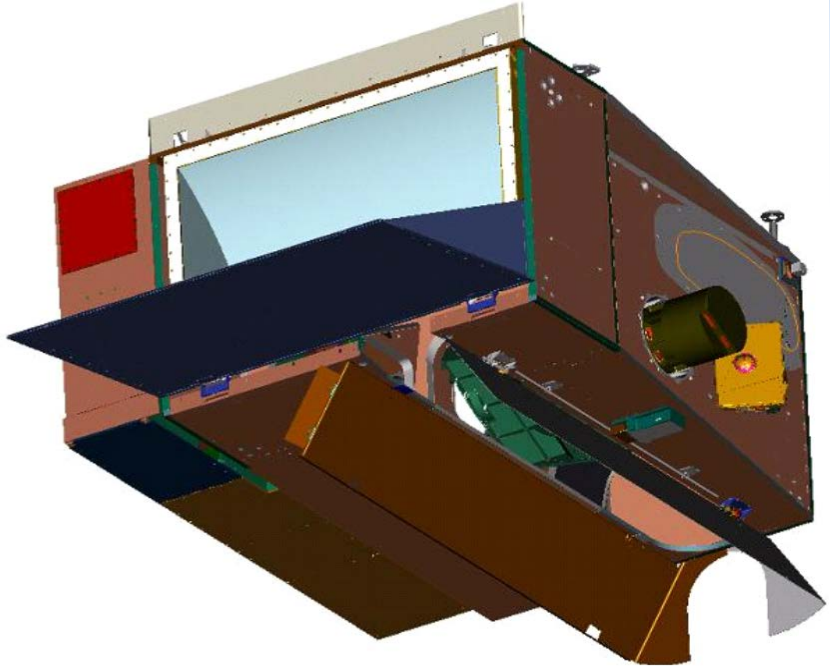

VisNIR Polarization Factor (%)

Band	Sensor	Scan Angle												
		-55	-45	-37	-30	-22	-15	-8	4	20	45	55	Max Pol.	Spec
I1	SNPP	1.5	1.24	~	~	0.93	~	0.85	~	0.7	0.64	0.62	**1.24**	2.5
	J1	0.81	0.74	0.75	0.73	0.73	0.79	0.76	0.8	0.82	0.85	0.85	**0.85**	2.5
I2	SNPP	0.29	0.27	~	~	0.34	~	0.37	~	0.47	0.51	0.51	**0.51**	3
	J1	0.73	0.62	0.54	0.47	0.36	0.37	0.37	0.43	0.5	0.61	0.66	**0.62**	3
M1	SNPP	2.99	2.63	~	~	1.95	~	1.79	~	1.42	1.21	1.4	**2.63**	3
	J1	5.13	5.26	5.35	5.52	5.54	5.56	5.65	5.7	5.66	5.51	5.37	**5.7**	3
M2	SNPP	2.11	1.97	~	~	1.63	~	1.53	~	1.28	1.17	1.29	**1.97**	2.5
	J1	3.72	3.79	3.85	3.95	3.9	3.89	3.94	3.95	3.9	3.99	4.04	**3.99**	2.5
M3	SNPP	1.2	1.14	~	~	0.9	~	0.82	~	0.61	0.7	0.8	**1.14**	2.5
	J1	2.89	2.85	2.83	2.85	2.73	2.69	2.68	2.63	2.62	2.8	2.84	**2.85**	2.5
M4	SNPP	1.05	1.1	~	~	1.19	~	1.16	~	1	0.88	0.84	**1.19**	2.5
	J1	3.61	3.9	4.08	4.16	4.17	4.22	4.18	4.18	4.04	3.89	3.8	**4.22**	2.5
M5	SNPP	1.19	1.02	~	~	0.85	~	0.84	~	0.76	0.73	0.69	**1.02**	2.5
	J1	1.9	1.86	1.9	1.86	1.82	1.85	1.79	1.83	1.81	1.8	1.8	**1.9**	2.5
M6	SNPP	0.99	0.96	~	~	0.94	~	0.94	~	0.88	0.82	0.76	**0.96**	2.5
	J1	1.62	1.32	1.13	0.99	0.86	0.85	0.79	0.75	0.73	0.75	0.76	**1.32**	2.5
M7	SNPP	0.17	0.19	~	~	0.25	~	0.28	~	0.38	0.42	0.41	**0.42**	3
	J1	0.73	0.62	0.54	0.46	0.36	0.36	0.32	0.39	0.45	0.55	0.6	**0.62**	3

- **Polarization using Broadband source was of high quality**
  - Uncertainty less than (0.4%), Repeatability within 0.13%
- **Polarization using Spectral source (T-SIRCUS): M1 and M4**
  - Agreement between Broadband and Spectral to within ~0.3 %
- **General agreement for high quality polarization testing**

VIIRS Integrate on J1 Spacecraft

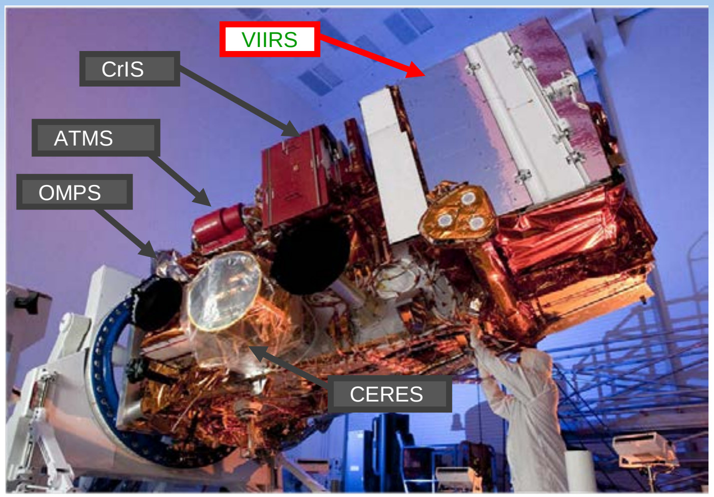

- ✓ J1 VIIRS is the follow on sensor after SNPP VIIRS
- ✓ J1 VIIRS completed successfully its sensor level testing program
- ✓ Sensor Shipped from Raytheon to Ball (spacecraft) on 2/6/15
- ✓ Sensor installed on spacecraft on 2/20/15
- ✓ J1 VIIRS completed its initial ambient testing on 03/17/2015.
- J1 VIIRS TV testing (as-you-fly), expected June 2016.
- J1 VIIRS Launch Janaury 2017

J1 VIIRS Sensor Integration to Spacecraft and Initial Performance Trending were Completed Successfully

TEB Radiometric Performance

Absolute Radiometric Uncertainty (ARD): Nominal

ARD Performance (%)								
Temp (K)	I4	I5	M12	M13	M14	M15	M16A	M16B
190	~	~	~	~	0.68	0.29	0.17	0.25
230	~	~	7.60	2.95	0.11	0.07	0.08	0.04
267	0.48	0.10	~	~	~	~	~	~
270	~	~	0.24	0.15	0.08	0.05	0.04	0.04
310	~	~	0.25	0.17	0.11	0.06	0.03	0.04
340	~	~	0.27	0.18	0.09	0.05	0.03	0.03
ARD Specification (%)								
Temp (K)	I4	I5	M12	M13	M14	M15	M16A	M16B
190	~	~	~	~	12.30	2.10	1.60	1.60
230	~	~	7.00	5.70	2.40	0.60	0.60	0.60
267	5.00	2.50	~	~	~	~	~	~
270	~	~	0.70	0.70	0.60	0.40	0.40	0.40
310	~	~	0.70	0.70	0.40	0.40	0.40	0.40
340	~	~	0.70	0.70	0.50	0.40	0.40	0.40

J1 ARD requirements met with margins

Uniformity – Det. Striping Nominal

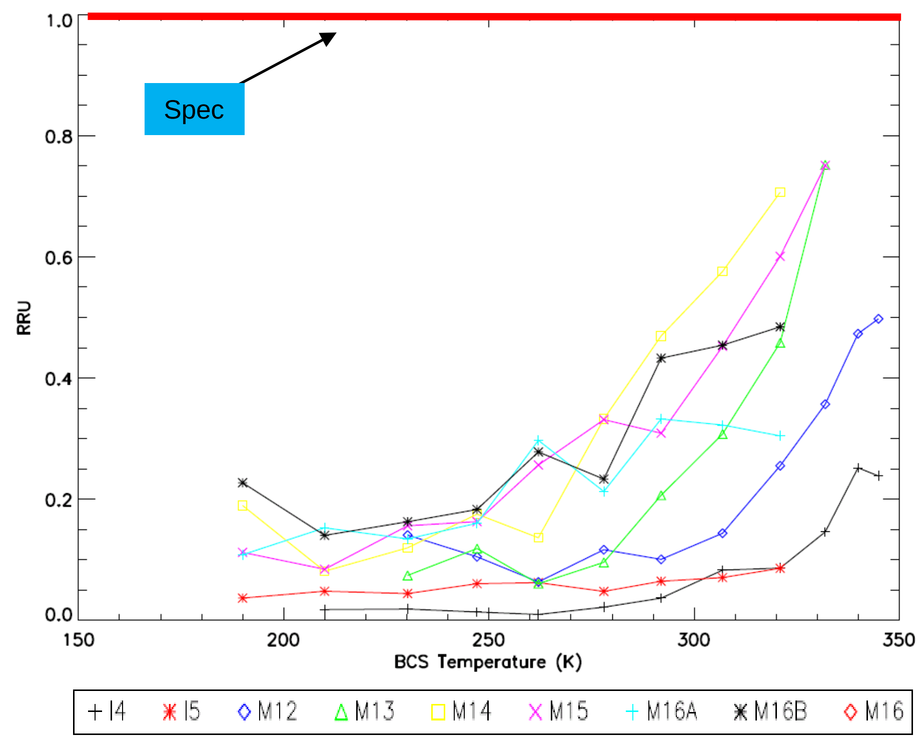

- **J1 TEB calibration shows very good performance for ARD and uniformity (striping).**
  - **ARD is below ~0.3 % except at low temperatures for the MWIR (as expected).**
  - **Detector-to-detector uniformity shows some small potential for striping at high temperatures in bands M12 – M14 (similar to SNPP).**

T-SIRCUS Polarization Measurements

T-SIRCUS polarization measurements were performed in December 2014.

Limited number of measurements made in terms of scan angle, HAM side, and wavelength.

FRED model data compared to measurement results:

1) Good agreement on general shape of wavelength dependence
2) Largest contributor to the polarization sensitivity comes from the edges of the bandpass
3) Some phase shifts in the center of M4 bandpass unexplained by model

Measurement

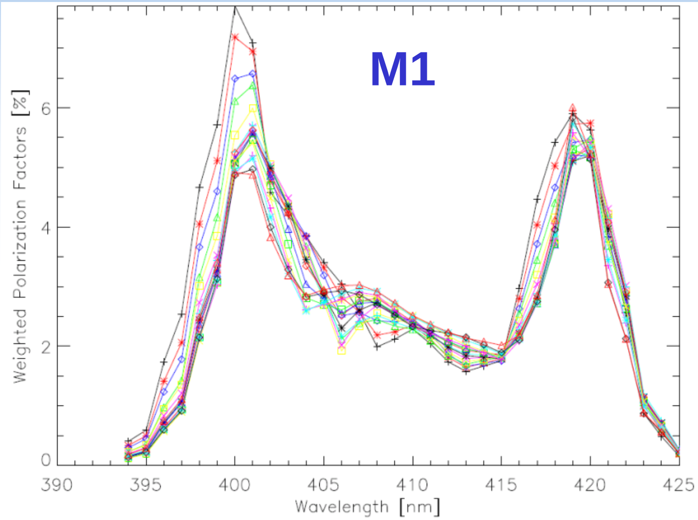

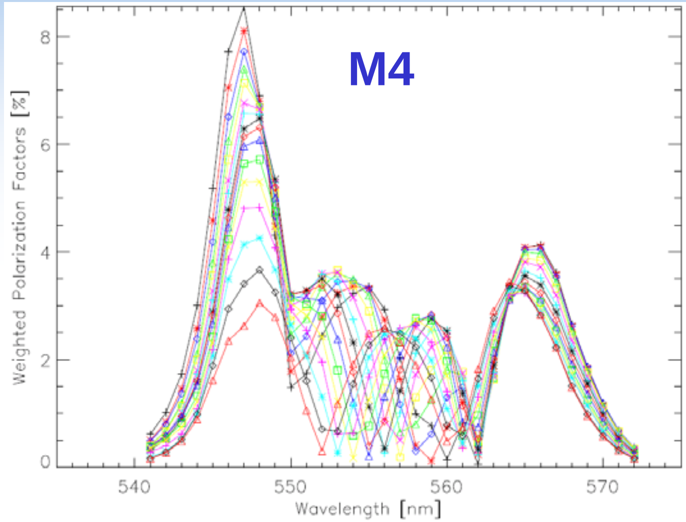

FRED model

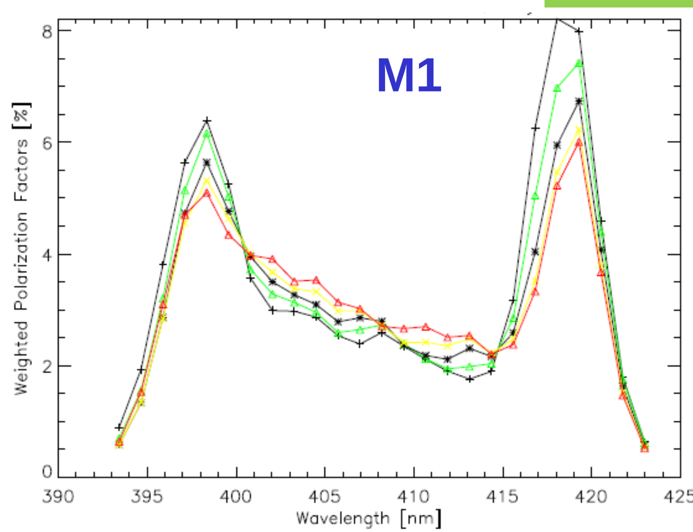

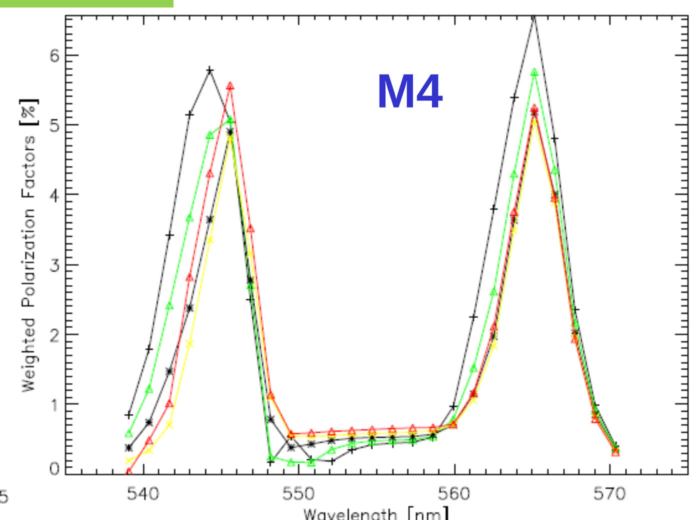

VIIRS geospatial calibration for SNPP, J1 and beyond

NASA VIIRS Characterization Support Team (VCST)
Geometric Calibration Group

Guoqing (Gary) Lin, SSAI/GSFC Code 619
Robert E. Wolfe, NASA/GSFC Code 619
John Dellomo, GST/GSFC Code 619
Zhangshi Yin, Bin Tan, Ping Zhang, SSAI/GSFC Code 619
James C. Tilton, NASA/GSFC Code 606

NASA Ocean Biology Processing Group (OBPG)

Fred Patt, SAIC/GSFC Code 616

NOAA STAR JPSS STM
College Park, Maryland
Tuesday, 9 August 2016

Acknowledgements

- Thanks the Raytheon VIIRS instrument test team for the efforts in addressing many concerns, including HW rework ones.
- Thanks the NOAA STAR team, NASA JPSS Project Science Office, NASA VCST Radiometric Calibration Team, UW spectral calibration team, Aerospace team, instrument on-site team & SC I&T on-site team for cooperation and assistance.
- Thanks NASA VIIRS Land SIPS Team for processing control point residuals from both IDPS and LSIPS forward-&re-processed VIIRS geolocation products, and testing Geo LUTs updates.
- Thanks past and current Geo JAMs – Alice Isaacman, Robert Williamson and Rosalie Marley (Rad+Geo now) -- for helping us resolving DRs in the DPE/DPA/AMP at the GRAVITE
- Thanks NOAA JPSS MOT, NASA FDF, BATC for assistance in understanding the SNPP altitude, ground speed and attitude issues.

Outline

- Optical calibration -- LSF, DFOV, MTF
- BBR calibration
- Geolocation calibration
- Challenges, concerns, Issues
  - Improvements are in the making
- Concluding Remarks

Optical calibration

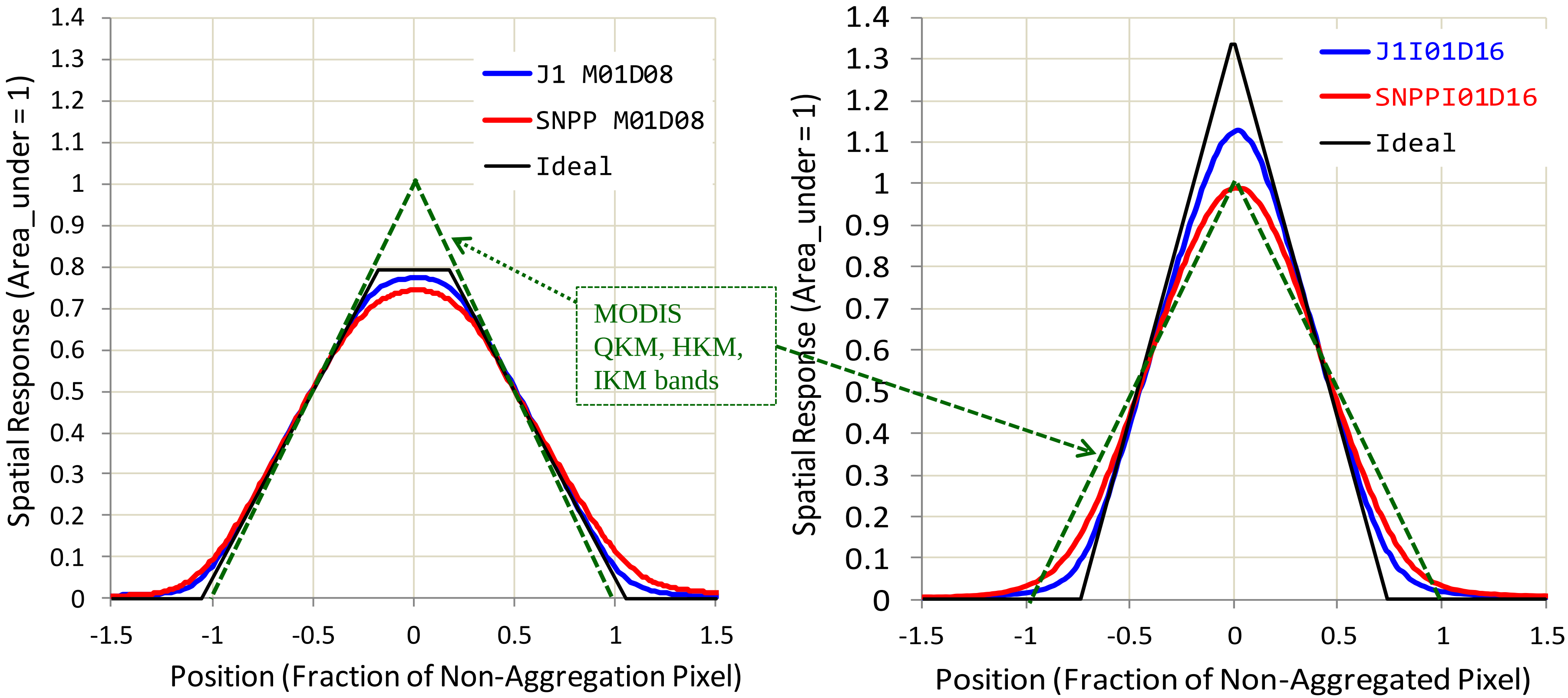

- J1 VIIRS has improved optical system over SNPP
- J2 ~= J1

Scan LSF → DFOV

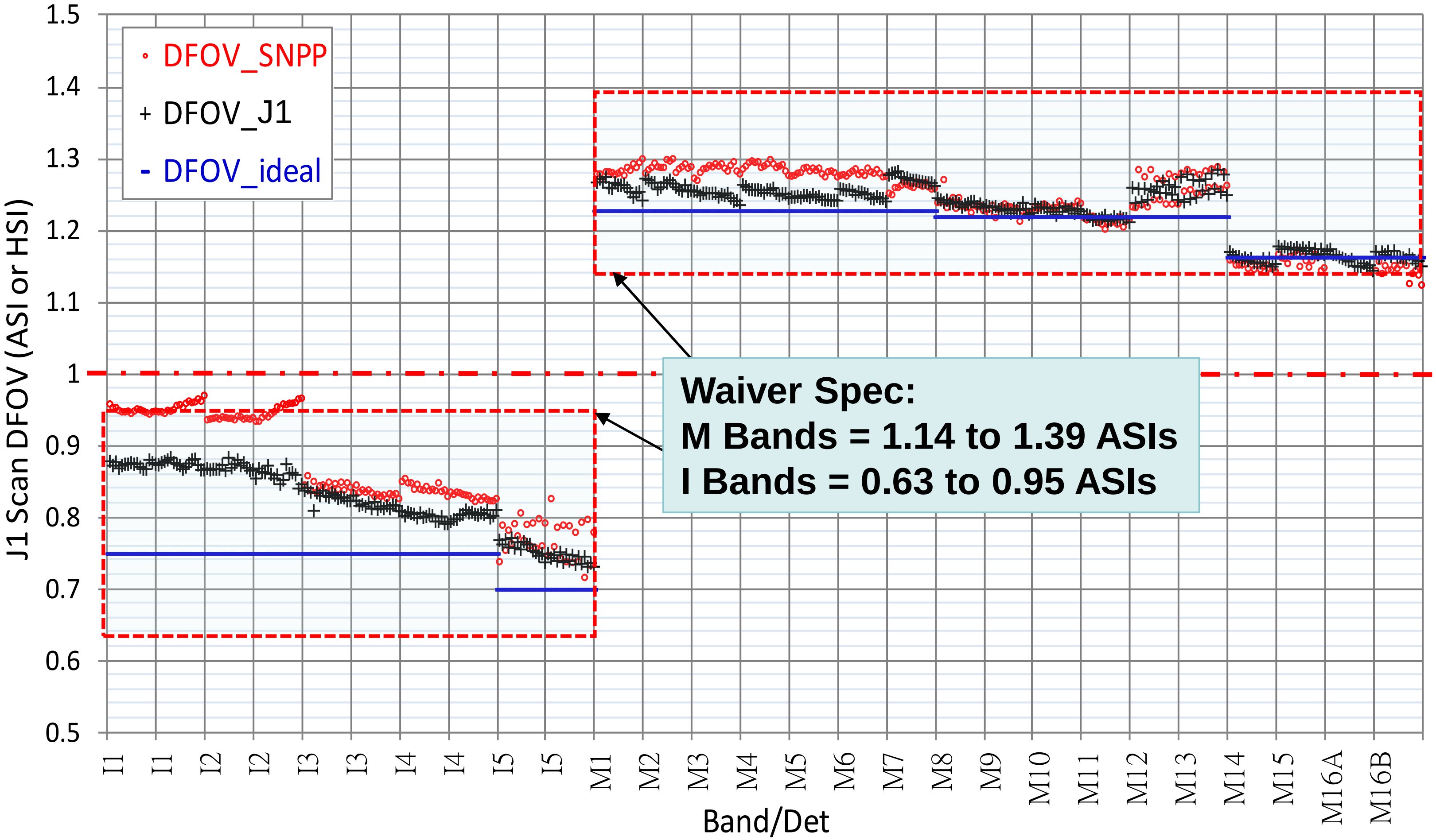

- SNPP VIIRS has de-focus in VisNIR bands
- J1 VIIRS has the right focus
- I-bands under-sample the earth at TOA in un-agg zones

Scan LSF → MTF

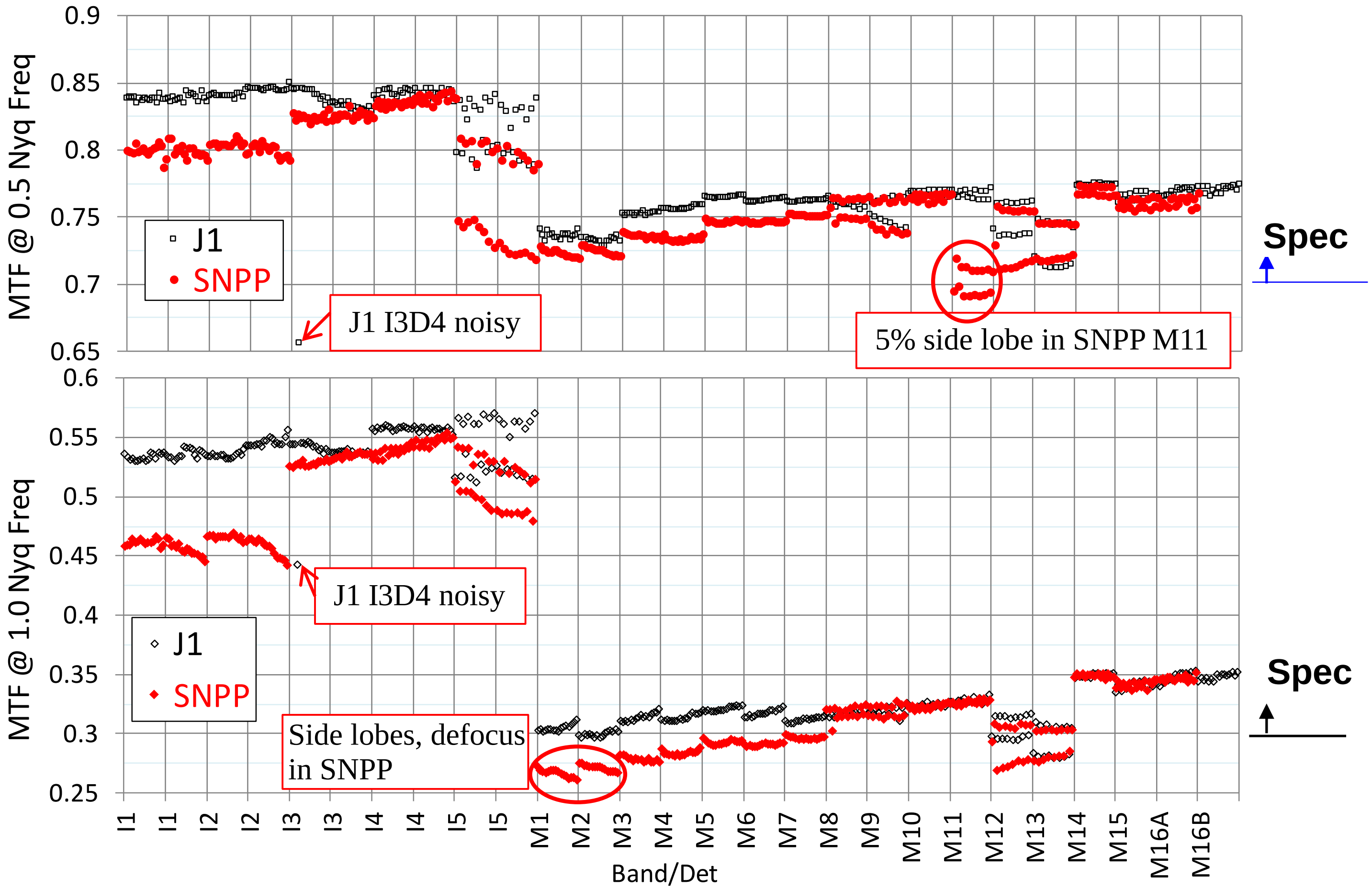

- J1 MTF performs better than SNPP
- I-bands images are sharp, at least at TOA (J1 I3D4 under-performs)
- Track direction LSFs are nearly square, MTF ~= 0.63 at 1.00NF (Nyquist Frequency)

BBR: M/I band offsets wrt I1

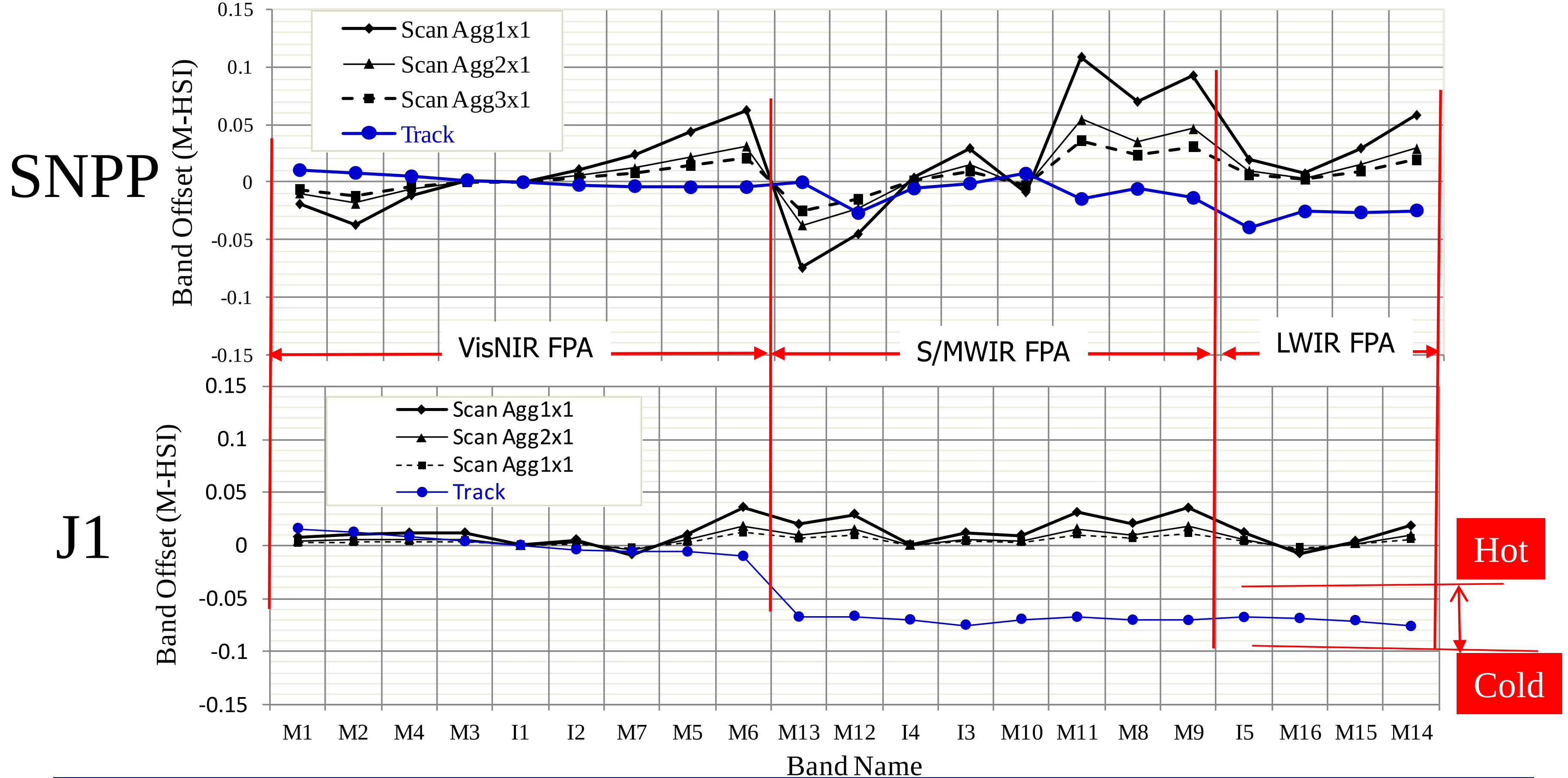

- J1 and SNPP are similar in the overall BBR band pair performances
- J1 BBR performs better than SNPP in the scan direction
- In the track direction, J1 Bands on cold FPAs shifted ~ 50 m from bands on VisNIR FPA

SNPP on-orbit geolocation calibration

w/ LUTs Updates

Update	Date	Description	Comments
a	*1/19/2012*	*Cryo-radiator door open*	*All VIIRS band available, LPEATE re-process start date*
1	2/23/2012	Initial mounting coef. update	Removed bias ~ 1.3 km
2	3/30/2012	Initial DNB FPA center update	Removed bias ~ 1 km
b	*11/22/2012*	*Scan control electronics (SCE) was switched from B-side to A-Side*	*Caused bias ~ 300 m for 19 days*
3	12/11/2012	Correction after SCE was switched from B-Side to A-side	Removed bias ~ 300 m
4	2/15/2013	Second, fine DNB FPA center update	Removed DNB bias ~ 300 m
5	4/18/2013	Second, scan angle dependent, fine Geo LUT update	Fine tuned and removed scan dependent biases
c	*4/25/2013*	*Star tracker maintenance/re-alignment*	*Caused bias ~ 25 m*
6	8/22/2013	Correction to the star tracker re-alignment	Removed bias ~ 25 m

Key: All bands impacted DNB only *External event*

➢ SNPP VIIRS on-orbit geolocation calibration went well

SNPP VIIRS track residual trends

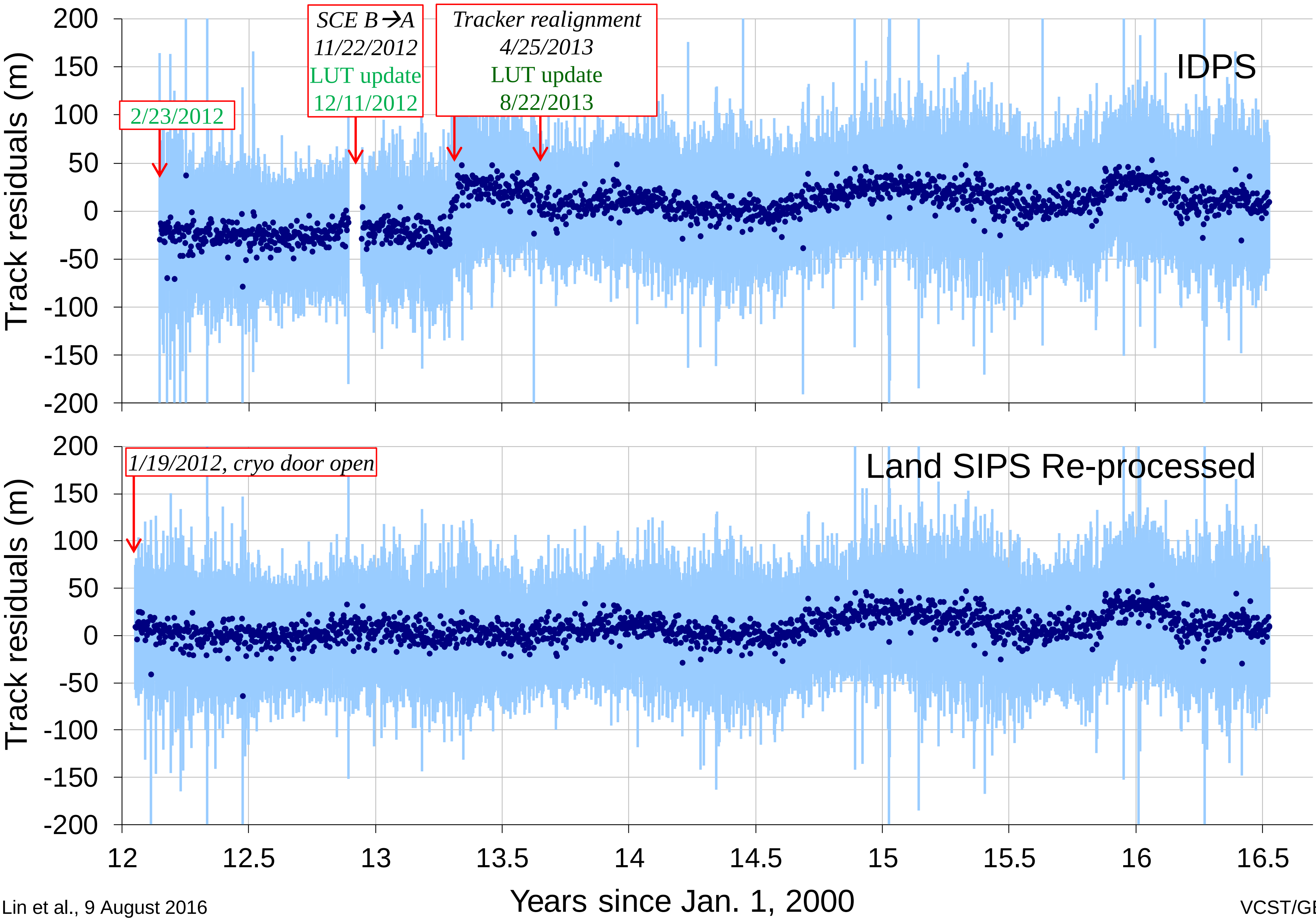

SNPP VIIRS scan residual trends

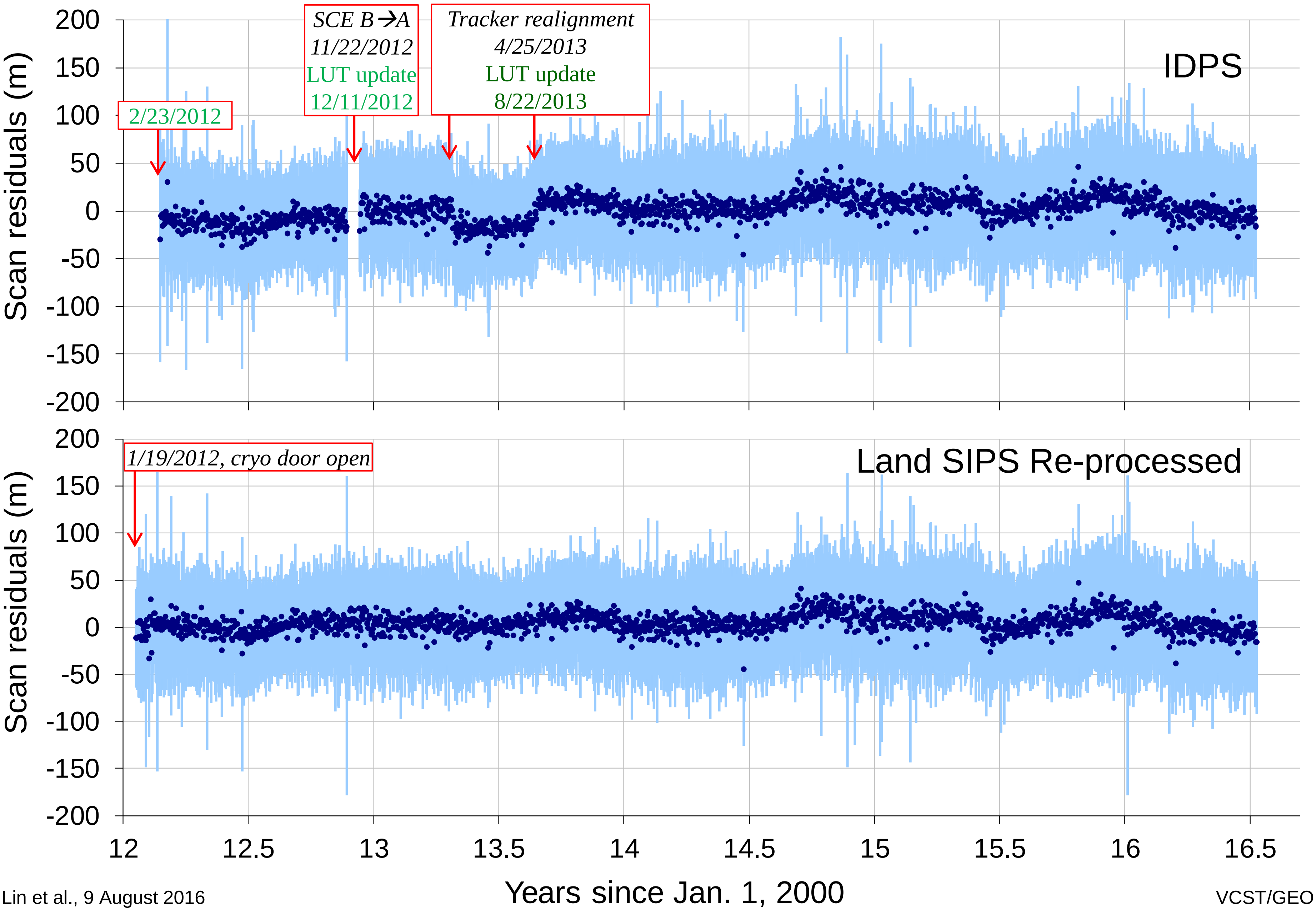

SNPP geo long-term trending

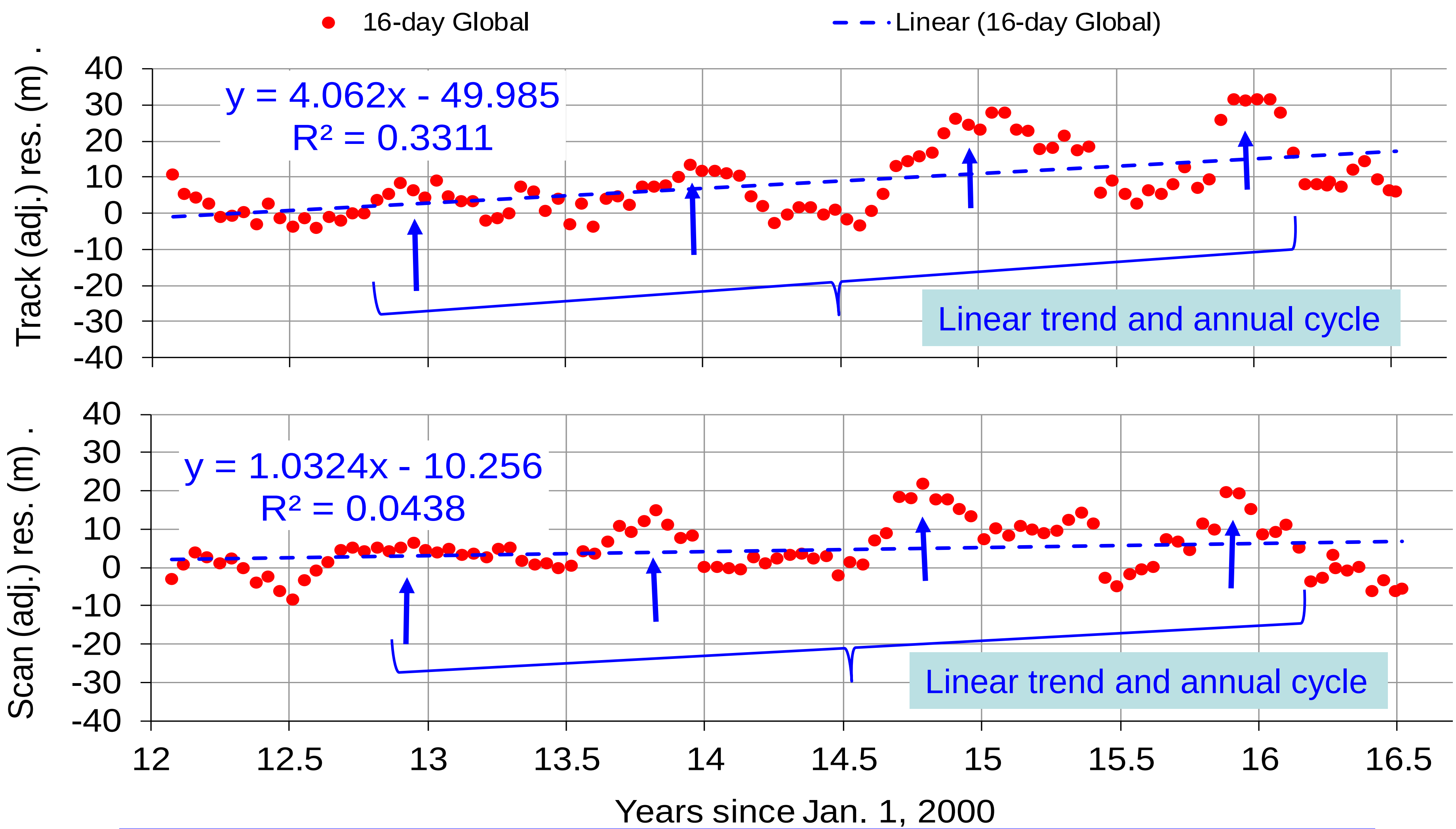

- Small trends and seasonal variations in VIIRS geolocation are correctible

Land SIPS Re-processed, can be corrected

SNPP DNB geolocation error trending
based on coastal area GCP matching

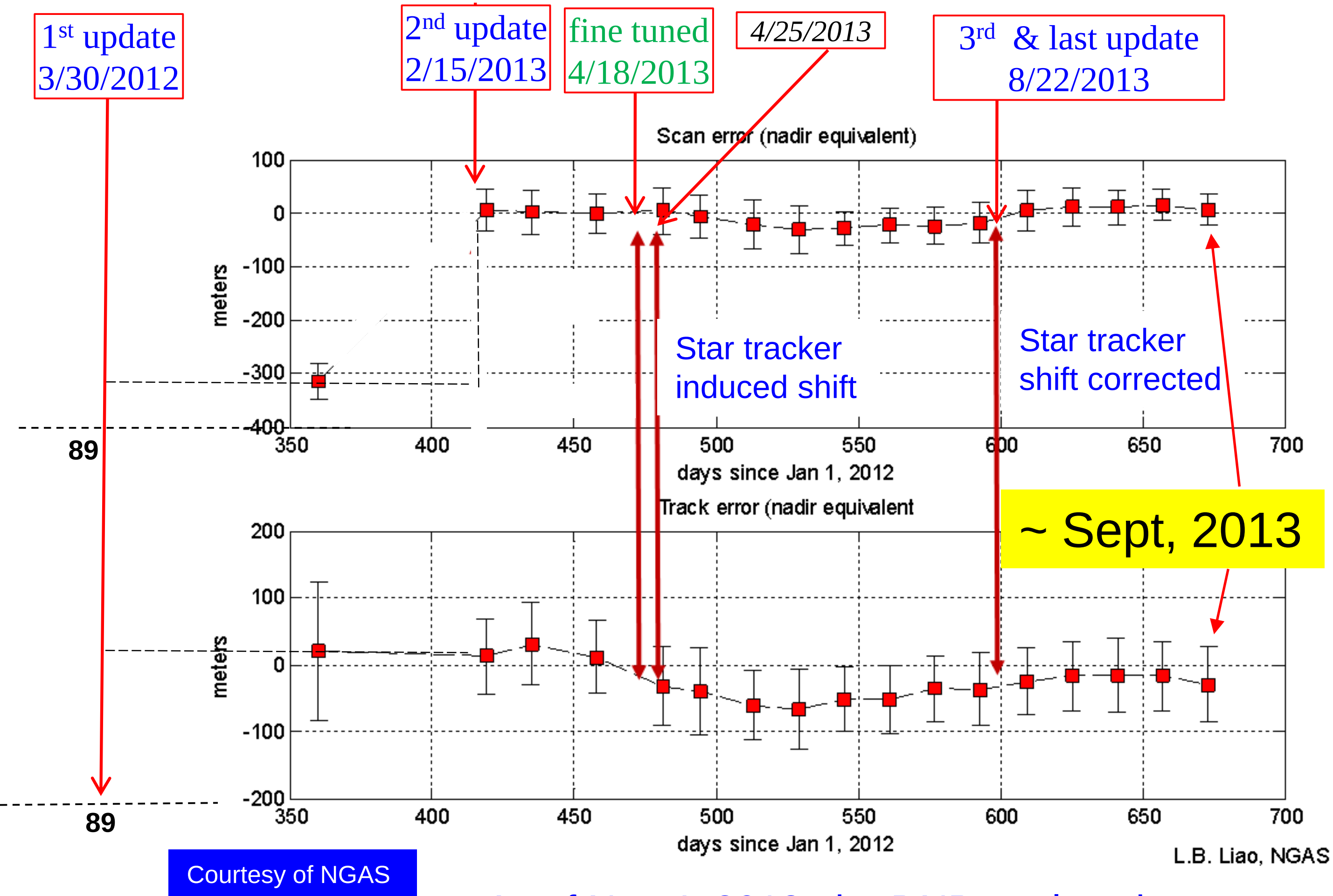

- DNB TC geolocation (appending fields (lat, lon, height, QF)_TC to the ellipsoid DNB geolocation product) was TTOed on **5/22/2014**, 14:30 GMT (data observation time) in IDPS.
- DNB errors track with I1 band errors

As of Nov 4, 2013, the DNB geolocation accuracy is
Scan: 8 ± 33 μrad   Track: -35 ± 68 μrad
Scan: 7 ± 28 m Track: -29 ± 57 m over coastal areas
(nadir equivalent with mean altitude of 838.8 km)

Overall SNPP geolocation performance

Residuals	**IDPS VIIRS**	**Land SIPS VIIRS**	Aqua MODIS C6	Terra MODIS C6
Track mean	**4 m**	**8 m**	2 m	2 m
Scan mean	**1 m**	**4 m**	0 m	-1 m
Track RMSE	**77 m**	**72 m**	46 m	43 m
Scan RMSE	**62 m**	**61 m**	53 m	44 m
Data-days	**1580 (4.3 yrs)**	**1635 (4.5 yrs)**	5040 (13.8 yrs)	5849 (16.0 yrs)
Missing days	**21**	**1**	10	62
Daily matched GCPs w/ I1/B1	**131**	**131**	189	218

- **Nadir equivalent** accuracy (RMSE – Root Mean Square Error) . (MODIS for reference)
  - Meet Spec: 133 m (1σ); **within 20% I1 HSI (375 m) = 75 m @ nadir for VIIRS**
  - Band-to-band mis-registration adds bias to RMSE to other bands**:** $RMSE = \sqrt{\sigma^2 + \mu^2}$
  - Periods: IDPS 2/23/2012 - - 7/11/2016 except 11/22/2012 – 12/11/2012;
    LandSIPS 1/19/2012 – 7/11/2016
- MODIS – VIIRS differences

  ➢ SNPP VIIRS geolocation uncertainty ~ 70 m (1σ)

  Aqua use definitive ephemeris data → 27 hour latency

  SNPP attitude data is not as good, see Slides18 & 28

  DEM resolutions: older 1 km for VIIRS vs newer 0.5 km for MODIS C6

SNPP & J1 DNB cell sizes in scan direction

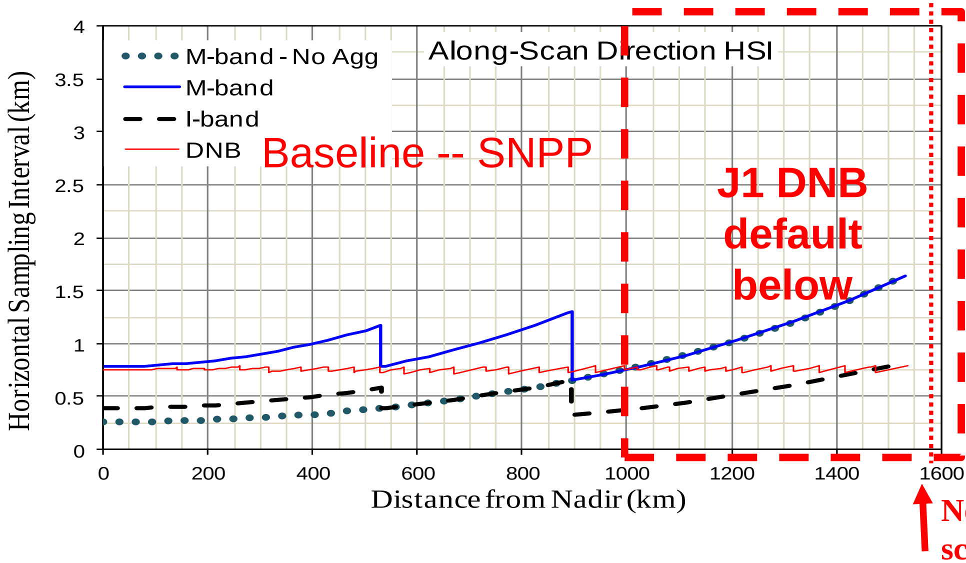

- DNB LSFs are mostly square
- Baselined pixel size is ~ 750 m
- "Option21" has pixel size up to 1.6 km within 56.5°
- Geolocation is extrapolated post-nadir for scan angle > ~56.5° (pixel size up to 3.9 km @60.5°)

J1 DNB cell sizes are not constant as SNPP VIIRS are

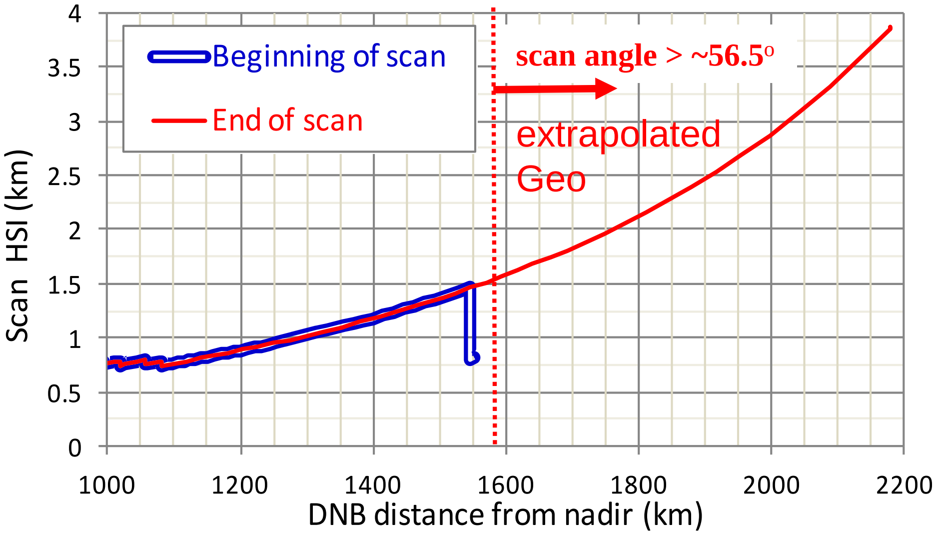

"Option21" – default, in km

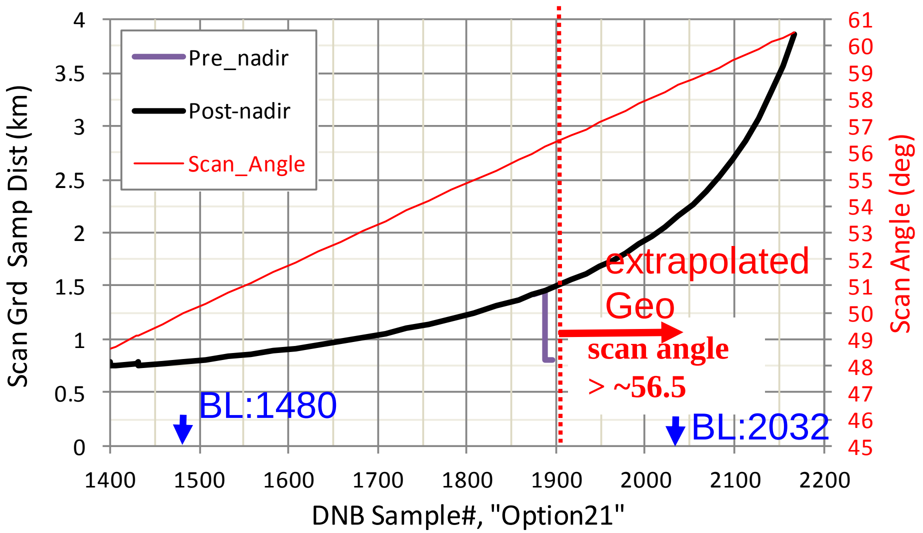

"Option21" – default, in Samp#

Issues, concerns, challenges

- J1, J2 scan-to-scan underlap

VIIRS ground track speed carried by SNPP

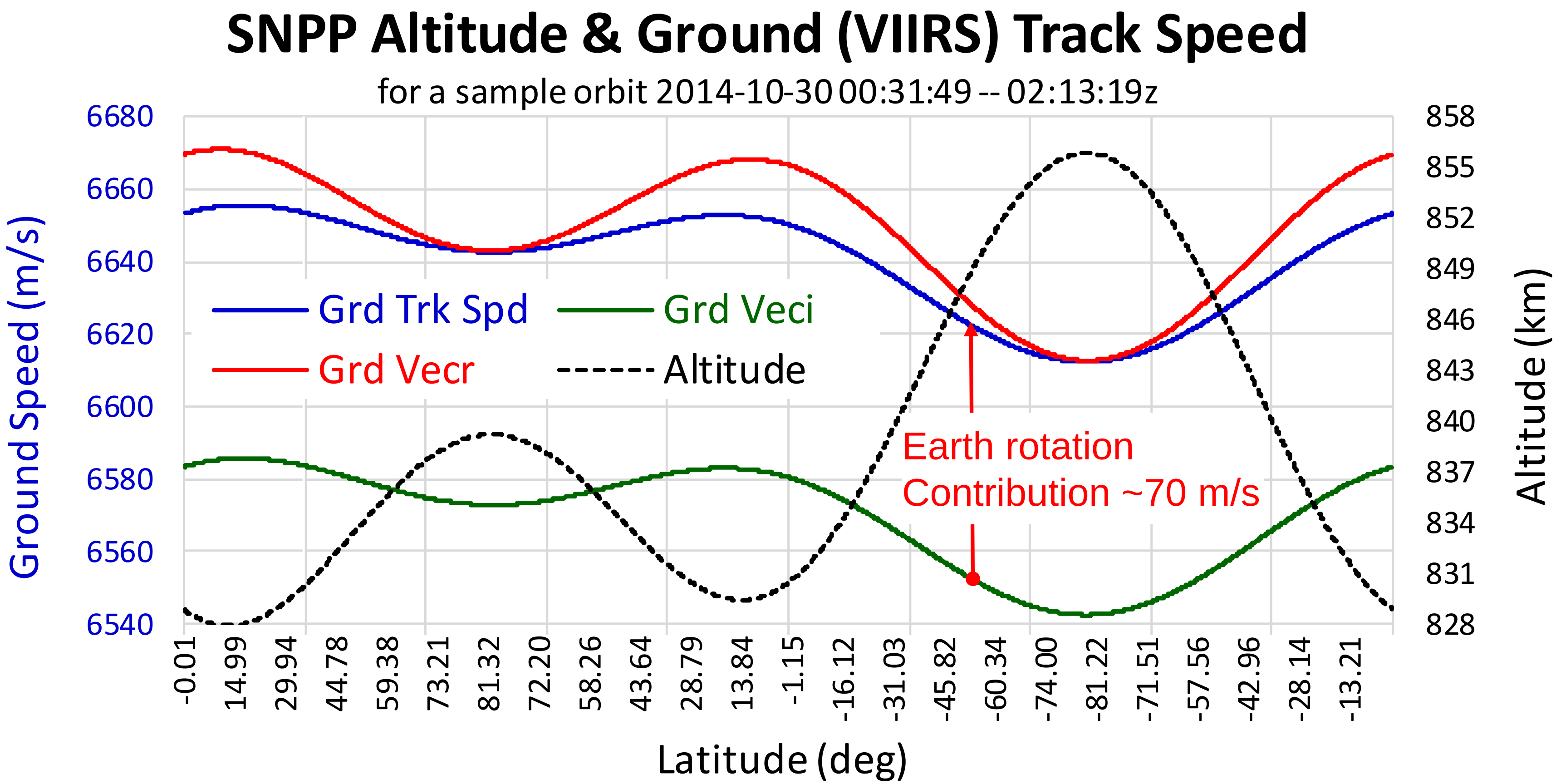

- Earth rotation contributes to speed in VIIRS track direction due to SNPP inclination angle
- Speed at sub-satellite point (SSP = Vg_ECR) should be a better parameter for future design of VIIRS FPA dimension in the track direction
- Variations in altitude (3.4%) and speed (0.6%) matter - - a 1% change induces ~1/3 I-pixel more/less overlap in the track Field of Regard (FOR) formed by 32 I-detectors

VIIRS nadir overlap/underlap

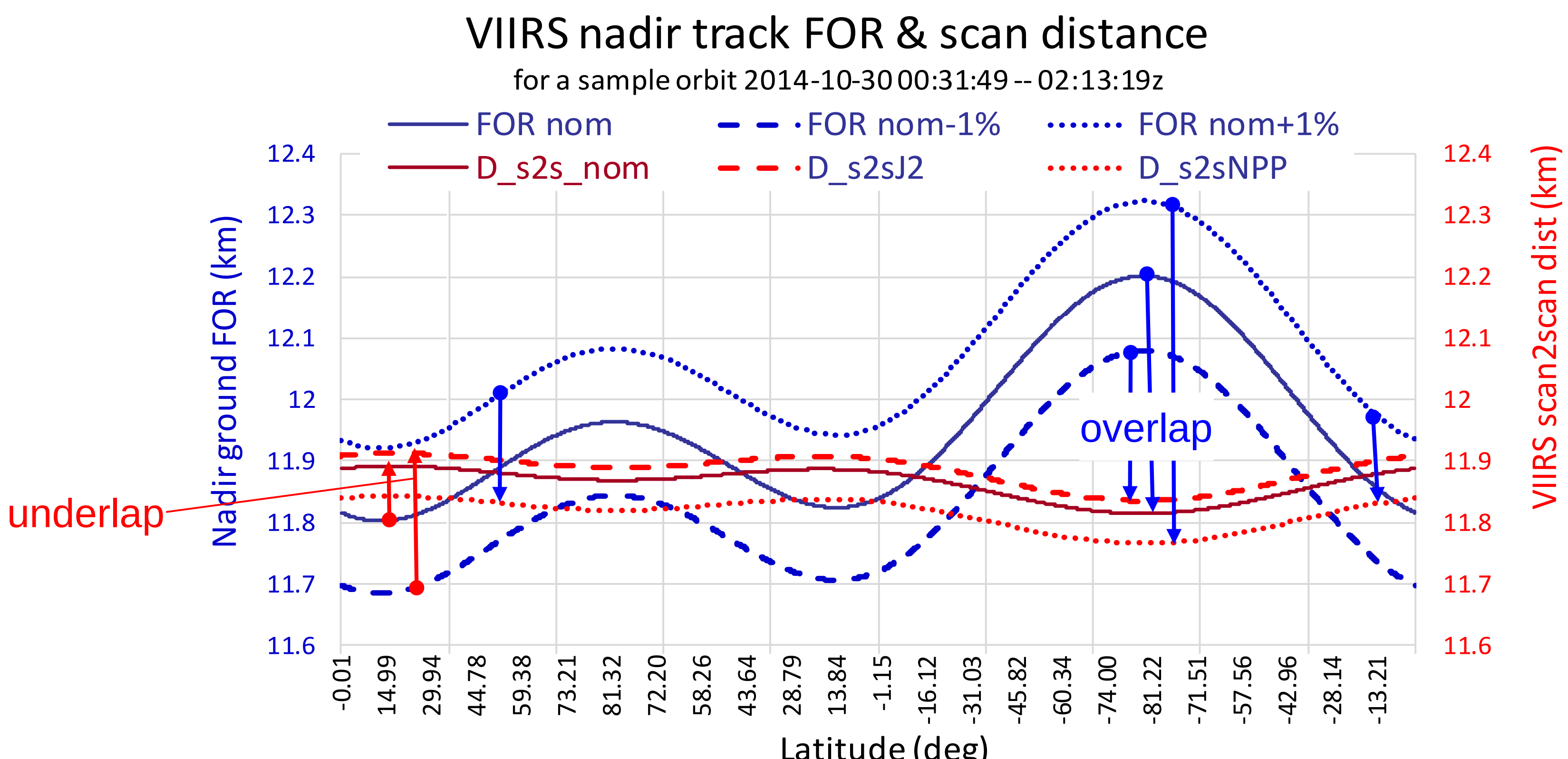

- Scan2scan distances are calculated using scan rate of 3.53107 rad/s for SNPP, nominal 3.51657 for J1, and proposed 3.5104 for J2.
- J1 & J2 VIIRS are expected to have underlap over the equator region
- J3+ should have fixed the problem probably by using SNPP shorter focal length and faster scan rate
- Contribution of earth rotation to the ground speed in the track direction might have been forgotten in the original “system” design

Issues, concerns, challenges

- SNPP attitude system degradation, that affects VIIRS geolocation accuracy

Attitude control & knowledge errors

2016-05-02 06:48:50 – 06:50:40z

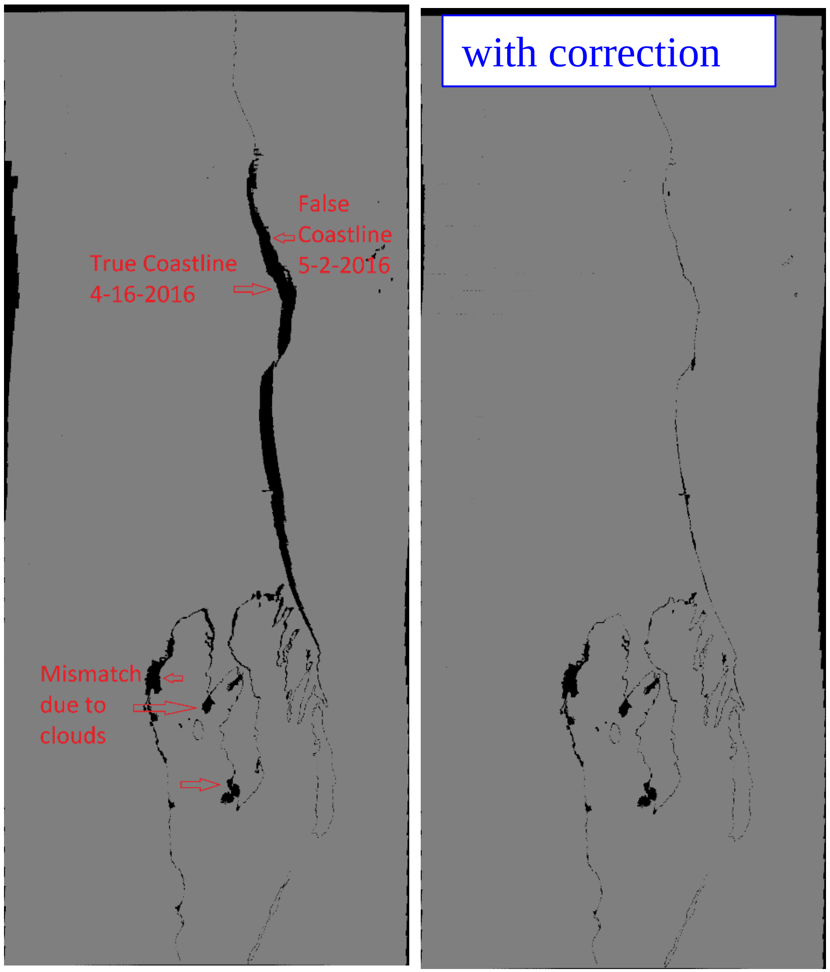

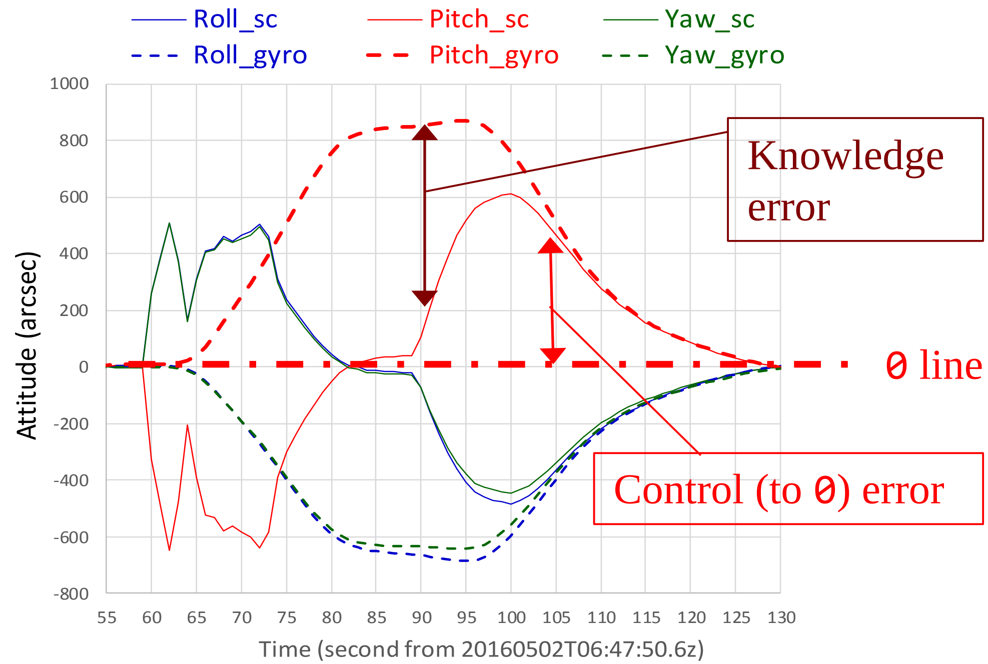

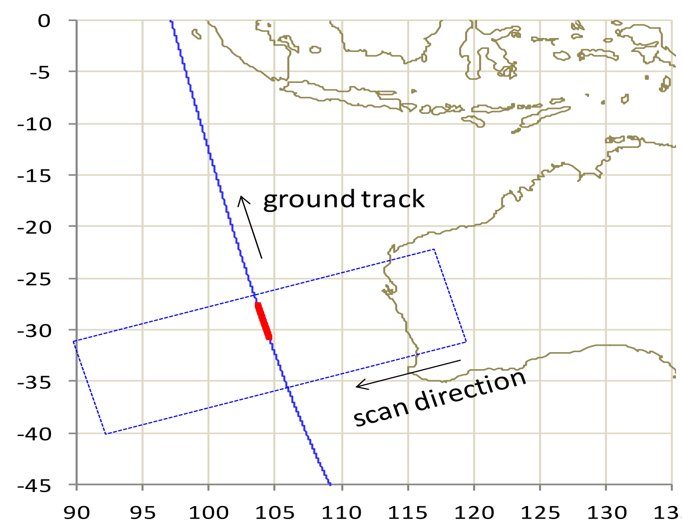

- Western Australian coast (south up)
- Difference in "land"/"Water" masks from data 16 days earlier

Requirements (NGIID, RevD, 2008-01-07)

Knowledge error: from truth orientation

IF230780 The spacecraft-supplied estimate of the inertial attitude of the Spacecraft Attitude Determination Frame shall be in the J2000.0 frame, be time-tagged and have an error during ***any orbit*** *of less than* ***30 arcsec*** *(3 sigma) per axis.*

Control error: from desired (0) orientation

IF230796 For NPP, the Spacecraft Attitude Control Error during ***any orbit****, excluding the effects due to jitter, shall be less than* ***108 arcsec*** *(3 sigma) per axis during all mission data collection periods.*

The "3 sigma" is interpreted as 99.73% confidence level, i.e., <= 16 second-points out of 6090 second-points per orbit when the error is outside the spec'd value.

Spec outage and trend

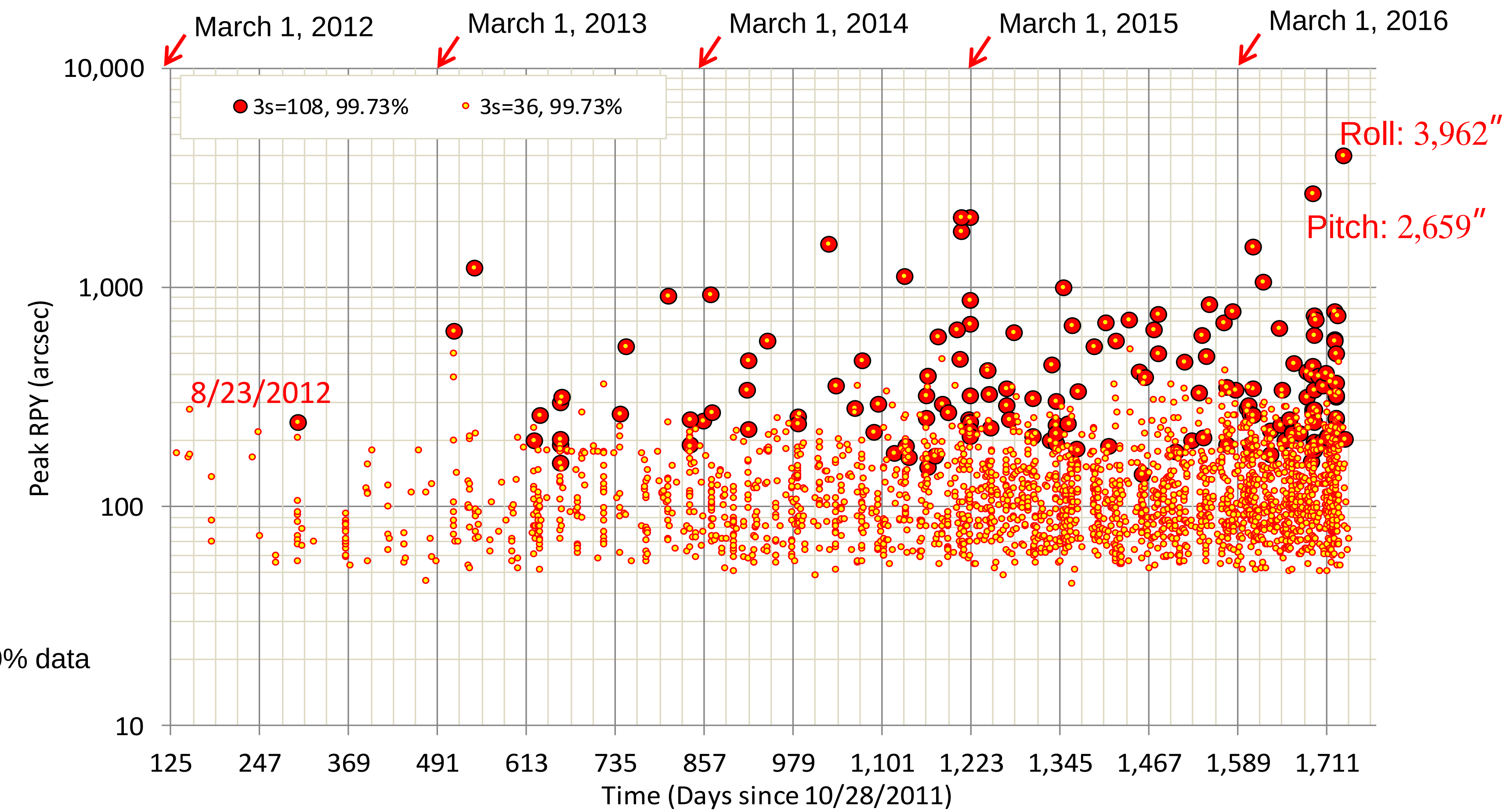

using ~90% data

- Large circles for control spec outage
- Small dots hint knowledge spec outage

Global distribution

1/1/2016 – 6/19/2016

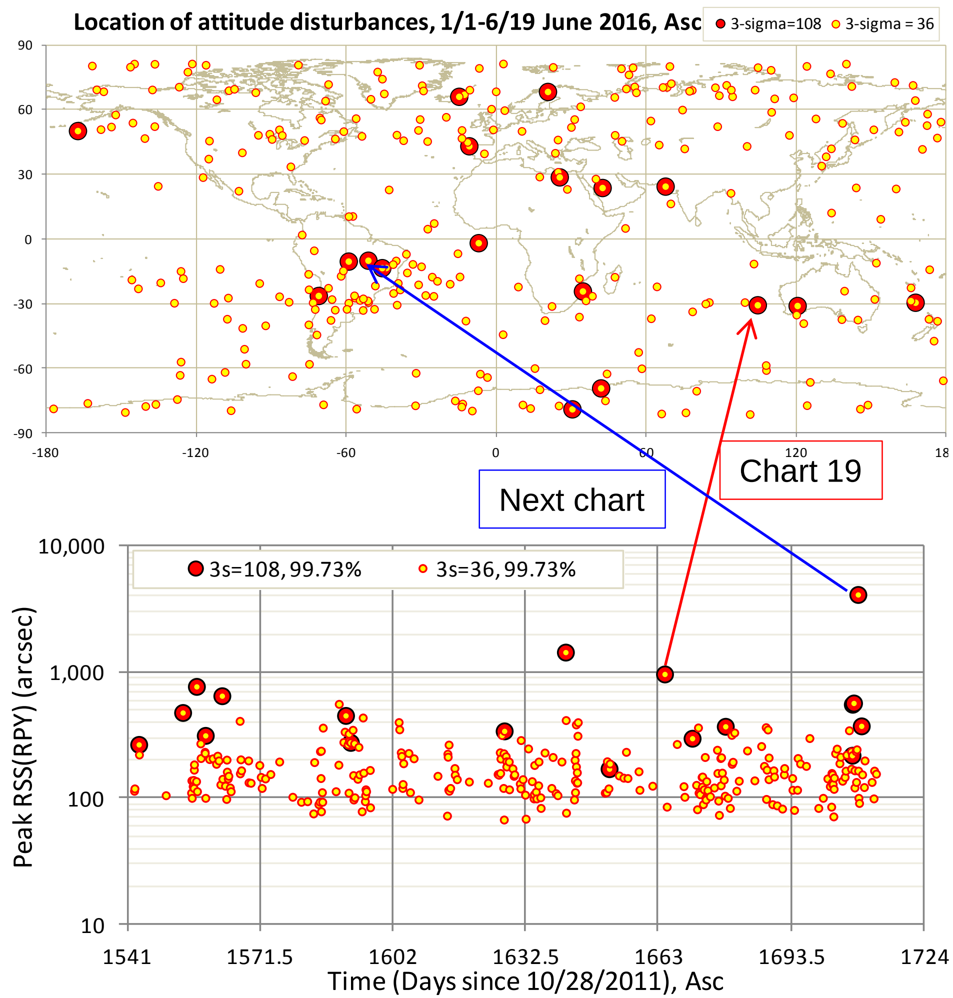

Ascending orbits

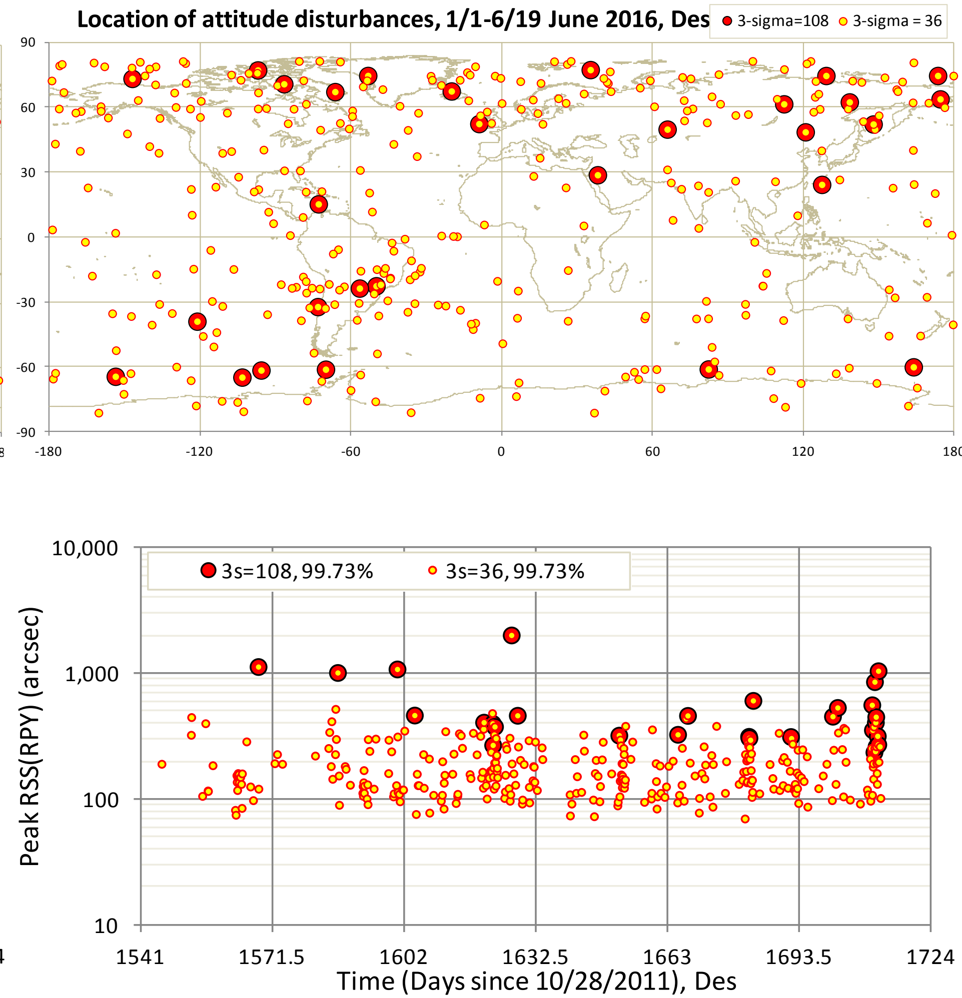

Descending orbits

➢ All over the places, day and night

Attitude errors over 0.7 deg!

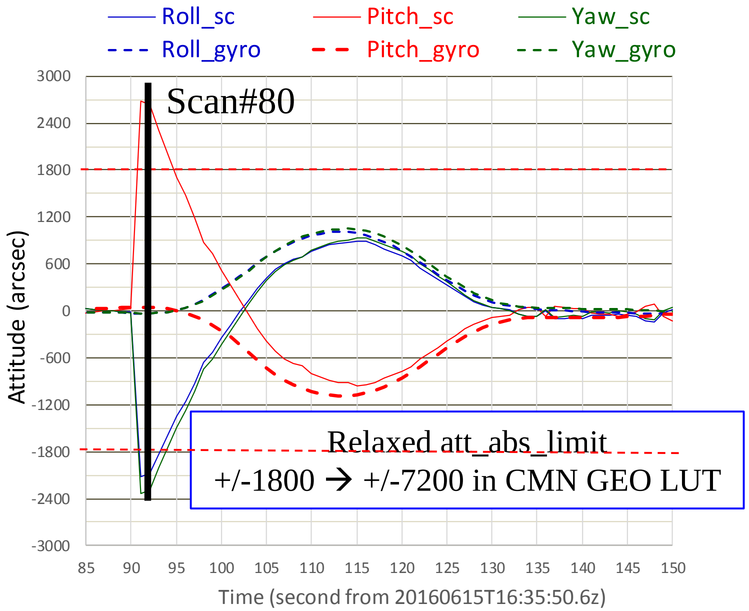

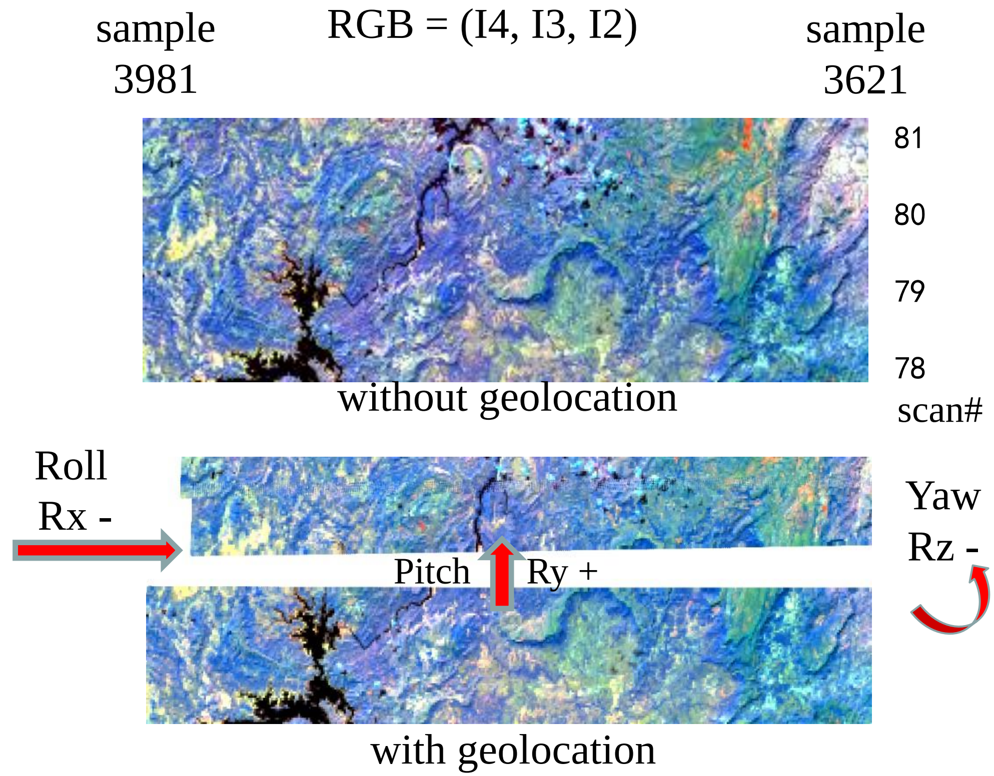

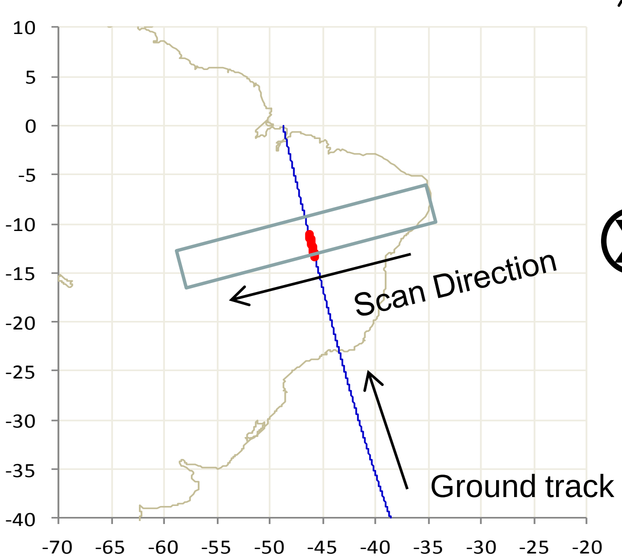

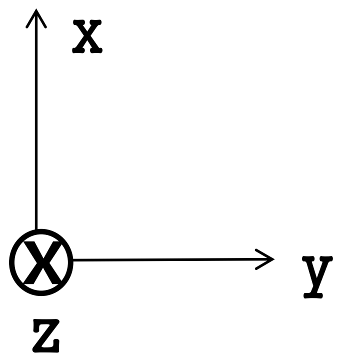

- 5 min granule from 16:35z

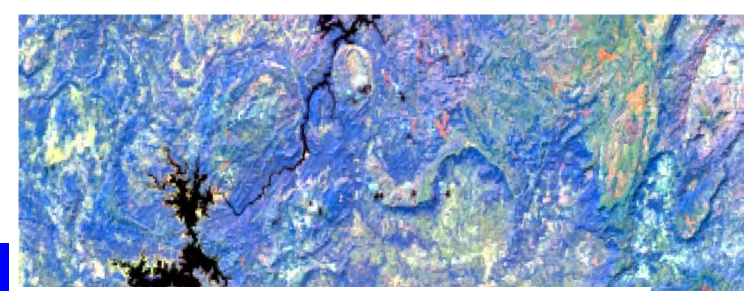

with geolocation, 16 days earlier

- ➢ VIIRS images “see” the attitude errors

Fewer and fewer stars are being tracked

Star counts in 2-hour windows

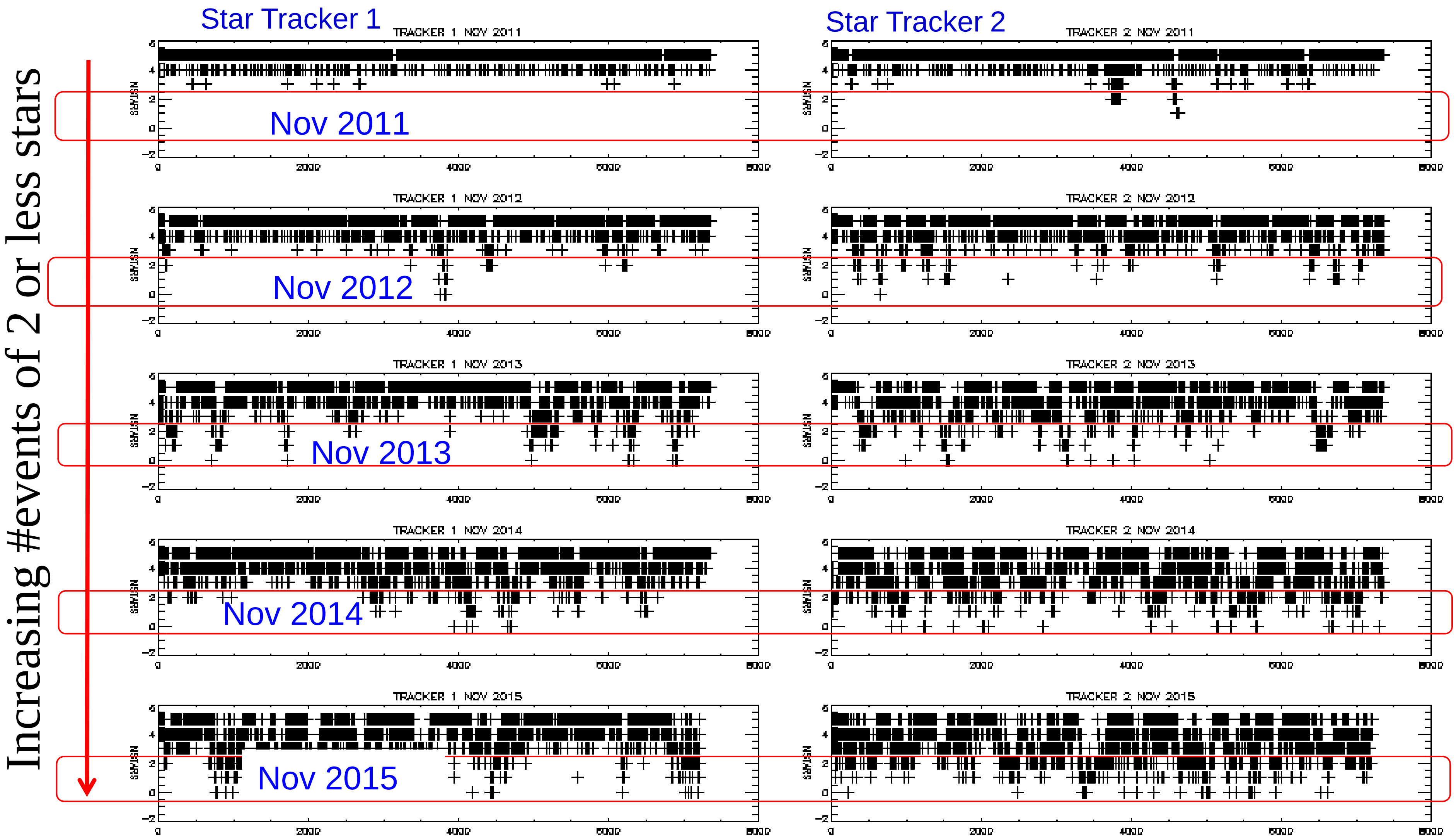

a minimum of 2 stars in both trackers are combined to do attitude determination

- **The attitude solution relies on one tracker more often**

Star trackers are getting noisier

max residuals in 2-hour windows

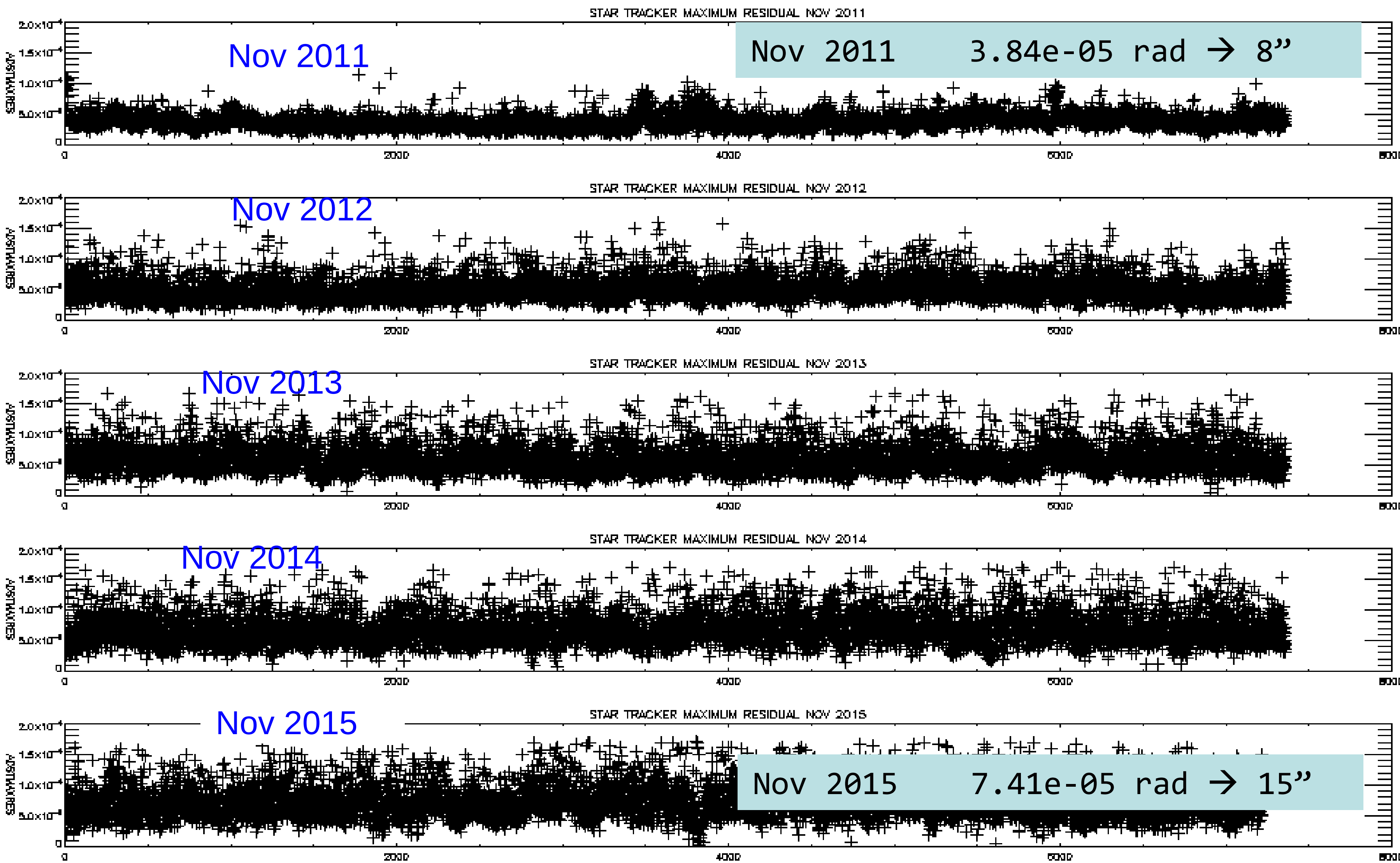

➢ The noise level ~ doubled over the 4+ year life

Gyros-only Test (1/2)

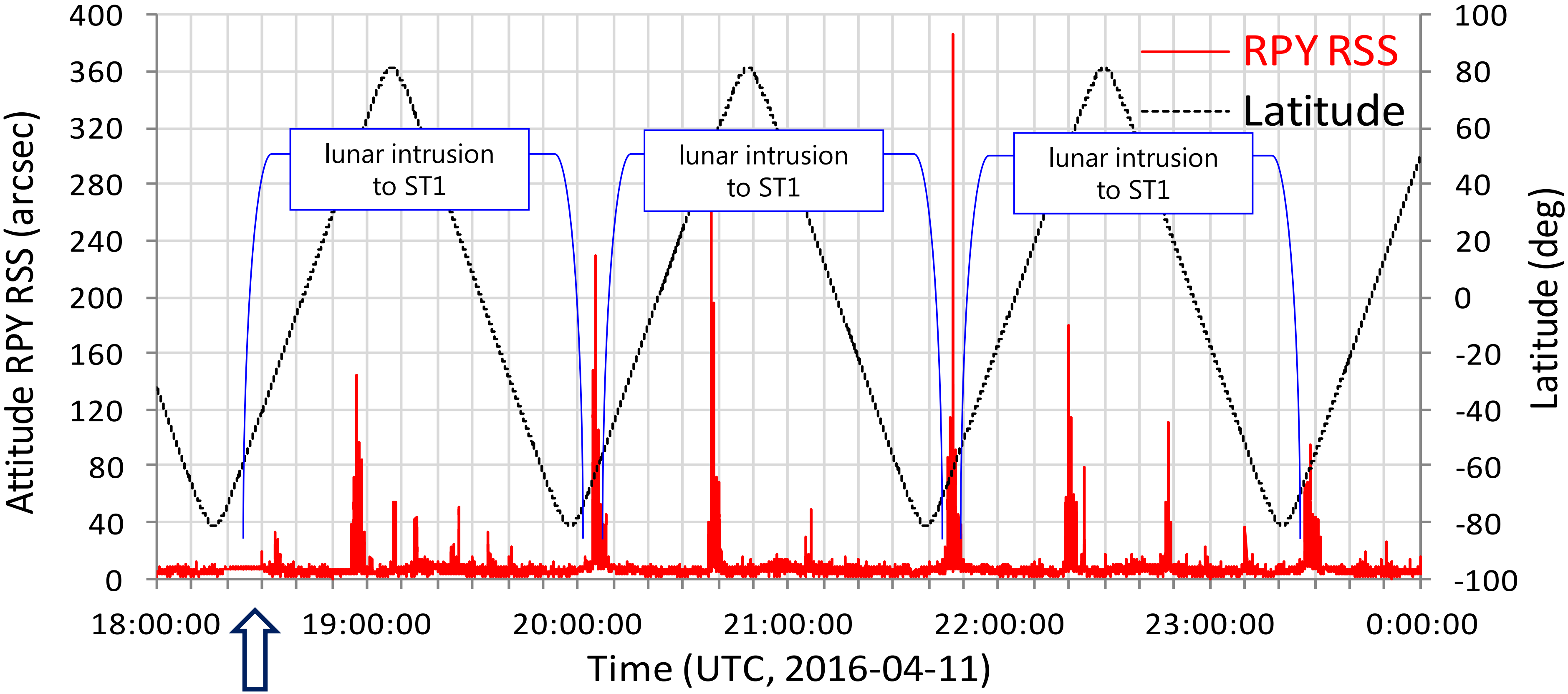

- A test of gyros only masked out attitude excursion induced by lunar intrusion

Gyros-only Test (2/2)

Results of Gyro-only Test 2016-04-11, 18:18:44 to 18:30:02z

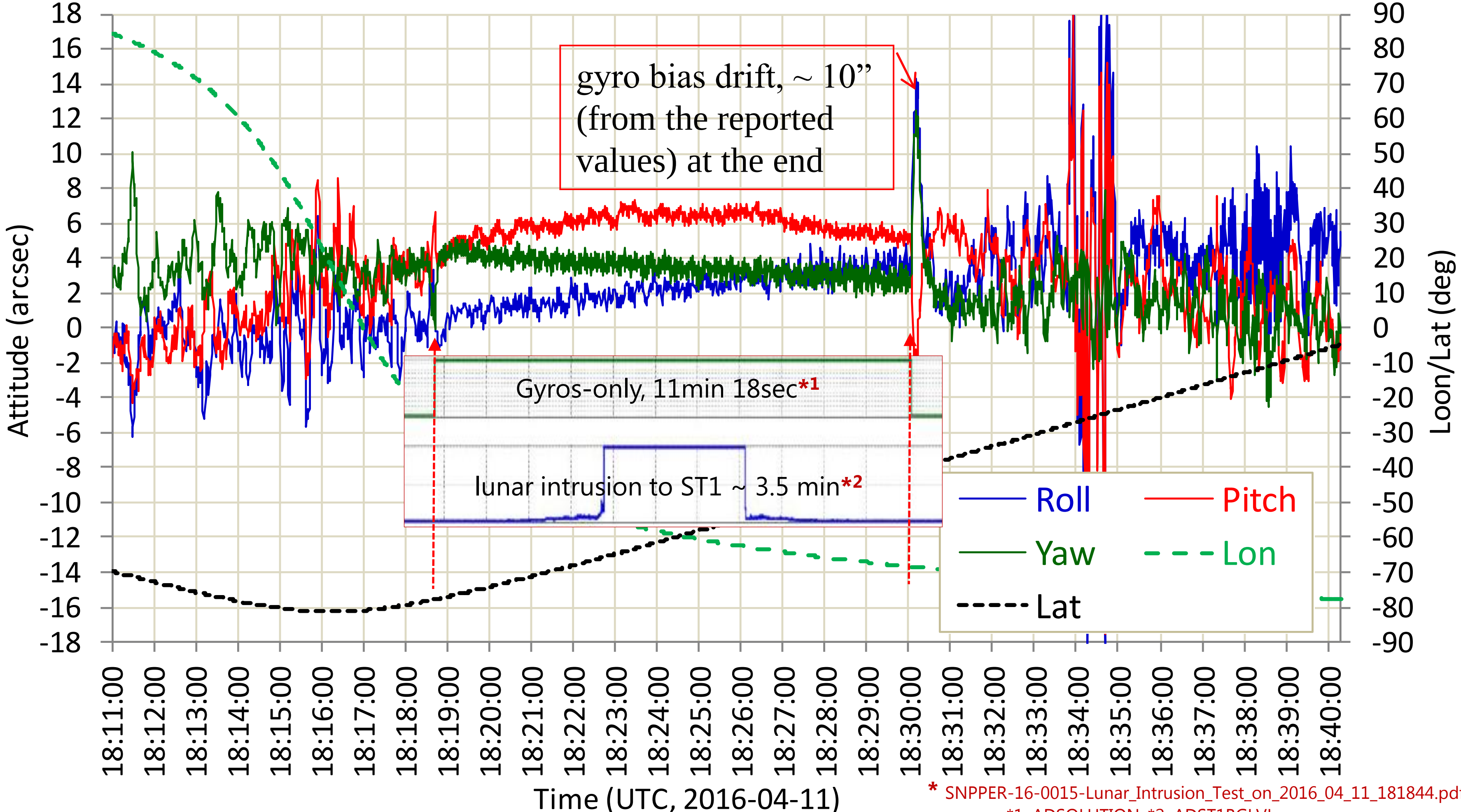

* SNPPER-16-0015-Lunar_Intrusion_Test_on_2016_04_11_181844.pdf
*1: ADSOLUTION; *2: ADST1BGLVL

➢ Gyros-only performed well, drifting ~ 10 arcsec @ end of 11 min 18 sec

Attitude re-generated using gyros data in TLM

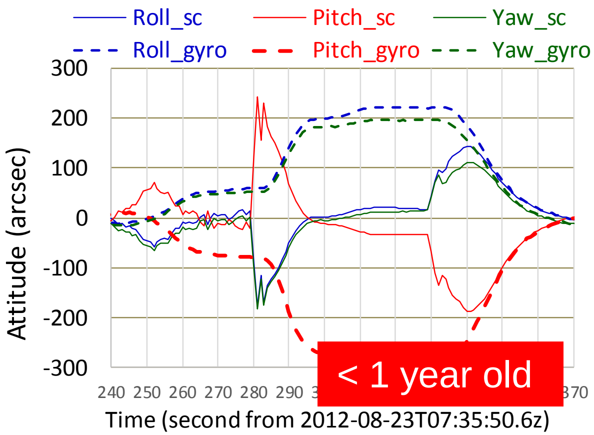

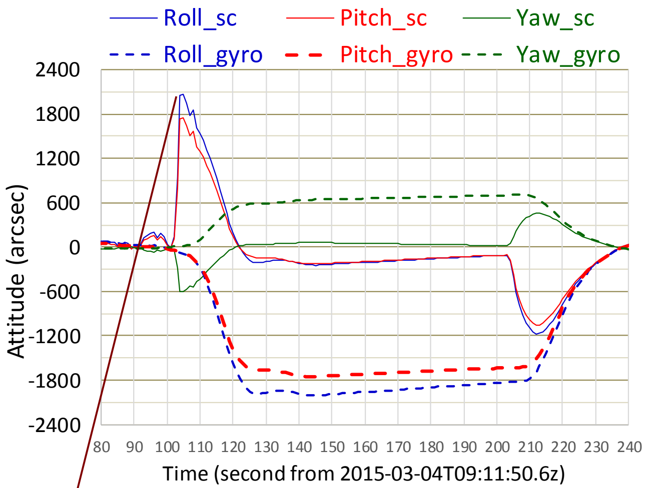

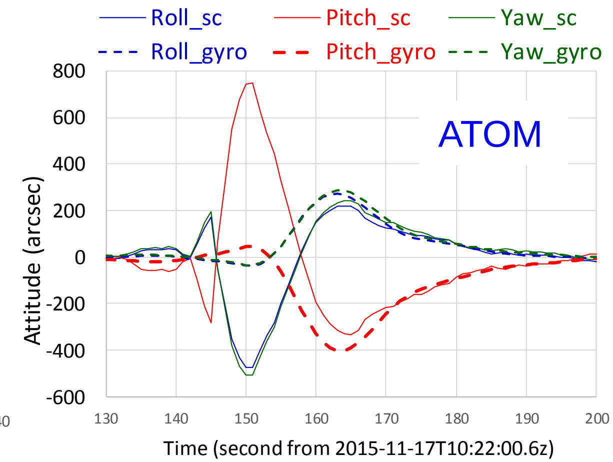

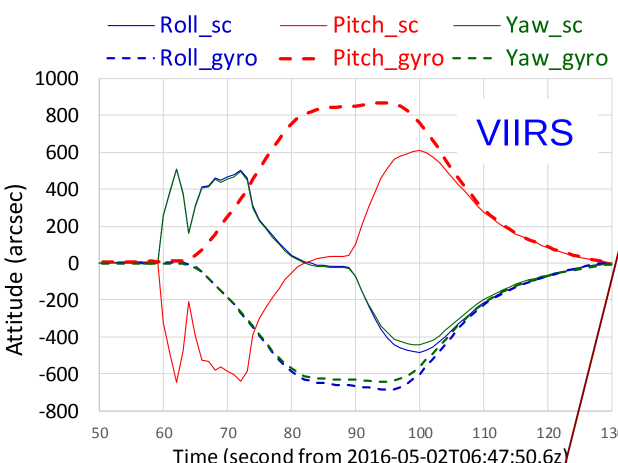

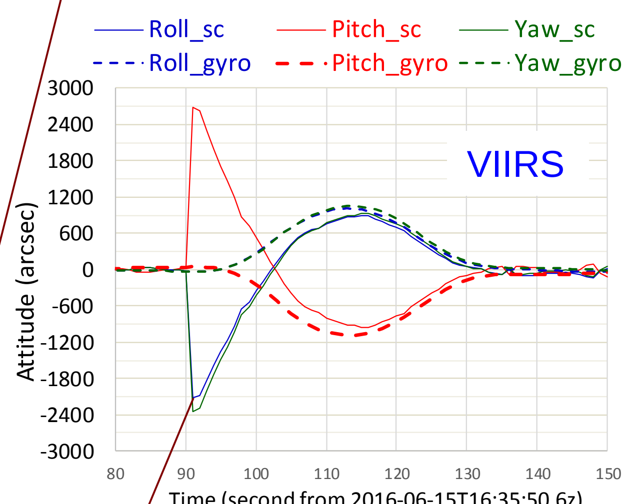

- Prototyping with gyros data looks good up to ~ 30 min, proven by test, VIIRS and ATOM data
- Geolocation errors > 7 km occasionally
- On-orbit system needs fixes to bring attitude to within spec

Un-physical. Indicator of deficiencies in HW/SW

The latest -- attitude Error > 1°

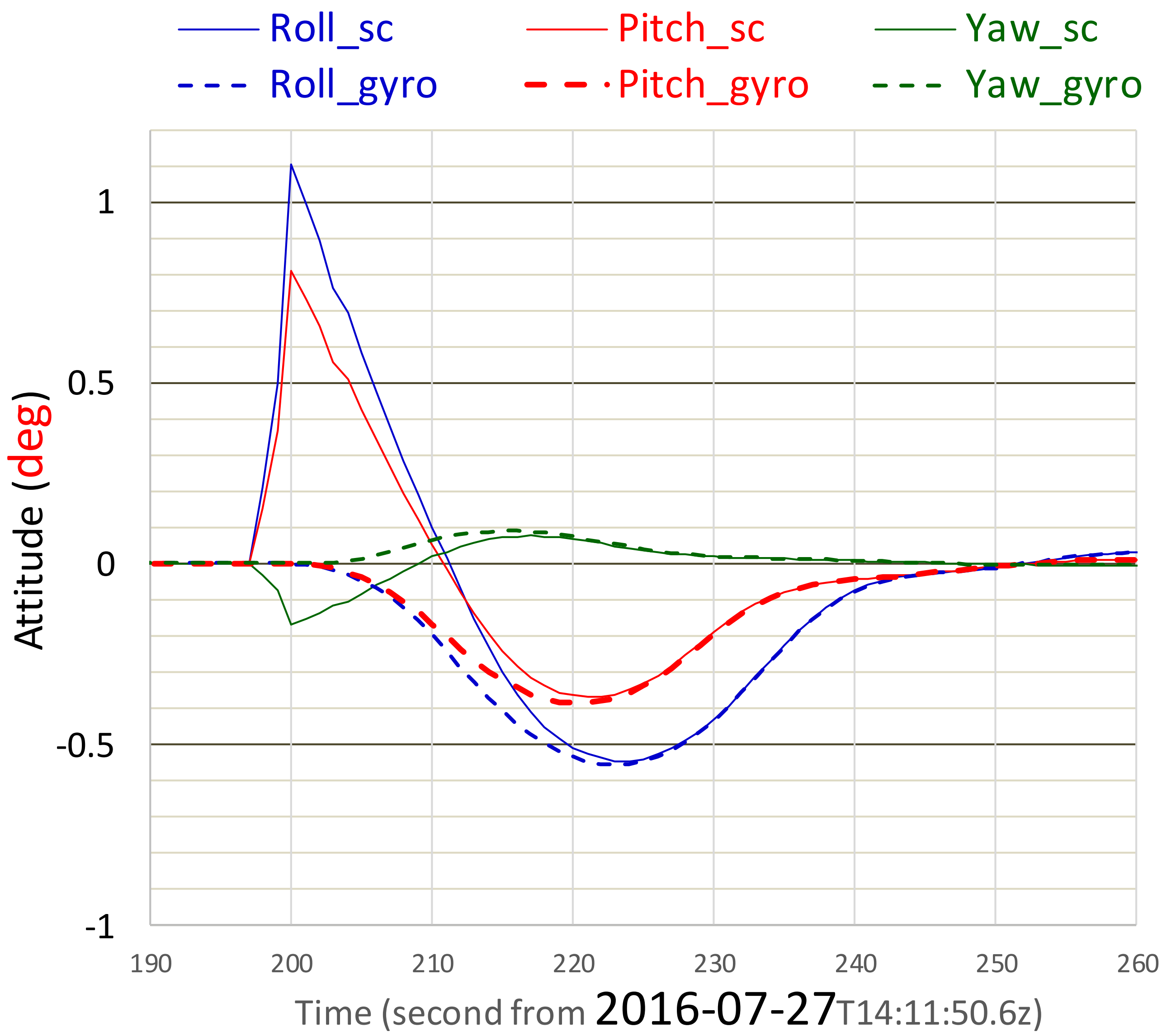

Potential paths forward

to correct the behaviors of the SNPP attitude system

1) Extend the time-out for gyros-only from 5-min to 15 min – test done, mostly useful to star catalog uploads
2) Adjust background noise thresholds to enable better star identification -- test done, might have helped reducing magnitude of attitude disturbances, but not enough
3) Lower the temperatures in the trackers – FSW patching under consideration, **scheduled at the end of September, 2016**
4) Adjust coefficients in the ADCS "mixing algorithm" to reduce the sensitivity to the star trackers data and thus reduce attitude errors
5) Map out and mask out malfunctioned CCD cells in the trackers CCD arrays for the attitude solution
6) others (implement Kalman Filter? urgent for J1, be a requirement for J2+)

- Some symptoms diagnosed and "medicines" prescribed
- The "medicines" need to be administered

Concluding remarks

- SNPP VIIRS Geolocation mean errors for I- & M-bands are near 0 and uncertainties are ~ 70 m at nadir, statistically
- J1 geolocation expectations
  - Geolocation will be calibrated on-orbit by control points through LUTs
  - Bands on VisNIR FPA should be good; Bands on cold FPAs will be off ~ 50 m in the track direction
  - DNB geolocation pixels will be larger beyond Sample#1500, 1100 km off nadir
- Challenges, concerns, and issues
  - Challenges: Scan-to-scan underlap, the expectations
    - SNPP VIIRS has no underlap owing to shorter focal length and faster scan rate
    - J1 has underlap of ~1/4 I-pixel near nadir over the equator region
    - J2 has larger underlap over a larger extent of the earth than J1
  - Concern: J1 attitude performance
  - Issue: The SNPP attitude system anomaly, error > 1 deg → geolocation error > 10 km occurred lately. The attitude system (HW & SW) needs maintenance.

Thank you !

Questions?

Be aware of assumptions in probability theory.

Be cautious in using statistical methods.

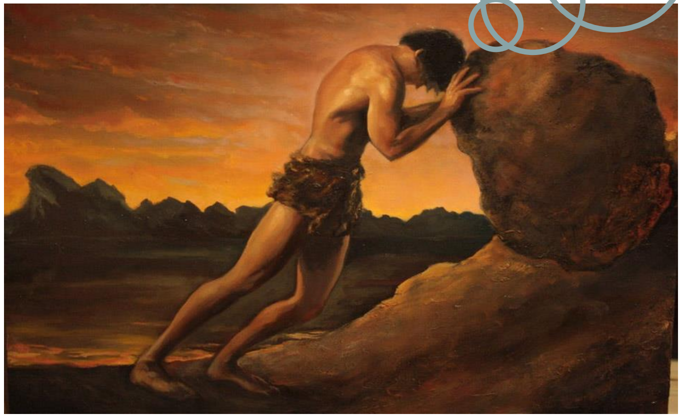

Backup Slides

Initial on-orbit geolocation LUTs Update

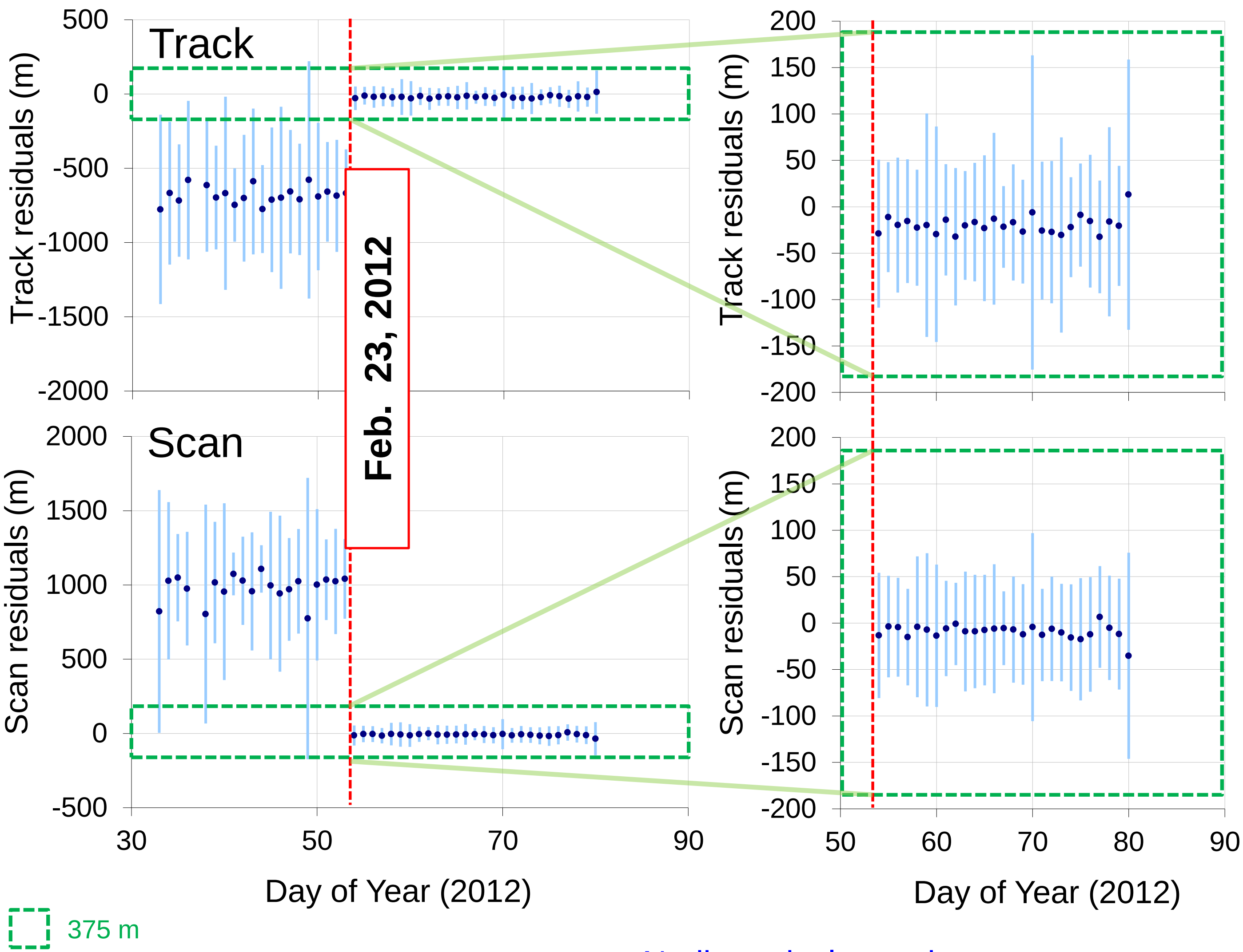

Error after
LUT update
(2/23/2012, doy 54)

	Bias (m)	RMSE (m)
Track	-21	80
Scan	-8	64

27 days with average of 142 matchups/day (minus 12 outliers/day)

Nadir equivalent units;

Biases removed: Track -755 m, Scan 1118 m

Scan Control Electronics (SCE) Side Switch, Geolocation Error and Correction

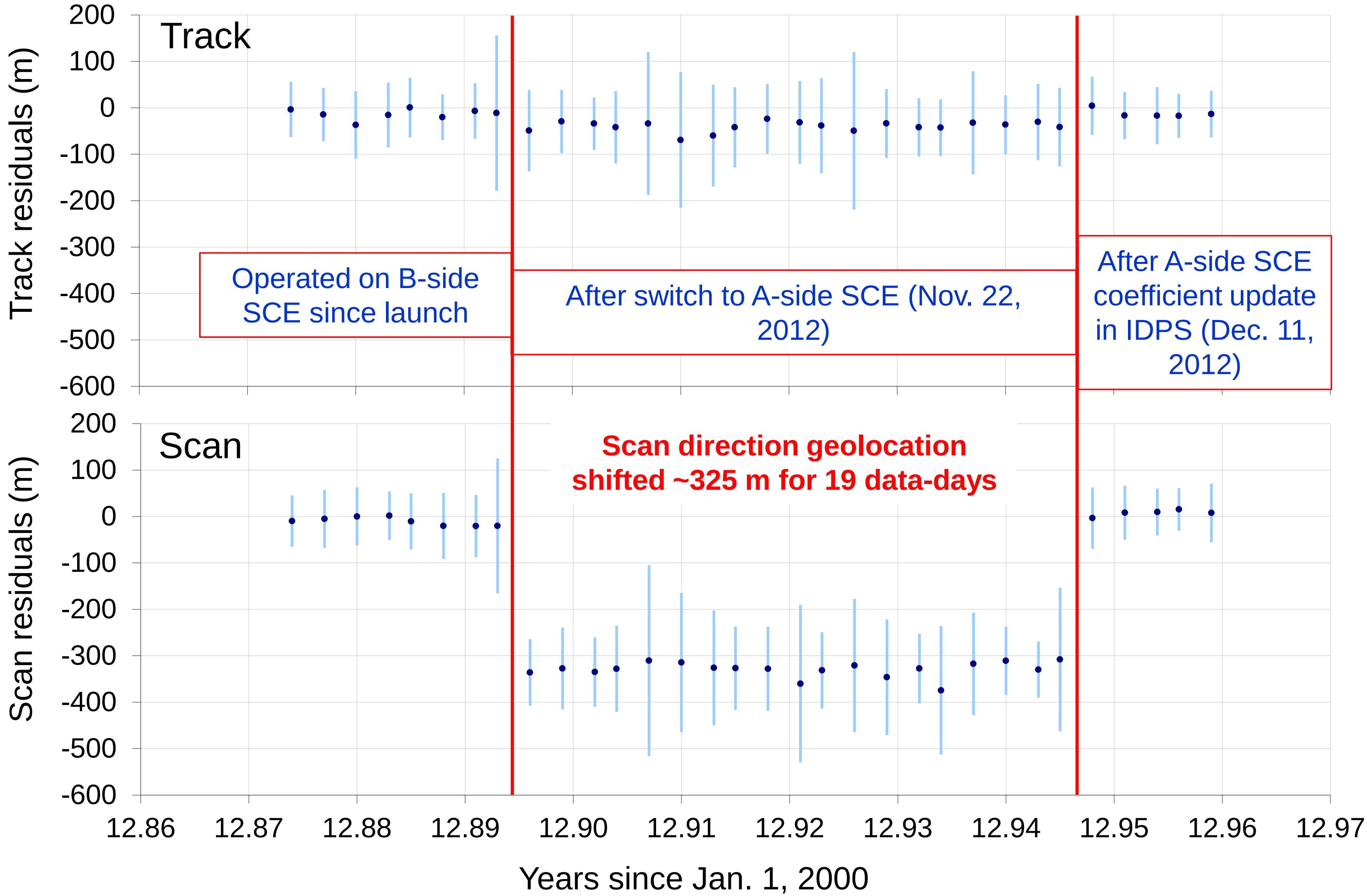

(Nadir equivalent units)

Star Tracker Re-alignment and Correction

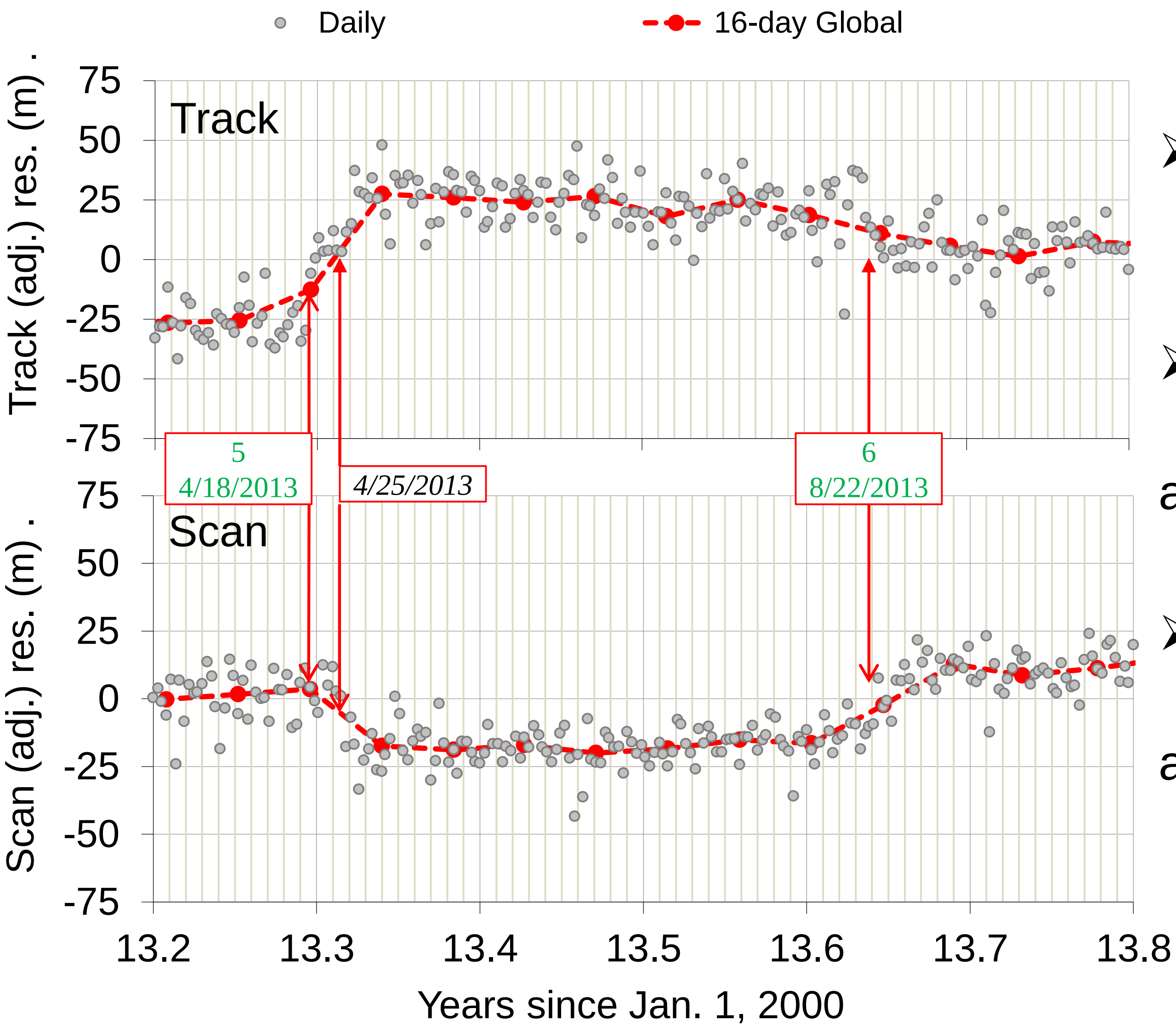

- 4/18/2013:
  Geo LUTs fine tuned
- 4/25/2013:
  Star tracker re-alignment
- 8/22/2013
  Error ~ 25 m found and corrected

JPSS-1 VIIRS V2 "At-Launch" RSR, Comparisons, Impacts, Etc.

Chris Moeller[a], Tom Schwarting[b], Jeff McIntire[b], Dave Moyer[c], Jinan Zeng[d]

[a]Univ. Wisconsin - Madison

[b]VCST

[c]Aerospace Corporation

[d]Fibretek Corporation

Acknowledgement to NIST T-SIRCUS Team, VIIRS instrument team at Raytheon Corp., Joel McCorkel (GSFC)

2016 STAR JPSS Science Teams Anuual Mtg

August 8-12, 2016

College Park , MD

RSR, Comparisons, Impact

- JPSS-1 V2 RSR
  - Pedigree/Analysis
  - Product
- Influence of RSR on SDR
  - Comparisons with SNPP
  - Detector dependence

JPSS-1 VIIRS RSR Version History: Version 0 (Beta)

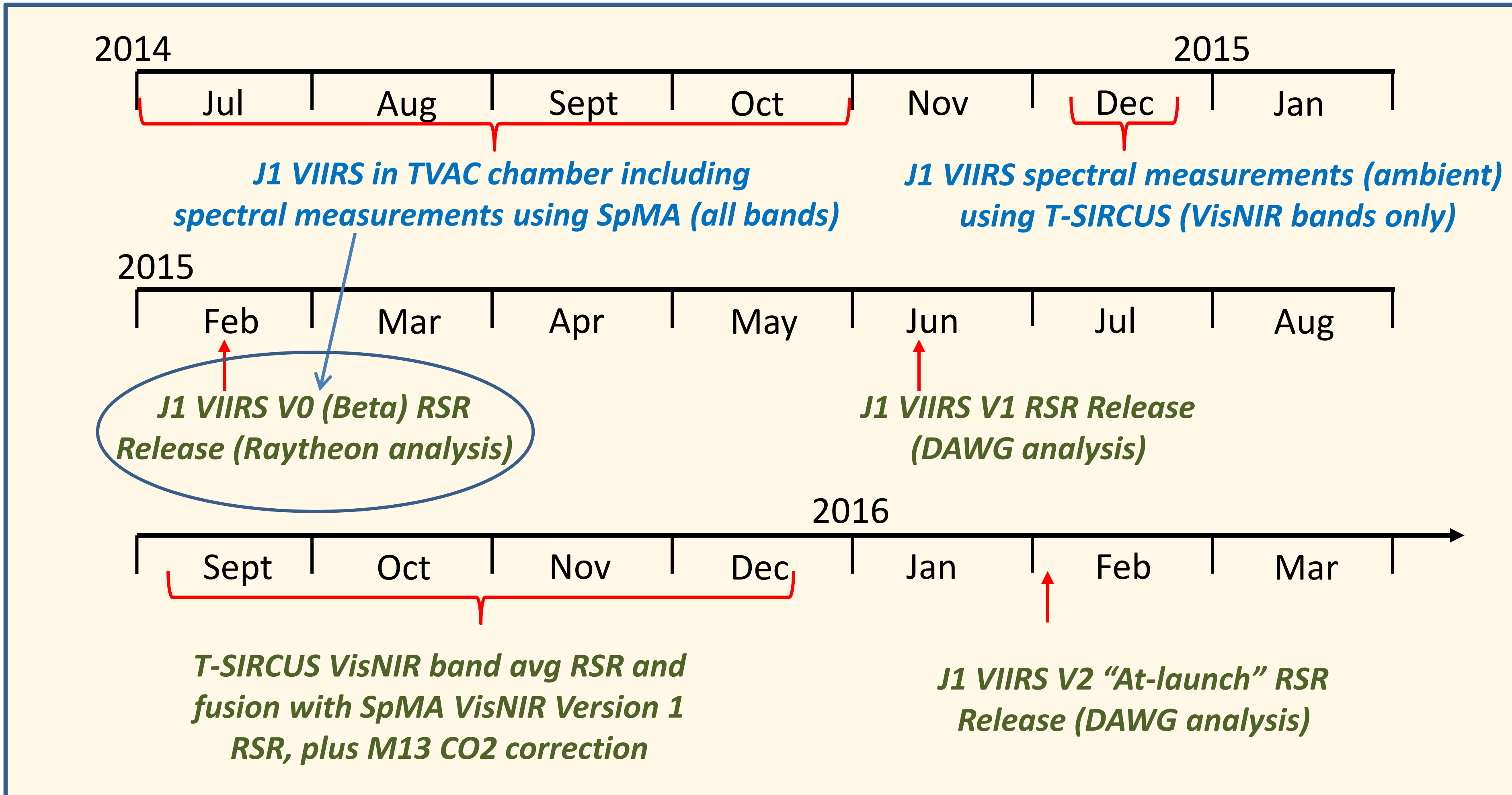

JPSS-1 VIIRS RSR Version History: Version 1

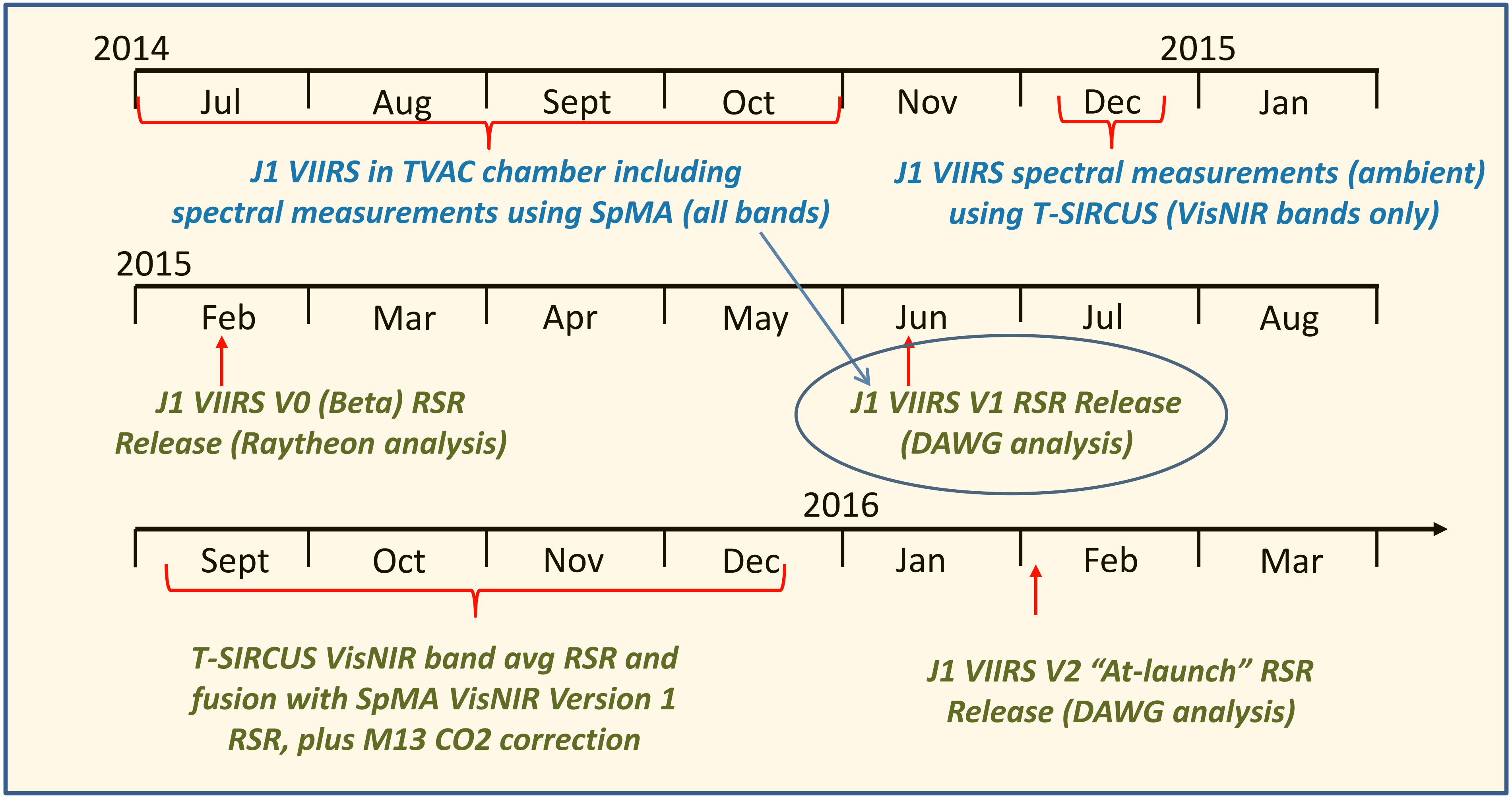

JPSS-1 VIIRS RSR Version History: Version 2 "At-Launch"

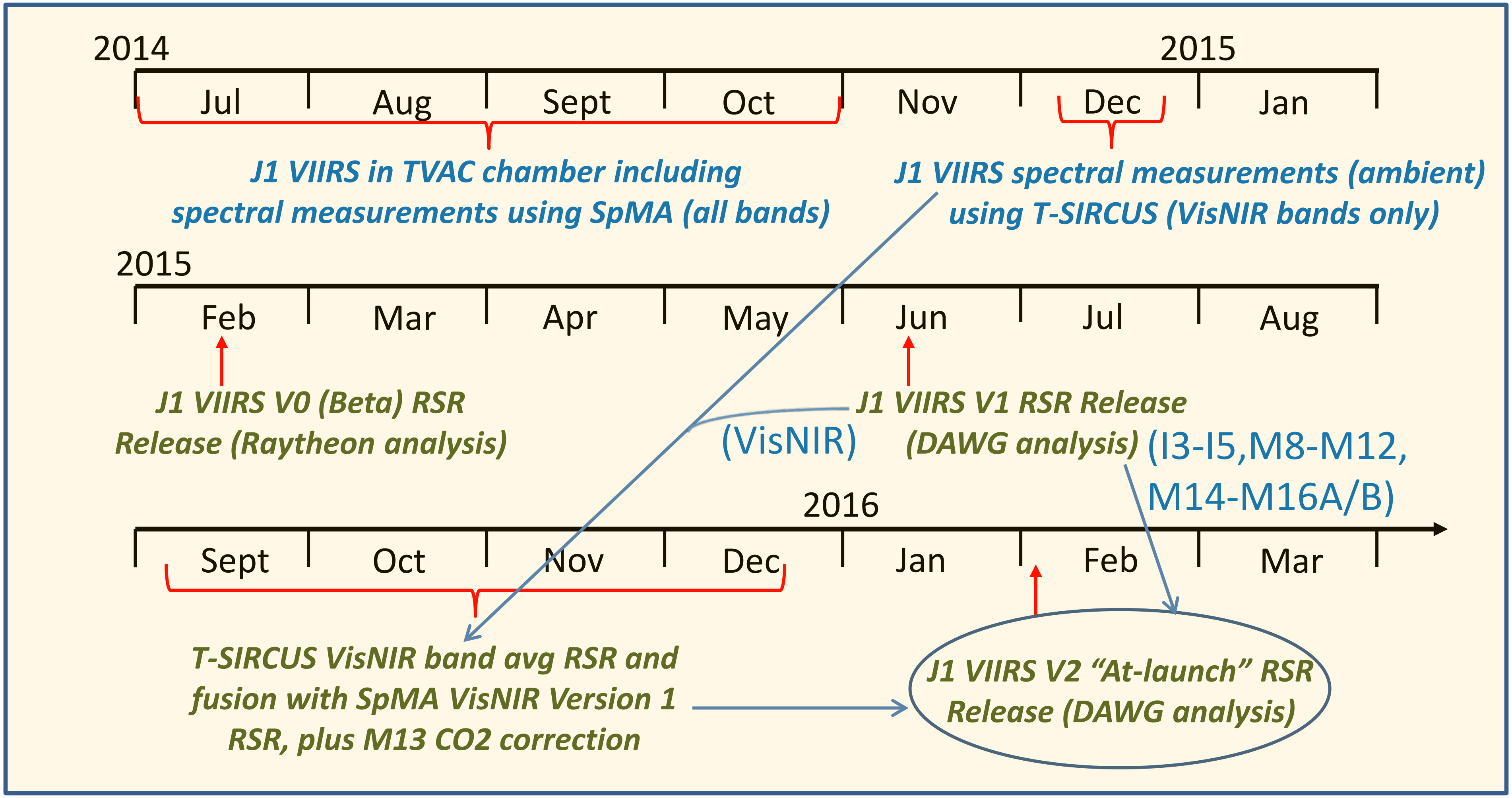

Measurements: Illumination Characteristics

TSIRCUS sampling strategy at each wavelength

- Light on detectors for 8-28 seconds (Dn_{open})
- Shutter closed (dark) for 8-28 seconds (Dn_{closed})

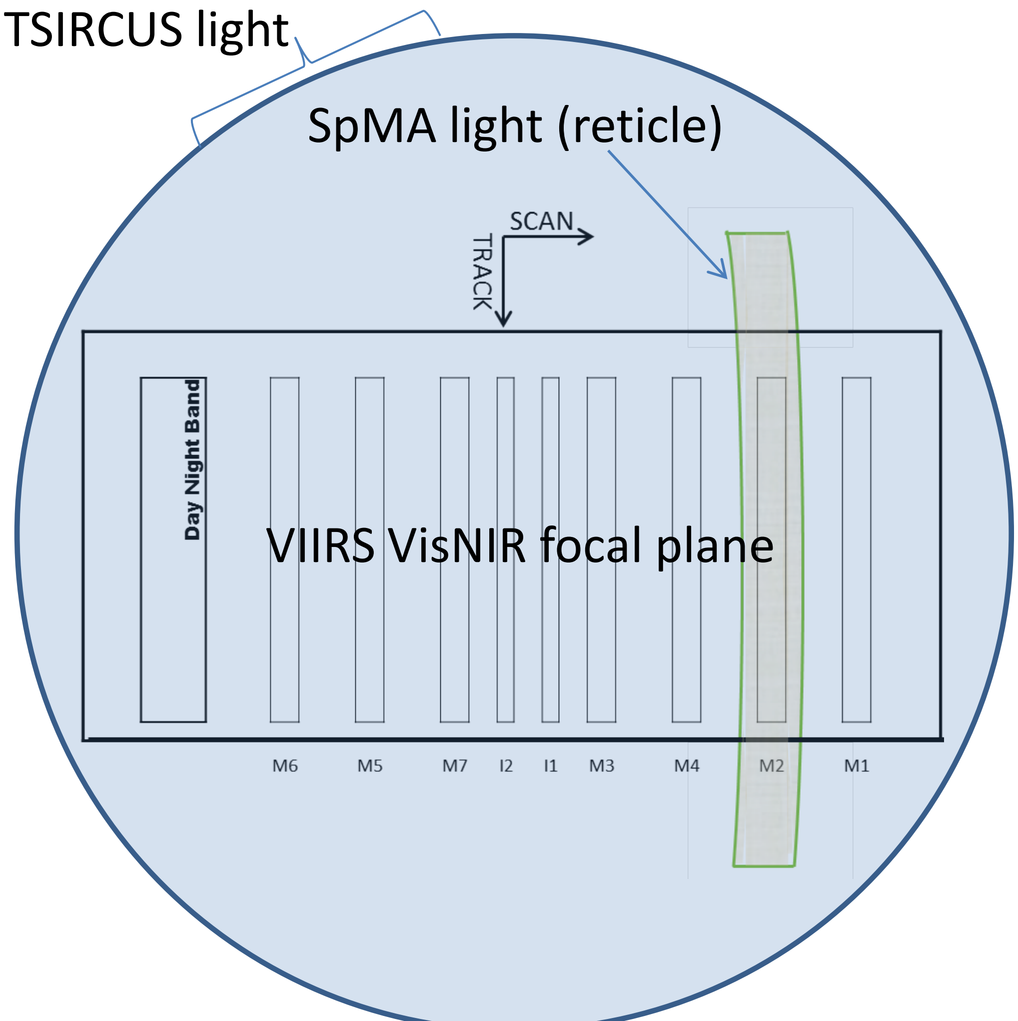

SpMA (V1 - All Bands)	TSIRCUS (V2 – VisNIR Bands)
• Slit illumination	• Flood illumination
• Polarized	• Unpolarized
• Spectral smile	• Spectrally flat
• >30% source non-uniformity along-track	• <10% source non-uniformity along-track
• Offline source monitoring	• Realtime source monitoring
• 5 to 6 decades of VisNIR response	• 4 to 5 decades of VisNIR response
• Contiguous spectral sampling	• “Picket-fence” spectral sampling

Analysis: 6 Steps to V2 Band Average "Fused" VisNIR RSR

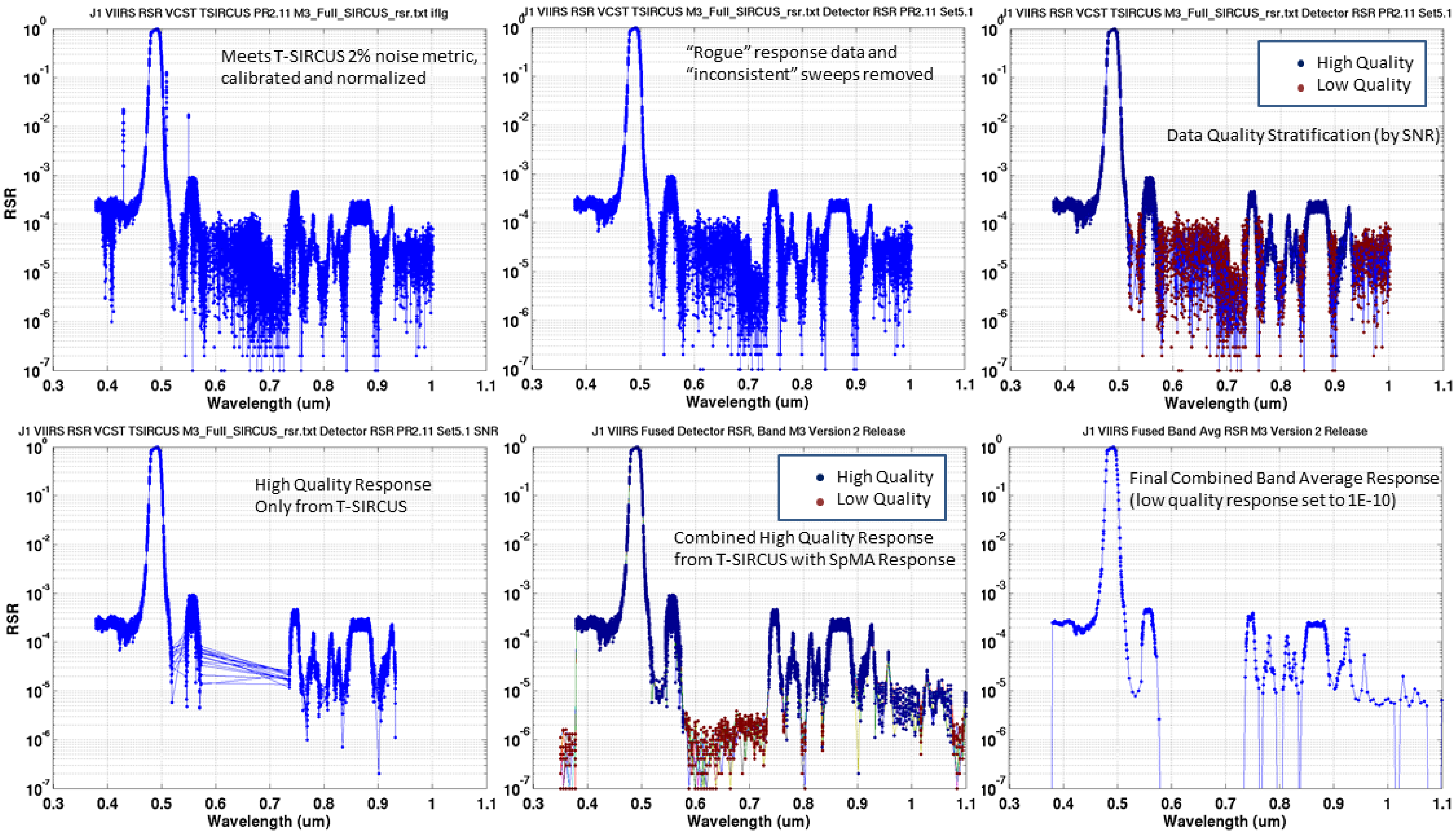

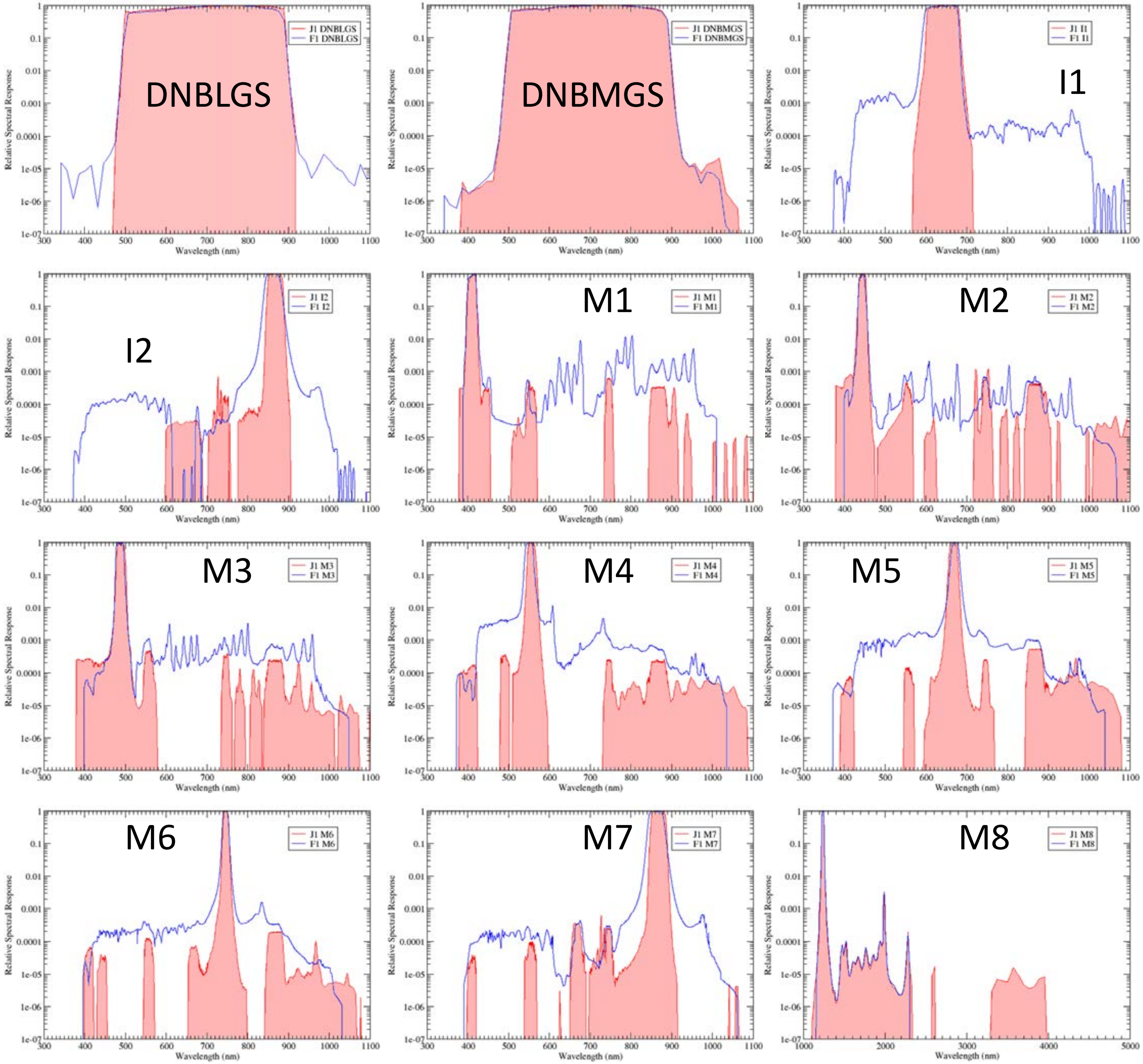
DNBLGS
J1 DNBLGS
F1 DNBLGS
DNBMGS
J1 DNBMGS
F1 DNBMGS
I1
J1 I1
F1 I1
I2
J1 I2
F1 I2
M1
J1 M1
F1 M1
M2
J1 M2
F1 M2
M3
J1 M3
F1 M3
M4
J1 M4
F1 M4
M5
J1 M5
F1 M5
M6
J1 M6
F1 M6
M7
J1 M7
F1 M7
M8
J1 M8
F1 M8
Relative Spectral Response
Wavelength (nm)

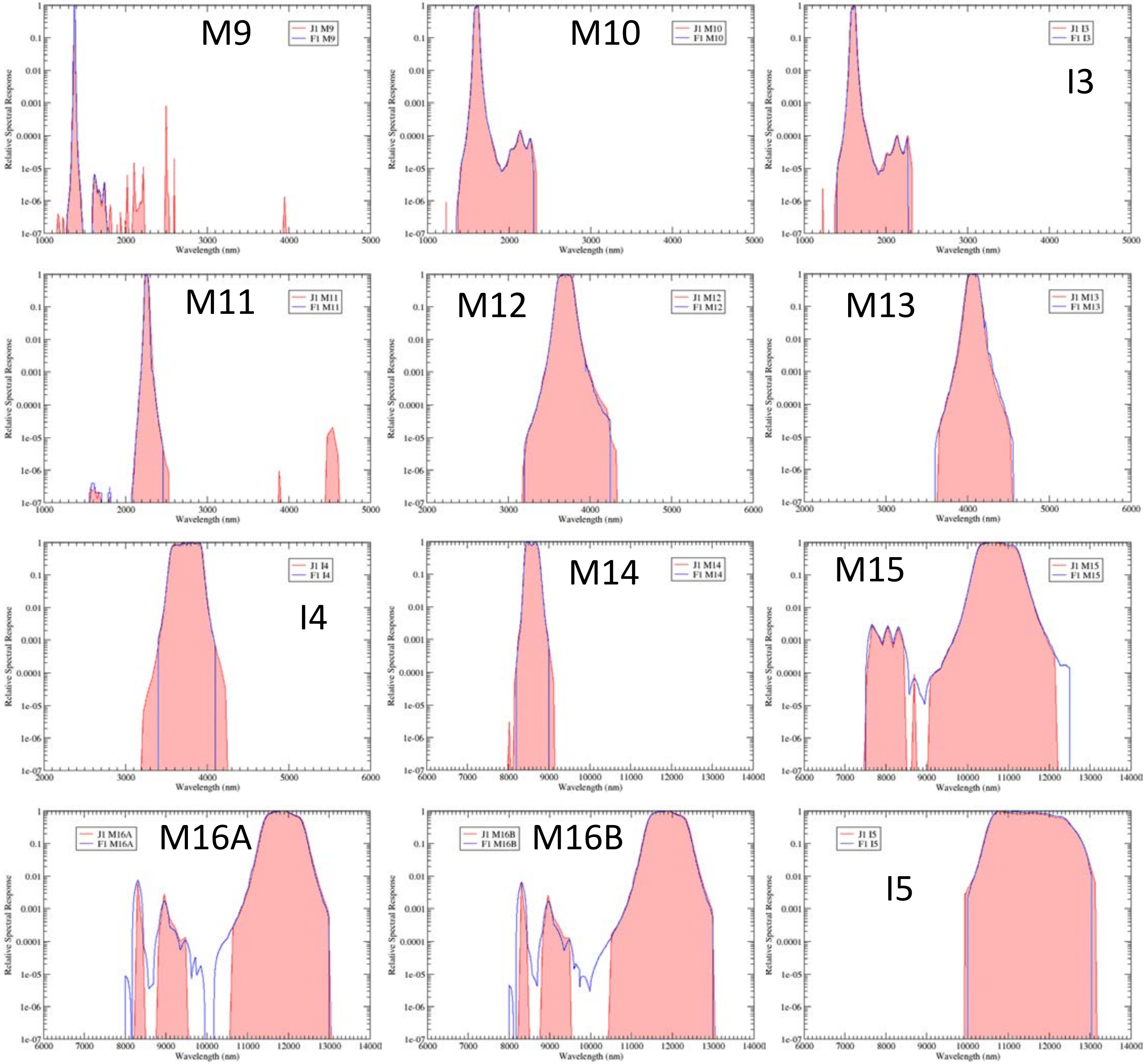
M9
J1 M9
F1 M9
M10
J1 M10
F1 M10
I3
J1 I3
F1 I3
M11
J1 M11
F1 M11
M12
J1 M12
F1 M12
M13
J1 M13
F1 M13
I4
J1 I4
F1 I4
M14
J1 M14
F1 M14
M15
J1 M15
F1 M15
M16A
J1 M16A
F1 M16A
M16B
J1 M16B
F1 M16B
I5
J1 I5
F1 I5
Relative Spectral Response
Wavelength (nm)

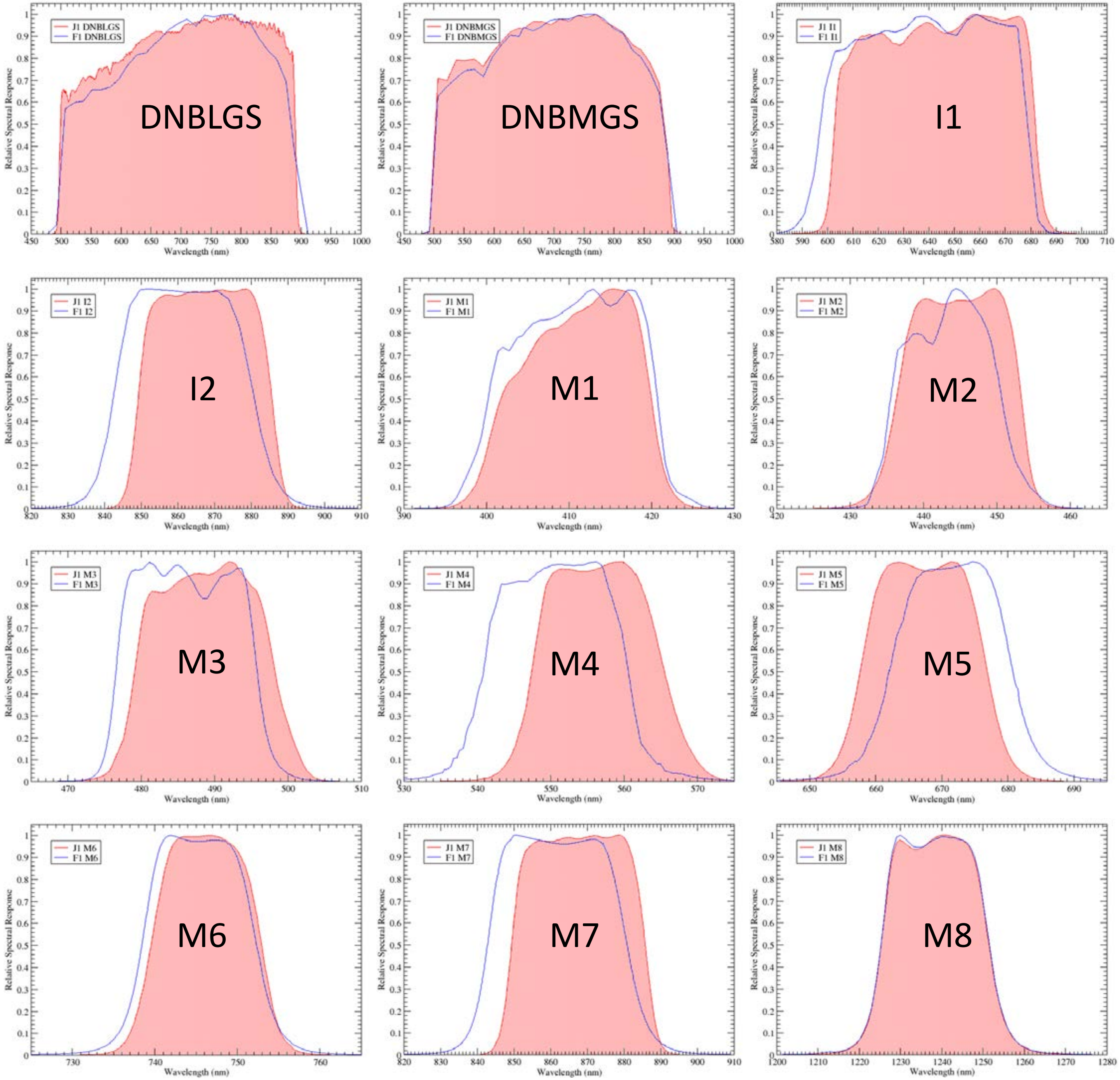
DNBLGS
J1 DNBLGS
F1 DNBLGS
DNBMGS
J1 DNBMGS
F1 DNBMGS
I1
J1 I1
F1 I1
I2
J1 I2
F1 I2
M1
J1 M1
F1 M1
M2
J1 M2
F1 M2
M3
J1 M3
F1 M3
M4
J1 M4
F1 M4
M5
J1 M5
F1 M5
M6
J1 M6
F1 M6
M7
J1 M7
F1 M7
M8
J1 M8
F1 M8
Relative Spectral Response
Wavelength (nm)

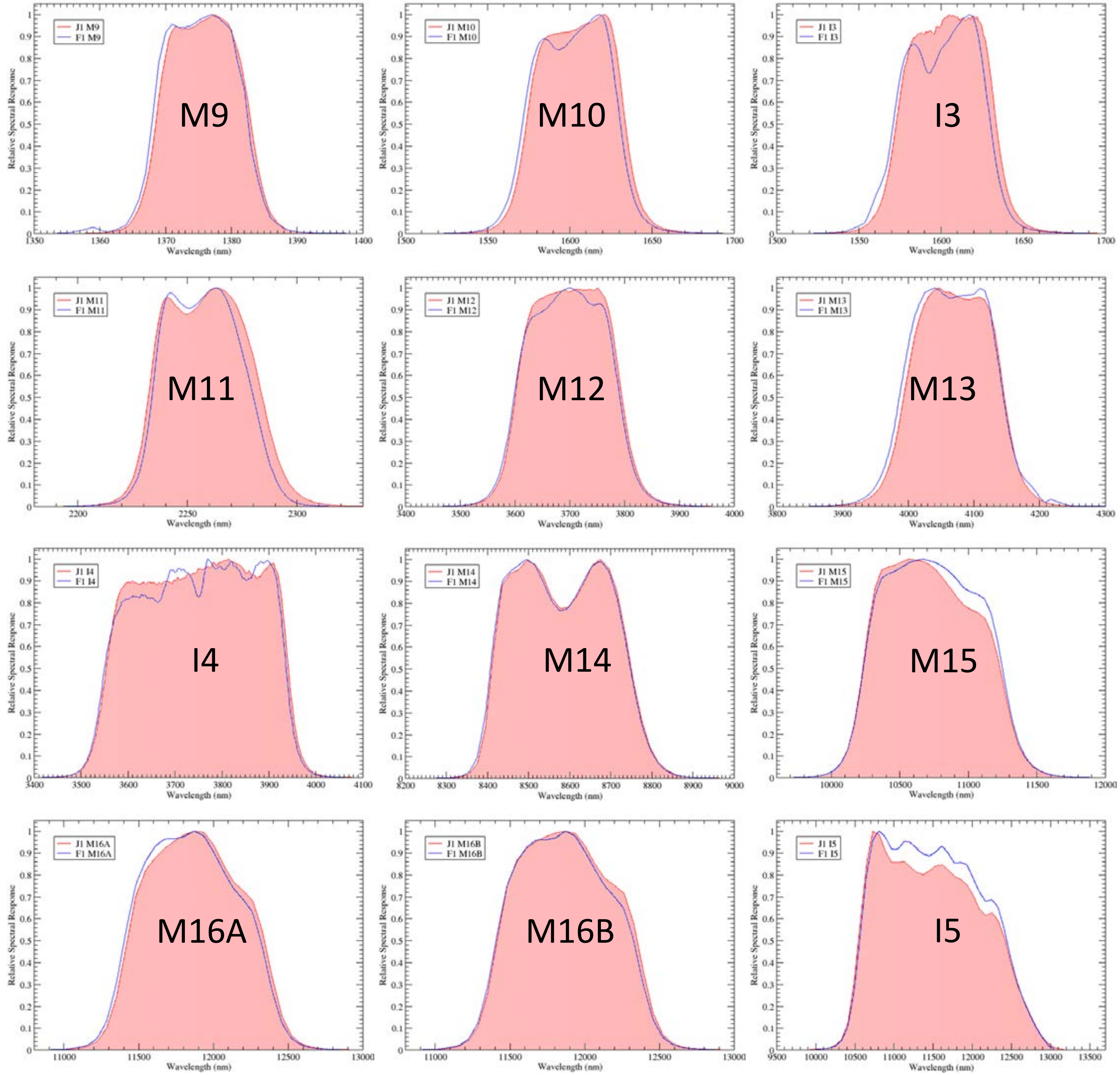
M9
J1 M9
F1 M9
M10
J1 M10
F1 M10
I3
J1 I3
F1 I3
M11
J1 M11
F1 M11
M12
J1 M12
F1 M12
M13
J1 M13
F1 M13
I4
J1 I4
F1 I4
M14
J1 M14
F1 M14
M15
J1 M15
F1 M15
M16A
J1 M16A
F1 M16A
M16B
J1 M16B
F1 M16B
I5
J1 I5
F1 I5
Relative Spectral Response
Wavelength (nm)

Band Average RSR Performance Against Compliance Metrics

Band	Specified Center (nm)	Measured Center (nm)	Specified 50% Bandpass (nm)	Measured 50% Bandpass (nm)	Specified Lower 1% Limit (nm)	Measured Lower 1% Limit (nm)	Specified Upper 1% Limit (nm)	Measured Upper 1% Limit (nm)	Specified IOOB (%)	J1 Measured IOOB (%)	S-NPP Measured IOOB (%)
I1	640 ±6	642.3	80 ±6	78.9	≥565	594.4	≤715	691.5	0.5	0.11	0.39
I2	865 ±8	867.4	39 ±5	36.5	≥802	842.7	≤928	892.3	0.7	0.12	0.52
I3	1610 ±14	1603.2	60 ±9	60.7	≥1509	1544.3	≤1709	1667.7	0.7	0.44	0.48
I4	3740 ±40	3747.6	380 ±30	387.5	≥3340	3474.1	≤4140	4015.2	0.5	0.16	0.16
I5	11450 ±125	11483.1	1900 ±100	1875.1	≥9900	10170.8	≤12900	13090.6	0.4	0.08	0.06
M1	412 ±2	410.9	20 ±2	18.2	≥376	395.6	≤444	425.1	1.0	0.35	2.19
M2	445 ±3	444.8	18 ±2	17.0	≥417	429.2	≤473	457.7	1.0	0.52	0.93
M3	488 ±4	488.7	20 ±3	19.1	≥455	472.9	≤521	504.4	0.7	0.43	1.15
M4	555 ±4	556.5	20 ±3	18.1	≥523	540.2	589	573.7	0.7	0.37	3.65
M5	672 ±5	667.3	20 ±3	19.3	≥638	649.7	≤706	685.1	0.7	0.37	2.70
M6	746 ±2	746.2	15 ±2	13.4	≥721	734.2	≤771	758.2	0.8	0.40	1.64
M7	865 ±8	867.6	39 ±5	36.5	≥801	842.8	≤929	892.5	0.7	0.16	0.62
M8	1240 ±5	1238.4	20 ±4	26.1	≥1205	1214.0	≤1275	1264.9	0.8	0.48	0.49
M9	1378 ±4	1375.8	15 ±3	14.5	≥1351	1362.0	≤1405	1390.0	1.0	0.41	1.01
M10	1610 ±14	1603.8	60 ±9	60.2	≥1509	1545.7	≤1709	1667.6	0.7	0.43	0.46
M11	2250 ±13	2258.2	50 ±6	52.0	≥2167	2209.4	2333	2314.4	1.0	0.35	0.40
M12	3700 ±32	3697.9	180 ±20	194.8	≥3410	3519.1	≤3990	3893.8	1.1	0.33	0.34
M13	4050 ±34	4070.0	155 ±20	153.0	≥3790	3909.1	≤4310	4224.7	1.3	0.40	0.35
M14	8550 ±70	8580.3	300 ±40	340.1	≥8050	8336.3	≤9050	8879.3	0.9	0.19	0.21
M15	10763 ±113	10730.9	1000 ±100	1001.7	≥9700	9916.9	≤11740	11638.7	0.4	0.35	0.40
M16A	12013 ±88	11882.8	950 ±50	914.6	≥11060	11104.1	≤13050	12692.5	0.4	0.39	0.39
M16B	12013 ±88	11883.0	950 ±50	934.5	≥11060	11101.5	≤13050	12698.5	0.4	0.38	0.37
M16[1]	12013 ±88	11882.9	950 ±50	924.8	≥11060	11102.8	≤13050	12695.7	0.4	0.39	-
DNBMGS[2]	700 ±14	693.1	400 ±20	381.1	≥470	487.8	≤960	906.9	0.1	0.00	0.00
DNBLGS	700 ±14	694.8	400 ±20	391.4	≥470	491.0	≤960	900.1	0.1	0.02	0.00

[1]M16 is an average of M16A and M16B.

[1]DNBMGS spectral characterization represents DNBHGS. DNBHGS not directly measured due to its high gain.

Summary: JPSS-1 VIIRS At-launch RSR

- JPSS-1 VIIRS RSR measurement and analysis program is complete, leading to the "at-launch" designation for the Version 2 (February 2016) release.
- Reductions in IOOB in VisNIR bands bring JPSS-1 VIIRS into compliance for these bands. Other minor non-compliances exist but are well characterized.
- Though the RSR are compliant on spectral position, there are differences in position/shape compared to SNPP.

V2 RSR Impact on SDR: RSB

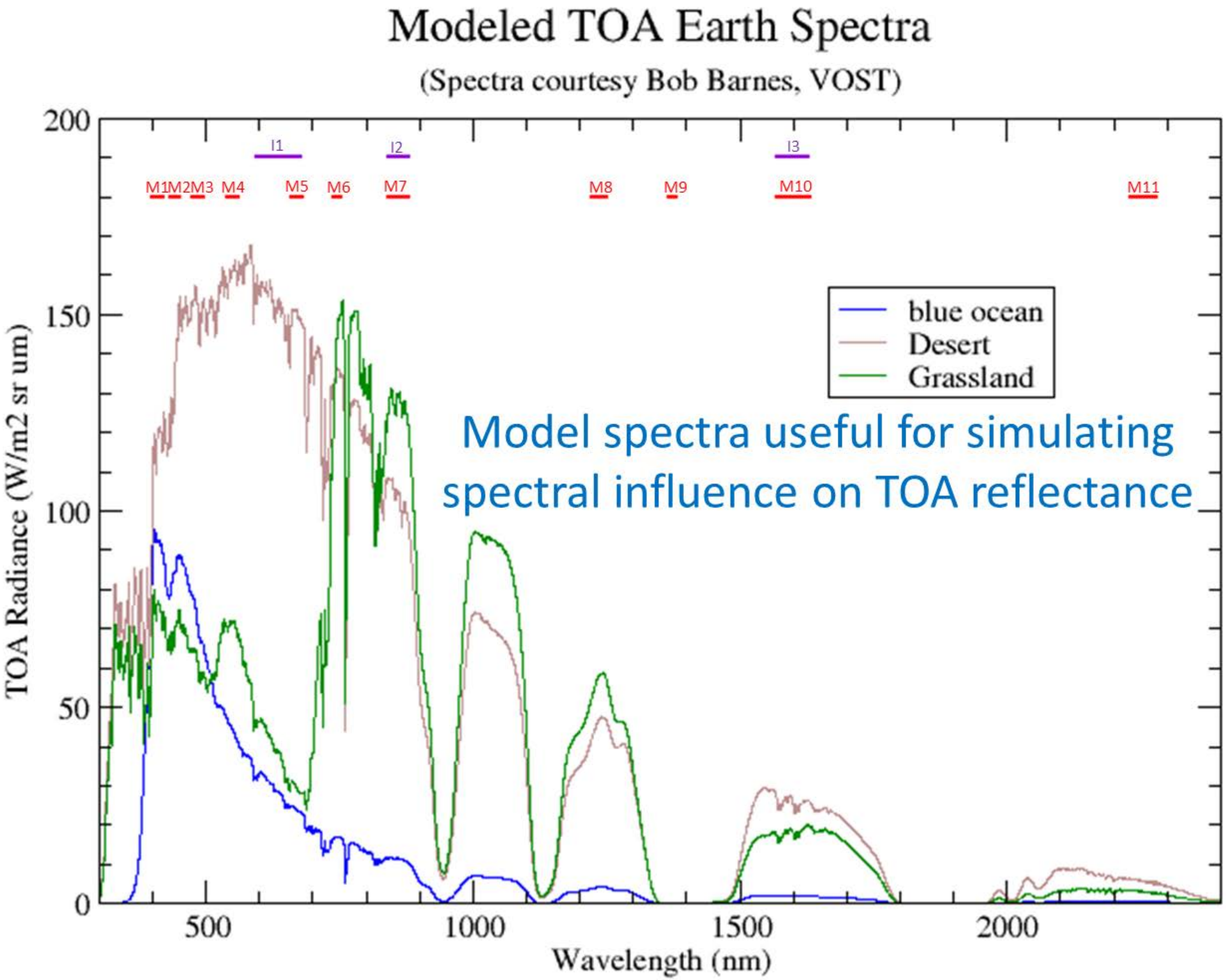

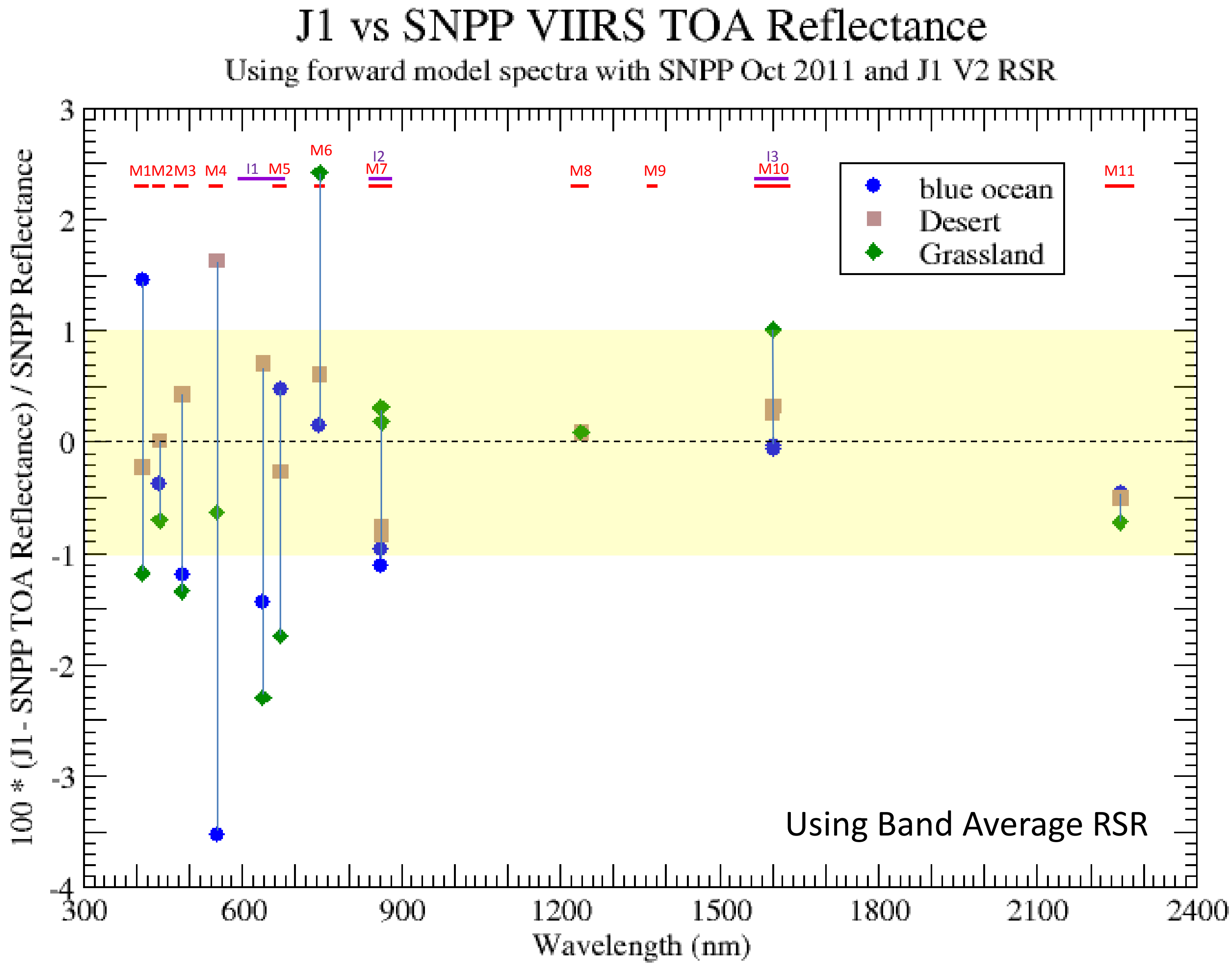

J1 vs SNPP VIIRS TOA Reflectance
Using forward model spectra with SNPP Oct 2011 and J1 V2 RSR
100 * (J1 - SNPP TOA Reflectance) / SNPP Reflectance
Wavelength (nm)
M1
M2
M3
M4
I1
M5
M6
I2
M7
M8
M9
I3
M10
M11
blue ocean
Desert
Grassland
Using Band Average RSR

VIIRS Detector Dependence: Blue Ocean Model

- Non-telecentric design causes variation in detector spectral coverage
- Simulated TOA reflectances show detector dependence

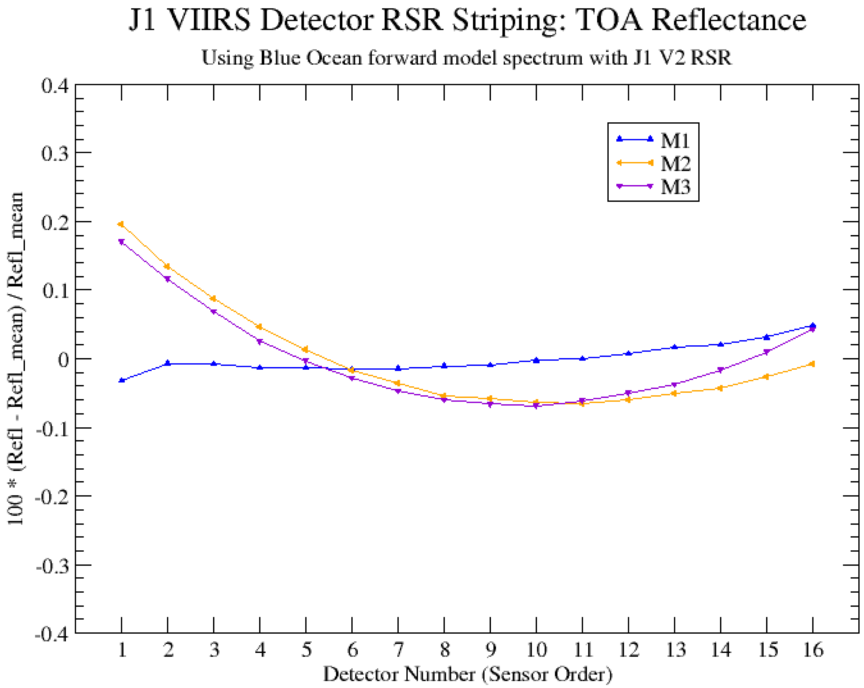

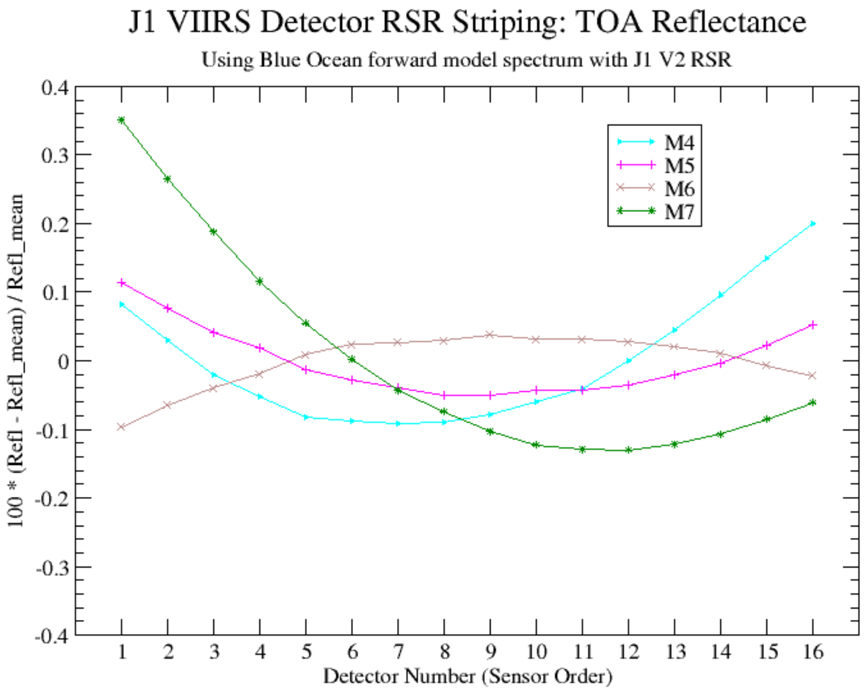

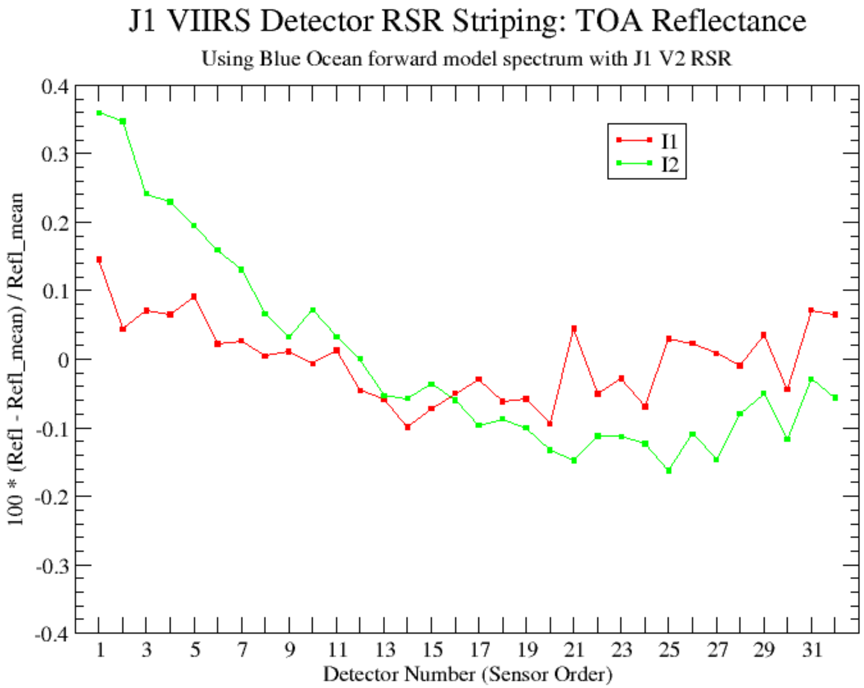

VIIRS Detector Dependence: Grassland Model

- Non-telecentric design causes variation in detector spectral coverage
- Simulated TOA reflectances show detector dependence

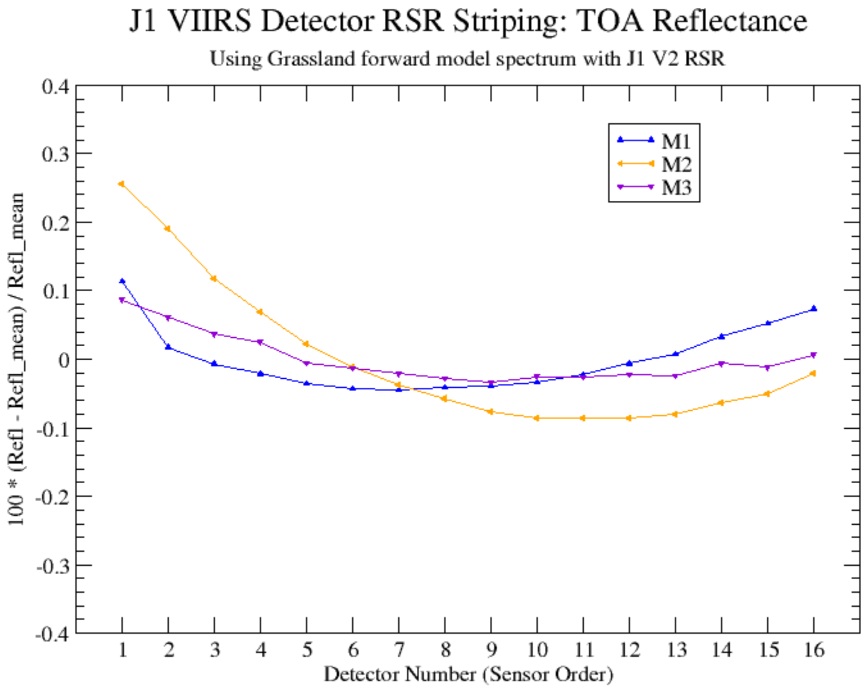

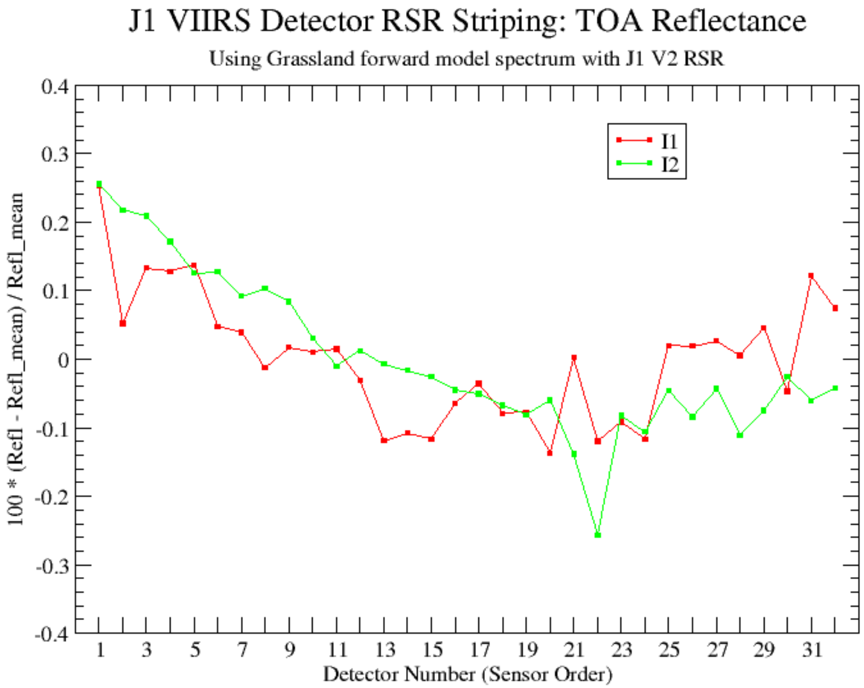

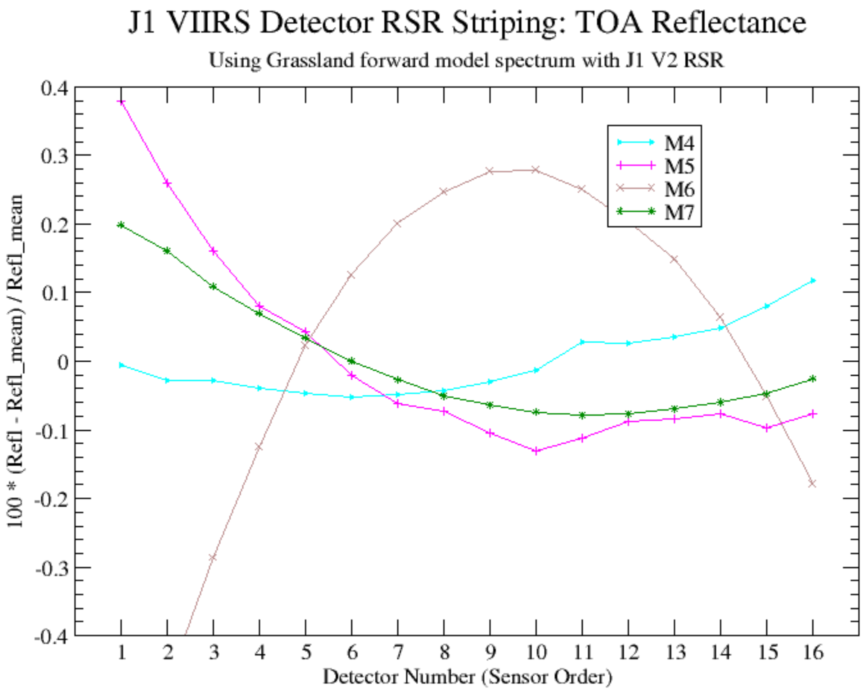

VIIRS Detector Dependence: Desert Model

- Non-telecentric design causes variation in detector spectral coverage
- Simulated TOA reflectances show detector dependence

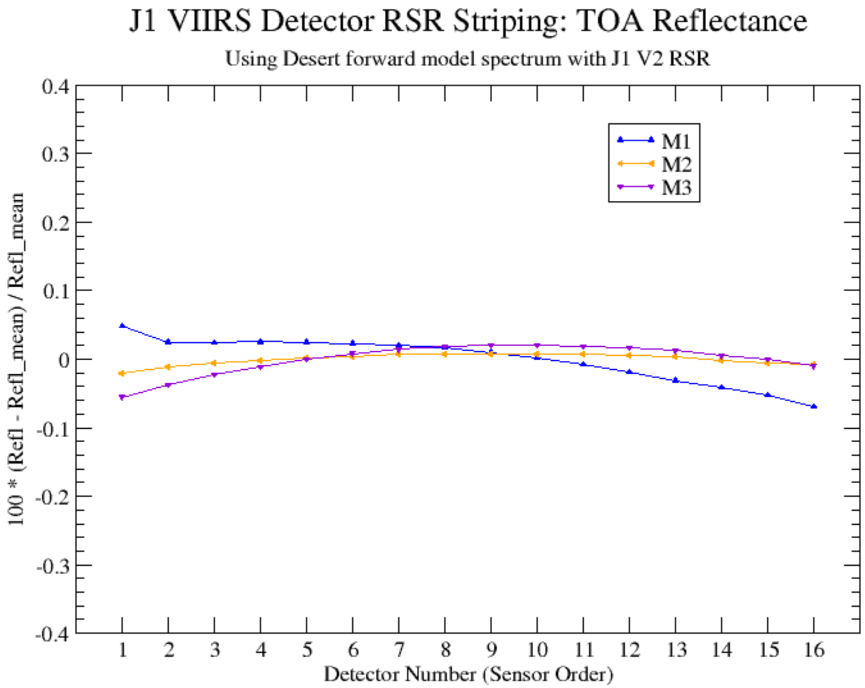

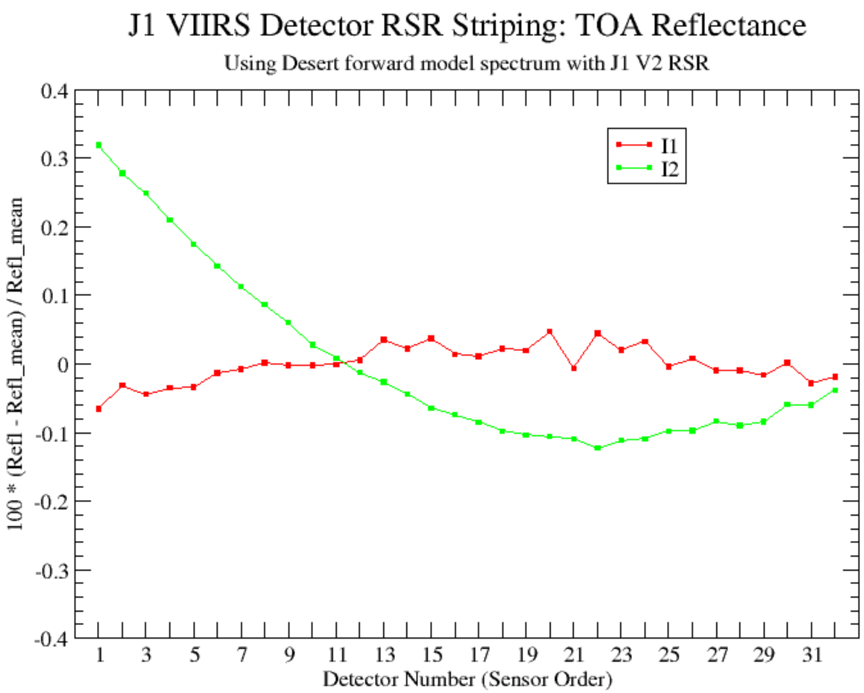

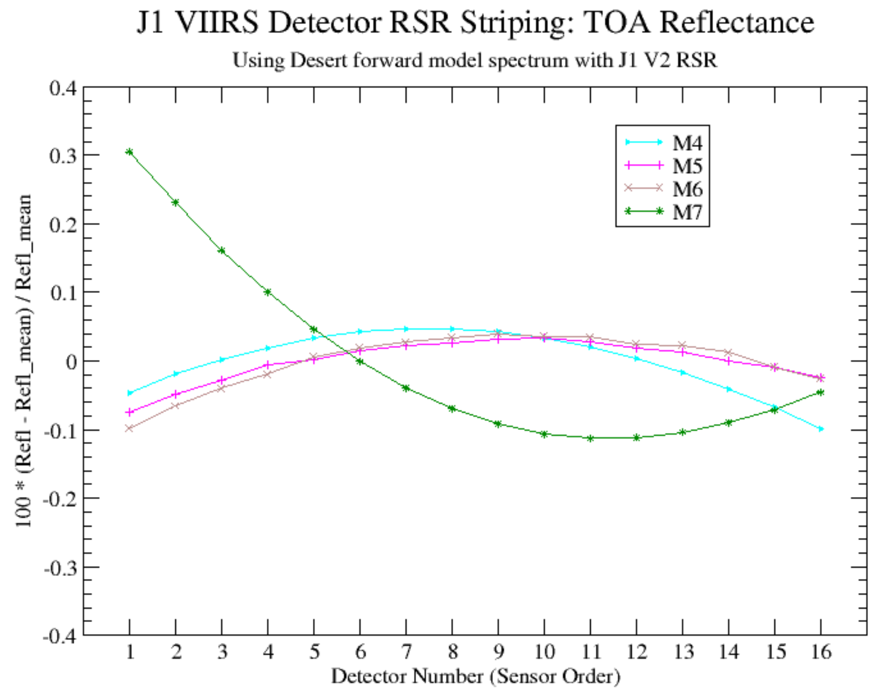

V2 RSR Impact on SDR: TEB

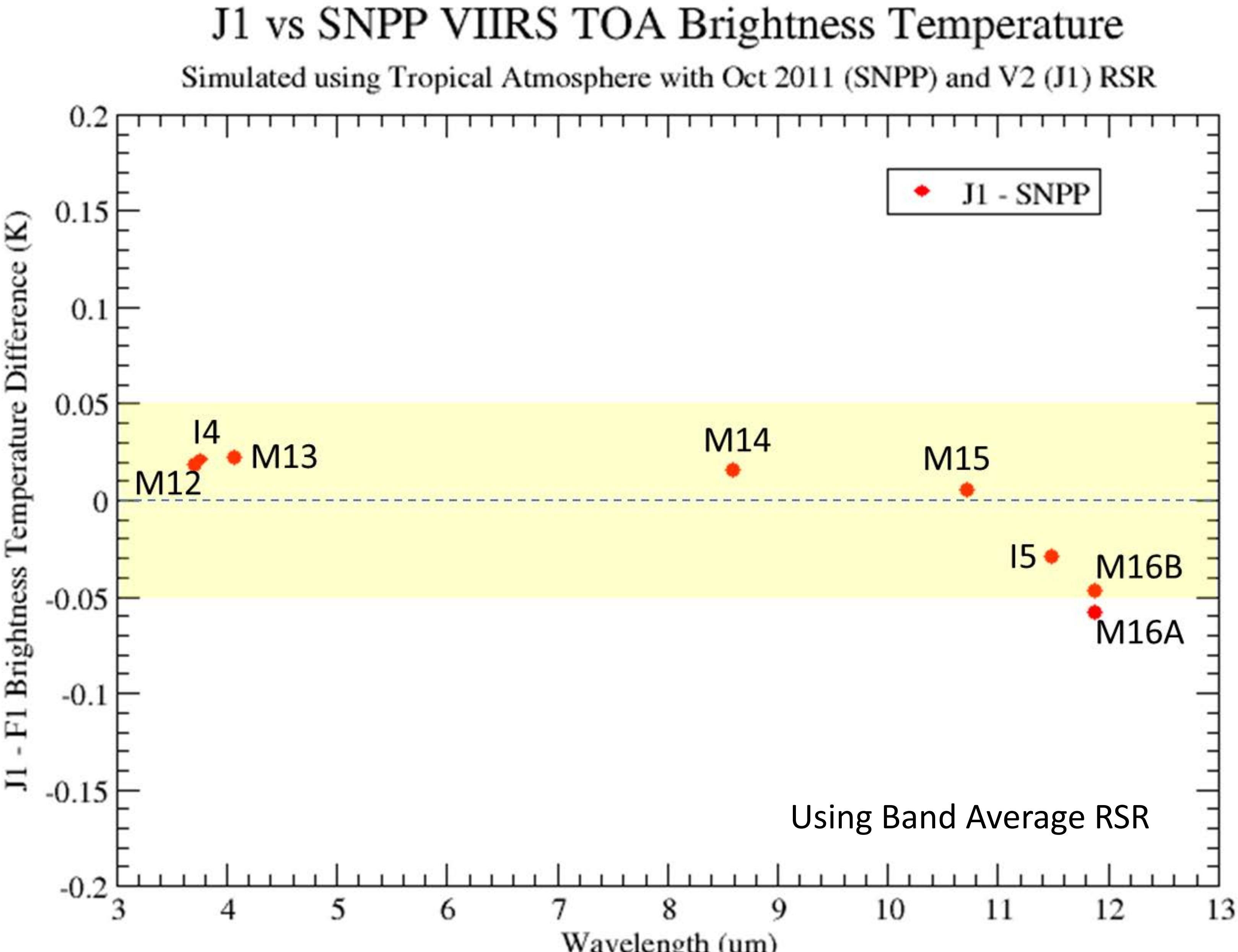

TEB Detector Dependence from RSR

Tropical Standard Atmosphere Model

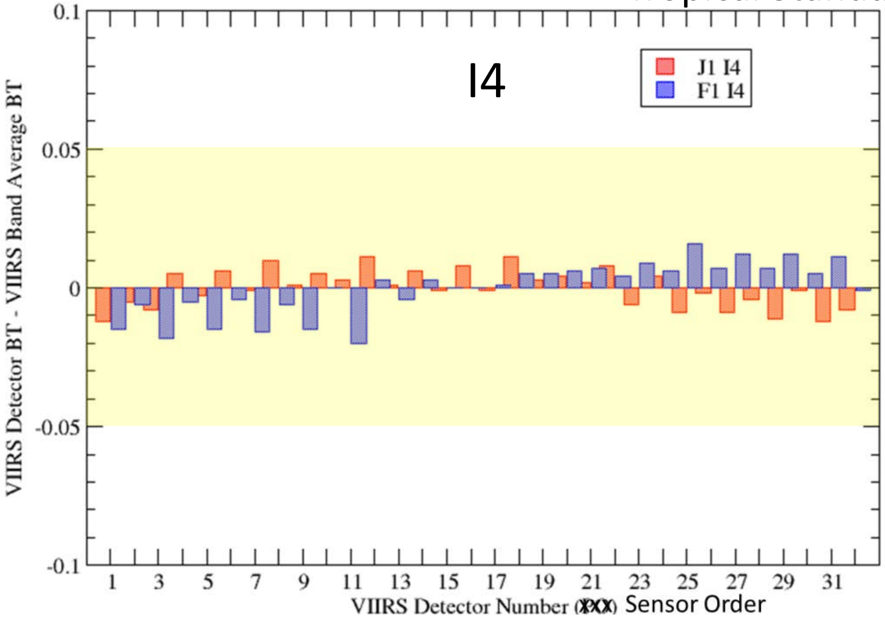

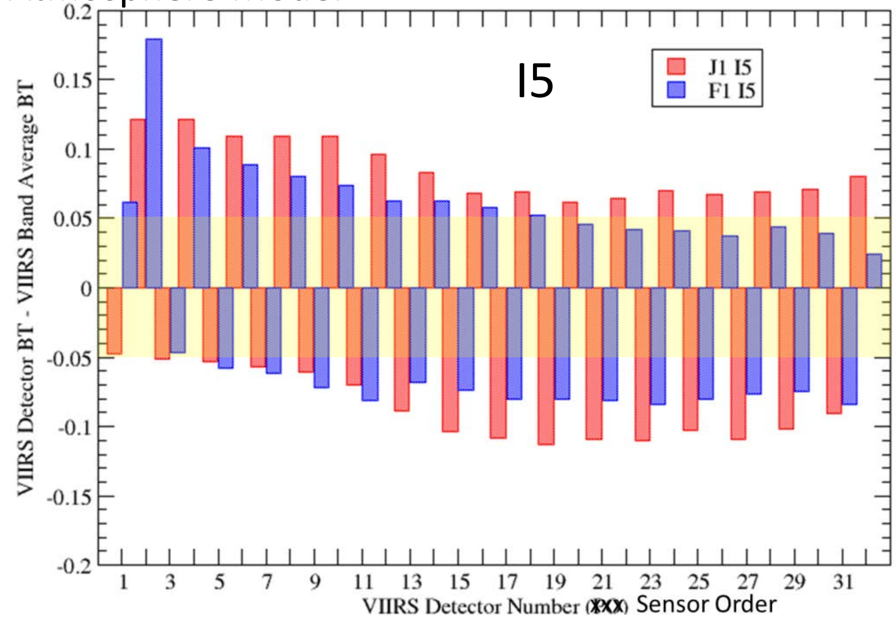

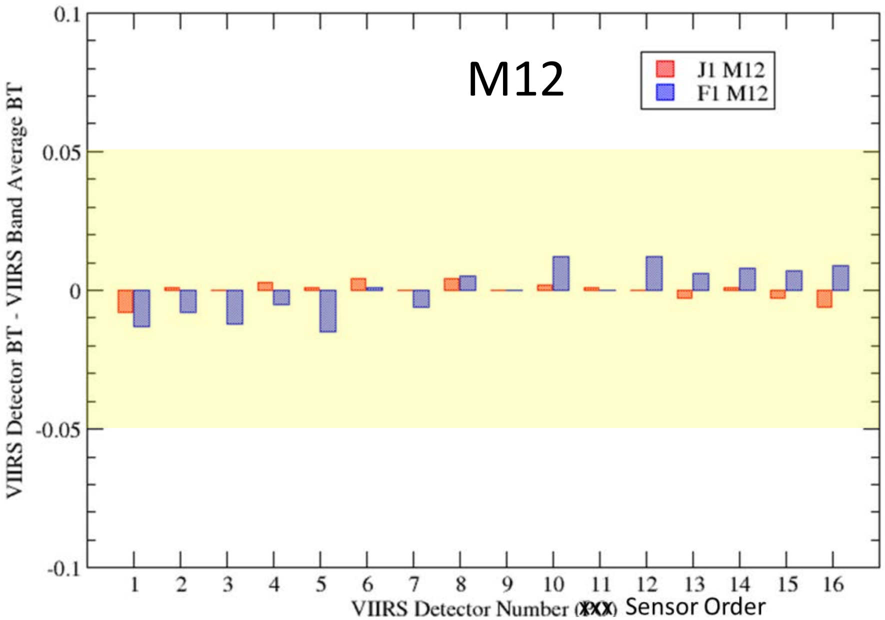

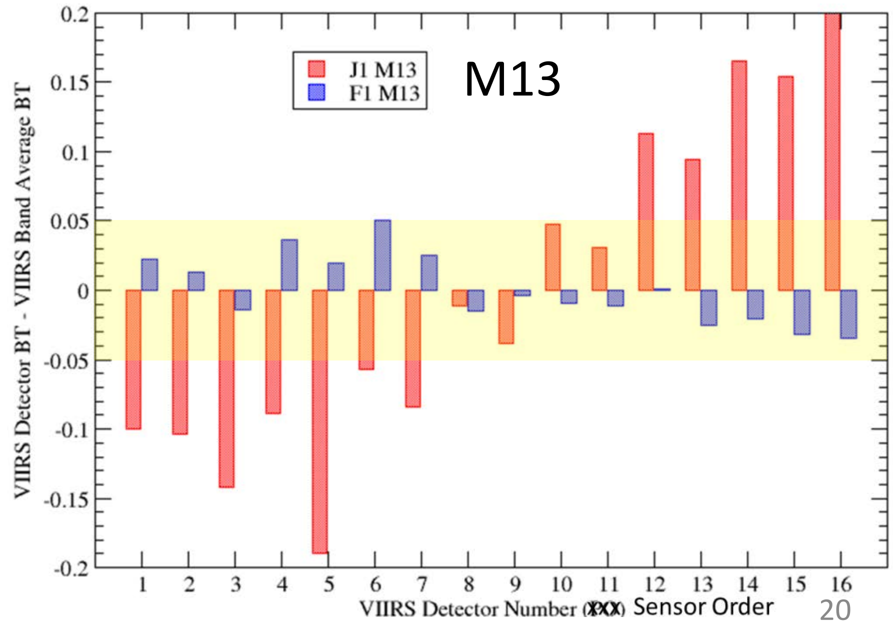

TEB Detector Dependence from RSR

Tropical Standard Atmosphere Model

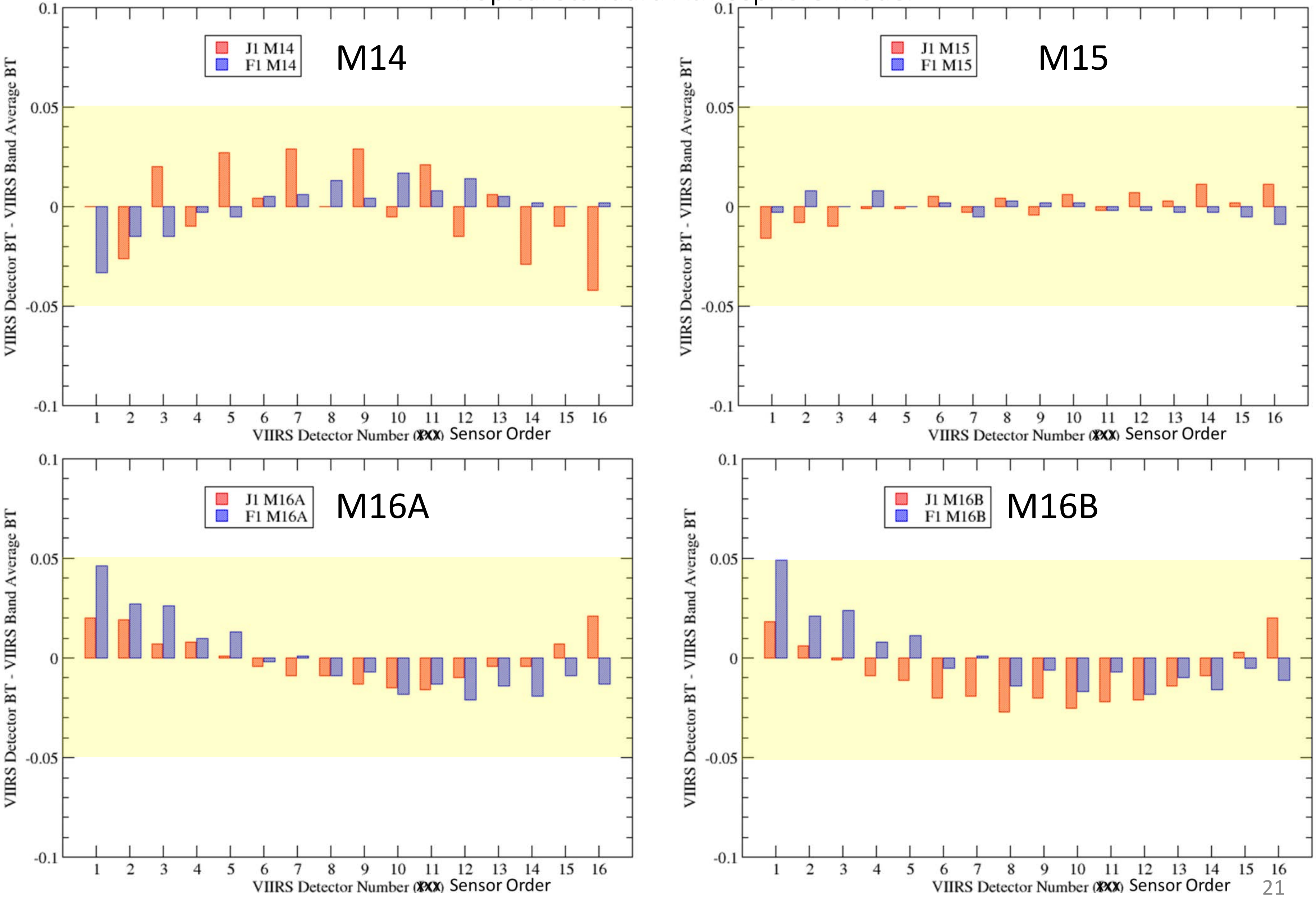

SNPP VIIRS Band I5 in the Indian Ocean

Day 2014080, 065522 UTC

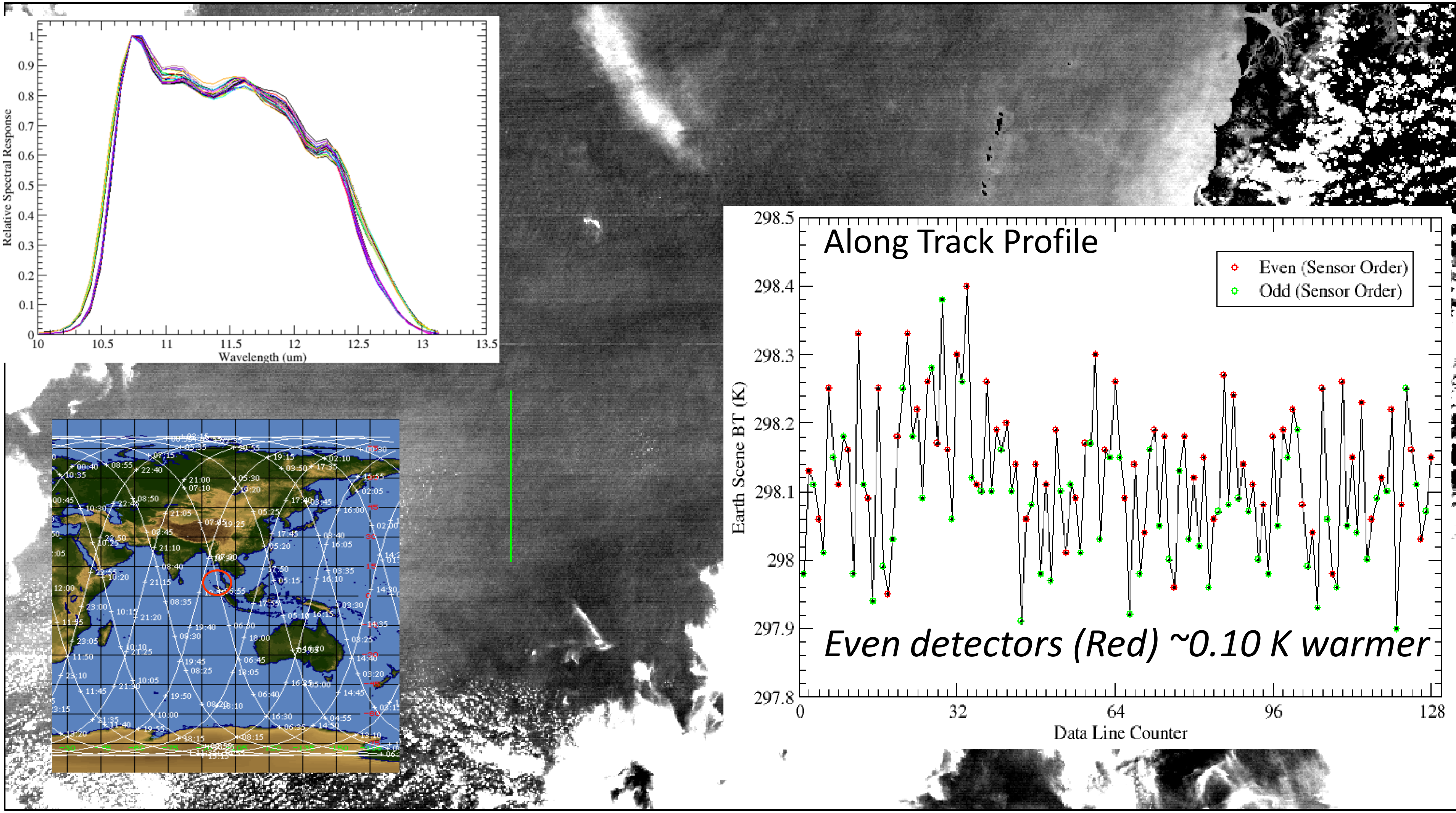

Along track profile taken from position of green line in imagery

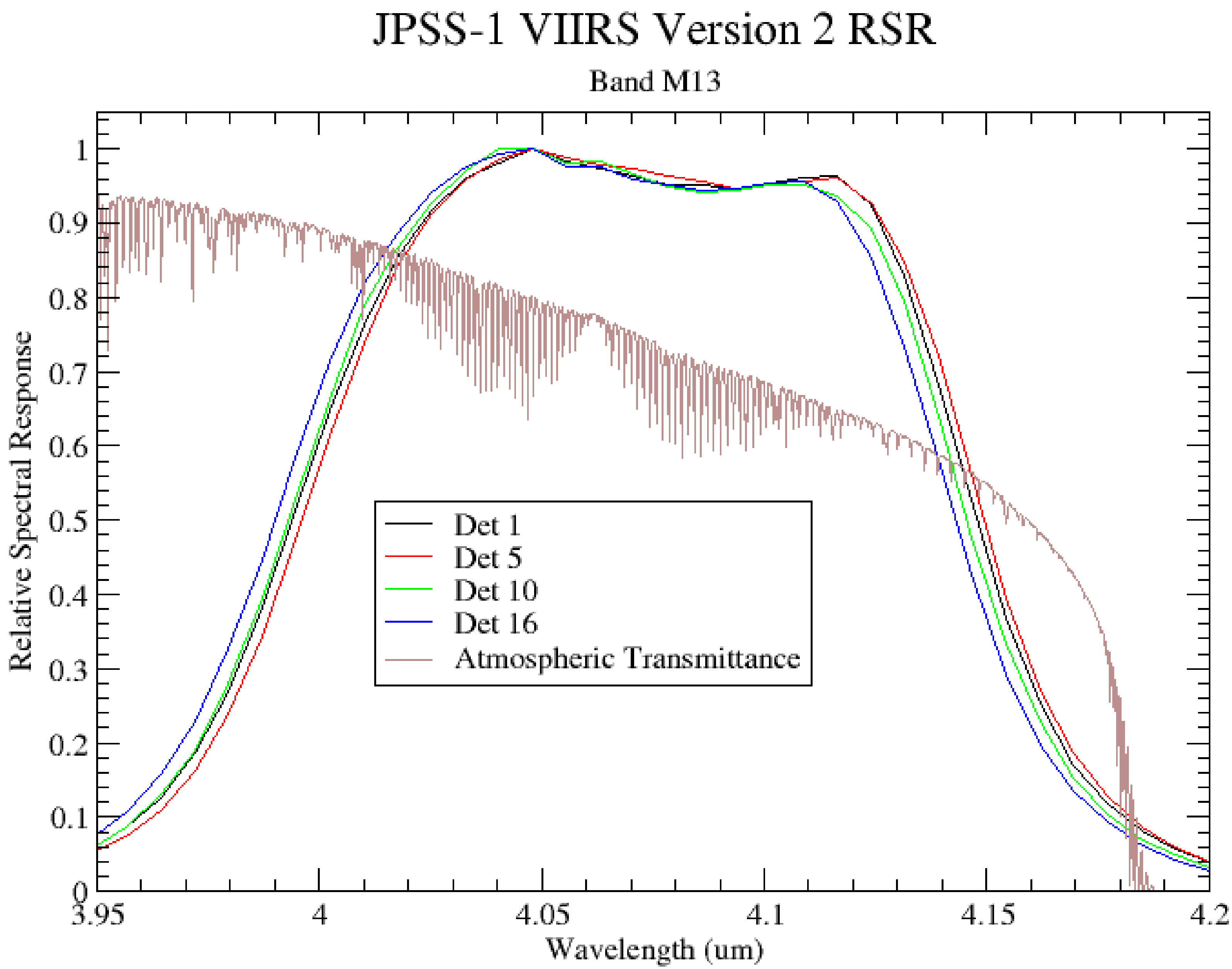

JPSS-1 VIIRS Version 2 RSR
Band M13
Relative Spectral Response
Wavelength (um)
0
0.1
0.2
0.3
0.4
0.5
0.6
0.7
0.8
0.9
1
3.95
4
4.05
4.1
4.15
4.2
Det 1
Det 5
Det 10
Det 16
Atmospheric Transmittance

Summary: JPSS-1 VIIRS RSR Influence on SDR

- Comparisons with SNPP
  - RSB TOA reflectance normalized difference mostly within 1% but as high as 4%
  - TEB TOA BT within about 50 mK
- Detector dependence
  - RSB TOA reflectance variation along focal plane up to 0.5% due to VIIRS non-telecentric optical design.
  - TEB detector striping similar to SNPP except M13 which appears larger.

JPSS-1 VIIRS RSR Availability

- JPSS-1 VIIRS At-launch RSR are awaiting approval for public release. Available now at password-protected NASA eRoom: https://jpss-erooms.ndc.nasa.gov/eRoom/JPSSInstruments/VIIRSF2_JPSS1/0_38007
- Band average and supporting detector RSR (Sensor order numbering), plus Readme and pptx with background information.

Water Vapor Band Trade Study

Slawomir Blonski, ERT, Inc.
Chris C. Moeller, CIMSS, U. Wisconsin
Changyong Cao, NOAA/NESDIS/STAR

JPSS Annual Science Team Meeting (August 9, 2016)

Background

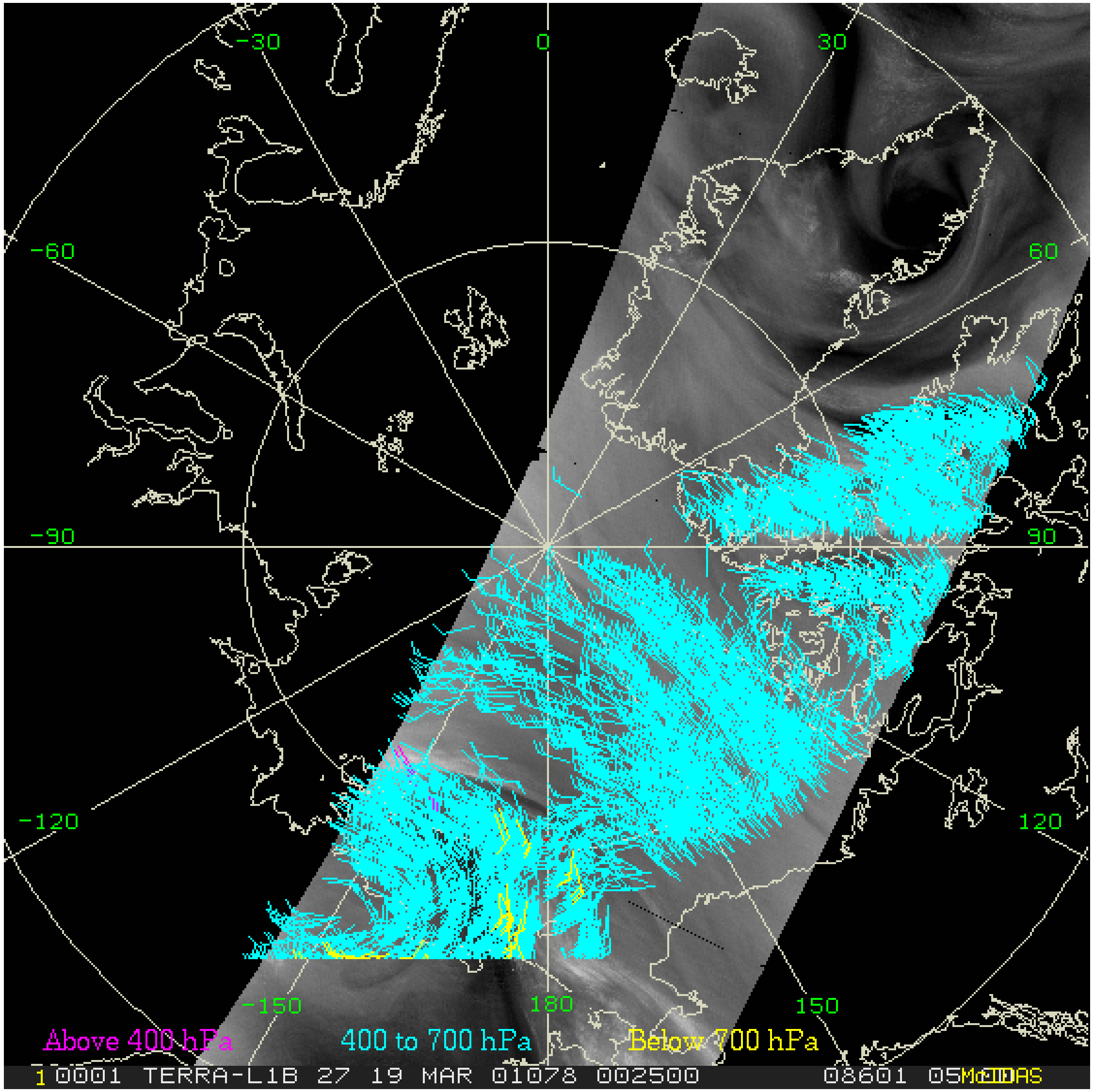

MODIS band 27 water vapor images and derived wind vectors over the North Pole
Courtesy of Paul Menzel, U. Wisconsin

- Polar wind vectors derived from satellite observations of cloud drift and water vapor motion improve weather forecasting
- MODIS instruments provide the cloud- and moisture-tracked winds currently assimilated into numerical weather prediction models
- Next generation weather observations are provided by VIIRS on S-NPP and future JPSS satellites
- VIIRS currently lacks a water vapor band at 6.7 µm, allowing only for cloud-tracking of winds
- An addition of a water vapor band to future VIIRS instruments has been proposed
- Potential impacts of the proposed modifications on VIIRS SDR are presented here

Additional Benefits of VIIRS Water Vapor Band

Improved cloud detection in polar night

Cloud detection over Antarctica
VIIRS data simulated from MODIS
23:40 UTC on 4 June 2001

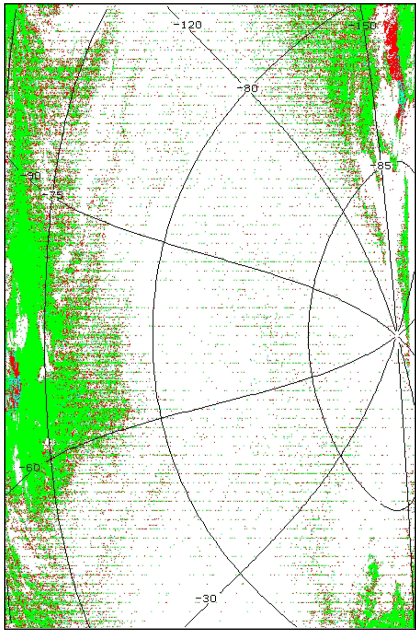

VIIRS cloud mask w/o 11-6.7μm test

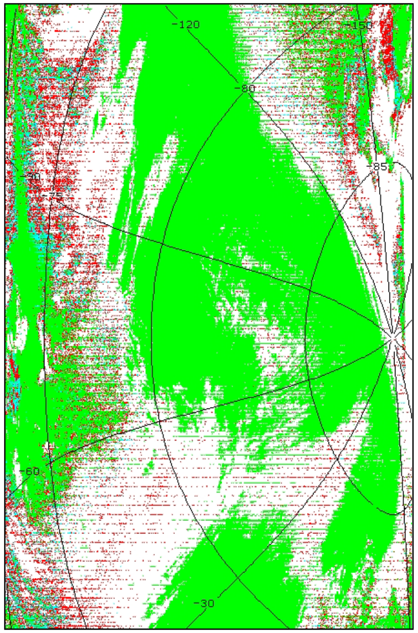

VIIRS cloud mask with 11-6.7μm test

green - clear
white - cloud
red - uncertain

- Better determination of night-time clear sky conditions

Improved cloud height/property retrievals

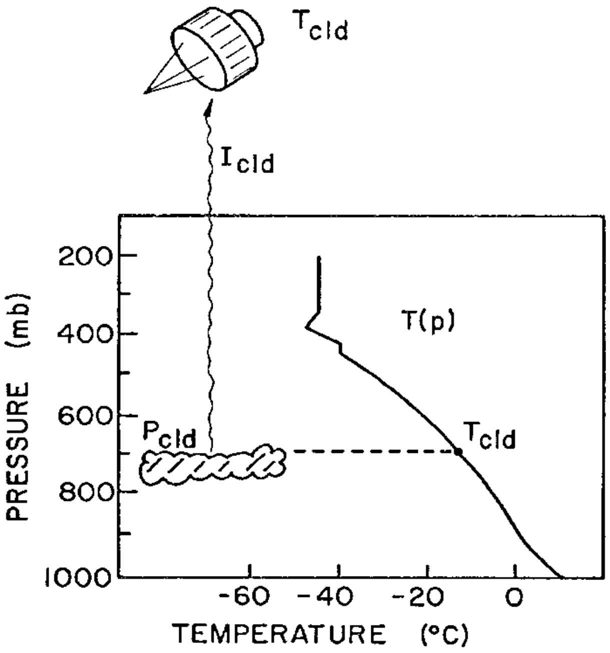

- Traditional relation of opaque cloud height and atmospheric temperature T(p) fails when radiation below cloud leaks thru, e.g., thin cirrus
- VIIRS is struggling to continue the MODIS cloud record without any CO_2 or H_2O sensitive bands

Water Vapor Channel Options

Three options for modifying the instrument have been identified:

1. Adding to the LWIR (long-wave infrared) FPA (focal plane array) one or more bands in the 6.7 µm water vapor spectral region
2. Replacing one of two TDI (time-delay and integration) stages of the M16 band with a water vapor band
3. Replacing an existing, but seemingly redundant spectral band such as M10 with a water vapor one

Option 1 has been studied (Puschell, Kim & Menzel, *AIAA SPACE 2010 Conference & Exposition*), and its feasibility has been confirmed, but necessary changes to the LWIR FPA and electronics can make this option very expensive:

- Additional filters, detectors and associated electronics for water vapor spectral bands
- Possible increase in Dewar window size and possible change in dichroic mirror design
- More mass from additional detector arrays, filters and electronics
- Higher data rate from additional detector samples
- Higher power required for additional detector arrays and electronics
- More heat dissipated by additional detectors and electronics in cold focal plane assembly, which affects cooler margin

M16 TDI Replacement Option

- Out of the three options, option 2 is perhaps the least expensive since it requires only minimal modifications, mainly to the spectral filter and possibly the microlenses: Puschell & Herbst, *Proc. SPIE* **8516** (2012) 851604
  - Band M16 uses TDI from its two components, M16A and M16B, to increase SNR (signal-to-noise ratio) of the measurements
  - Based on on-orbit performance of the S-NPP VIIRS, this redundancy may not be necessary, meaning that M16A alone can meet the performance requirements, and M16B can be changed to a water vapor band
  - In this option, no substantial change occurs in VIIRS system level size, mass, power, and heat dissipated by detectors and electronics in the LWIR FPA
  - In the study presented here, effects of implementing option 2 on M16 SNR have been investigated to assess potential impacts of the modifications on the VIIRS data product users

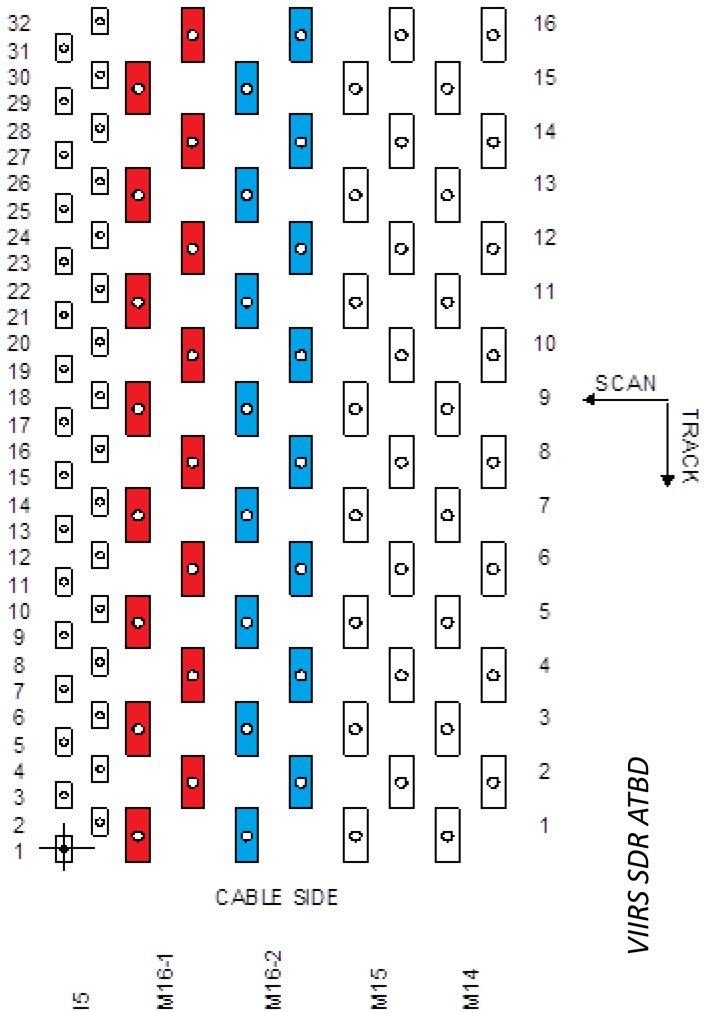

LWIR FPA

M16 SNR Measurements

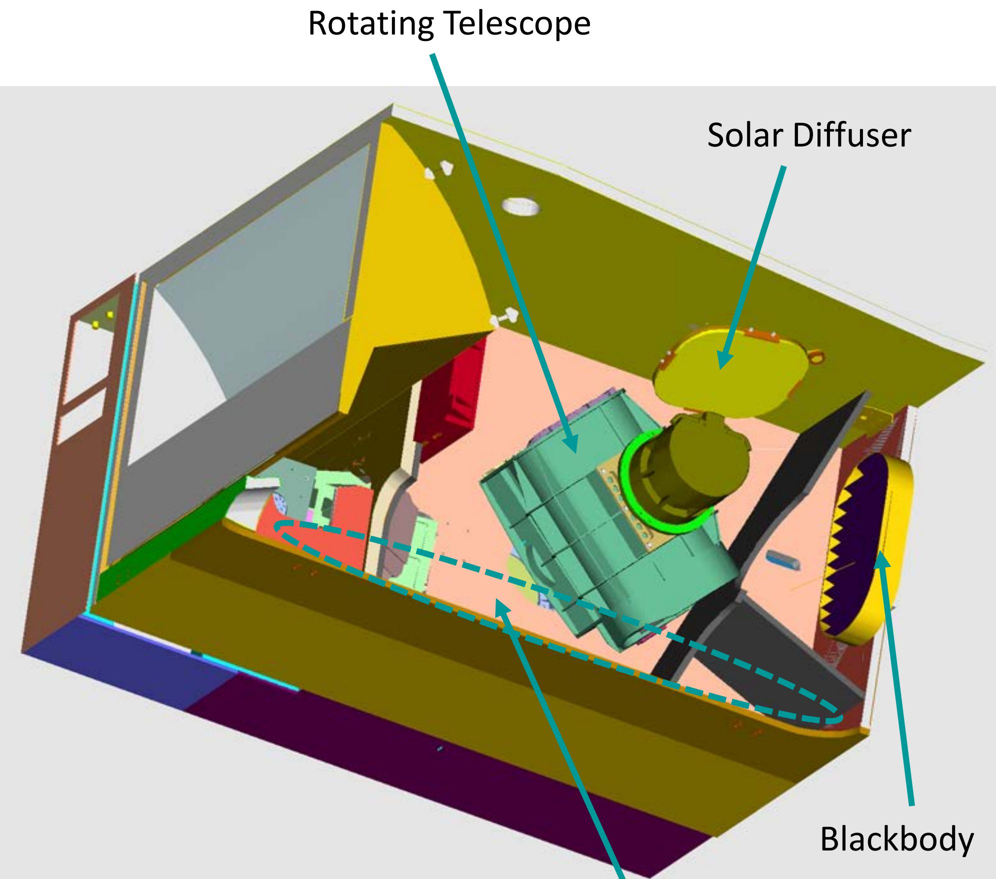

VIIRS SDR User's Guide

- In addition to scanning Earth during each telescope revolution, VIIRS also measures radiance emitted from the blackbody (BB) and from the solar diffuser (SD), which are parts of the onboard calibrator
- While only the combined M16 data are available from the Earth observations, the BB/SD calibrator data are provided separately for M16A and M16B
- During each scan, 48 measurements are collected for each M16 detector from BB and SD as well
- **SNR = mean(ΔDN) / st.dev.(ΔDN)** is calculated from the 48 samples (without outlier rejection); the signal (ΔDN) includes Space View (SV) subtraction

SNR Comparison for BB and SD Measurements

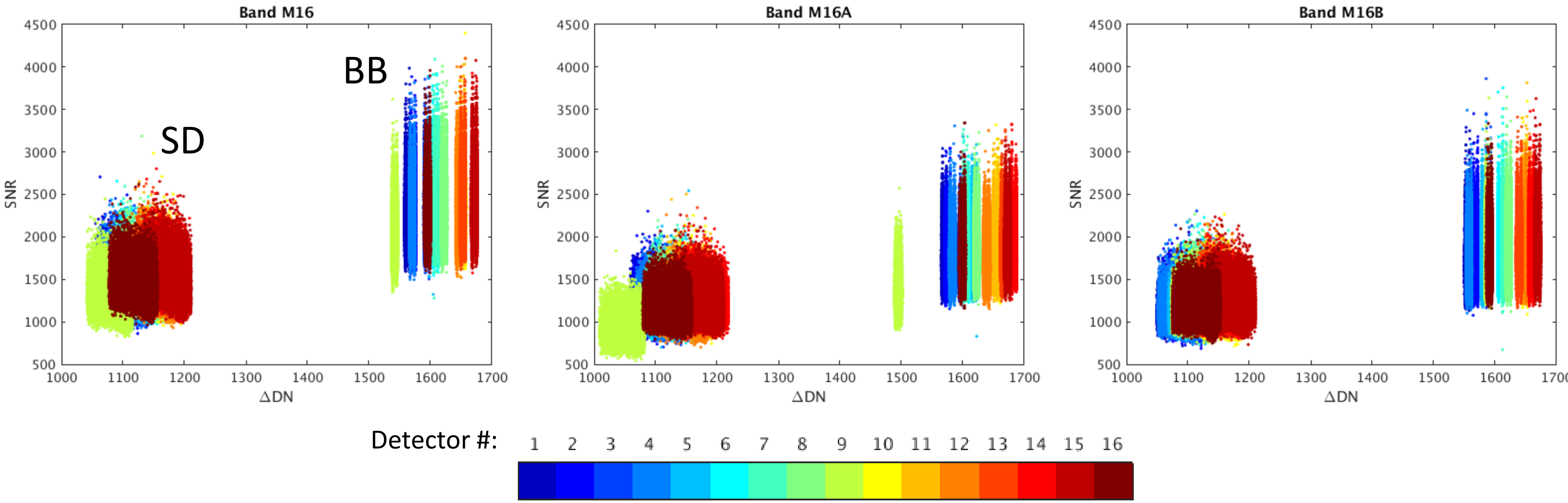

- BB and SD data from all S-NPP orbits on September 23, 2015 are analyzed (~48,000 scans) for each of the bands M16, M16A, and M16B
- SNR data for each detector are shown on the graphs with a different color, with both HAM (half-angle mirror) sides analyzed together
- 14-bit BB/SD measurements are truncated to 12 bits to match the Earth observations
- BB temperature is stable throughout each orbit while SD temperature varies
- M16 SNR improvement by averaging M16A and M16B can be seen
- M16A detector #9 is out-of-family with lower gain and SNR;
  TDI partially mitigates this non-uniformity

M16A/B vs. M16 SNR Comparison

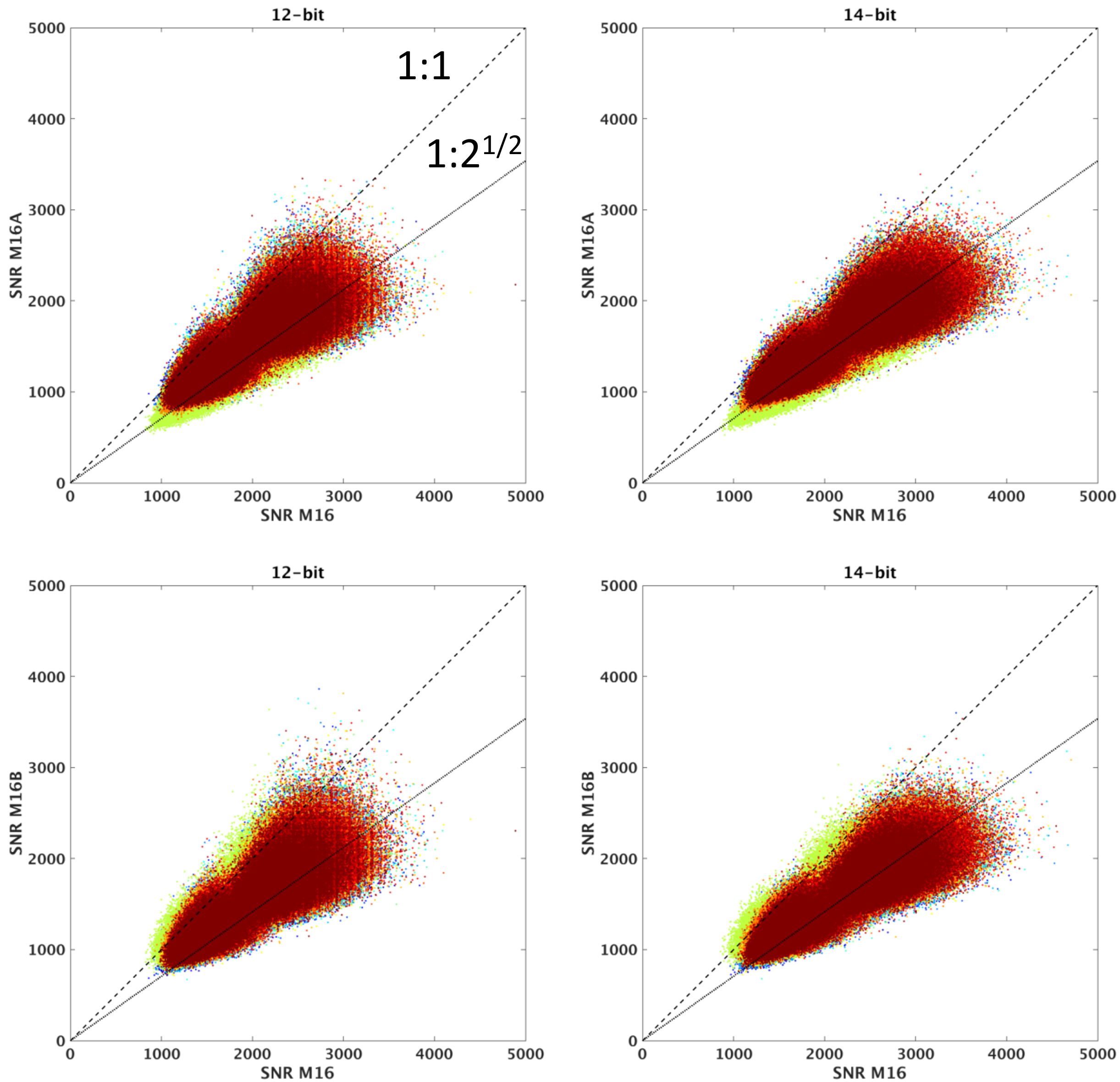

- M16 SNR is larger by the factor of square root of 2 than SNR for either M16A or M16B, as predicted by statistics
- There is only a small impact from the 12-bit quantization
- M16 NEΔT measured in prelaunch tests and on orbit has a large margin (~100%) from the NEΔT requirement
- Without TDI, M16 NEΔT would still be within the requirement (increase from 0.03 K to ~0.04 K)
- However, potential FPA non-uniformity would not be reduced

SNR for M10 Replacement with Aggregated I3

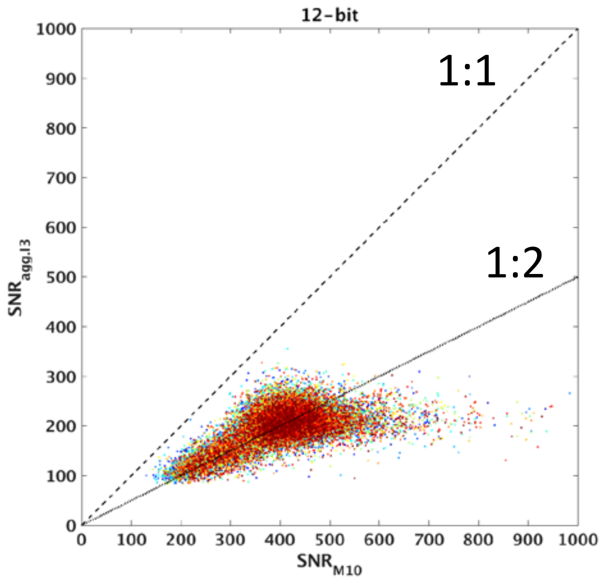

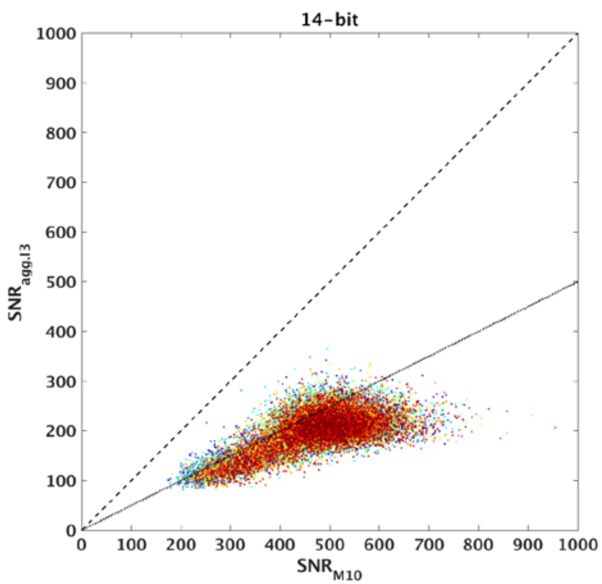

- In option 3, the additional, water vapor channel could replace a 750-m channel at 1.6 µm (M10) that shares spectral response characteristics with a 375-m channel (I3)
- M10 data would then be synthesized by the 2-by-2 aggregation of I3 pixels
- SNR for the actual and synthesized band M10 was calculated from measurements of light reflected from the SD during solar calibration events occurring on each satellite revolution around the Earth near the night/day terminator crossing in the southern hemisphere
- September 23, 2015 data were used in this study
- SNR of synthesized M10 (aggregated I3) is always lower than SNR of actual M10
- On averaged, SNR differs by a factor near 2 (especially with the 12-bit quantization)
- Apparently, pixel field-of-view and integration time differences between the I3 and M10 bands are not compensated by the spatial aggregation of the I3 pixels
- Band I3 with the 2-by-2 pixel aggregation can be substituted for M10, but with a reduced SNR

Option of Replacing M10 with Aggregated I3

- Prelaunch tests have shown that the M10 SNR exceeds the requirements by a factor larger than two
- Thus, even with the 50% reduction shown on the previous chart, the synthesized M10 should fulfill the requirements, although with only a small margin

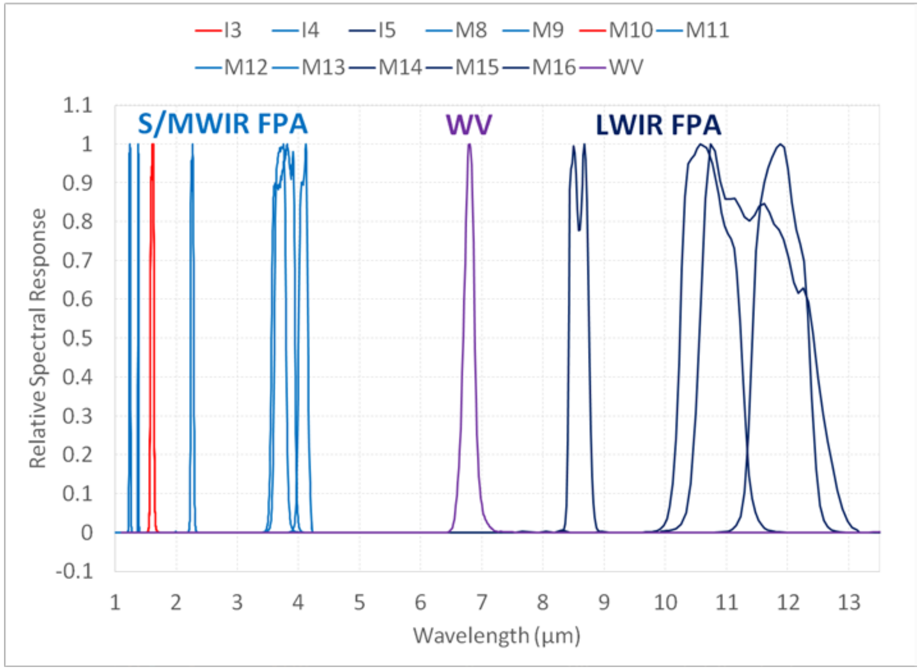

- However, detectors for bands M10 and I3 are located on the S/MWIR (short-/mid-wave infrared) FPA, and all bands from that FPA have spectral responses in the range of 1.2 to 4.1 µm
- Since the water vapor (WV) band is proposed to be at 6.7 µm, extensive modifications of the S/MWIR FPA may be needed to ensure the required spectral response of the water vapor band

Summary

- From the three options that were identified for adding a water vapor band to VIIRS, creating new detectors on the LWIR FPA is preferable for the data users because of the minimal impact on the other bands, but this option also requires the most extensive hardware modifications
- Removing TDI from band M16 and using the second set of the M16 detectors for the water vapor band will increase M16 noise, but a substantial margin from the noise requirement will remain
  - Without TDI risk of non-uniformity for M16 will be similar to the other thermal emissive bands such as M15
  - This option may be preferable because it requires fewer hardware modifications than the one above
  - Additional analysis using M16A and M16B data will be needed to fully assess the impact on SST
- Replacing M10 with aggregated I3 data and using the M10 detectors for the water vapor band will reduce M10 SNR to a level that would leave no margin from the requirements
  - This option may also require extensive hardware modifications because of the large wavelength difference between the water vapor band and the one it would replace

VIIRS RSB Calibration for Ocean Color Applications

Junqiang Sun[1,2] and Menghua Wang[1]

[1]NOAA/NESDIS Center for Satellite Applications and Research
E/RA3, 5830 University Research Ct., College Park, MD 20740, USA
[2]Global Science and Technology, 7855 Walker Drive, Maryland, USA

8/9/2016 13:15-13:35 PM

Outline

- Introduction
  - VIIRS Instrument Background
  - Reflective Solar Bands (RSB) On-Orbit Calibration
- SDSM Calibration
  - Algorithms, data analysis, and performance
- SD Calibration
  - Algorithms, data analysis, and performance
- Lunar Calibration
  - Algorithms, data analysis, and performance
- Hybrid Approach
  - Algorithms and hybrid calibration coefficients
- Improvements in Ocean Color Products
- Summary

VIIRS Background

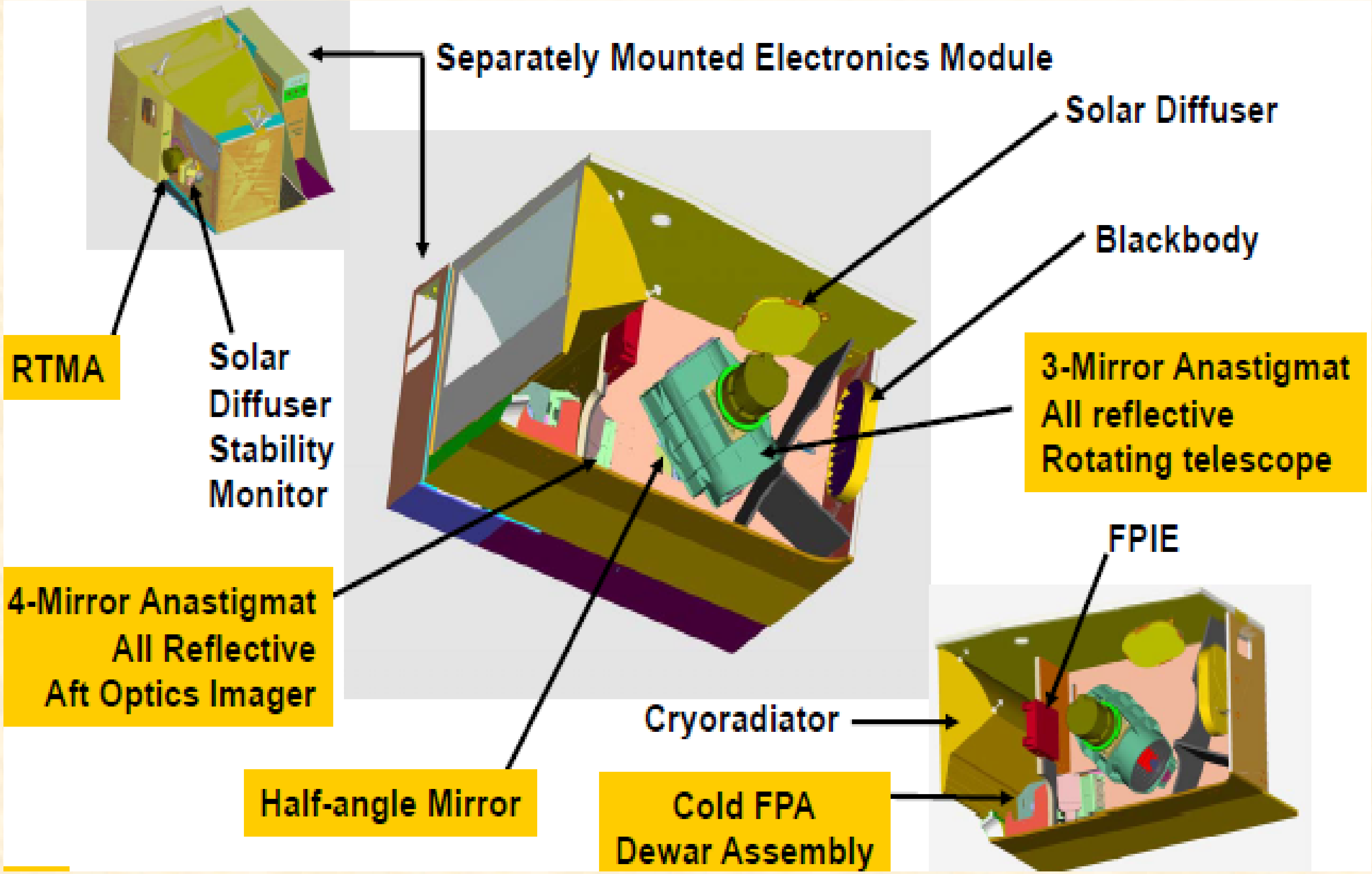

RSB On-Orbit Calibration

- 22 spectral bands - 410 nm to 12.013 μm spectral range
- 14 Reflective Solar Bands (RSB) : 3 image bands, I1-I3, and 11 moderate bands, M1-M11
- The VIIRS RSB are calibrated on orbit by SD/SDSM calibration
- Monthly lunar observation through its space view (SV) since launch.
- For VIIRS, the angle of incidence (AOI) of the SV is exactly the same as that of the SD. Lunar observations should provide identical on-orbit gain change for VIIRS RSB as SD/SDSM calibration.

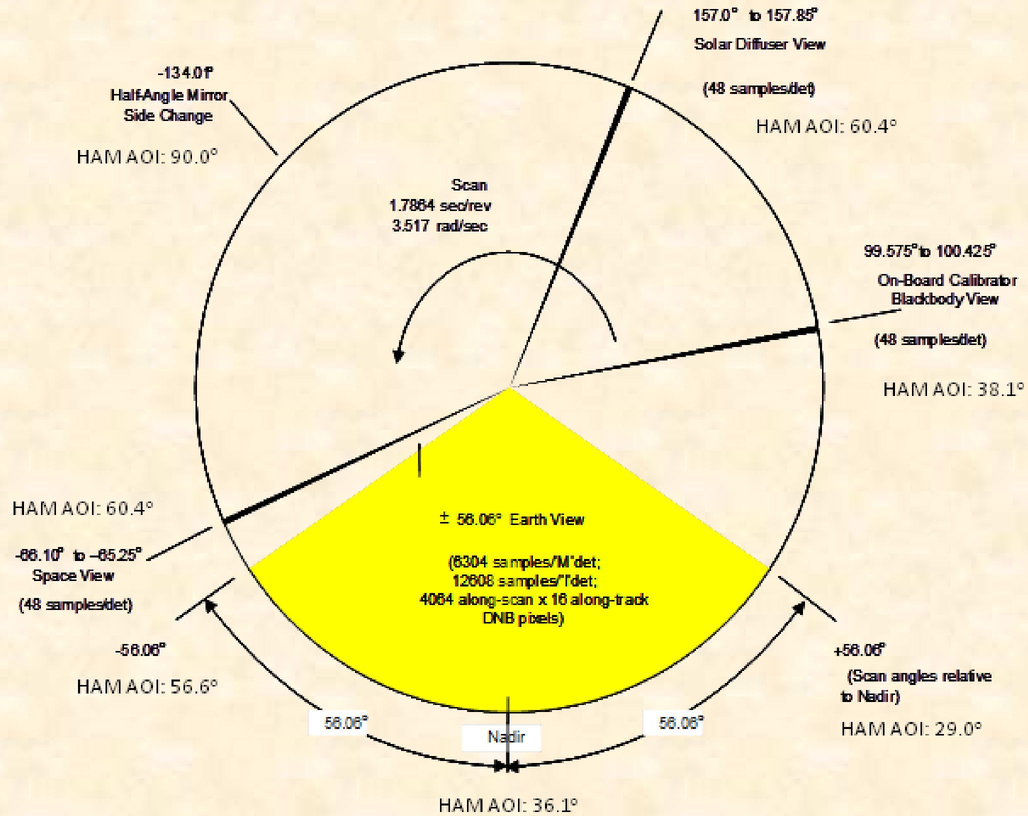

VIIRS RSB uncertainty specification is 2%; For ocean color EDR products, the ocean bands (M1-M7) are required to be calibrated with an uncertainty of ~0.1-0.3%.

Key Improvements: Overview

- BRF and VF from yaw measurements
  - Modified procedure
  - Proper data selection
- H-factors (SD degradation from SDSM)
  - Correct initial characterization
  - Identified "SD degradation nonuniformity effect"
- F-factors (RSB Calibration Coefficients)
  - time-dependent relative-spectral-response
- New: Hybrid Coefficients
  - Improved lunar results – geometrical factor
  - Combination algorithm

(*Each step has been thoroughly described in publication*)

Part 1: Standard RSB Calibration with Solar Diffuser

- Solar Diffuser provides quantifiable illumination on orbit
- Currently the official calibration baseline

SD/SDSM Calibration Overview

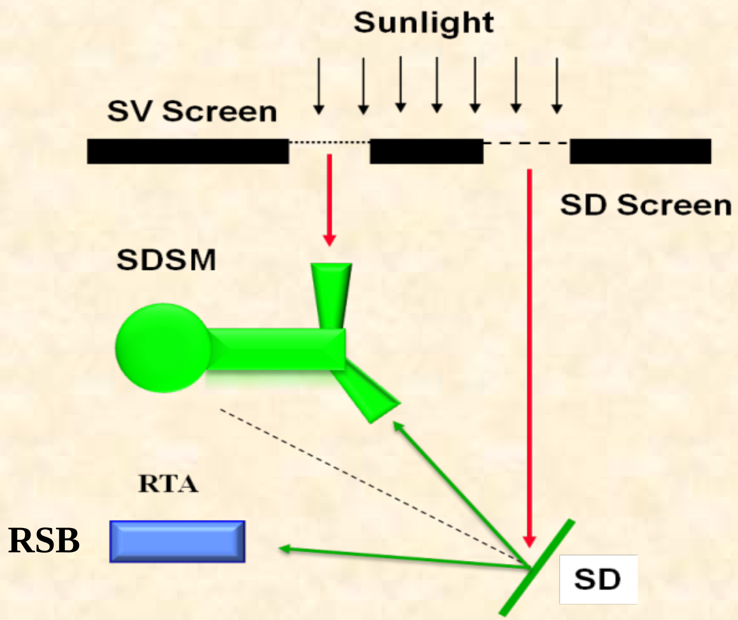

- *SD and SDSM sun view screens:*
  - *Prevent RSB and SDSM saturation*
  - *Vignetting functions (VFs)*
  - *VFs measured prelaunch and validated by yaw measurements*
  - *SD bidirectional reflectance factors (BRFs)*
- *BRFs measured prelaunch and validated by yaw measurements*
  - *SD on-orbit degradation is tracked by the SDSM measurements at 8 wavelength from 412 nm to 935 nm*

- ***Key assumption: SD degrades uniformly with respect to both incident and outgoing directions***

Fist step: Carefully derive BRFs and VFs from the yaw measurements

J. Sun and M. Wang, "On-orbit characterization of the VIIRS solar diffuser and solar diffuser screen," Appl. Opt., 54, 236 -252 (2015).

SDSM Calibration Algorithm

- SDSM is a ratio radiometer, which views SD, Sun, and an internal dark scene successively in three-scan cycles.

- SD BRF for SDSM view direction

$$BRF_{SD,SDSM}(\lambda) = \rho_{SD,SDSM}(\lambda)H(\lambda)$$

  - $\rho_{SD,SDSM}(\lambda)$: Prelaunch BRF for SDSM view direction
  - $H(\lambda)$ is solar diffuser degradation since launch

- SD degradation, H factors, for SDSM view direction at the wavelength of the SDSM detector D

$$H(\lambda_D) = \left\langle \frac{dc_{SD,D}}{\rho_{SD,SDSM}(\lambda_D)\tau_{SDS}\cos(\theta_{SD})} \right\rangle_{Scan} \Bigg/ \left\langle \frac{dc_{SV,D}}{\tau_{SVS}} \right\rangle_{Scan}$$

- ***Improvements***
  - ***Carefully derived the VFs and BRFs from yaw measurements***
  - ***Ratio of the averages***
  - ***Sweet spots selection***

SDSM operations: Every orbit first few months, then once per day for about two years, and once per two days since May, 2014.

J. Sun and M. Wang, "Visible infrared image radiometer suite solar diffuser calibration and its challenges using solar diffuser stability monitor," Appl. Opt., 53, 8571-8584 (2014).

SDSM Calibration Results

SD Degradation (H-Factors)

Sweet spots

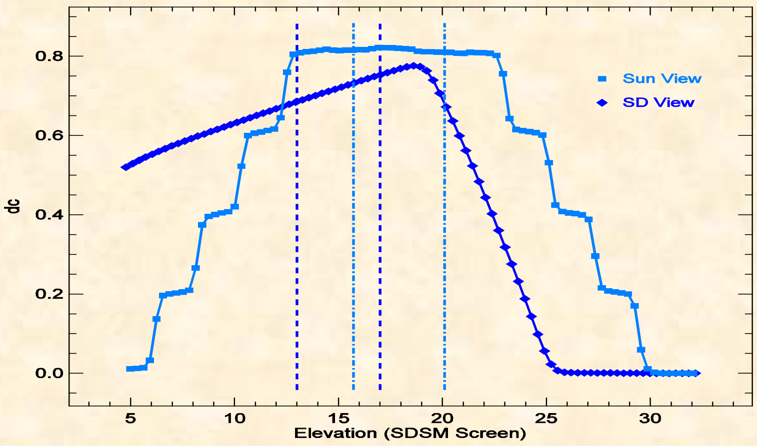

SD Degradation – First 70 days

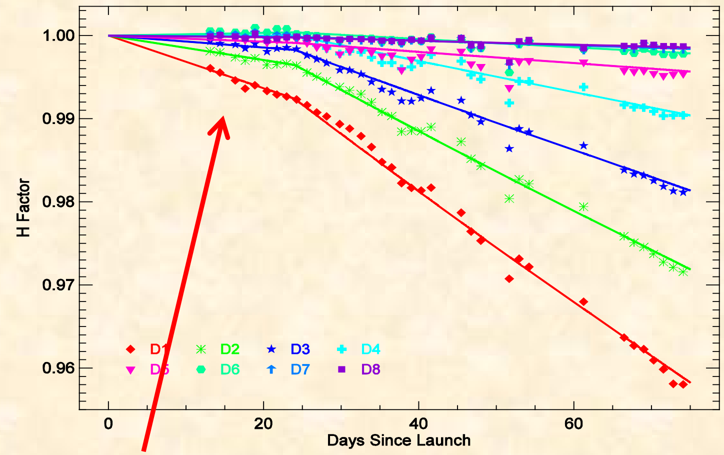

SD degradation

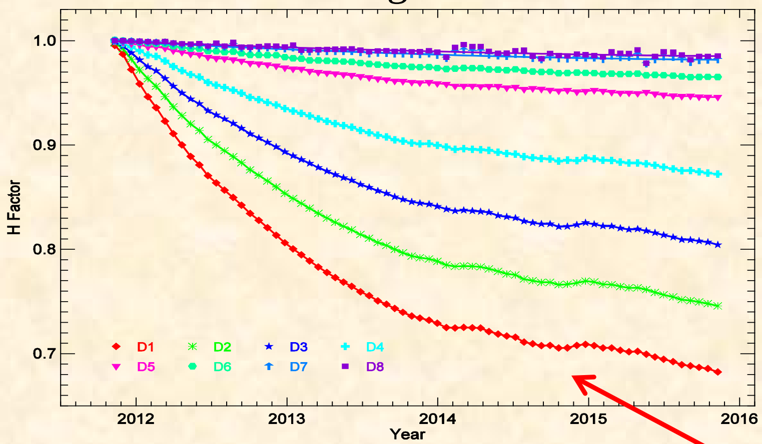

- ***First 25 days must be done right, or 1% error!***
- ***Results very stable, very accurate, no average over orbit, no smoothing, actual measurements***
- ***SDSM can accurately track the SD degradation for SDSM direction***
- ***But in different direction from RSB view direction – KEY ISSUE***
- ***Unexpected but real degradation (Nov., 2014)***

J. Sun and M. Wang, "Visible infrared image radiometer suite solar diffuser calibration and its challenges using solar diffuser stability monitor," Appl. Opt., 53, 8571-8584 (2014).

SD Calibration Algorithm

- SD is made of Spectralon®, near Lambertian property
- Solar radinace reflected by the SD

$$L_{SD}(\lambda) = I_{Sun}(\lambda)\cdot\tau_{SDS}\cdot\cos(\theta_{SD})\cdot\rho_{SD,RTA}(\lambda)\cdot h(\lambda)/d_{VS}^2$$

  - $\rho_{RSD,RTA}(\lambda)$: Prelaunch BRF for RTA view direction
  - $h(\lambda)$: SD degradation for SDSM view direction is used as the SD degradation for the RTA direction

- RSB calibration coefficients, F factors

$$F(B,D,M,G) = \frac{RVS_{B,SD}\cdot\int RSR_B(\lambda)\cdot L_{SD}(\lambda)\cdot d\lambda}{\sum_i c_i(B,D,M,G)\cdot dn^i\cdot\int RSR_B(\lambda)\cdot d\lambda}$$

  - *B, D, M, G*: Band, Detector, HAM side, and gain status

J. Sun and M. Wang, "On-orbit calibration of Visible Infrared Imaging Radiometer Suite reflective solar bands and its challenges using a solar," Appl. Opt., 54, 7210-7223 (2015).

SD Calibration: Every orbit

- ***Improvements***
  - ***Carefully derived the VFs and BRFs from yaw measurements***
  - ***Improved H factors***
  - ***Sweet spot selection***
  - ***Time-dependent RSR***

SD Calibration Results

RSB Calibration Coefficients (SD F-Factors)

Sweet spot

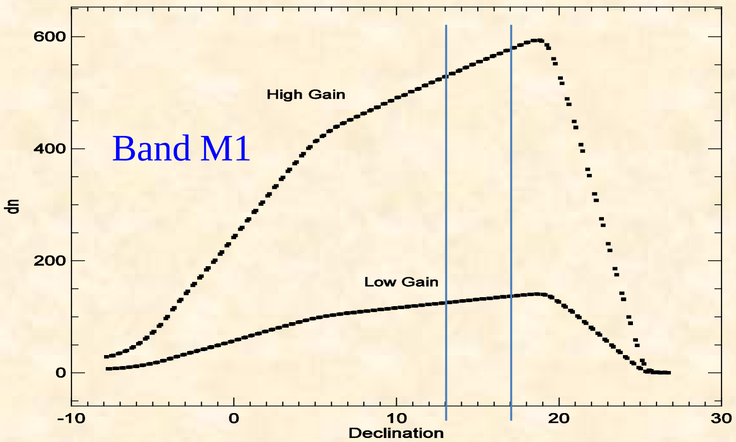

Band averaged HAM 1 HG F-factors

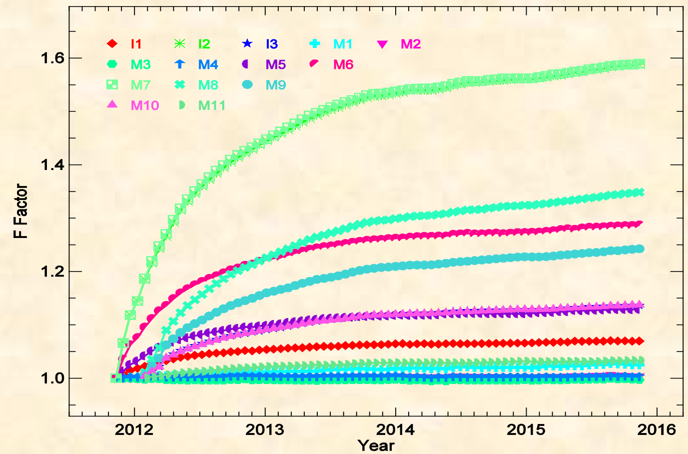

HG = High Gain
LG = Low Gain

Band M1 HAM 1 HG F-factors

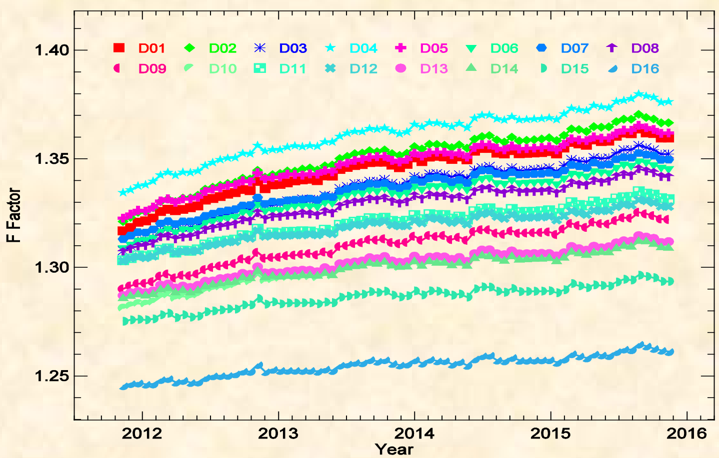

Band averaged gains

- ***SD can accurately track the RSB gain change as long as SD degradation for the RTA view can be approximated as that for the SDSM view.***
- ***Stable and smooth***

Part 2: Lunar Calibration

- Not an official part of the RSB official calibration algorithm
- Not in IDPS processing
- Important calibration baseline

Lunar Calibration Algorithm

- Moon is very stable in its reflectance

- RSB calibration coefficients , F factors, from lunar observations

$$F(B,M) = \frac{g(B)N_{t,M}}{\sum_{D,S,N} L_{pl}(B,D,S,N)\delta(M,M_N)},$$

  - *g(B)*: View geometric effect correction (ROLO lunar model and extra correction)

SNPP VIIRS is scheduled to view the Moon approximately monthly (about nine months every year)

- ***Advantages***
  - ***Lunar surface reflectance has no observable degradation***
  - ***Can be used for inter-comparison***

J. Sun, X. Xiong, and J. Butler, "NPP VIIRS on-orbit calibration and characterization using the moon", Proc. SPIE, 8510,85101I, (2012).
X. Xiong, J. Sun, J. Fulbright, Z. Wang, and J. Butler, "Lunar Calibration and Performance for S-NPP VIIRS reflective Solar Bands", IEEE Trans. Geosci. Remote Sens., **54**, 1052-1061, (2016).

Lunar Calibration Results

RSB Calibration Coefficients (Lunar F-Factors)

Lunar image (M6 in April, 2012)

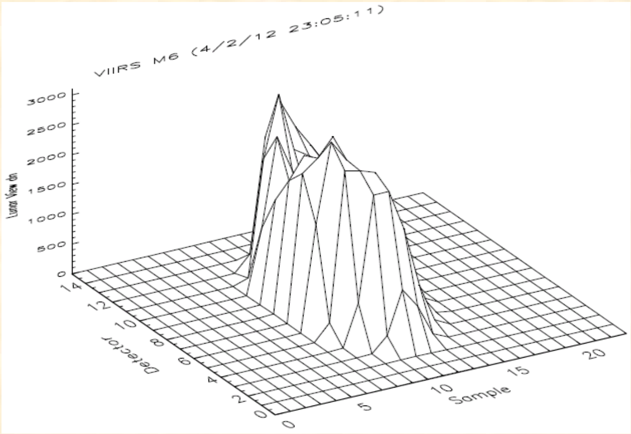

Lunar and SD F factors (M1-M4)

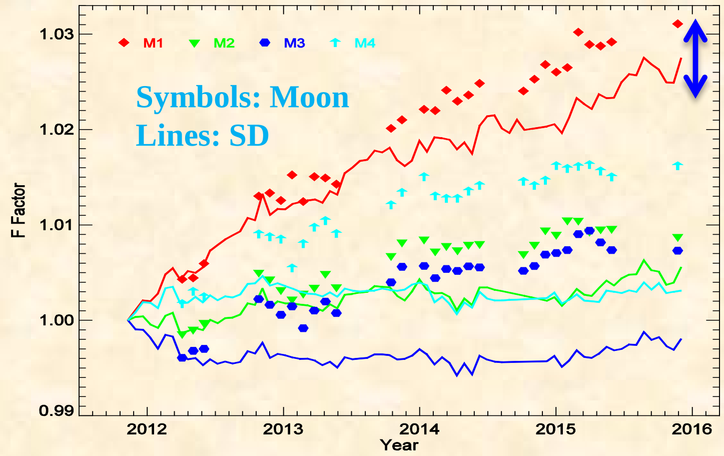

Ex: Relative Bias

Lunar and SD F Factors

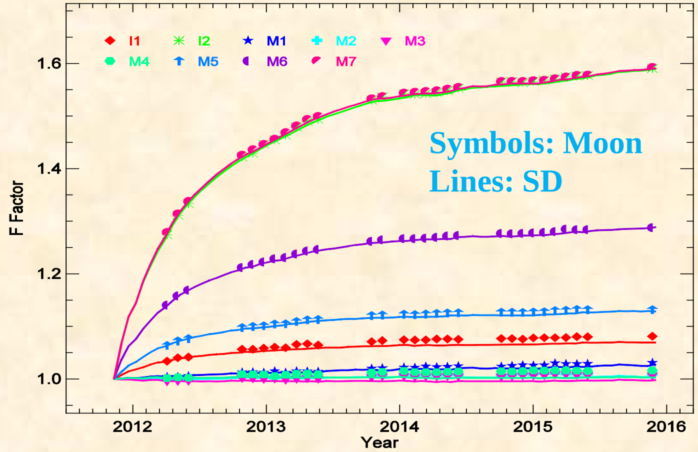

- ***Own Lunar model and correction beyond ROLO model***
- ***New Lunar results much improved – smooth, no oscillation***
- ***0.2% stability***
- ***The differences between the SD F-factor and lunar F-factors diverge, especially for short wavelength RSB***
- ***Which is correct?***

Part 3: Hybrid Methodology Mitigation

- Essential mitigation
- Takes full advantage of the strength in both SD/SDSM and Lunar Calibration Results

Non-Uniformity of the SD Degradation

Non-uniformity of SD degradation

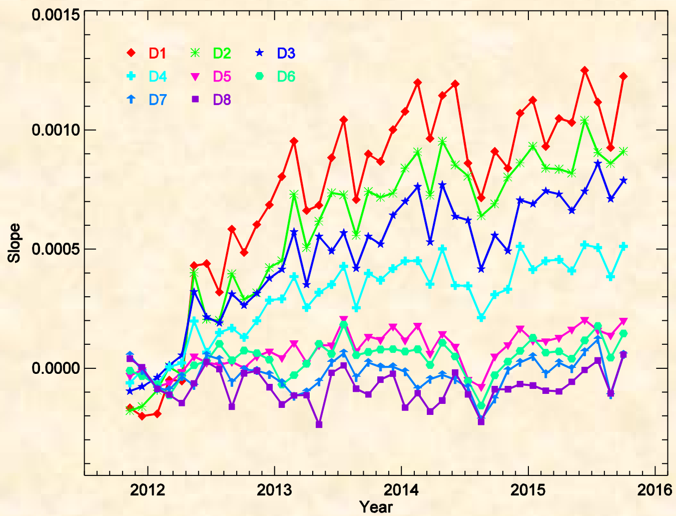

Slopes of H-factors in each individual event with respect to solar declination

SDSM and RTA views

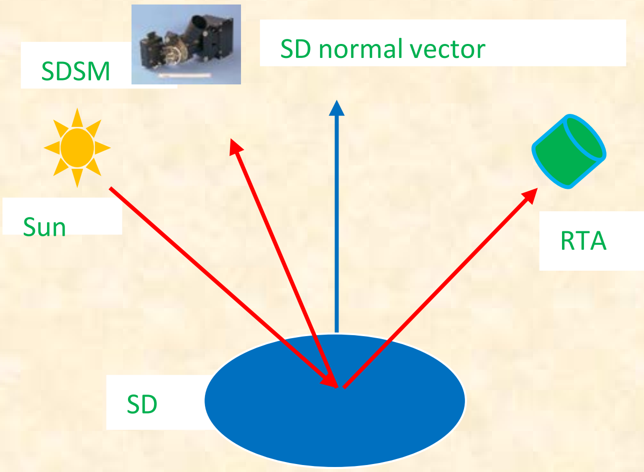

- SD degrades non-uniformly with respect to the incident angle for SDSM view direction
- According to *optical reciprocity*, then SD also degrades non-uniformly with respect to the outgoing direction
- SD calibration is may bring non-negligible errors for RSB characterization

J. Sun, M. Chu, M. Wang, "Degradation nonuniformity the solar diffuser bidirectional reflectance distribution factor," Appl. Opt., 55, 6001-6016 (2016).

Hybrid Approach

- SD Calibration
  - SD degrades non-uniformly, resulting long-term drifts
  - Results are stable and smooth
  - Observation in every orbit
- Lunar Calibration
  - No degradation issue
  - Infrequent and no observation in three months every year

- **Hybrid Approach**

F-Factors Ratios are fitted to quadratic polynomials of time

$$\mathcal{F}(B,D,M,G) = R(B,t) \cdot F(B,D,M,G)$$

$$R(B,t) = \left\langle f(B,M,t) \right\rangle_M / \left\langle F(B,D,M,0,t) \right\rangle_{D,t-15<t_i<t+15,M}$$

  - **Lunar calibration provides long-term baseline**
  - **SD calibration provides smoothness and frequency**

- *J. Sun and M. Wang, "Radiometric Calibration of the VIIRS Reflective Solar Bands with Robust Characterizations and Hybrid Calibration Coefficients," Appl. Opt., 54, 9331-9342 (2015).*
- *J. Sun and M. Wang, "VIIRS Reflective Solar Bands Calibration Progress and Its Impact on Ocean Color Products," Remote Sensing, 8, 194 (2016).*

Hybrid Calibration

Calibration coefficients Ratios

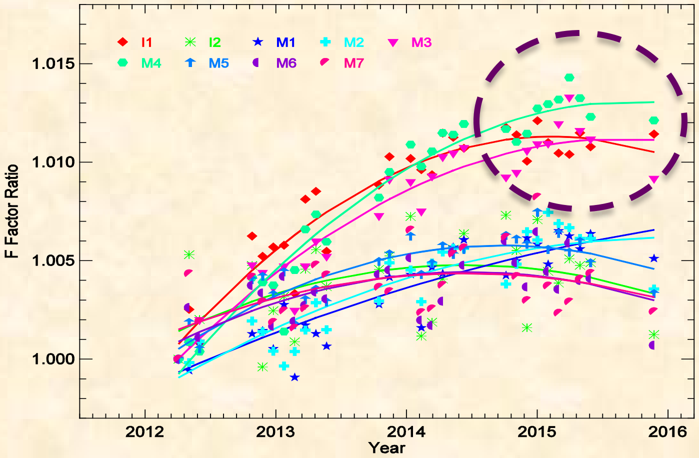

Calibration Coefficients (M4)

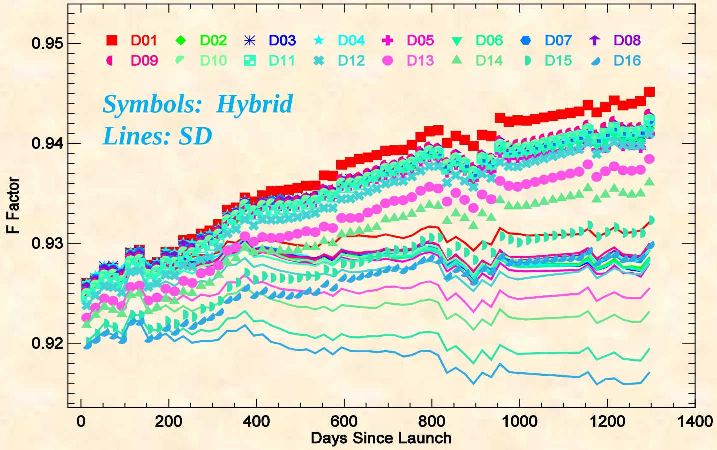

Calibration Coefficients

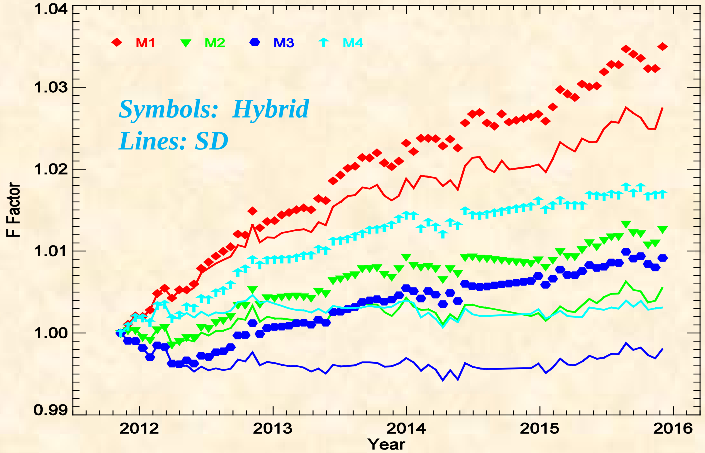

Earth-based SDR studies show that Hybrid-mitigated SDRs give correct time series

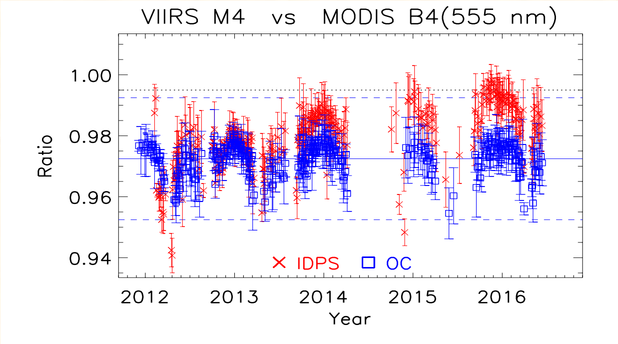

Poster: "Radiometric Comparison of the RSBs of the SNPP VIIRS and Aqua MODIS through SNO analysis" by M. Chu, J. Sun and M. Wang.

Improvements in Ocean Color Products

- VIIRS data were reprocessed using **MSL12** with SDR generated with updated hybrid calibration coefficients.
- NOAA ocean color products produced with the hybrid calibration coefficients have met validated maturity in March 2015.
- **Hybrid results agree with MOBY in situ!**
- **Hybrid LUTS have been used for forward science quality products since Dec 2015.**

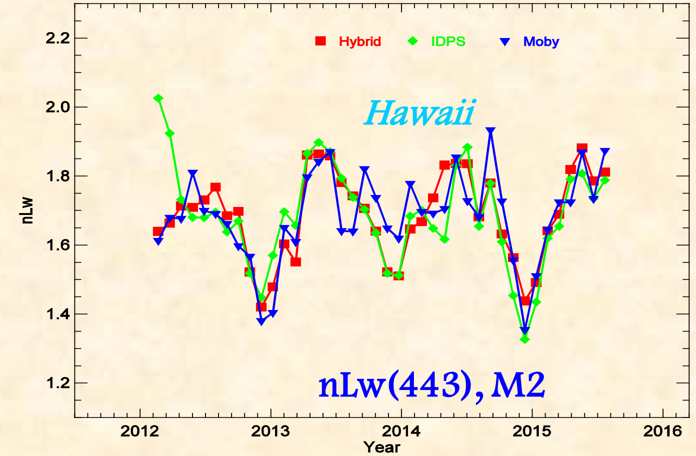

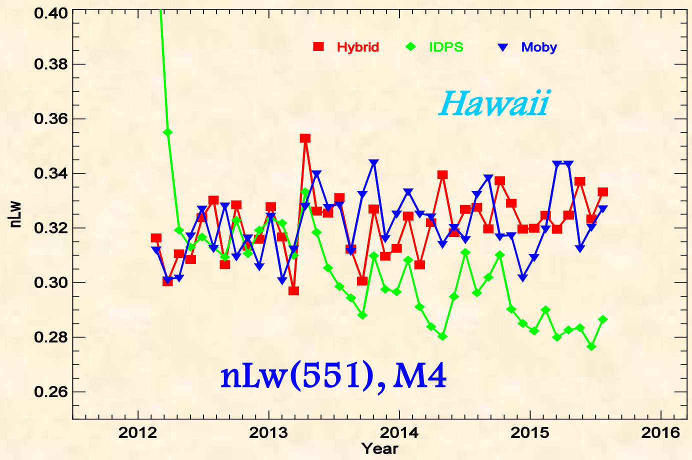

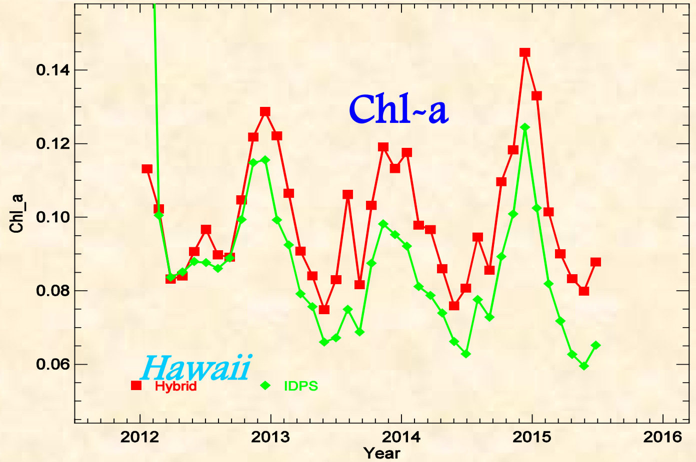

Green: VIIRS IDPS; Red: VIIRS Hybrid; Blue: Moby in Situ

- *J. Sun and M. Wang, "VIIRS Reflective Solar Bands calibration prog," Proc. SPIE, 9264, 92640L (2014).*
- *M. Wang, et al, "Evaluation of VIIRS ocean color products," Proc. SPIE 9261, 92610E (2014).*
- *M. Wang, et al, "VIIRS ocean color products: A progress update," Proc. IGARSS, Beijing, China (2016).*

Summary

- Robust RSB calibration of all components has been done to achieve ~0.2% stability – very clean, smooth result.
- The "*SD degradation nonuniformity effect*" has been discovered to impact RSB calibration, but "hybrid method" mitigation combining SD and Lunar calibration restores RSB calibration accuracy.
- The hybrid coefficients remove long-term bias in ocean color EDR products and enables the VIIRS ocean products for science quality applications. Similar issues expected in J1-J4 VIIRS.
- Identity real and critical issues is a must
- **We have successfully completed VIIRS Ocean Color EDR mission-long data reprocessing with Hybrid Coef. F-LUTS this year, and have begun forward delivery of science quality EDR since May 2016.**
- ***We anticipate more challenging issues to come and we are preparing.***

******More technical discussions will be presented in Wednesday ocean color breakout session.***

Backup

Table 1. Specification for SNPP VIIRS RSBs and SDSM detectors.

VIIRS Band	CW* (nm)	Band Gain	Detectors	Resolution*	SDSD Detector	CW* (nm)
M1	410	DG	16	742m x 776m	D1	412
M2	443	DG	16	742m x 776m	D2	450
M3	486	DG	16	742m x 776m	D3	488
M4	551	DG	16	742m x 776m	D4	555
I1	640	SG	32	371m x 387m	NA	NA
M5	671	DG	16	742m x 776m	D5	672
M6	745	SG	16	742m x 776m	D6	746
M7	862	DG	16	742m x 776m	D7	865
I2	862	SG	32	371m x 387m	D7	865
NA	NA	N	16		D8	935
M8	1238	SG	16	742m x 776m	NA	NA
M9	1378	SG	16	742m x 776m	NA	NA
M10	1610	SG	16	742m x 776m	NA	NA
I3	1610	SG	32	371m x 387m	NA	NA
M11	2250	SG	16	742m x 776m	NA	NA

*CW: Center Wavelength; DG: Dual Gain; SG: Singla Gain; Resolution: Track x Scan at Nadir after aggregation

Suomi NPP VIIRS Reflective Solar Band (RSB) Calibration Stability Assessments

8/9/2016

Jason Choi, Changyong Cao, Slawomir Blonski, Sirish Uprety, Xi Shao (NOAA VIIRS SDR team),

Jack Xiong, Ning Lei (NASA VCST)

Outline

- Introduction
  - About S-NPP VIIRS
- RSB calibration
  - RSB F/H factors
  - Lunar F-factor
- Results
  - VIIRS Reflective Solar Band (RSB) Look-Up Tables (LUTs)
    - NOAA VIIRS SDR team RSBAutoCal vs. NASA VCST LUTs
  - Lunar F-factors
  - Solar Diffuser F-factor correction using lunar F-factors
  - Validation Example
- Summary

The Suomi National Polar-orbiting Partnership (S-NPP) Visible Infrared Imaging Radiometer Suite (VIIRS)

- Descriptions of S-NPP VIIRS
  - A whiskbroom scanning radiometer
  - Sun synchronous orbit
  - Field of view of 112.56^{o}
  - Nominal altitude of 829 km
  - A large scan coverage of 3060 km
  - Equator crossing local time of approximately 1:30 pm
  - 22 spectral bands covering a spectral range of 412nm to 12 μm.

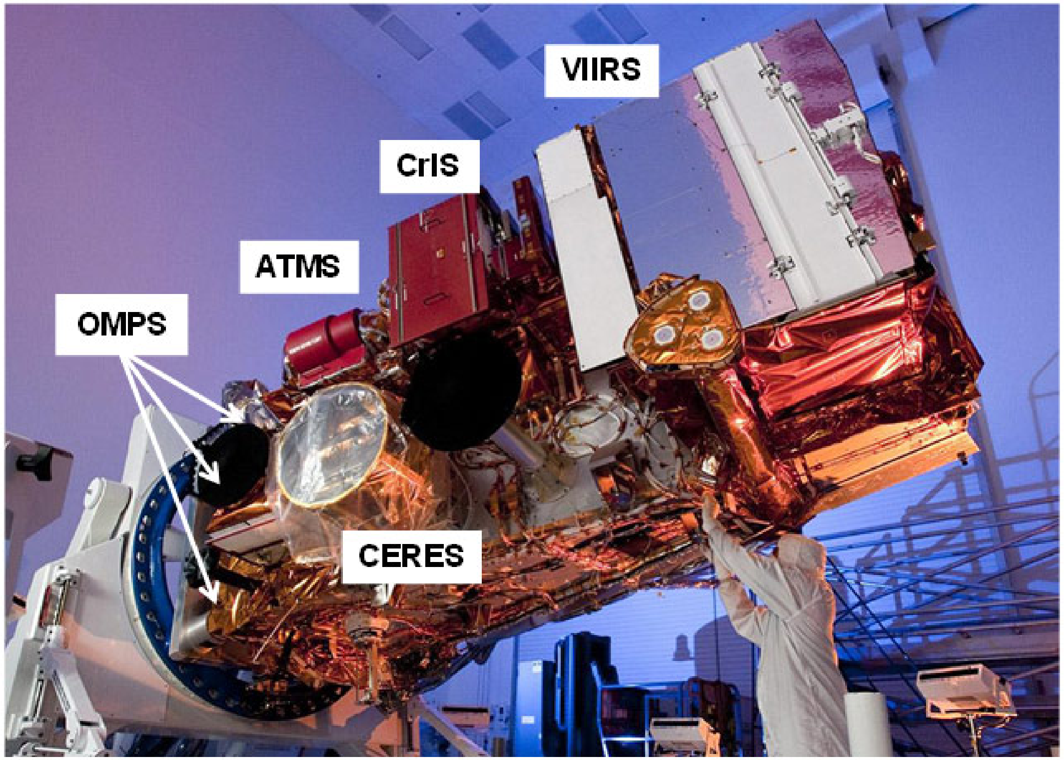

From ICVS webpage
http://www.star.nesdis.noaa.gov/icvs/index.php

Introduction

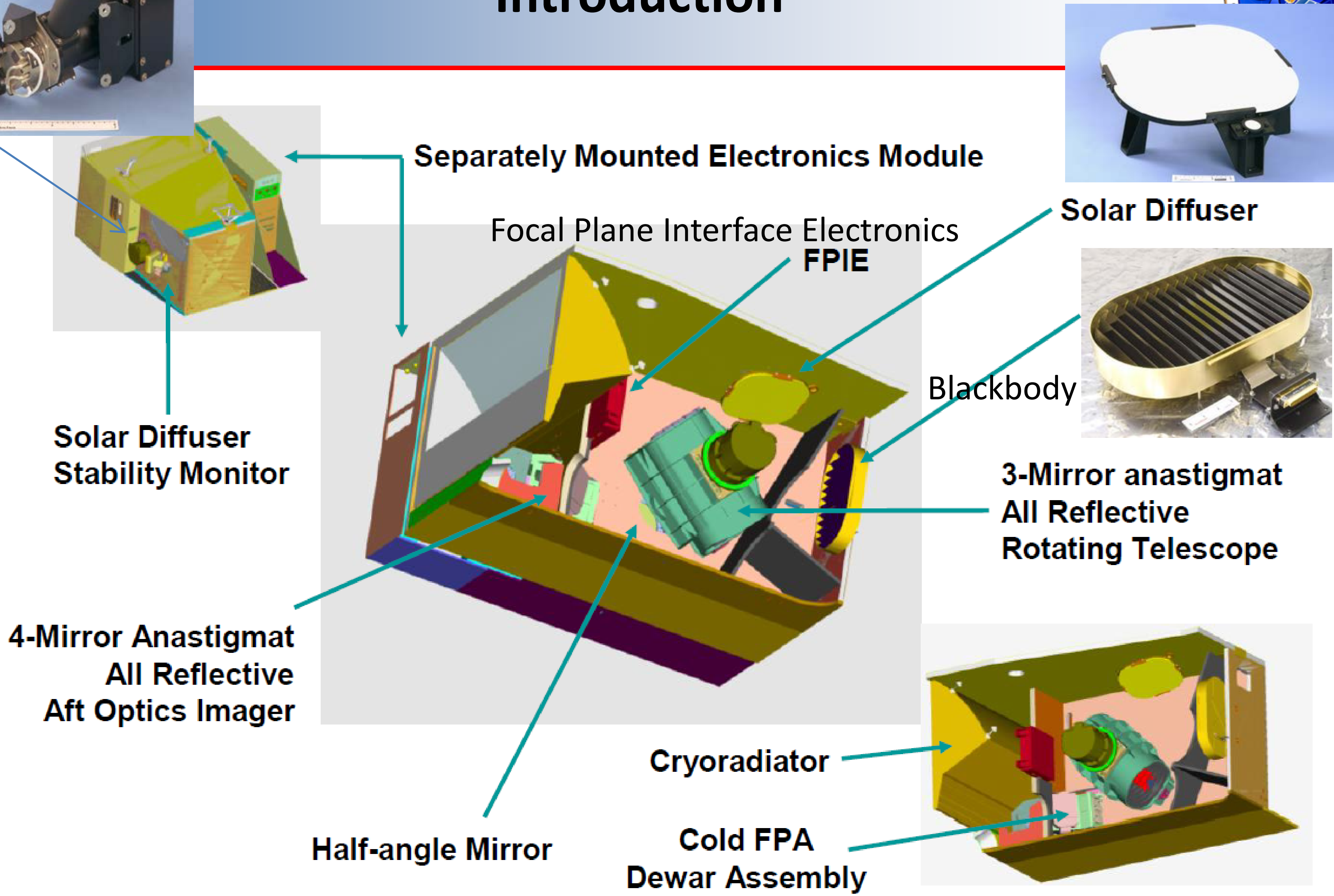

From VIIRS Radiometric ATBD.

Introduction

- Spectral Responses of the VIIRS RSB
  - RSB cover a spectral range from 412nm to 2.25 μm.
  - There are 14 RSB with 3 image bands (I1-I3) and 11 moderate bands (M1-M11).
  - RSB band calibration is dependent on Solar Diffuser (SD) and Solar Diffuser Stability Monitor (SDSM) observations.
  - The required RSB calibration uncertainty is 2 percent.
    - Ocean Color group wants 0.2 percent level.

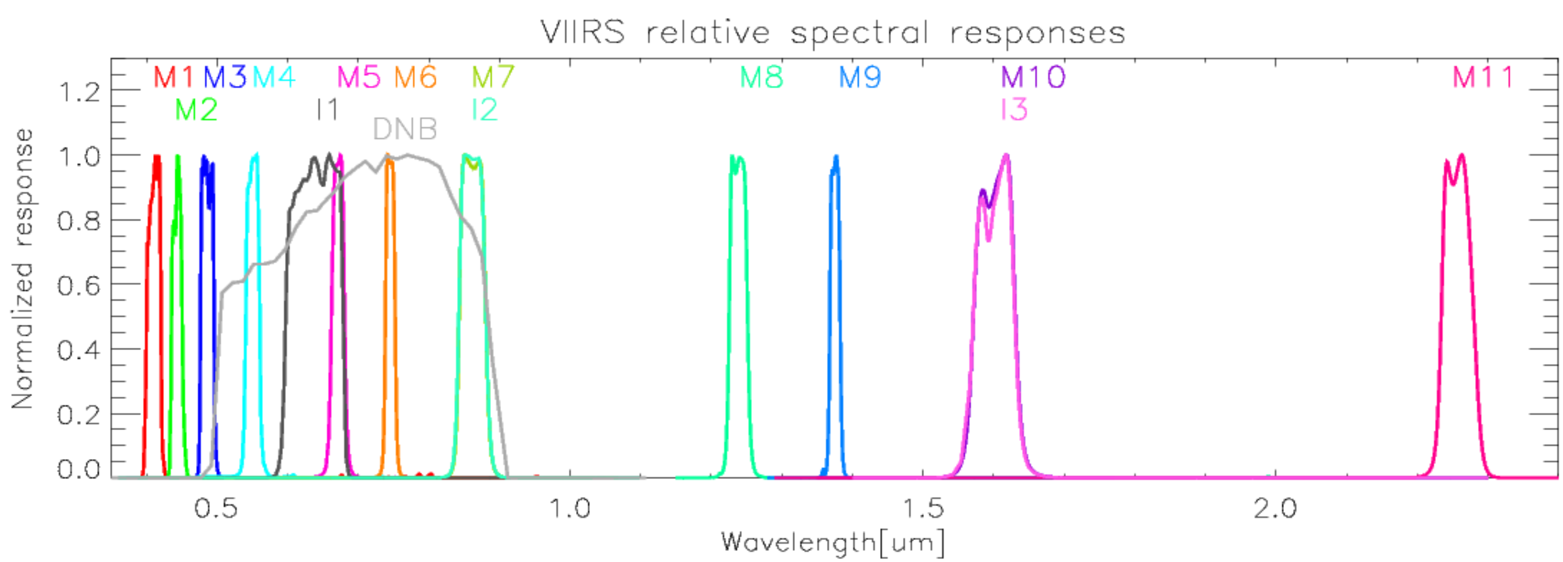

RSB Calibration: SD F-factor

- The RSB F-factor is just a ratio of computed sun radiance from SD over observed SD radiance from the VIIRS detectors.

$$F = \frac{L_{Sun\_Model}}{L_{Sun\_Observation}} = \frac{Computed\_L_{Sun}}{Observed\_L_{Sun}}$$

$$F = \frac{\cos(\theta_{inc}) \cdot \left[E_{sun} \cdot \tau_{sds} \cdot BRDF(t)\right] \cdot RVS_{SD}}{c_0 + c_1 \cdot dn_{SD} + c_2 \cdot dn_{SD}^2}$$

dn_{SD} : offset corrected SD DN, RVS_{SD} : response versus scan function at the angle of SD, $C_{0,1,2}$: detectors and electronics temperature dependent calibration coefficients, θ_{inc}: solar incident angle to the SD screen, *Esun* :solar irradiance, τ_{sds} : screen transmittance function, *BRDF*: the BRDF function out of on-orbit yaw maneuvers, *H(t):* SD degradation over time

$$BRDF(t) = H_{Norm}(t) \cdot BRDF(t_0)$$

$$H_{Norm}(t) \propto \frac{SD\_response(t)}{SUN\_response(t)}$$

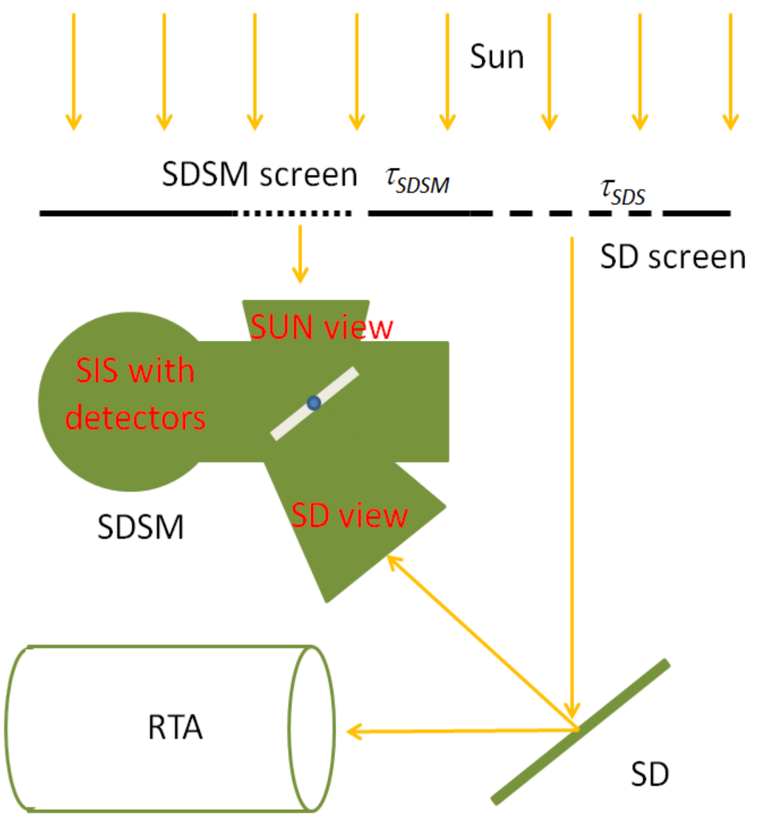

RSB Calibration: Lunar F-factor

- Lunar F-factor: as a Secondary calibration coefficient
- The lunar F-factor is calculated as a ratio between the theoretical lunar irradiance and observed lunar irradiance [2]

$$\mathrm{F(B,D)} = \frac{I_{GIRO}(B)}{Irrad(B,D)} = \frac{I_{GIRO}(B)}{L_{Avg}(B,D) \cdot \frac{\pi \cdot R_{moon}^2}{Dist_{Sat\_Moon}^2} \cdot \frac{1+\cos(\phi)}{2}}$$

$$L_{Avg} = \sum_{Pixel} L_{pix} \,/\, Number\_of\_effective\_pixels$$

I_{GIRO} : band dependent lunar irradiance value from the the Global Space-based Inter-Calibration System (GSICS) Implementation of RObotic lunar observatory (GIRO v1.0.0) model (at https://gsics.nesdis.noaa.gov/wiki/Development/LunarWorkArea), ϕ: moon phase angle, L_{Avg}: averaged radiance of the effective lunar pixels, R_{moon}: moon radius, $Dist_{Sat\_Moon}$: distance between satellite and moon

[2] Choi, T., Shao, X., Cao, C., Weng, F., Radiometric Stability Monitoring of the Suomi NPP Visible Infrared Imaging Radiometer Suite (VIIRS) Reflective Solar Bands Using the Moon. Remote Sens. 2016, 8, 15.

Introduction

- Different version of RSB LUTs are available
- SD H & F-factor LUTs
  - Aerospace (Fast track & RSBAutoCal)
  - NASA VCST
  - NOAA Ocean Color group
  - NOAA VIIRS RSBAutoCal & ICVS
- Lunar F-factor LUTs
  - NASA VCST (ROLO, GIRO)
  - NOAA Ocean Color (ROLO)
  - NOAA VIIRS (GIRO, Miller Turner)
- Lunar Band Ratio (LBR)
  - NOAA VIIRS

Results: RSBAutoCal vs. NASA VCST LUTs

- Aerospace RSB LUTs
  - Bi-weekly fast-track LUTs were operational from the start of mission to November 2015.
  - RSBAutoCal LUTs currently operational since November 2015.
- The operational F-factors are monitored by Integrated Calibration/Validation System (ICVS) F-factors
  - ICVS web-page at http://www.star.nesdis.noaa.gov/icvs/status_NPP_VIIRS.php
- **NOAA VIIRS SDR team** produces a new set of VIIRS lifetime **RSBAutoCal LUTs** for reprocessing.
  - Applying current operational LUTs from IDPS [1].
  - very similar to NOAA ICVS LUTs.
- NOAA Ocean Color group produces their own RSB LUTs.
  - With their own screen transmission, BRF, and sweet spot Defs.
- **NASA VIIRS Calibration Support Team (VCST)** produces several different version of RSB LUTs.
  - NASA VCST provided latest RSB LUTs to validate.
  - Lunar correction, time dependent RSR corrections, Out-of-band H-factor correction and normalization, Screen transmission table updates, SWIR SD deg.

[1] Blonski & Cao, *Remote Sens.* **2015**, *7*(12), 16131-16149; doi:10.3390/rs71215823

Results: RSBAutoCal vs. NASA VCST LUTs

- NOAA VIIRS SDR team prepared a set of initial version of reprocessing LUTs.
  - Using RSBAutoCal from the start of S-NPP launch
  - 3236 RSBAutoCal LUTs are generated
    - Covering 11/8/2011 to 4/25/2016.
  - RSBAutoCal LUTs provide
    - RSB F/H factors
- NASA VCST H/F LUTs
  - VCST provided H(v25) and F(v20) LUTs.
    - 22,864 data points for F-factors (11/8/2011 ~ 5/22/2016)
    - 2,258 data points for H-factors (11/8/2011~5/16/2016)
  - F-factors include middle detectors, HAM side A, HG states for dual-gain bands.
    - The middle detectors are detector 8 for M bands and detector 16 for I bands starting from detector index 1.
  - F-factor comparisons are performed in
    - HAM side A, HG state, Middle detectors.

Results: RSBAutoCal vs. NASA VCST LUTs

- RSBAutoCal vs. VCST F-factors in VIS and NIR bands
  - M1 (412nm) F-factors show ~3% differences.
  - M5 (672nm) 1%, I2/M7 (867nm) 0.4% → getting smaller.
  - VCST F-factors are larger than RSBAutoCal LUTs.

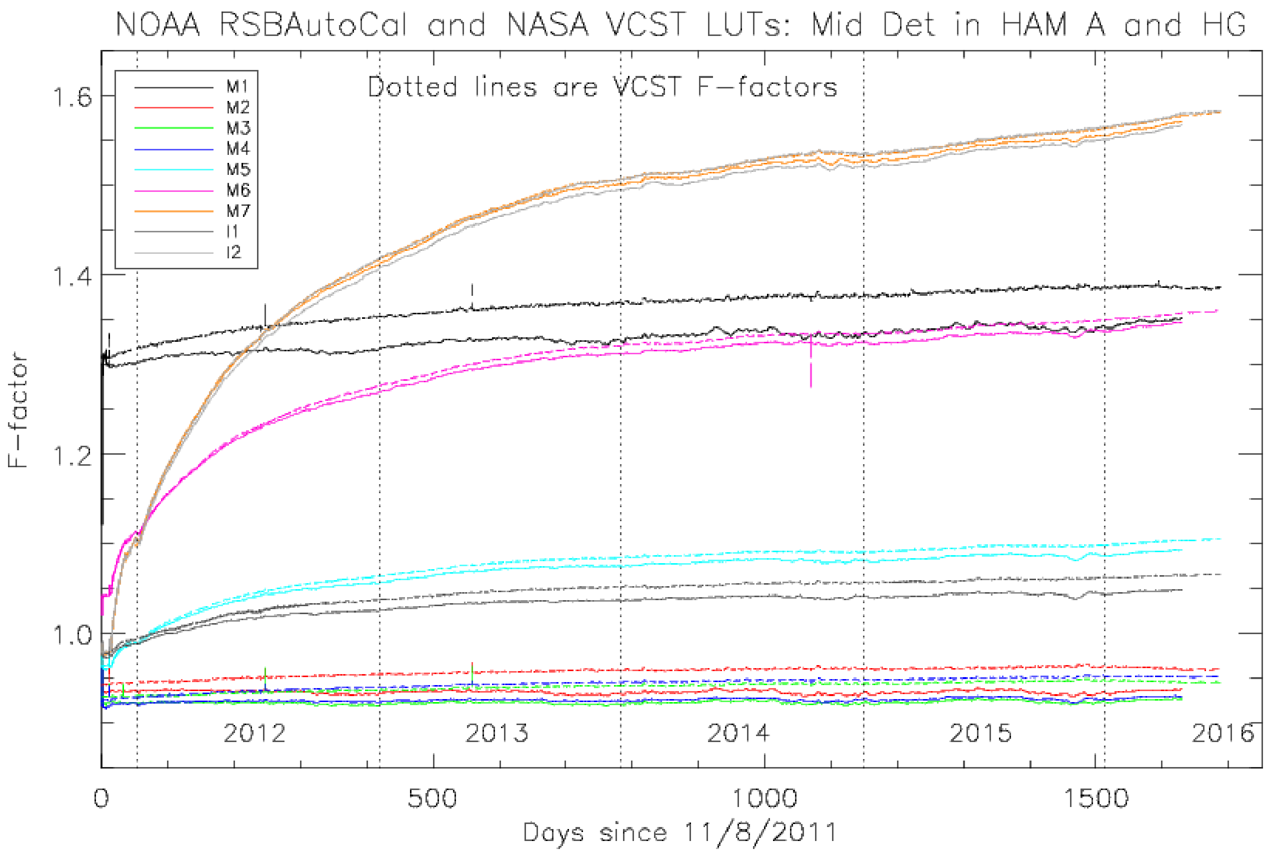

Results: RSBAutoCal vs. NASA VCST LUTs

- RSBAutoCal vs. VCST F-factors in SWIR bands
  - I3 and M10 differences are large (>0.5%) with NASA VCST LUTs.
  - VCST LUTs are below RSBAutoCal LUTs.

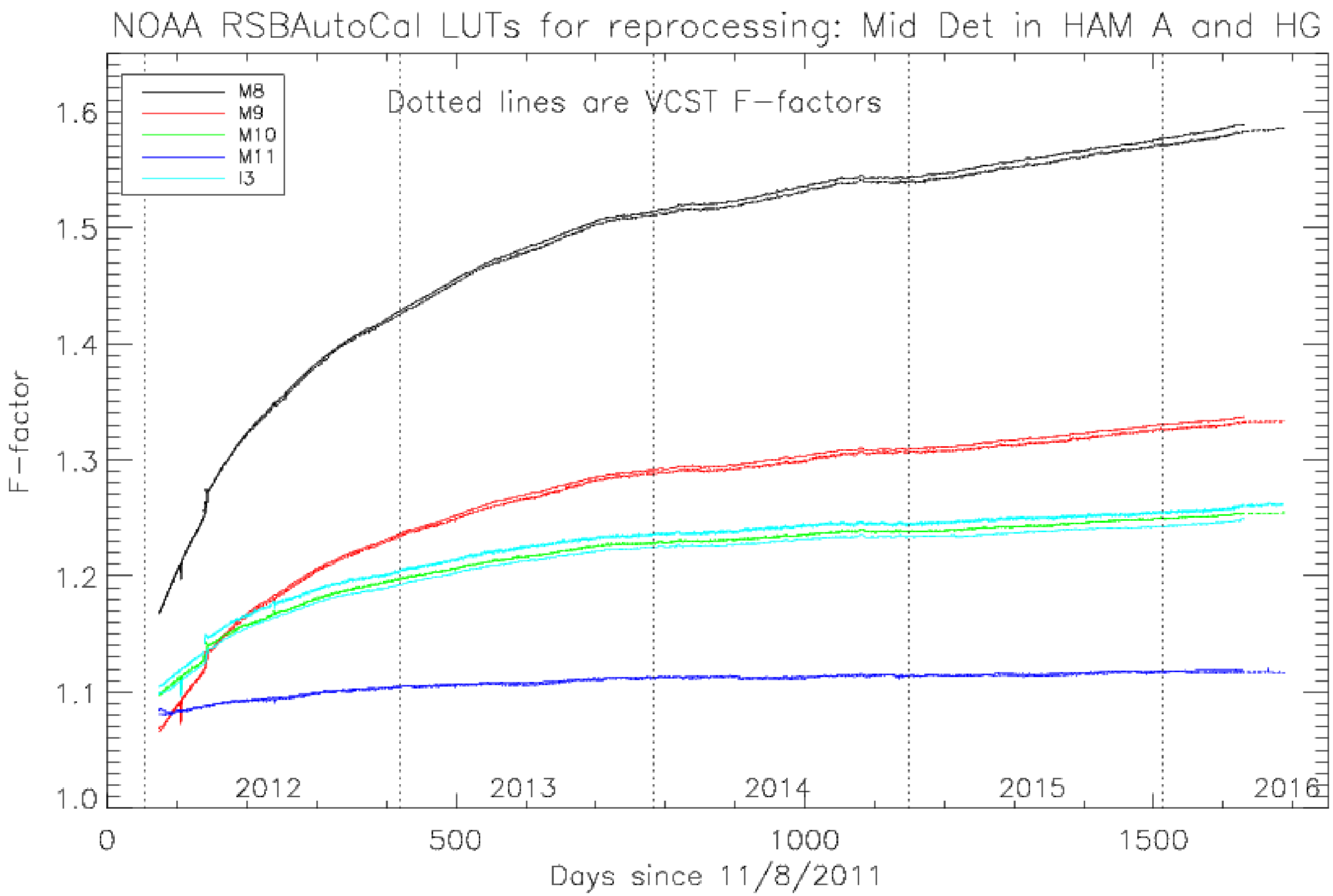

Results: RSBAutoCal vs. NASA VCST LUTs

- F-factor ratio plot in VIS and NIR bands
  - There are initial offsets and long-term drifts.
  - The differences are larger in short wavelength bands and getting smaller in longer wavelengths.

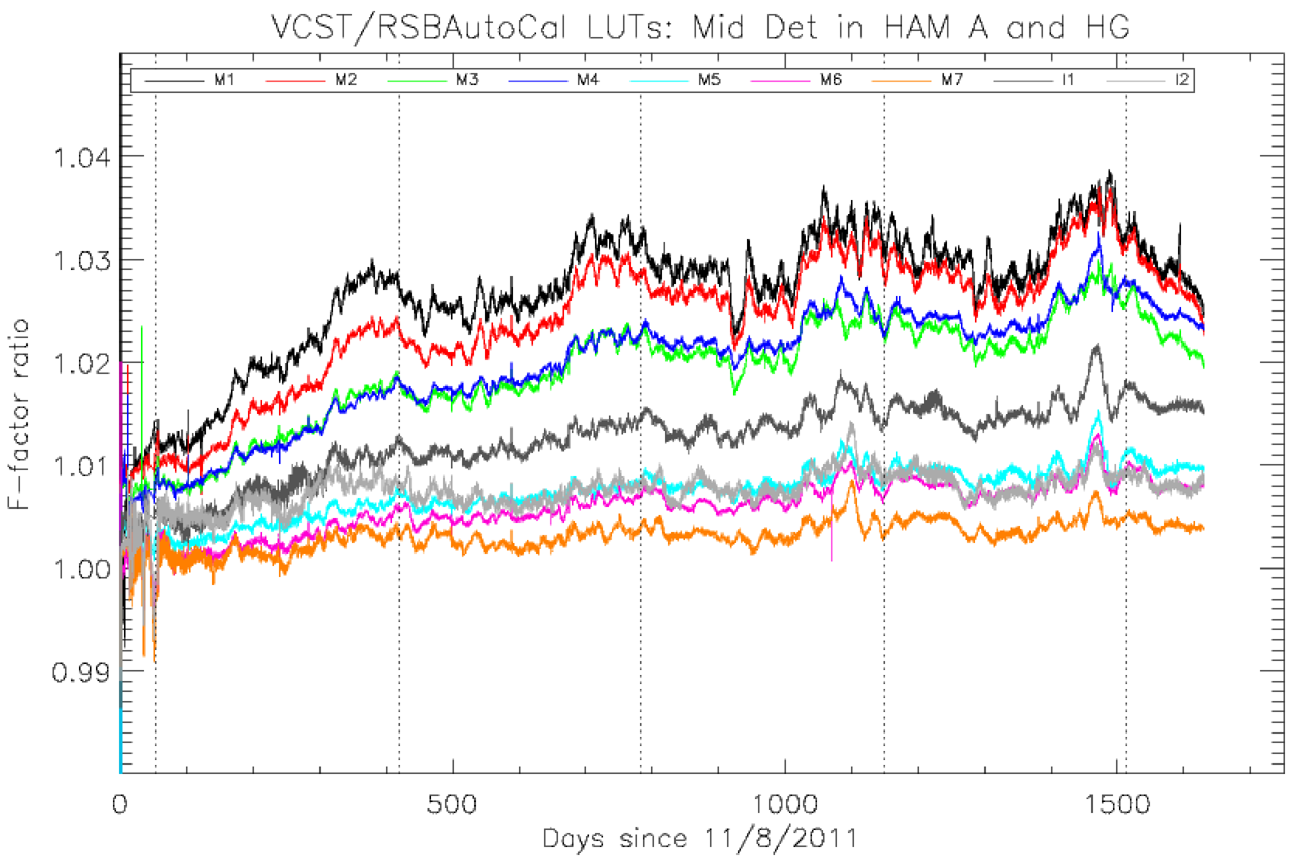

Results: RSBAutoCal vs. NASA VCST LUTs

- F-factor ratio plot in SWIR bands
  - H-factor (SD degradation) free bands show long-term drifts.

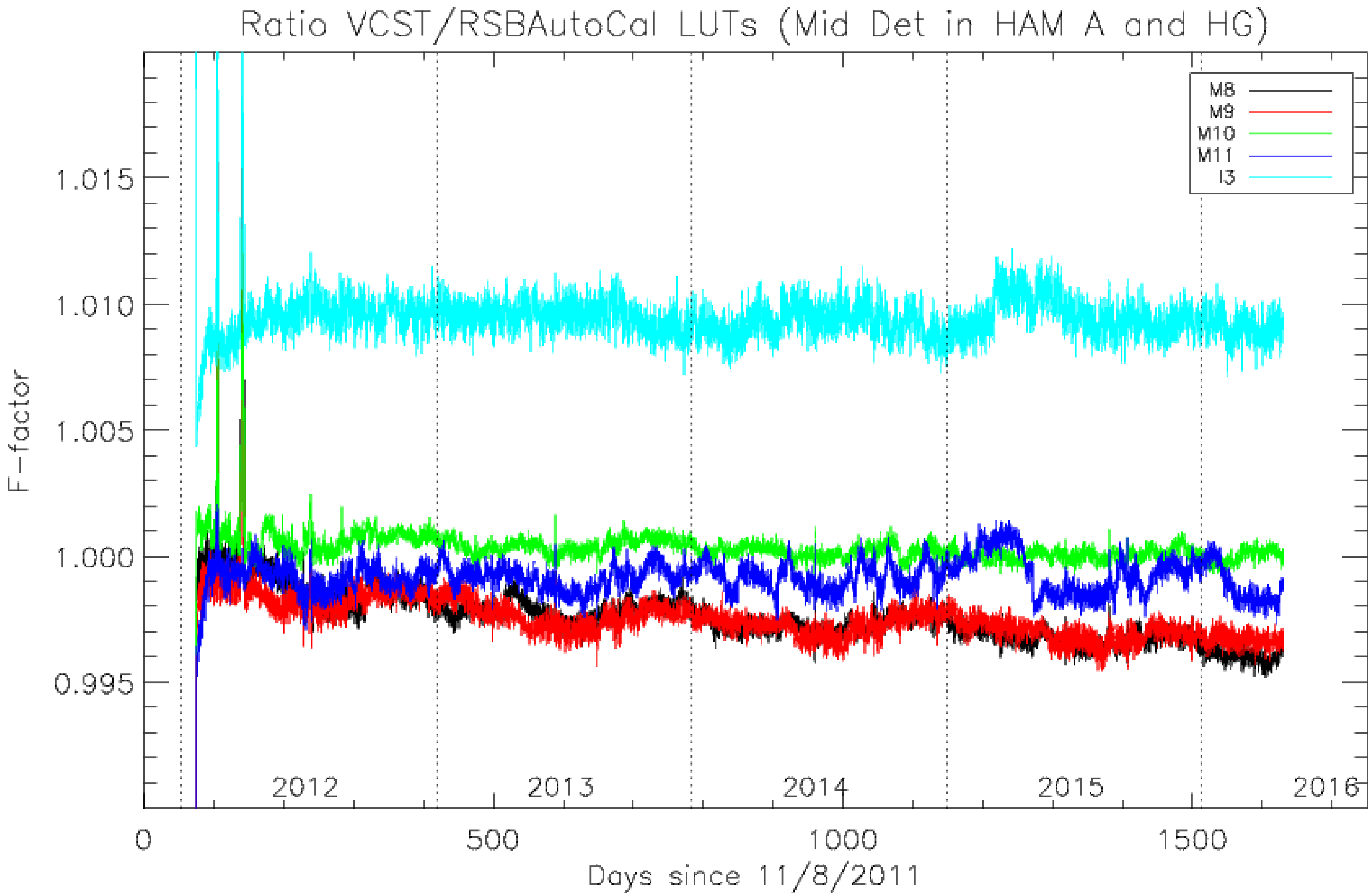

Results: RSBAutoCal vs. NASA VCST LUTs

- RSBAutoCal (dotted line) vs. VCST H-factor over plot
  - VCST H-factors are larger than RSBAutoCal.
  - The differences seem to be dependent on wavelengths.
  - There are initial sate differences.

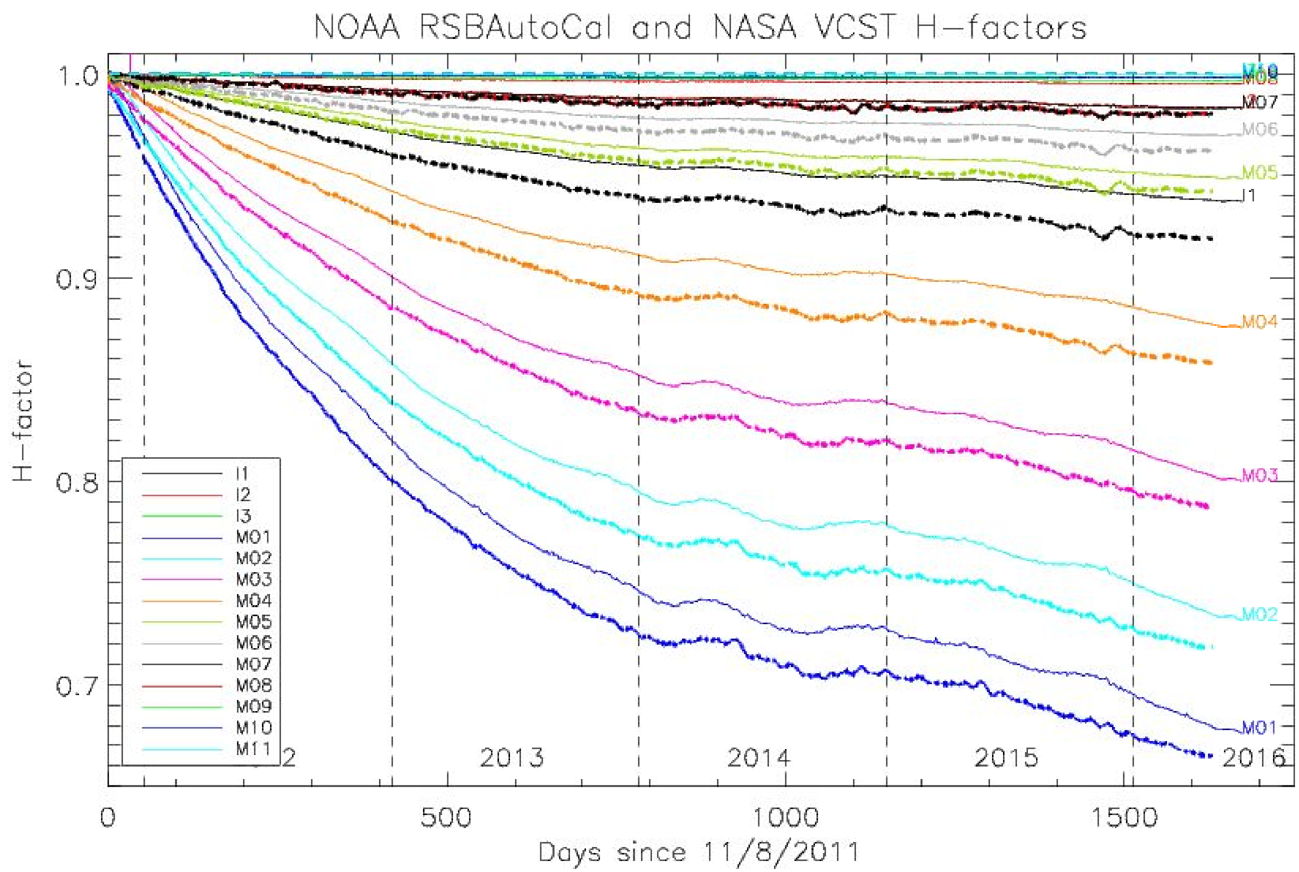

Results: RSBAutoCal vs. NASA VCST LUTs

- RSBAutoCal vs. VCST H-factor over plot
  - Thick lines are RSBAutoCal and narrow lines are VCST H-factors.
  - RSBAutoCal H-factors are set to be 1 in M8~M11, I3.
  - VCST has corrected for SD degradation.

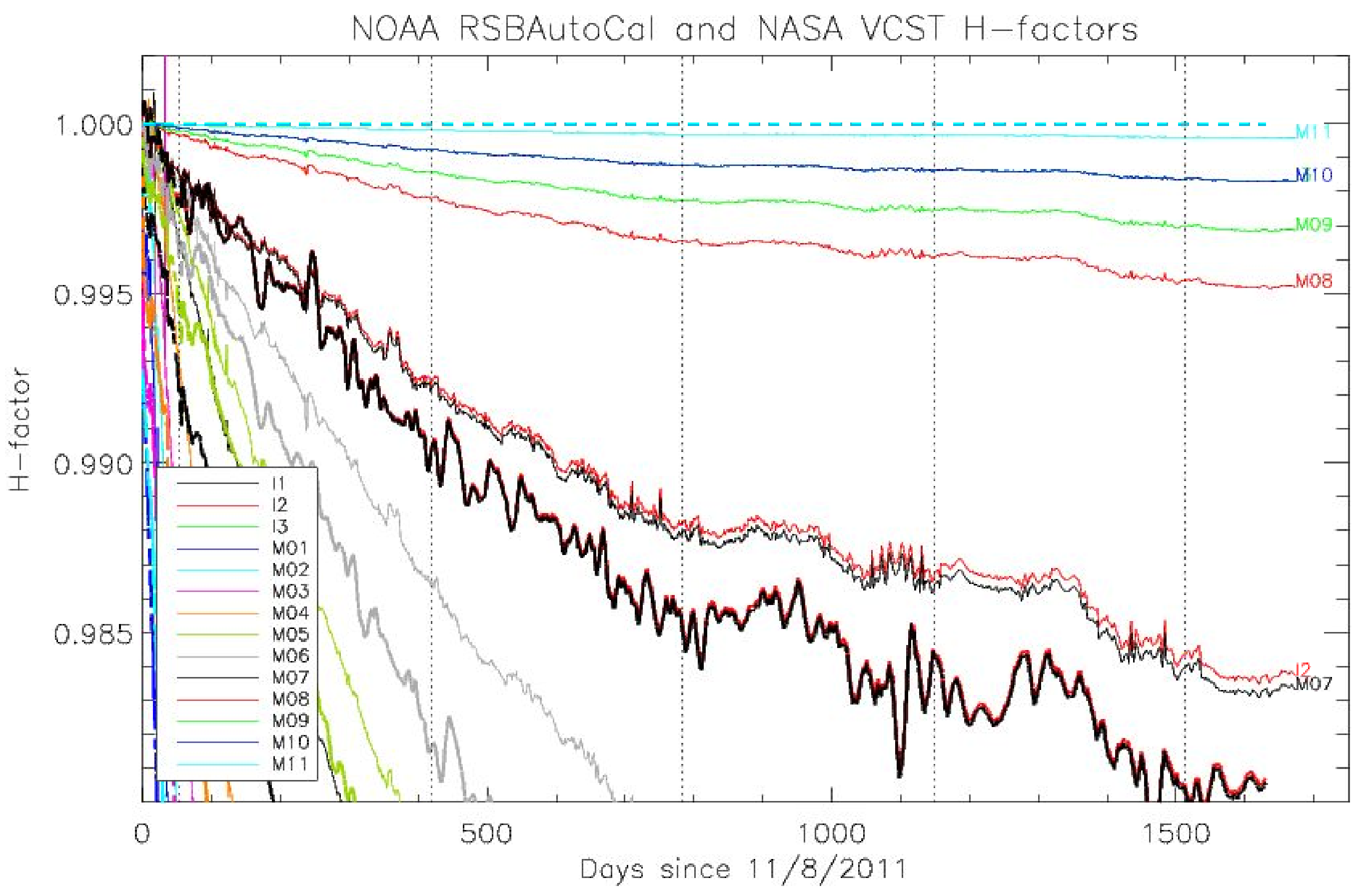

Results: RSBAutoCal vs. NASA VCST LUTs

- H-factor ratio plot
  - H-factor differences are very similar to the F-factor differences.
  - F-factor differences are caused by the H-factors.

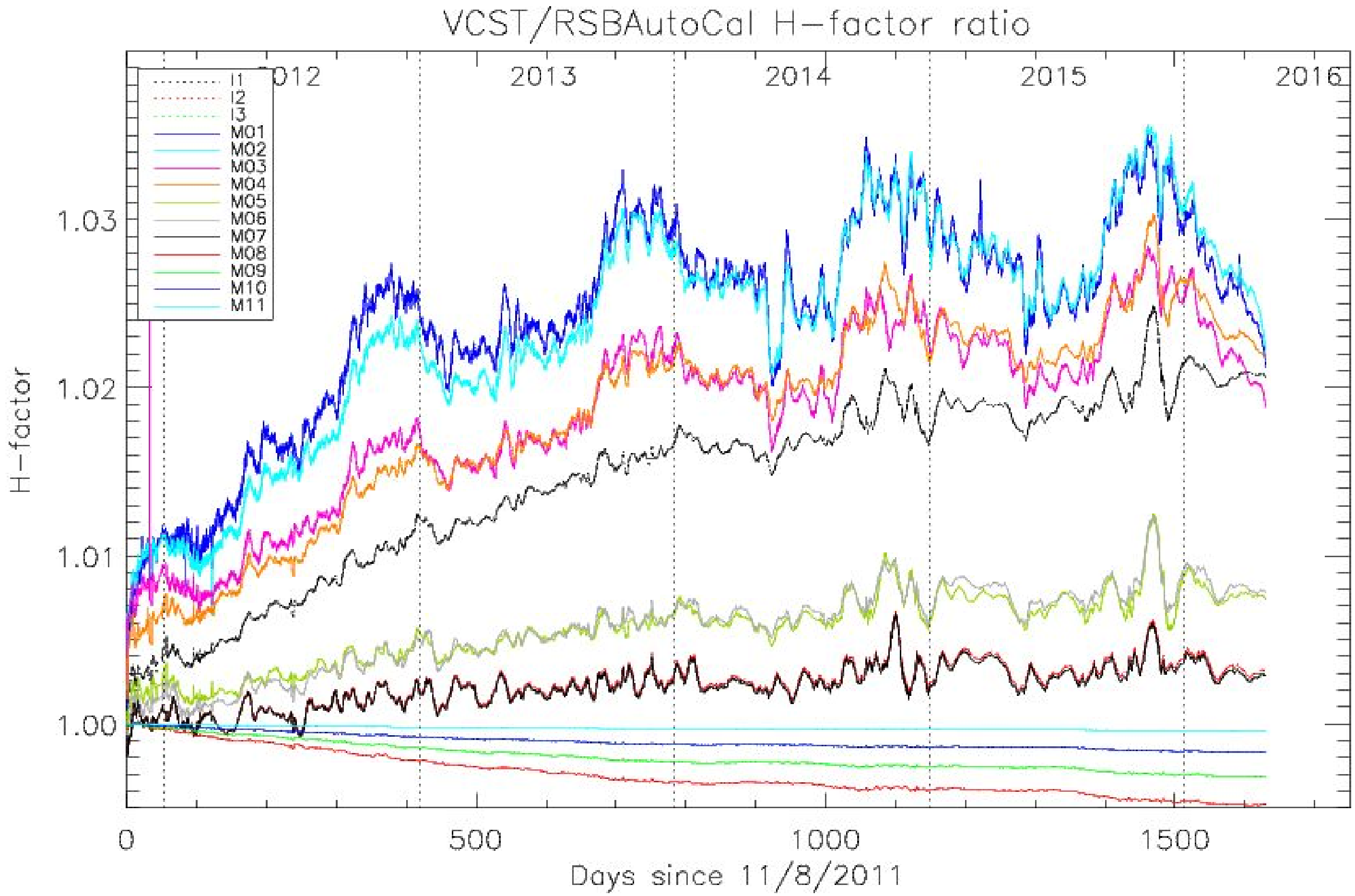

Results: Lunar F-factor comparisons

- The two F-factors need to be normalized (or scaled) properly because of the different solar irradiance models.
- The SD F-factors (solid lines) are normalized for better comparison and visualization in the figures.
- The best fitting scaling factors are calculated and applied for lunar F-factors (symbols).
- Lunar and SD F-factors are showing similar annual trends in starting from end of 2014 to current time.
- The first two lunar points are below the SD F-factors.
  - Potential errors in SD F-factors.

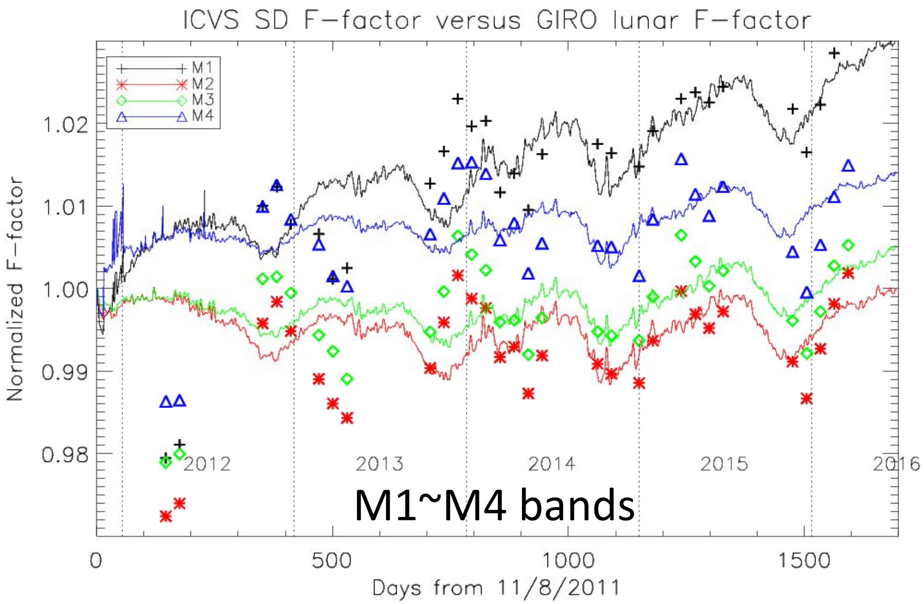

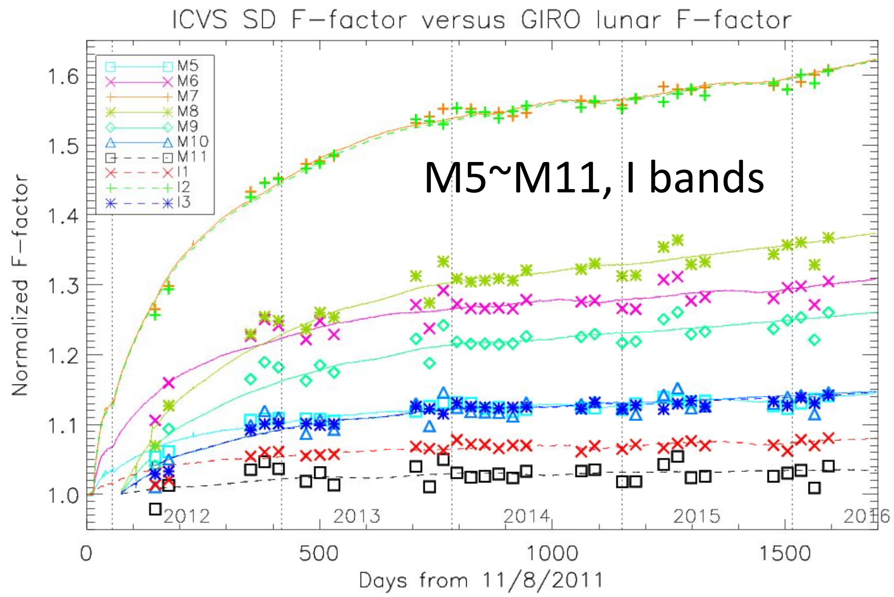

Results: Lunar F-factor comparisons

- The one-sigma root mean square(RMS) of the differences between SD and lunar F-factors are also shown in Table 1.
  - The SD F-factors are interpolated at the lunar collection time.
  - The short wavelength bands (M1~M4) are well within one percent level.
  - Other bands also show agreements less than 2 percent level.

Table 1. One-sigma RMS of the percentage differences between the SD and lunar F-factors.

Band	RMS	Band	RMS
M1	0.90	M8	1.70
M2	0.83	M9	1.59
M3	0.71	M10	1.46
M4	0.73	M11	1.33
M5	0.70	I1	0.75
M6	1.66	I2	0.90
M7	0.87	M3	0.73

Results: SD F-factor Correction

- SD F-factor correction to Lunar F-factor
  - Lunar F-factors are fitted.

    $Y = a \cdot log(x-b) + c \cdot x + d$
  - SD F-factors are fitted to a quadratic polynomial.

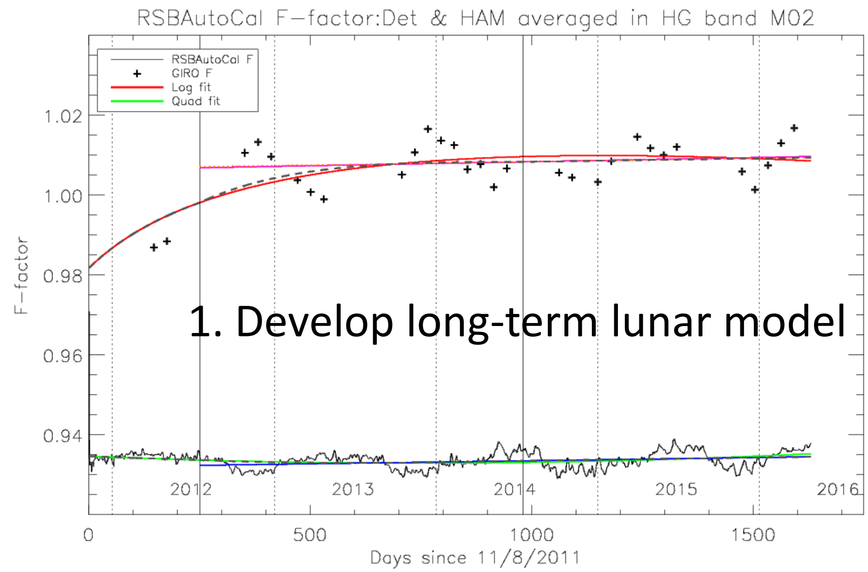

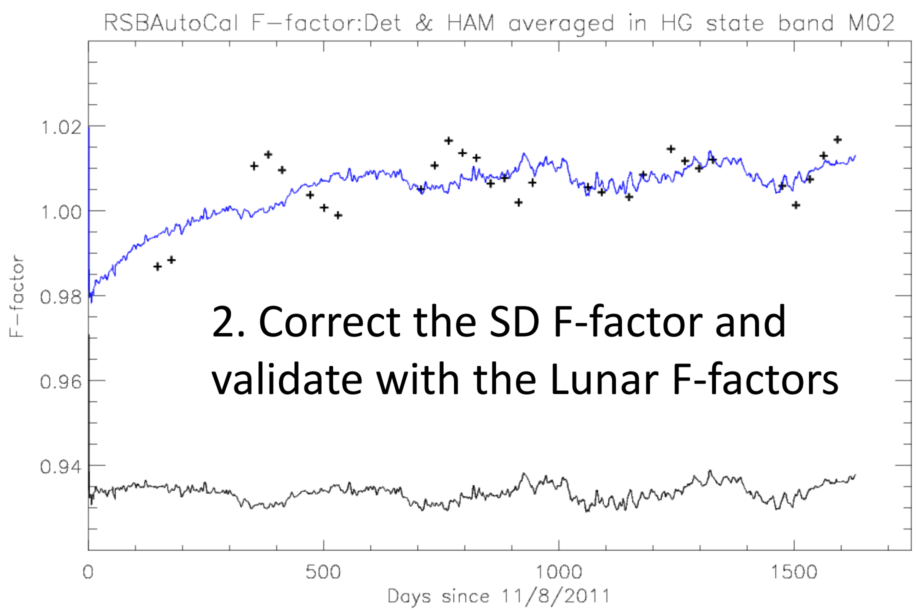

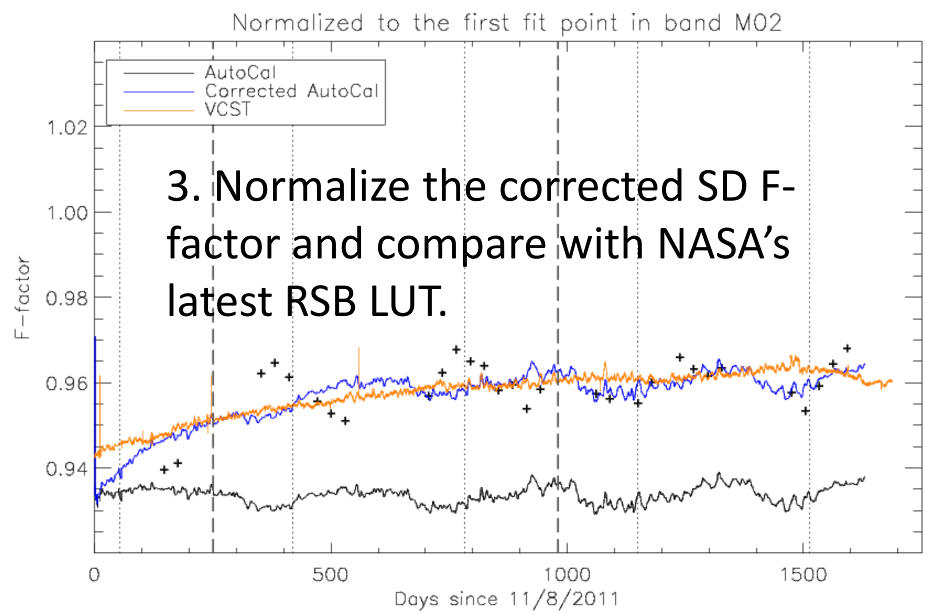

Results: SD F-factor Correction

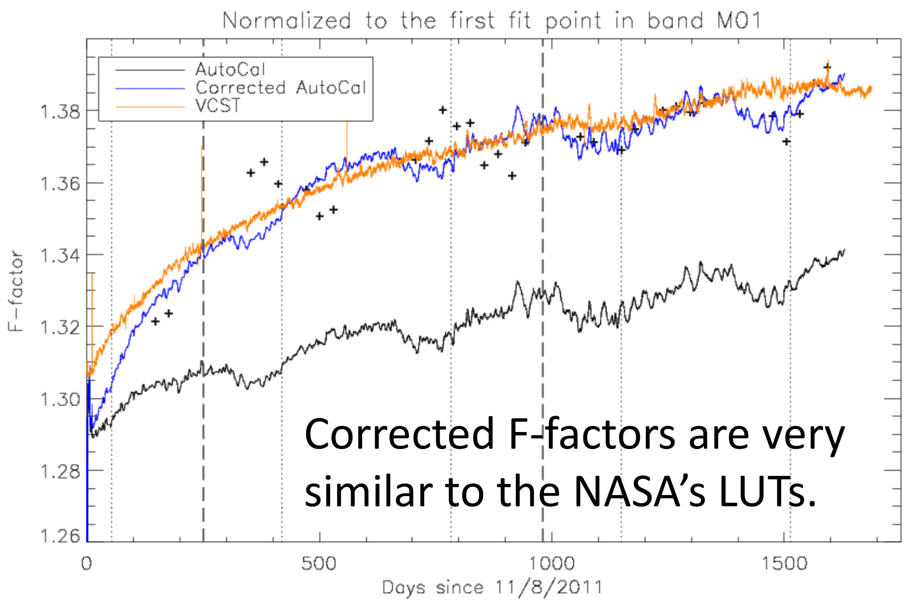

Corrected F-factors are very similar to the NASA's LUTs.

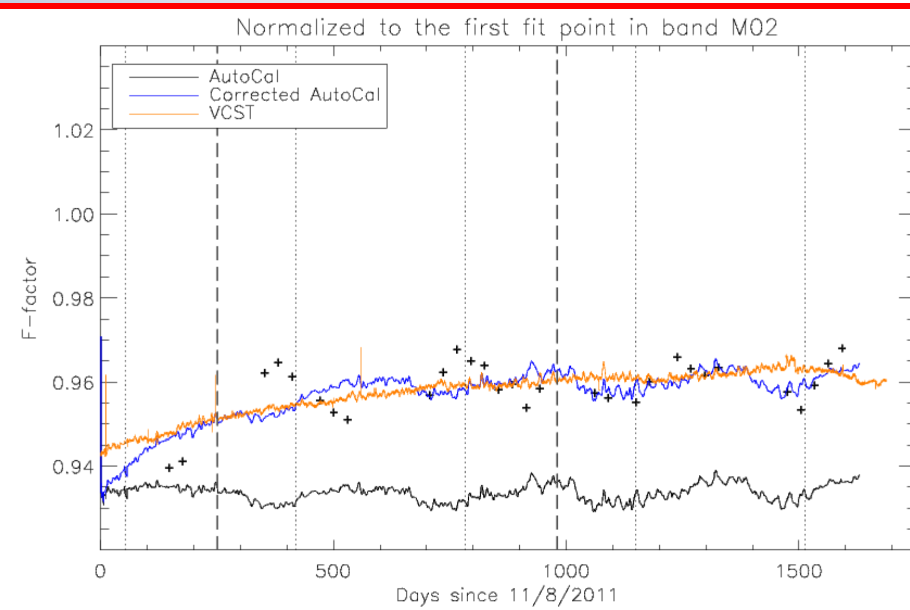

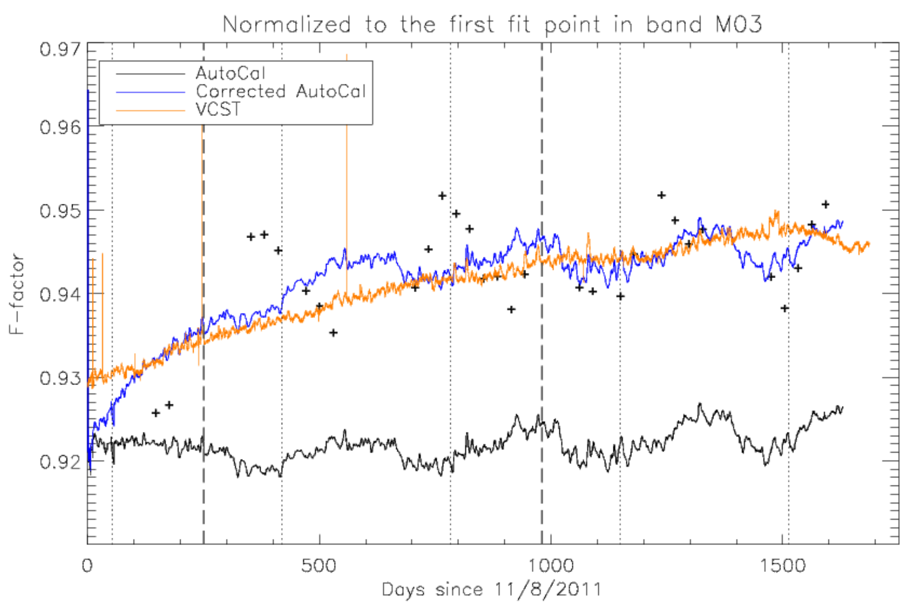

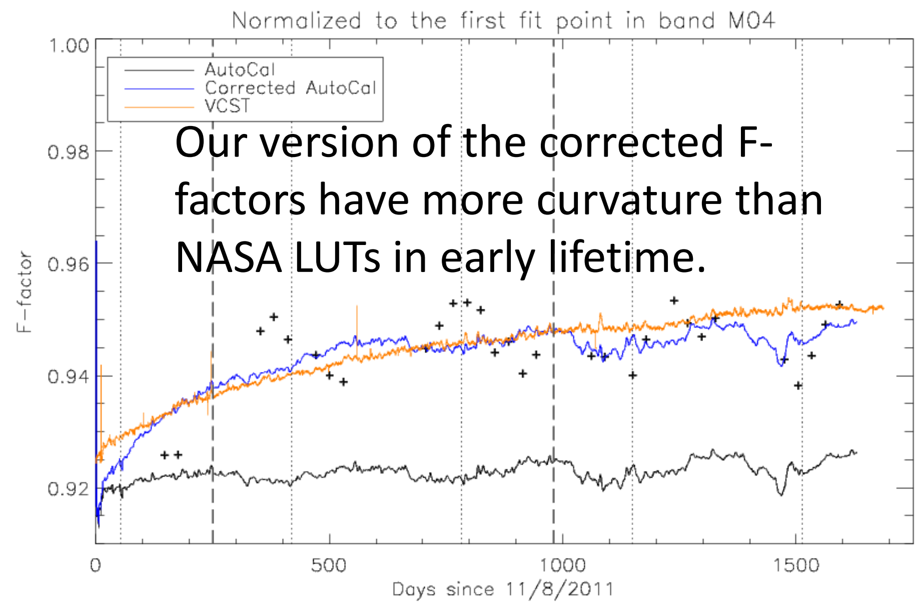

Our version of the corrected F-factors have more curvature than NASA LUTs in early lifetime.

Validation Example

- Radiance ratio of VIIRS data generated from IDPS and NASA Land SIPS is obtained for bands M1 through M7 near MOBY site.
- The ratio trends suggest the calibration differences among two products.
- All bands suggest agreement to within ±1% except M1 that shows almost ±2% difference mainly in 2014.
- It is to be noted that SIPS data are reprocessed data whereas IDPS is near real time data.

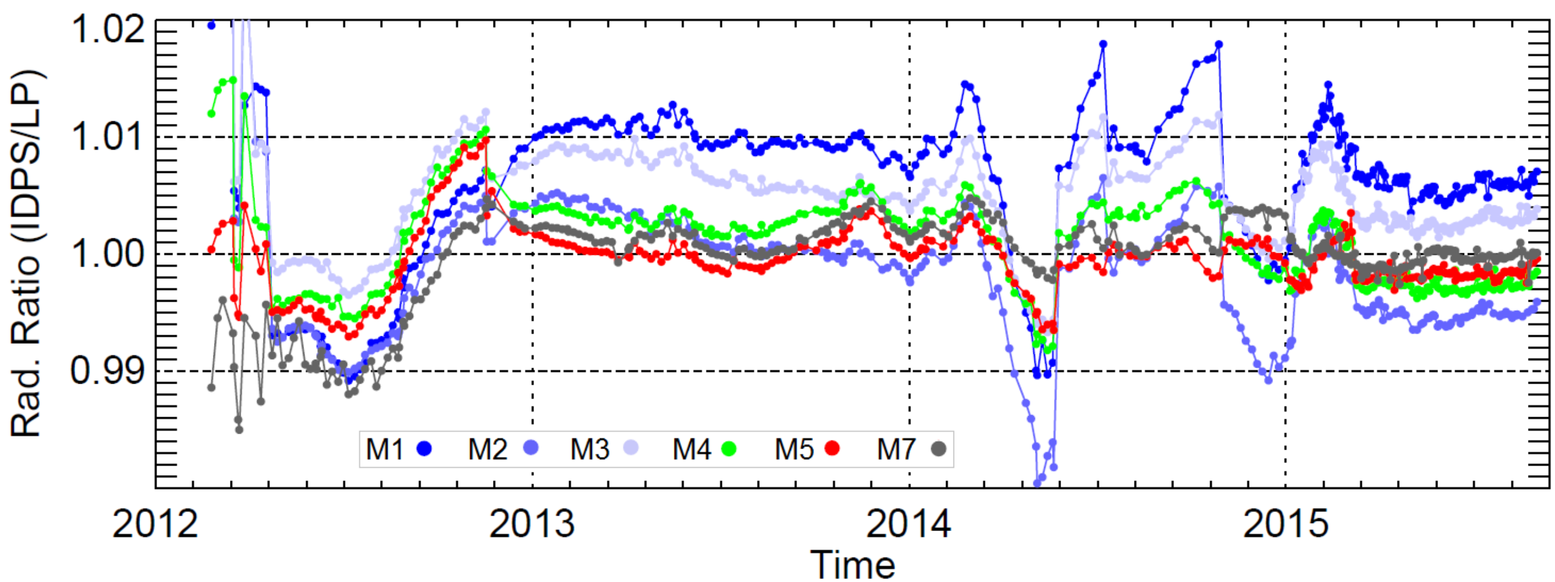

Summary (1/2)

- RSBAutoCal vs. NASA VCST LUTs
  - Reprocessing LUTs are compared between
    - RSBAutoCal and NASA VCST.
  - There are some initial state differences with long-term drifts up to 3% in band M1 (1% initial and 2% long-term drift).
    - Because of the normalization of H factors.
    - The differences are band wavelength dependent.
  - The F-factor differences are directly caused by the H-factor differences.
  - NASA VCST has corrected for SD degradation in SWIR bands.
    - In the H-factor free bands (M8~M11 and I3).

Summary (2/2)

- The SD and lunar F-factors suggested potential differences.
  - Up to 3 % in band M1 and M2.
  - The SD F-factors can be scaled to match lunar F-factors.
  - The corrected F-factors needs to be validated by other evidences.
    - Deep convection clouds (DCC), pseudo-invariant calibration sites, or sensor cross calibration using simultaneous nadir observations (SNOs).
    - Before applying to operational production and reprocessing.
- The long-term lunar corrections models are developed and applied.
  - Producing very similar results to NASA VCST's LUTs.
- NOAA VIIRS team will continue to monitor on-orbit calibration coefficients and vicarious observations.
  - Among different agencies (NASA, NOAA, and Aerospace)
  - And different working groups (**Ocean Color**, and NASA VCST)

Acknowledgements

- Authors thank to EUMETSAT sharing the GIRO version 1.0.0 with NOAA VIIRS team.
  - Global Space-based Inter-Calibration System (GSICS) Implementation of RObotic lunar observatory (GIRO v1.0.0) model
  - https://gsics.nesdis.noaa.gov/wiki/Development/LunarWorkArea

- Backup slides

- Reflective Solar Band (RSB) F-factor Calculation
  - F: RSB Calibration coefficient.
  - H: SD degradation factor.

$$L_{EV} = \frac{F \cdot (c_0 + c_1 \cdot dn_{EV} + c_2 \cdot dn_{EV}^2)}{RVS_{EV}}$$

$$F = \frac{L_{Sun\_Model}}{L_{Sun\_Observation}} = \frac{Computed\_L_{Sun}}{Observed\_L_{Sun}}$$

$$F = \frac{\cos(\theta_{inc}) \cdot [E_{sun} \cdot \tau_{sds} \cdot BRDF(t)] \cdot RVS_{SD}}{c_0 + c_1 \cdot dn_{SD} + c_2 \cdot dn_{SD}^2}$$

$$BRDF(t) = H_{Norm}(t) \cdot BRDF(t_0)$$

$$H_{Norm}(t) = \frac{H(t)}{H(t_0)}$$

$$H(t) = \frac{dc_{SD} \cdot \tau_{SDSM}}{dc_{SUN} \cdot BRDF(t_0) \cdot \tau_{SDS} \cdot \cos(\theta_{inc}) \cdot \Omega_{SDSM}}$$

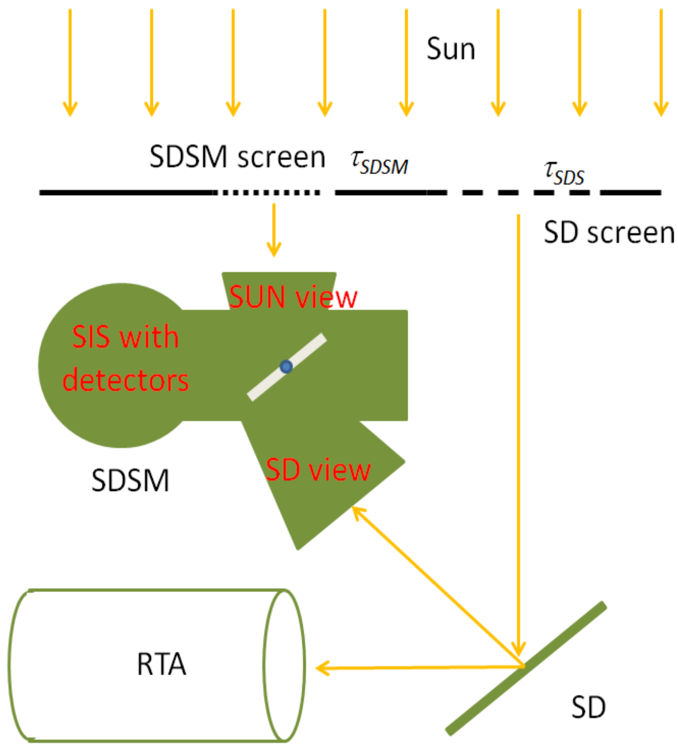

dn: VIIRS bias removed response
dc: SDSM bias removed response

Backup Slides

- Lunar F-factor Calculation from the Scheduled Lunar Collections
  - Moon observation made through the Space View (SV)
  - During the sector rotation, the VIIRS observations are set to be fixed High Gain (HG) mode.
  - Spacecraft roll maneuvers are required.
  - To avoid the complex oversampling factor calculation,
  - Center 5 scans with full moon in the entire scan are used.

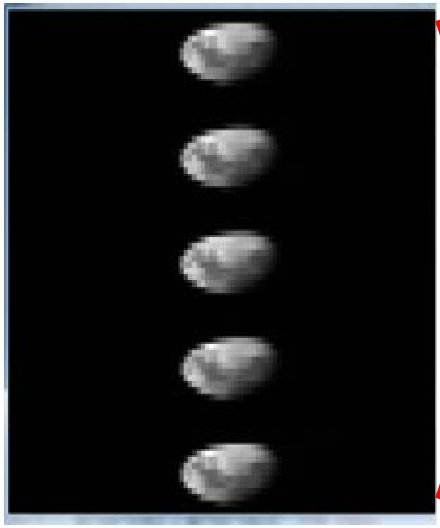

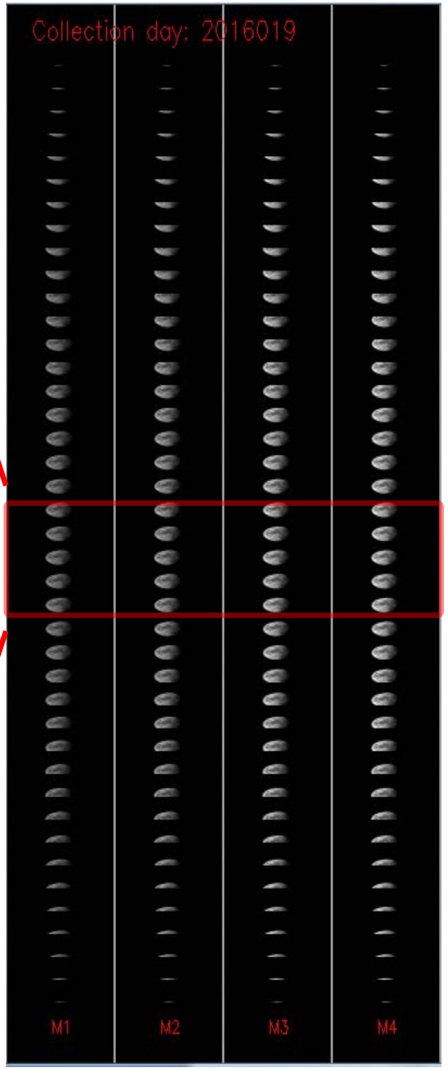

Backup Slides

- Lunar Band Ratio (LBR)
  - Lunar data processing
    - Lunar area is properly trimmed.
    - Based on all the valid bias corrected lunar pixels.
    - Bias is calculated from the background value.
  - LBR is now calculated using M11 as a reference band

$$\mathrm{LBR(B)} = \frac{\sum dn_{Pixel}(B)}{\sum dn_{Pixel}(Band\ M11)}$$

- LBR is compared to the SD F-factor ratios
  - Using M11 as a reference band.

Backup Slides

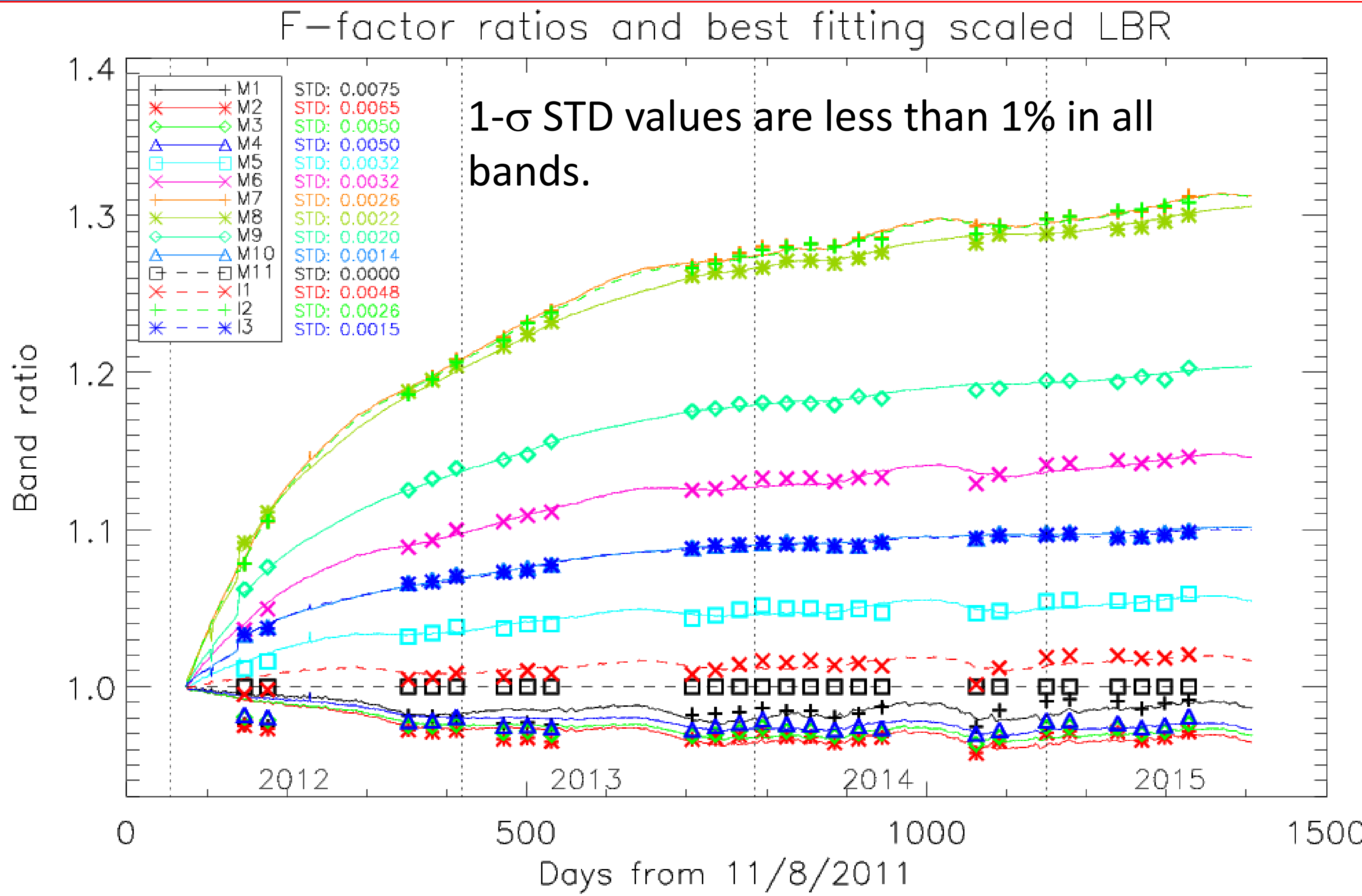

Backup Slides

- Zoomed in for M1~M4
  - LBR and F-factor ratios are very consistent except the first two points.

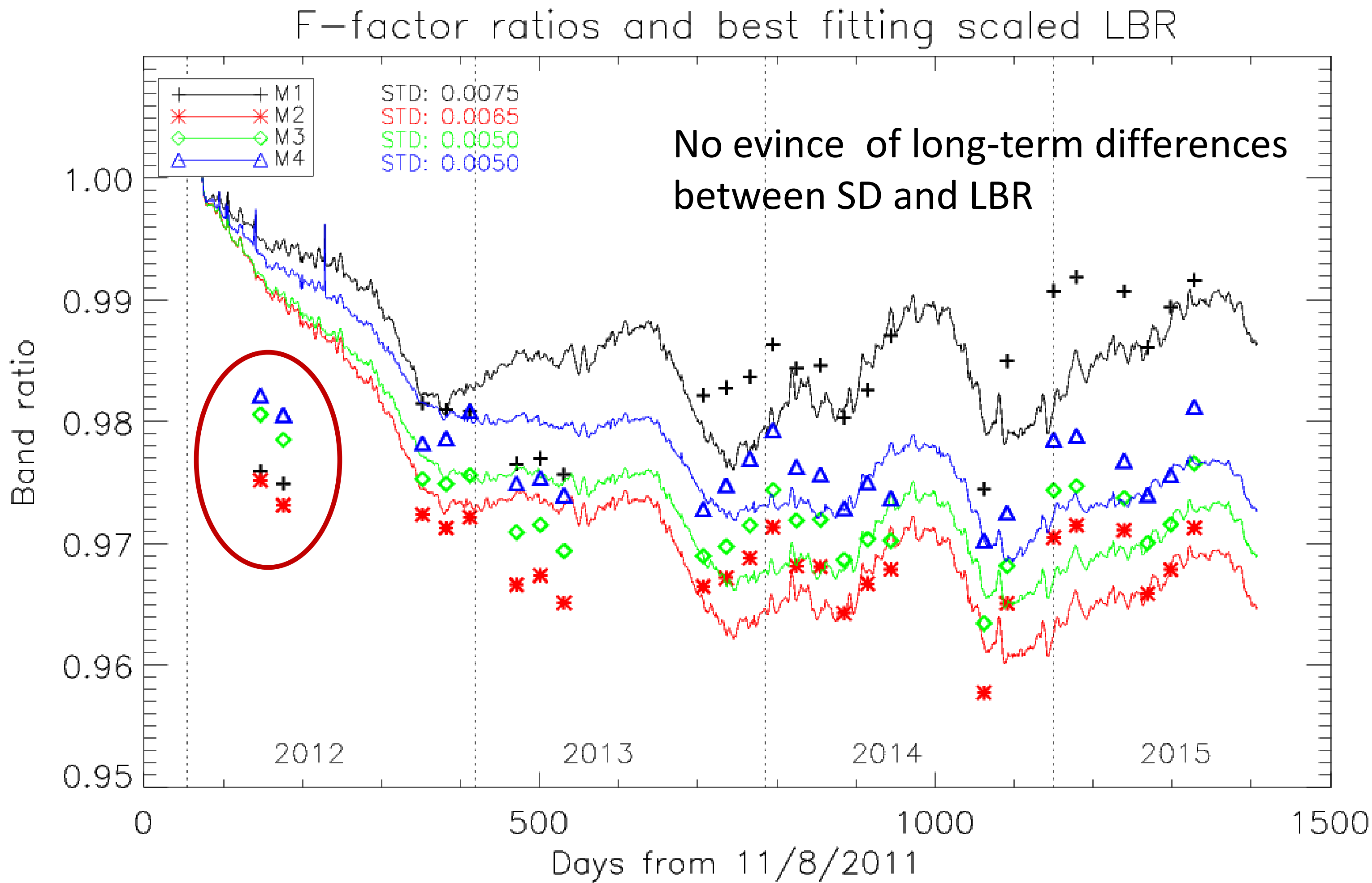

Backup Slides

- SD F-factor correction to Lunar F-factor
  - SD F-factor linear fit to blue solid line.
  - Linear transition between t1 and t2 with Quad fit and linear fit.
  - Linear lunar F-factor is calculated after t1.
  - Constant ratio was found from SD to lunar F-factor after t1.

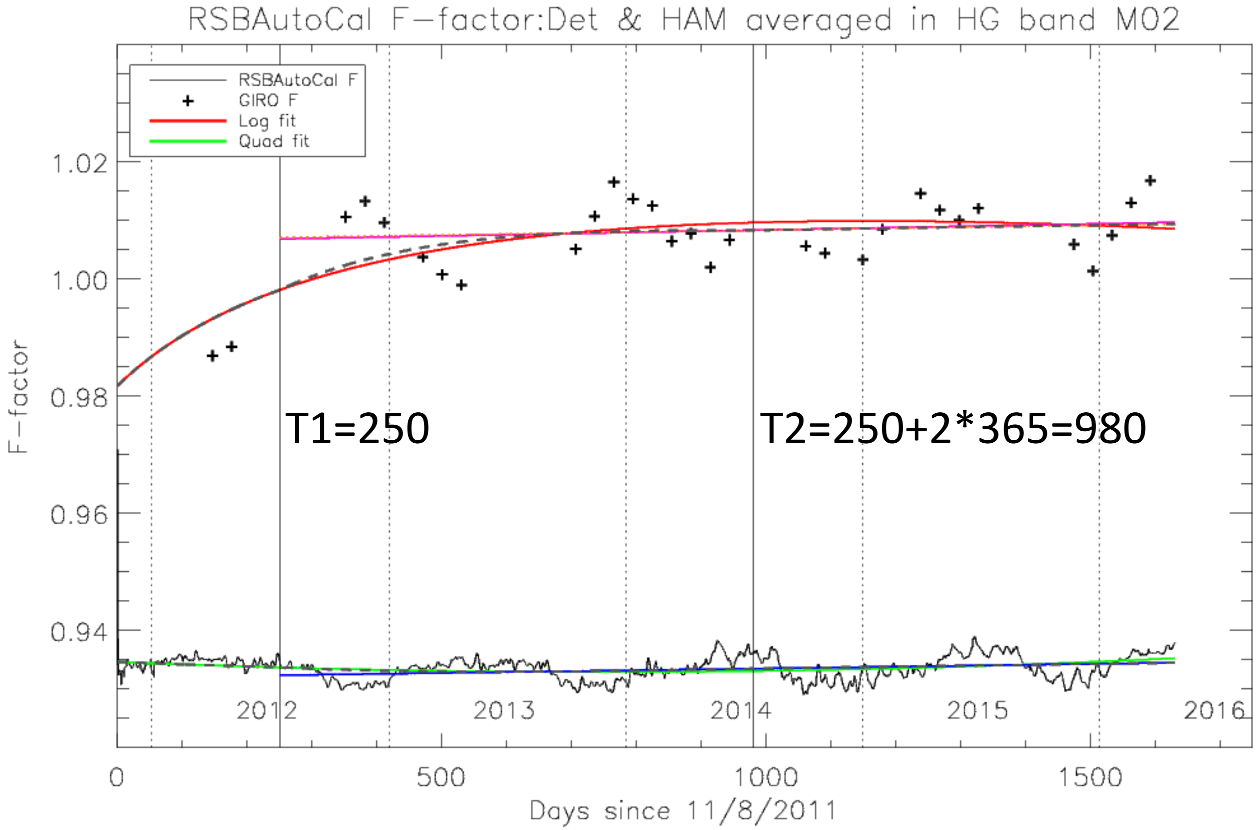

Comparing Reprocessed IDPS Data with Land SIPS

- Previous slide suggests that 2014 exhibits the largest discrepancies between IDPS and NASA Land SIPS data.
- Few IDPS data over desert for 2014 were reprocessed using calibration coefficients generated at STAR.
- Radiance ratio trends between the reprocessed IDPS and Land SIPS data indicates much smaller differences between the two products.
- Blue bands (M1-M3) agrees mostly to within 0.5% and M4 through M8 agree to within 0.3%.

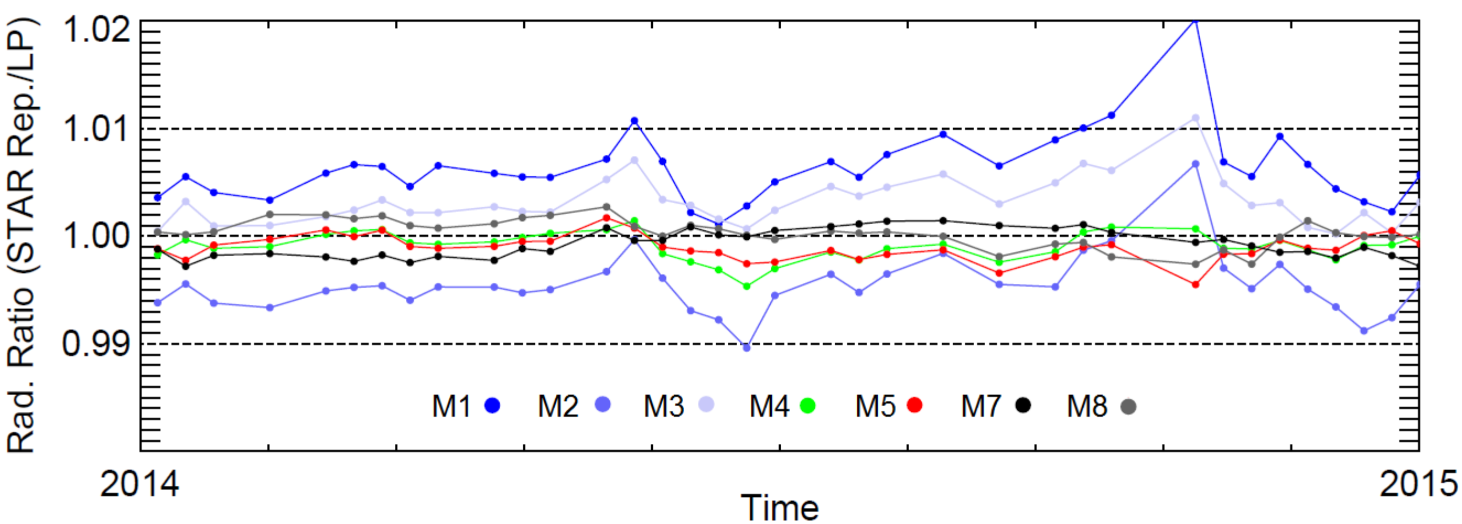

SNPP VIIRS Reflective Solar Bands On-orbit Radiometric Calibration Performance and Improvements

Ning Lei[1], Xuexia Chen[1], Zhipeng Wang[1], Vincent Chiang, and Jack Xiong[2]

1. VIIRS Characterization and Support Team (VCST), SSAI, Lanham, MD, USA
2. NASA GSFC, Greenbelt, MD, USA

August 9, 2016

Thanks to other VCST members

VIIRS RSB On-orbit Calibration

TOA spectral hemispherical reflectance is estimated by (Eq. 81, ATBD vF)

$$\rho(\lambda_{\mathrm{B}}) = \frac{\pi F(B) \times \left(c_0 + c_1 dn_{\mathrm{EV}} + c_2 dn_{\mathrm{EV}}^2\right)}{\mathrm{RVS}(\theta_{\mathrm{EV}}, B) \cos\theta_{\mathrm{sun-earth}} \overline{E_{\mathrm{sun}}}(\lambda_{\mathrm{B}}, d_{\mathrm{sun\text{-}viirs}})} \qquad (1)$$

Focus: correctly calculate *F* (correction factor)

$$F = \frac{\int \mathrm{RSR}(\lambda, B, t) \times L_{\mathrm{SD}}(\lambda, t, \vec{\phi})}{\left(c_0 + c_1 dn_{\mathrm{SD}} + c_2 dn_{\mathrm{SD}}^2\right) \times \int \mathrm{RSR}(\lambda, B, t) d\lambda} \qquad (2)$$

L_{SD} : improved

$\mathrm{RSR}(\lambda, B, t)$: slightly improved

Improved Calculated Sunlit SD Spectral Radiance

$$L_{SD} = E_{sun}(\lambda)\cos(\theta_{SD-sun})\tau_{SAS}\,\mathrm{BRDF}_{RTA}(\lambda, t=0, \vec{\phi})H_{RTA}(\lambda, t, \vec{\phi}) \quad (3)$$

★ $H_{RTA}(\lambda, t, \vec{\phi})$ (SD BRDF degradation factor): biases removed and screen transmittances are more accurate (computed from H_{SDSM})

$\tau_{SAS}(\lambda, \vec{\phi})\mathrm{BRDF}_{RTA}(\lambda, t=0; \vec{\phi})$: one bias removed, 0.05% along solar azimuth direction

Improvements on H_{SDSM} : part 1

(1) SDSM screen transmittance is more accurately calculated

use both yaw maneuver and a small portion (~3-month) of regular data

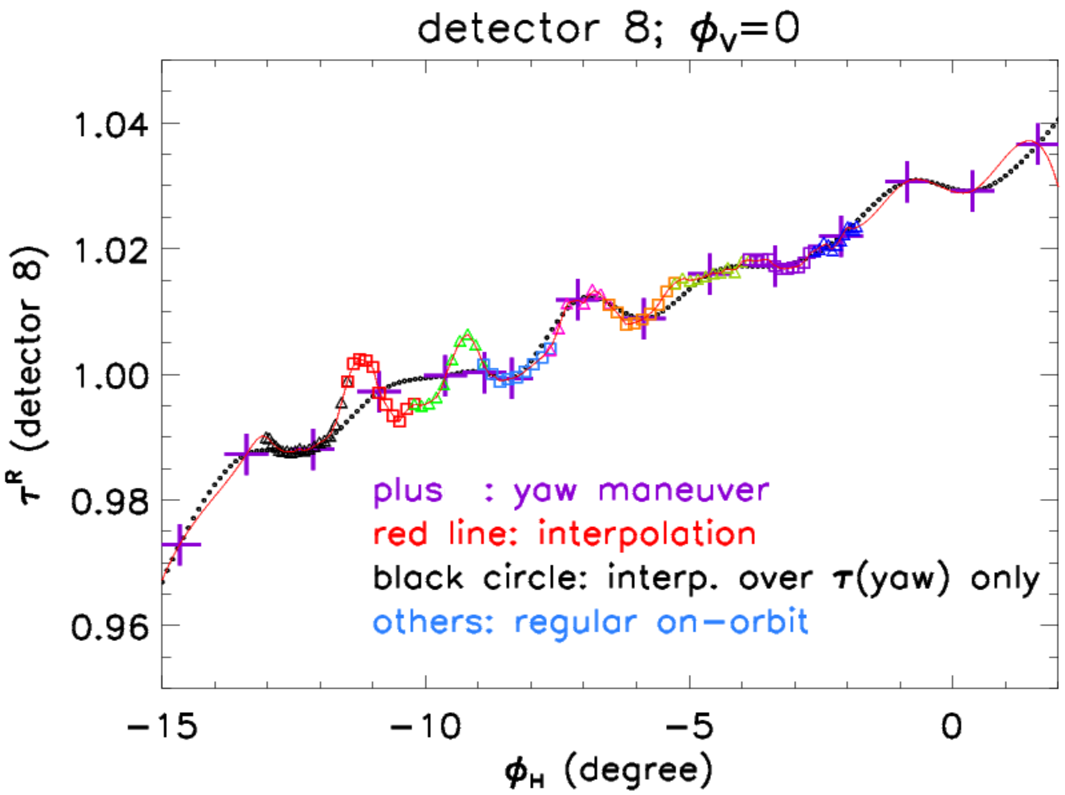

SDSM screen coord.

Improvements on H_{SDSM} : part 2

(2) Improved relative τ(SD)*BRDF(t=0; SDSM)

use both yaw maneuver and a small portion of regular data

and remove bias from the angular dependence of H_{SDSM}

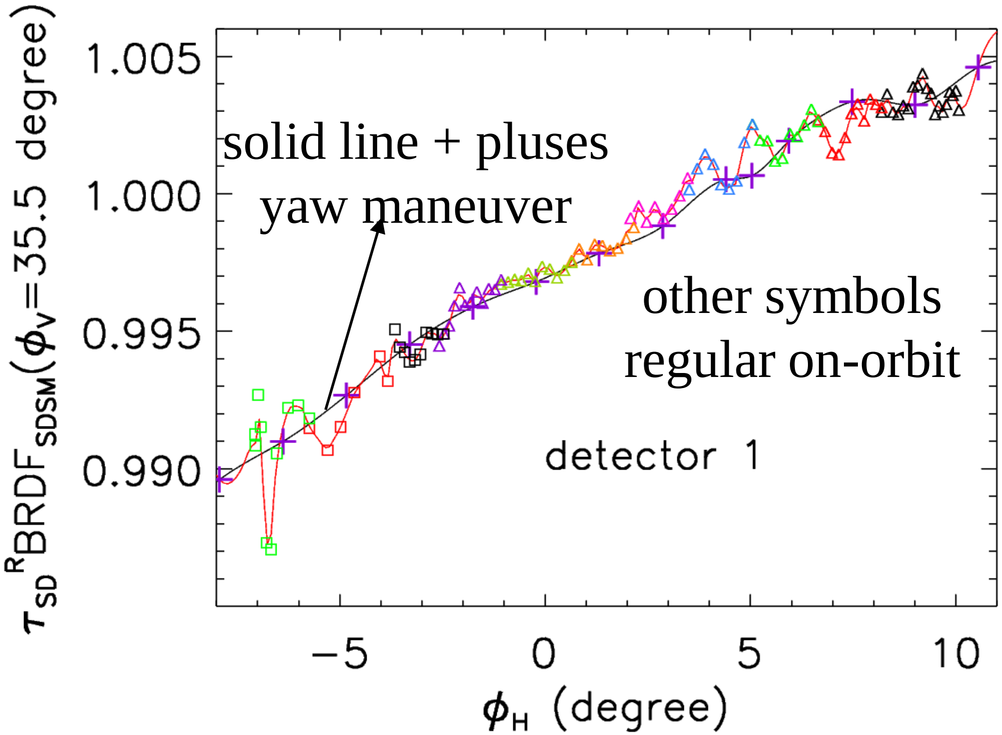

SD coord.

Solar angular dependence of SD BRDF degradation factor

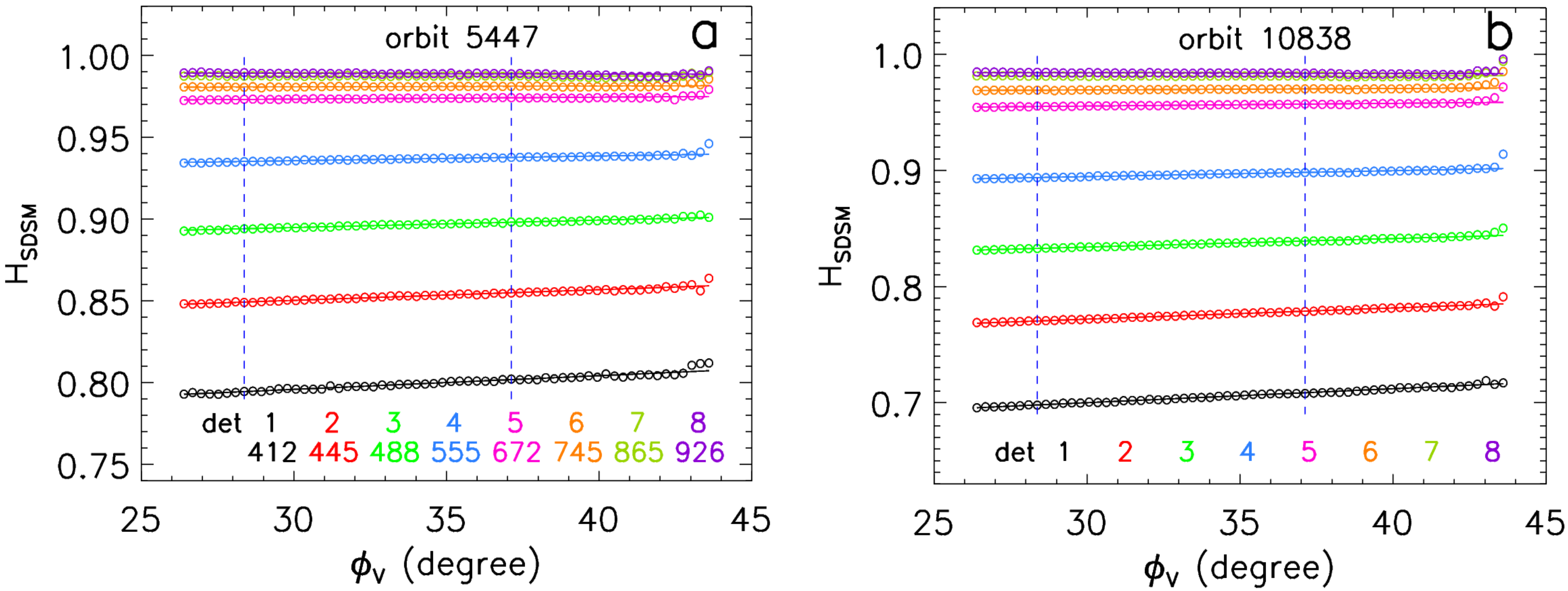

H_{SDSM} depends on solar vertical angle

- the dependence is stronger with smaller H_{SDSM}

Improvements on H_{SDSM} : part 3

(3) Rescale H_{SDSM}

effectively move up H_{SDSM} at the wavelength of 412 nm (M1) by about 1.0%

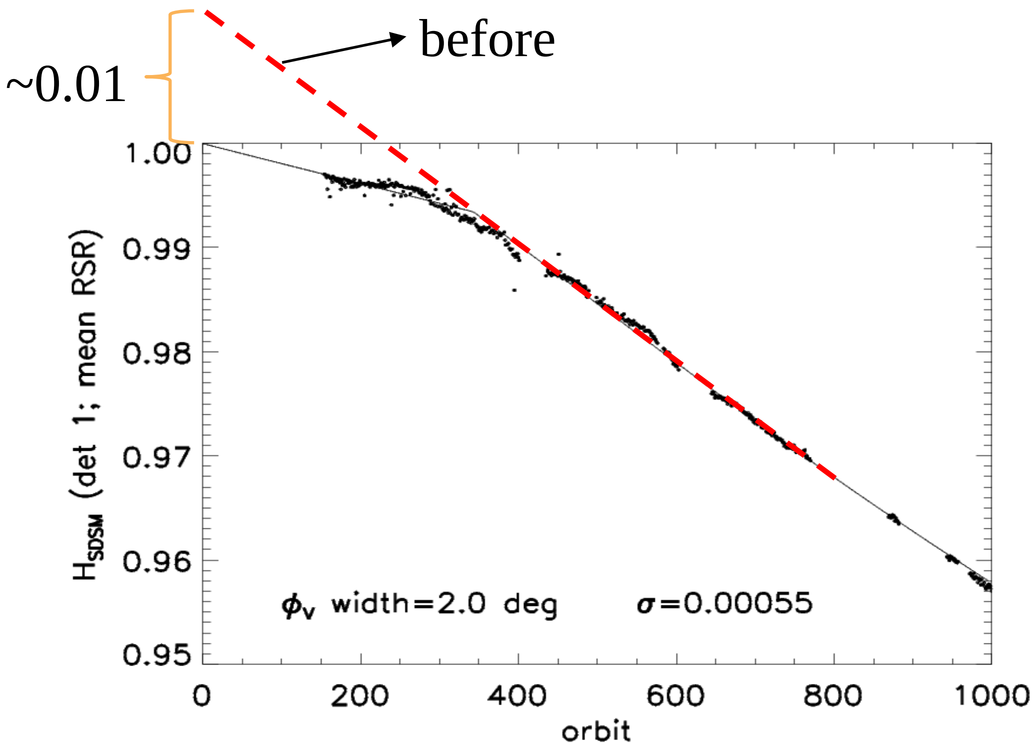

Improvements on H_{SDSM} : part 4

(4) Model H_{SDSM} at SWIR band wavelengths

originally H_{SDSM}(SWIR wavelength)=1

$$1 - H(\lambda, t) = \frac{\alpha(t)}{\lambda^{4.07}} \qquad \alpha(t) = \left\langle (1 - H(\lambda, t)) \times \lambda^{4.07} \right\rangle_{\lambda = (\lambda_{\text{det }5}, \lambda_{\text{det }6}, \lambda_{\text{det }7}, \lambda_{\text{det }8})}$$

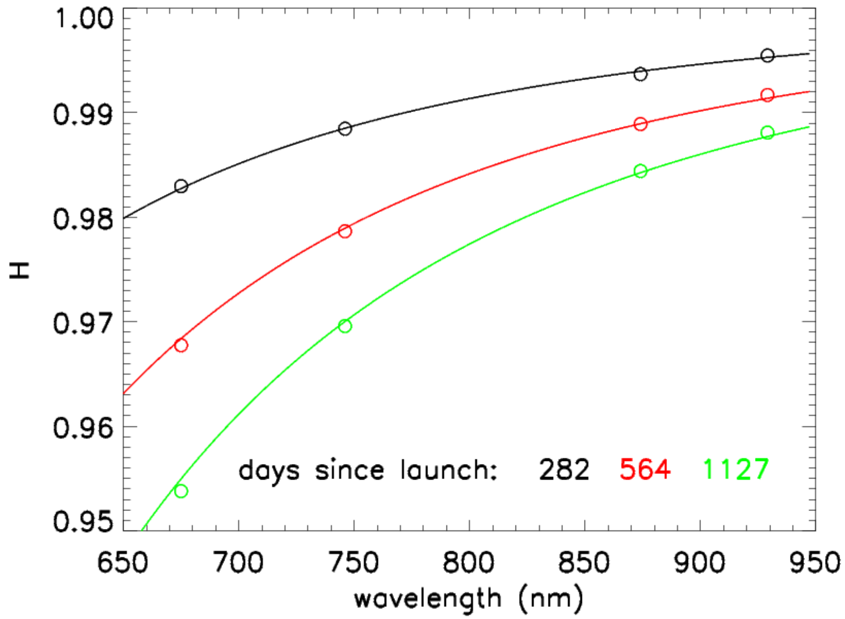

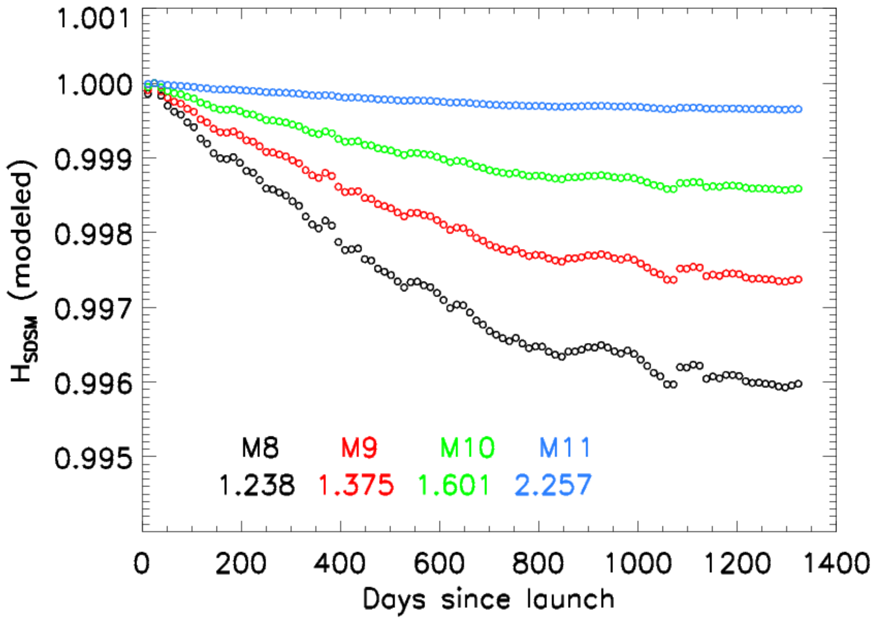

Improved H_{SDSM} (SDSM SD view)

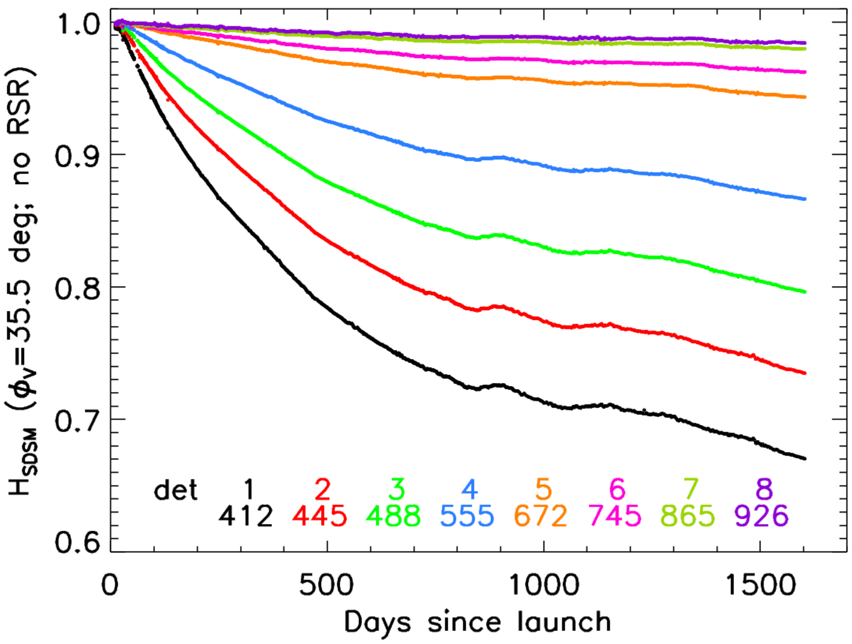

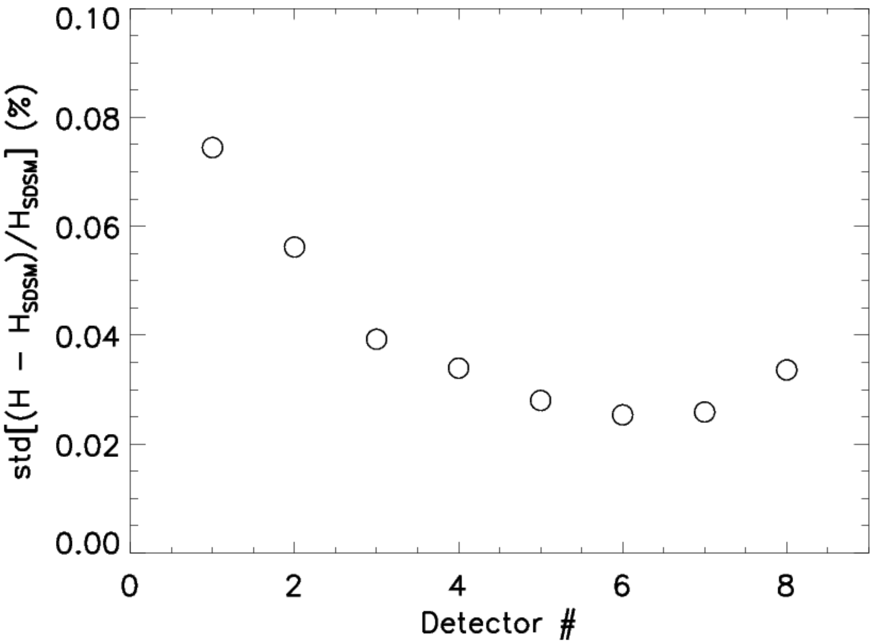

H_{SDSM} can be precisely measured with a relative error mainly in the mid to low 0.0001

Improvements on H_{RTA} : part 1

(1) H_{RTA} dependence on solar azimuth angle ϕ_H

non-observable dependence on φ_H

F calculated with H_{SDSM}

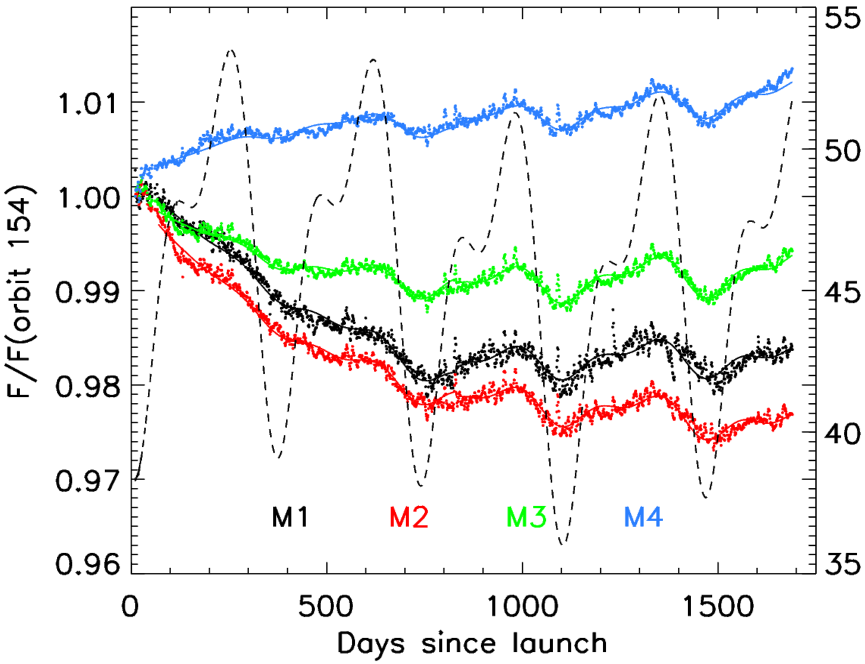

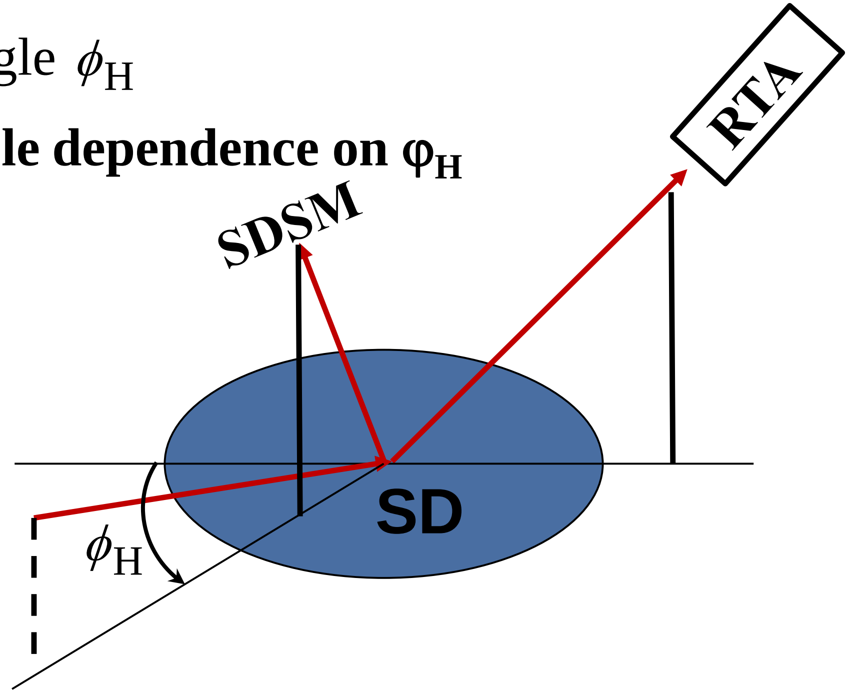

$$F \propto 1 + \beta(\lambda) * \left(H_{SDSM,\ mean\ RSR}(t_{mid}) - H_{SDSM,\ mean\ RSR}\right) * (\phi_H - 48.0°) \quad (4)$$

Improvements on H_{RTA} : part 1

(1) H_{RTA} dependence on solar azimuth angle ϕ_{H}

$$F_1 = F / \left[1 + \beta(\lambda) * \left(H_{\mathrm{SDSM,\ mean\ RSR}}(t_{\mathrm{mid}}) - H_{\mathrm{SDSM,\ mean\ RSR}}\right) * (\phi_{\mathrm{H}} - 48.0°)\right] \qquad (5)$$

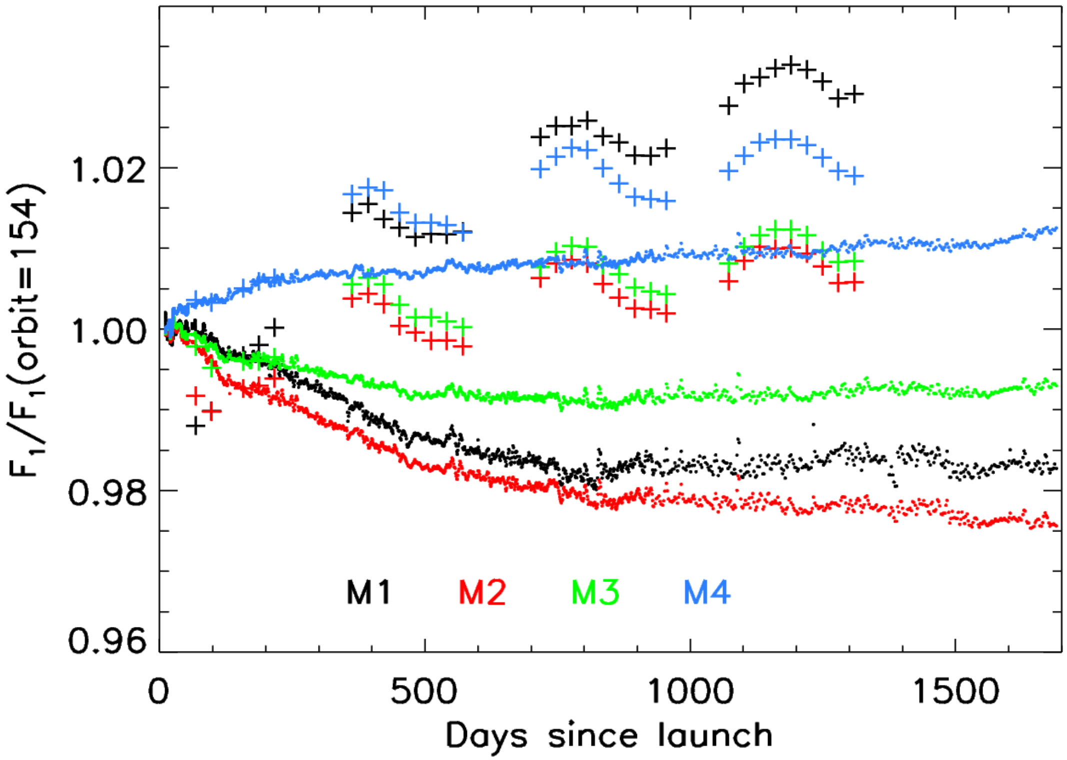

plus: lunar F
dot: SD F

Improvements on H_{RTA} : part 2

(2) H_{RTA} from H_{SDSM}: match scaled lunar results through least-squares fitting

(2.1) $$F_2 = F_1 \times [1 + \gamma(\lambda) * (1 - H_{SDSM})]$$ ➡ update RSR

$$H_{RTA} = H_{SDSM} \times \frac{[1 + \gamma(\lambda) * (1 - H_{SDSM})]}{1 + \beta(\lambda) * (1 - H_{SDSM}) * (\phi_H - 48.0°)}$$

F (5)

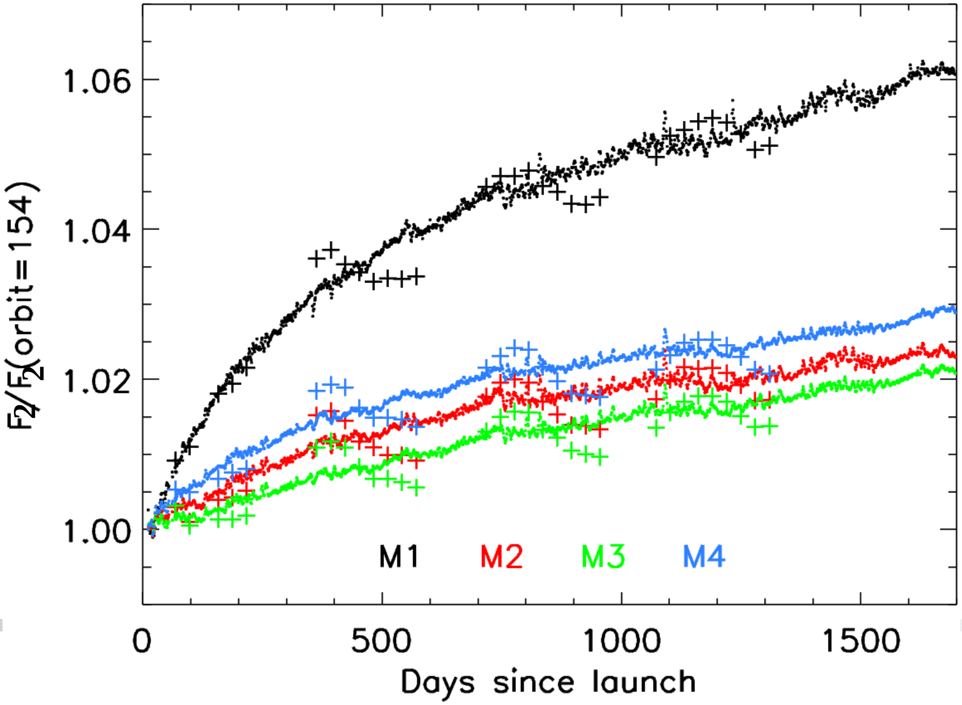

plus: lunar F
dot: SD F

Calculated Detector Gain

gain:=1/F

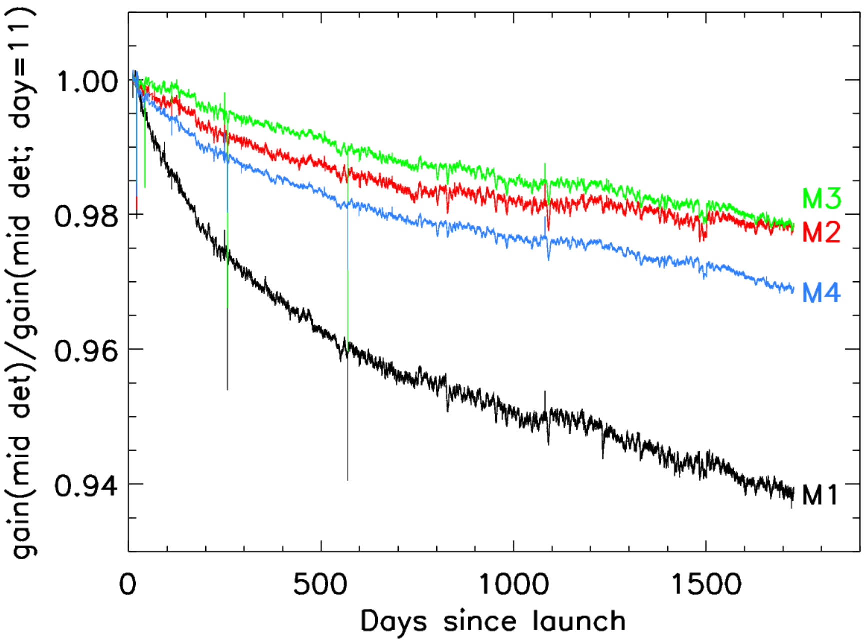

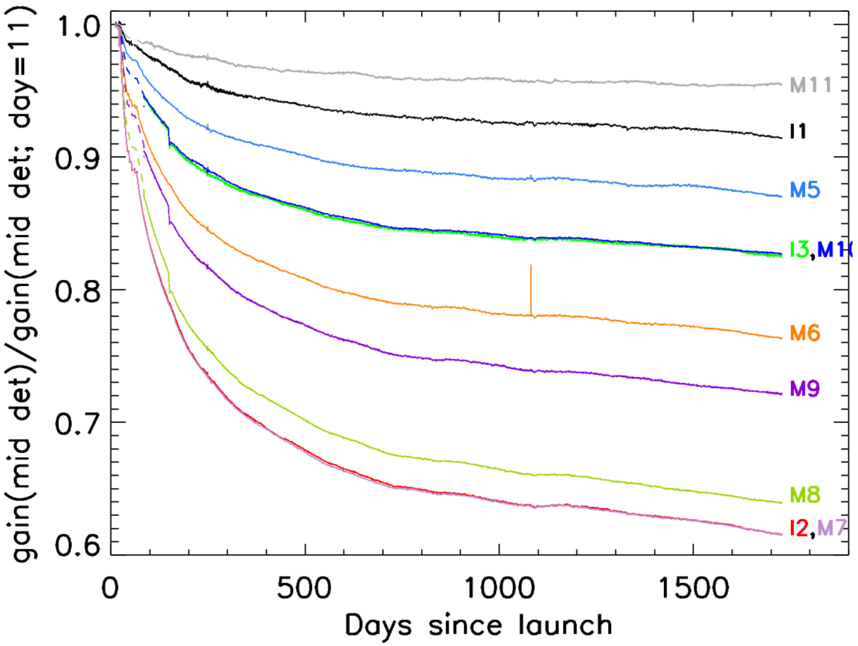

Calculated Gain: new vs old

Old (last version)

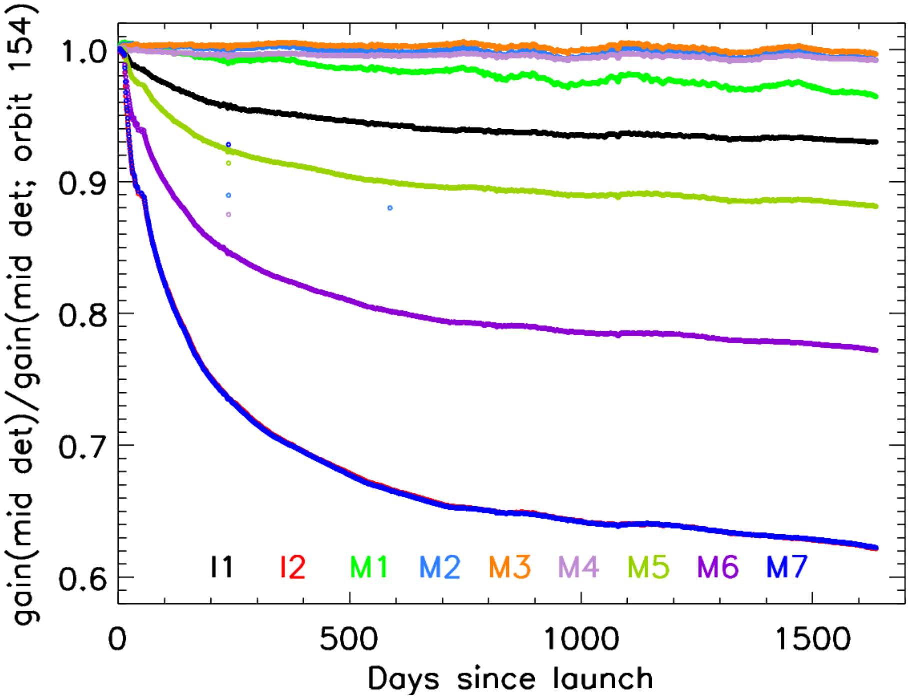

New (current version)

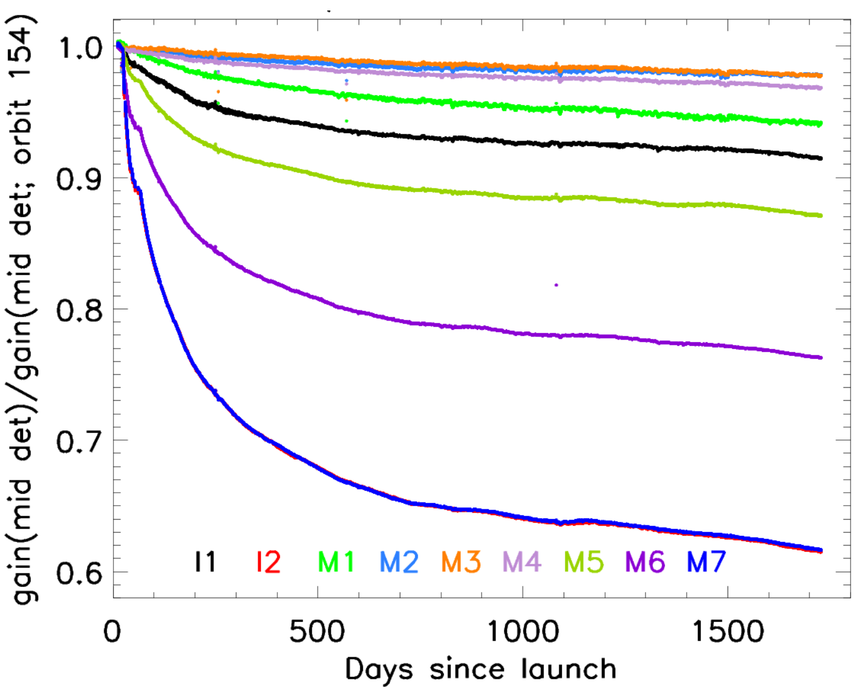

F Precision Estimation

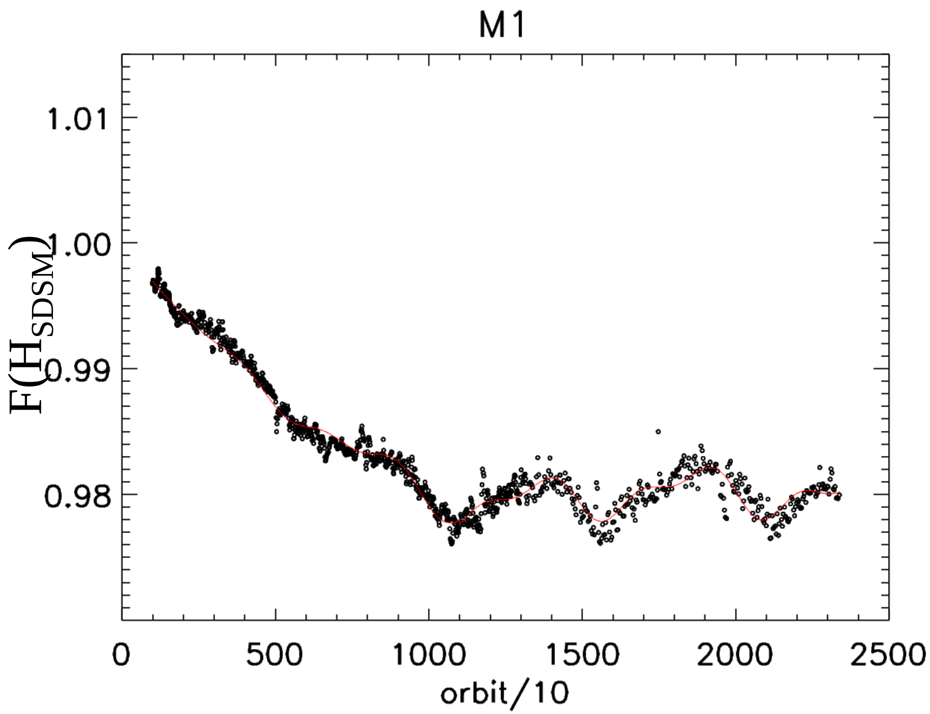

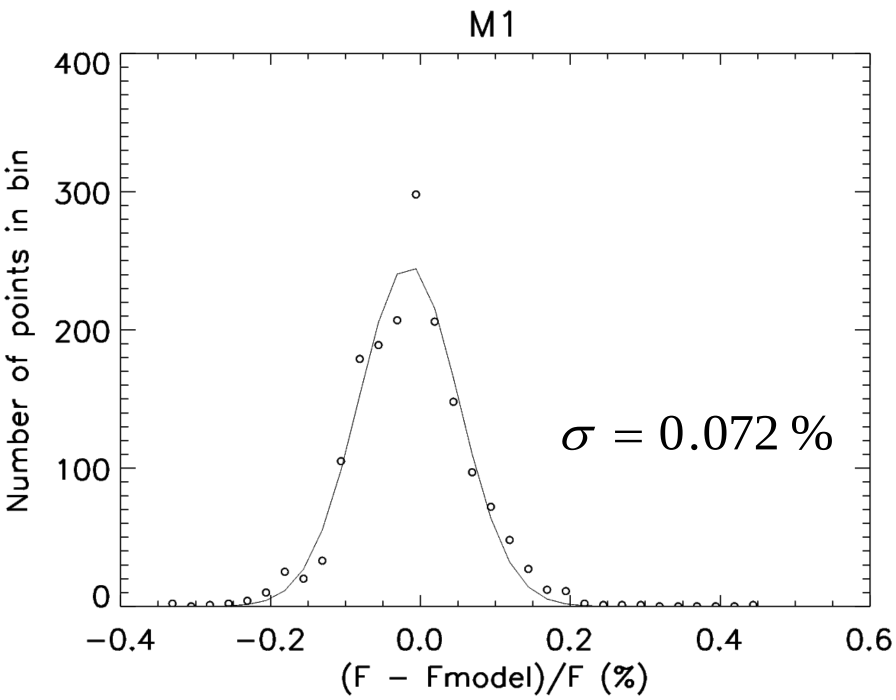

M1:0.07%, M2:0.07%, M3:0.06%, M4:0.04%, I1:0.06%, …, M11:0.05%

Summary

- ***F* calculation accuracy has been improved**
  (1) removed yearly detector gain undulations (as large as 0.5% for M1)
  (2) removed biases (originally observed as large as 1.5% for M1) relative to lunar observations
  (3) removed bias due to incorrect H_{SDSM} normalization at t=0 (~1% for M1)
  (4) removed bias in the original $\tau_{SD}\,\mathrm{BRDF}_{RTA}(t=0)$ (>0.05%; yaw)
  (5) removed bias for the calculated SWIR band throughput (0.4% for M8)
  (6) improved accuracies in $\tau_{SD}^{R}\,\mathrm{BRDF}_{SDSM}(t=0)$ and τ_{SDSM}^{R} (yaw+non-yaw)
  ⇨ H_{SDSM} precision of 0.0003 to 0.0007
- ***F* precisions are around 0.05% on a per satellite orbit basis**
  (M1:0.07%, M2:0.07%, M3:0.06%, M4:0.04%, I1:0.06%, …, M11:0.05%)

VIIRS TEB Potential Improvements

Wenhui Wang and Changyong Cao

NOAA/NESDIS/STAR

With contributions from: Likun Wang (STAR CrIS SDR team), Jason Choi, Bin Zhang , and Zhou Wang

JPSS Annual Science Team Meeting (August 9, 2016)

Outline

- Background
  - Remaining issues with SNPP VIIRS TEB calibration
- Potential Improvements to TEB calibration
  - Review of the Aerospace's method
  - Alternative method
  - Other potential improvements
- Summary

Three Remaining Issues with TEB Calibration

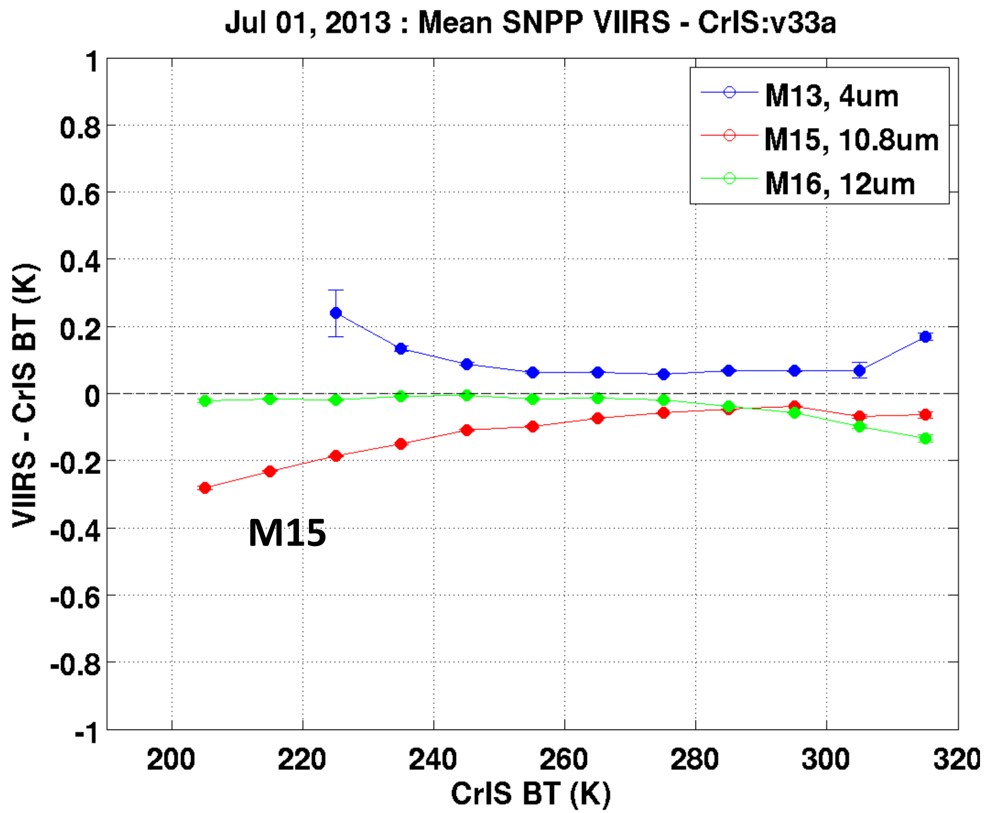

Courtesy of Chris Moeller, 2014 JPSS Annual Science Team Meeting

Issue 1: M15 has a cold bias at low scene temperature (~0.3 K at 200 K)
Issue 2: Constant bias also exist at SST and other temperatures for M15

Three Remaining Issues with TEB Calibration

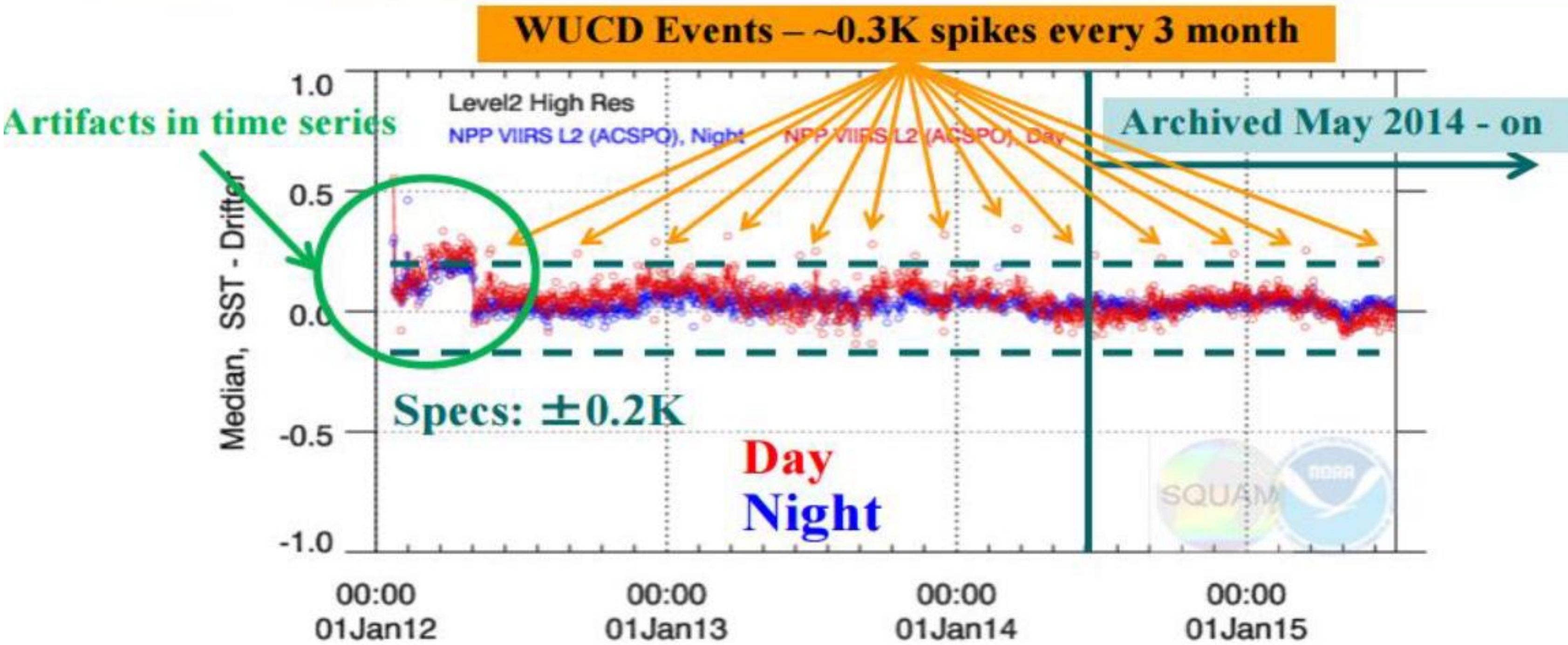

Courtesy of Dr. Ignatov, 2015 JPSS Annual Science Team Meeting

- **VIIRS SST product is generally consistent with drifter measurements, except**
- **Issue 3: "Global warming of ~0.3K" occurs in VIIRS SST every 3 months, due to warm up cool down (WUCD) calibration anomaly.**

STAR ICVS TEB F-Factor Time Series

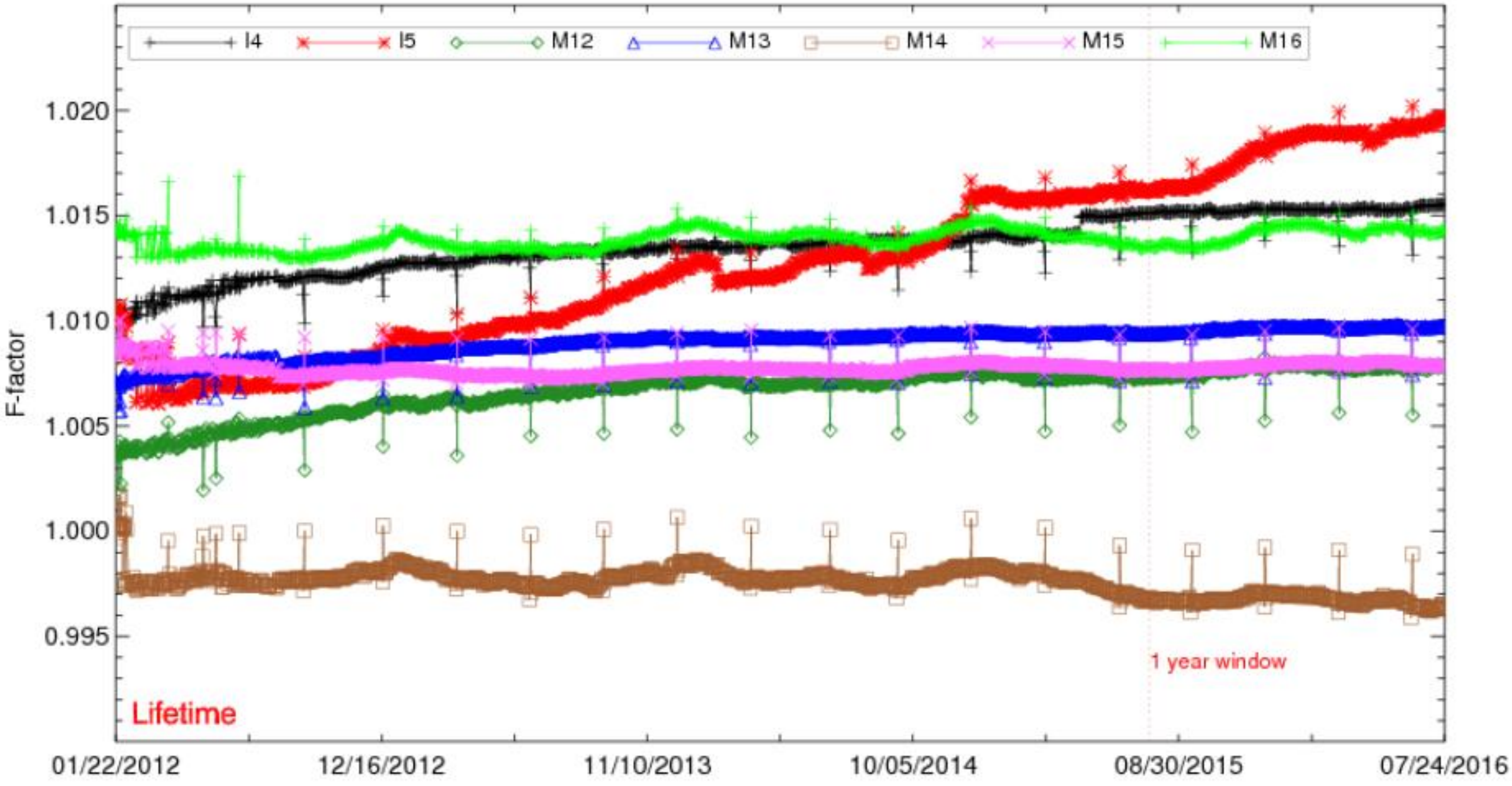

TEB F-factors behave differently during WUCD compared to during nominal blackbody (BB) temperature setting (292.5 K).

M15 F-factor for March 2016 WUCD Event

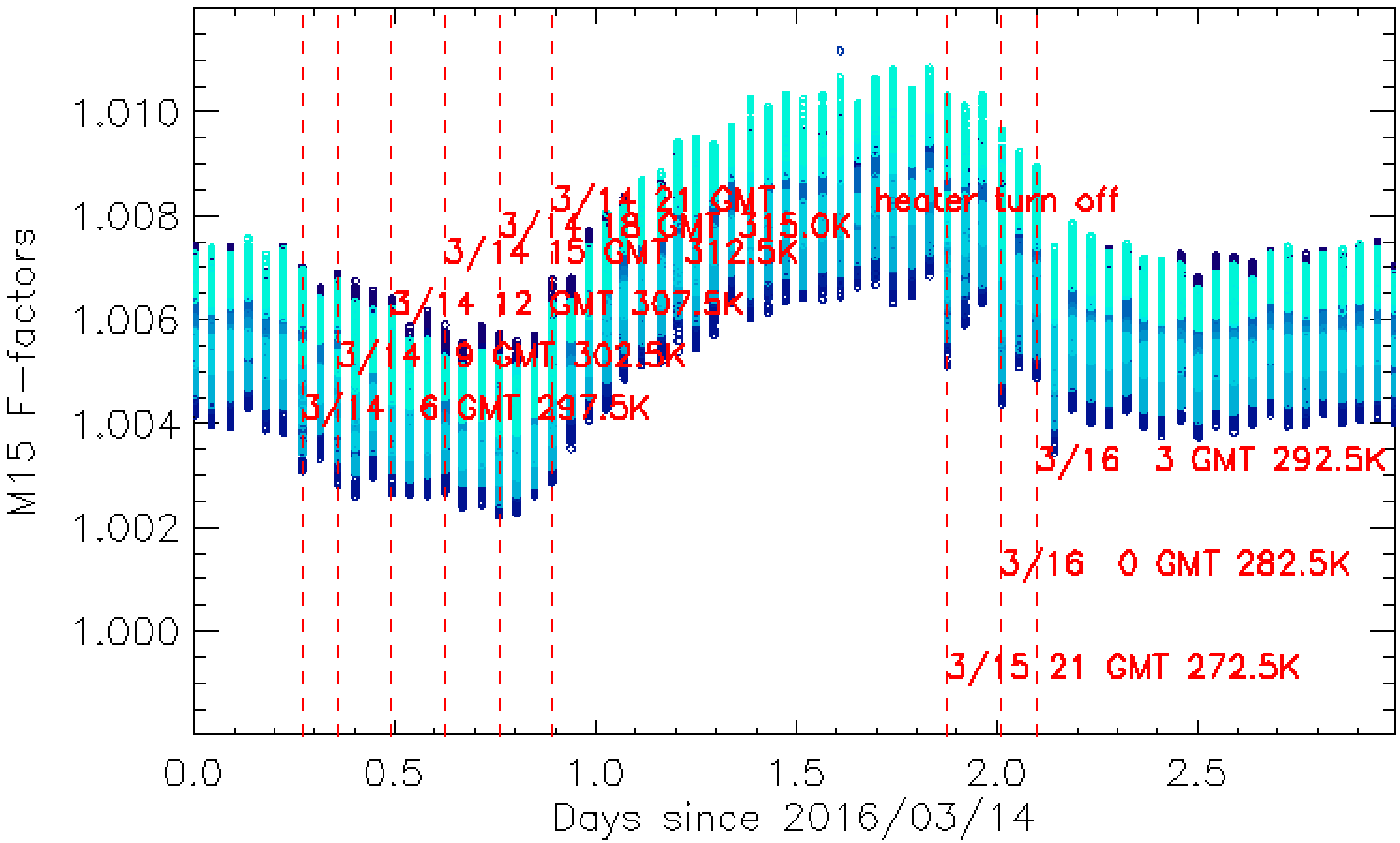

M15 F-factors have large warm biases during cool down→ warm bias in scene BT

small cold bias during warm up → small cold bias in scene BT

Overall: warm bias during WUCD

Summary of Aerospace's Method

- Aerospace proposed a method to reduce F-factor anomalies and scene temperature biases during WUCD (October 7, 2015, Option 1):
  - OBCBB Response Versus Scan (RVS) was changed to optimized values (band-averaged corrections);
  - Half Angle Mirror (HAM) emitted radiance LUT was modified to better represents true HAM radiance;
  - Only #3 and #6 Blackbody (BB) thermistors were used in radiance calculation;
  - Three TEB calibration LUTs in total were changed, no code change required.
  - The method was applicable to all TEB bands.
- The initial proposed method was further updated to flatten F-factors during WUCD by implementing (August 3, 2016, Option 2) :
  - Detector dependent corrections to OBCBB RVS;
  - Detector dependent modification of HAM emitted radiance LUT and using Emission Versus Scan (EVS) to better represents true HAM radiance;
  - Require changes of 3 LUTs + VIIRS SDR science code change;
  - The updated method can be applied to all TEB bands.

Details of Aerospace's method are available on GRAVITE Information Portal under VIIRS SDR telecon documentation directory.

Summary of Aerospace's Method
-Band M15 F Factor Trending Over Historical WUCDs

M15, HAM-A, D1

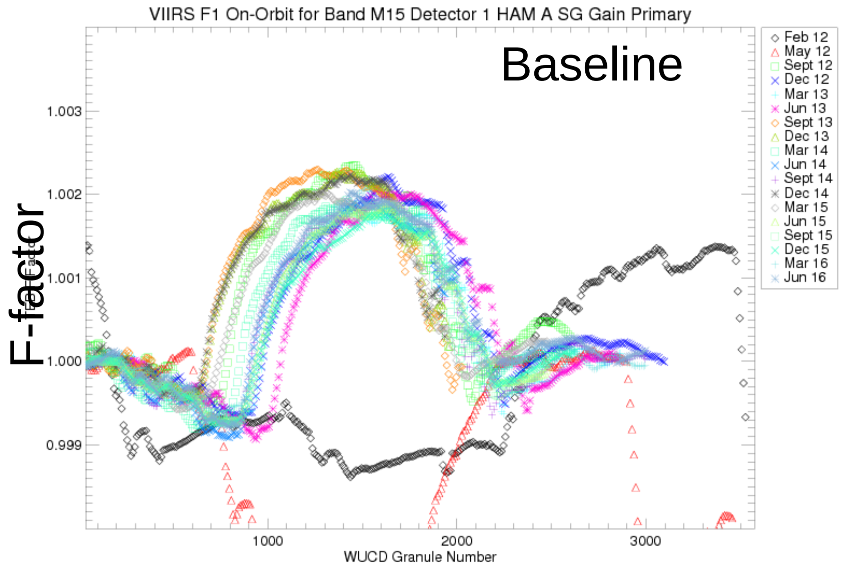

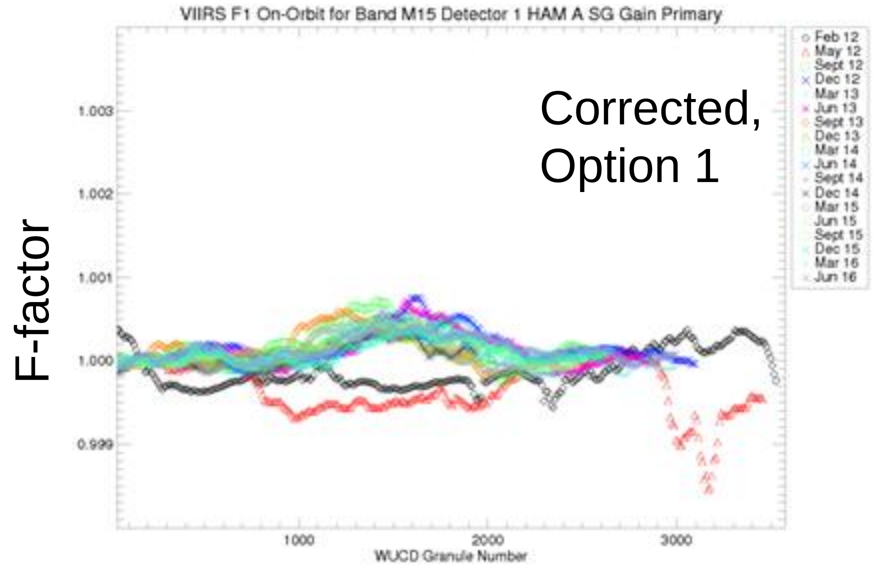

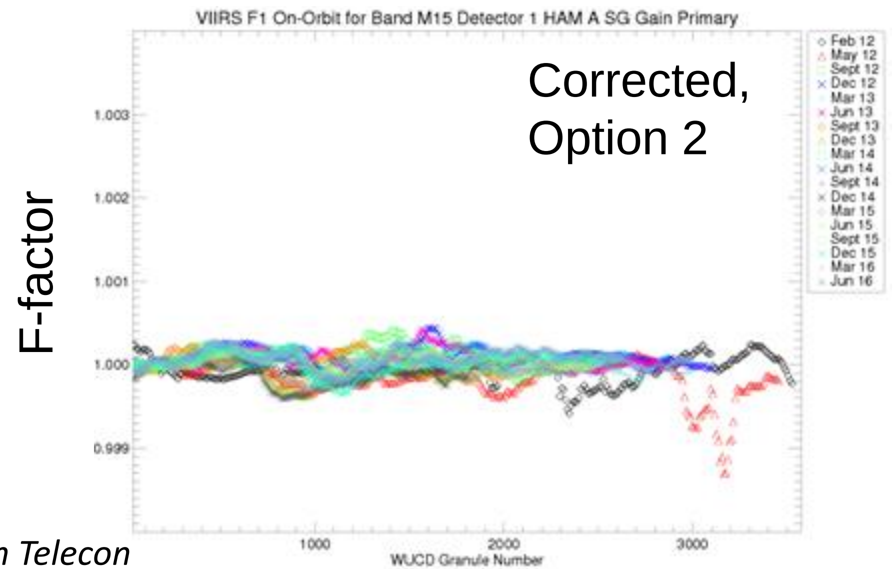

Other detectors/bands show similar patterns
F Factors Smoothed Over Orbits

Courtesy of David Moyer, Aerospace, Aug 3, 2016 VIIRS SDR Team Telecon

Summary of Aerospace's Method Pros and Cons

- Aerospace's method can effectively reducing F-factor anomalies for all TEB bands and reduce scene BT bias during WUCD at SST temperatures
- It can also reduce M15 constant scene BT bias under nominal BB temperatures
- However, it will increase M15 cold scene bias;
- Three LUTs needed to be modified;
- Code change is require for detector dependent HAM radiance correction (option 2);
- Only use 2 out of 6 BB temperature thermistors.

Alternative Method to Improve TEB Calibration

Prelaunch versus WUCD derived C Coefficients

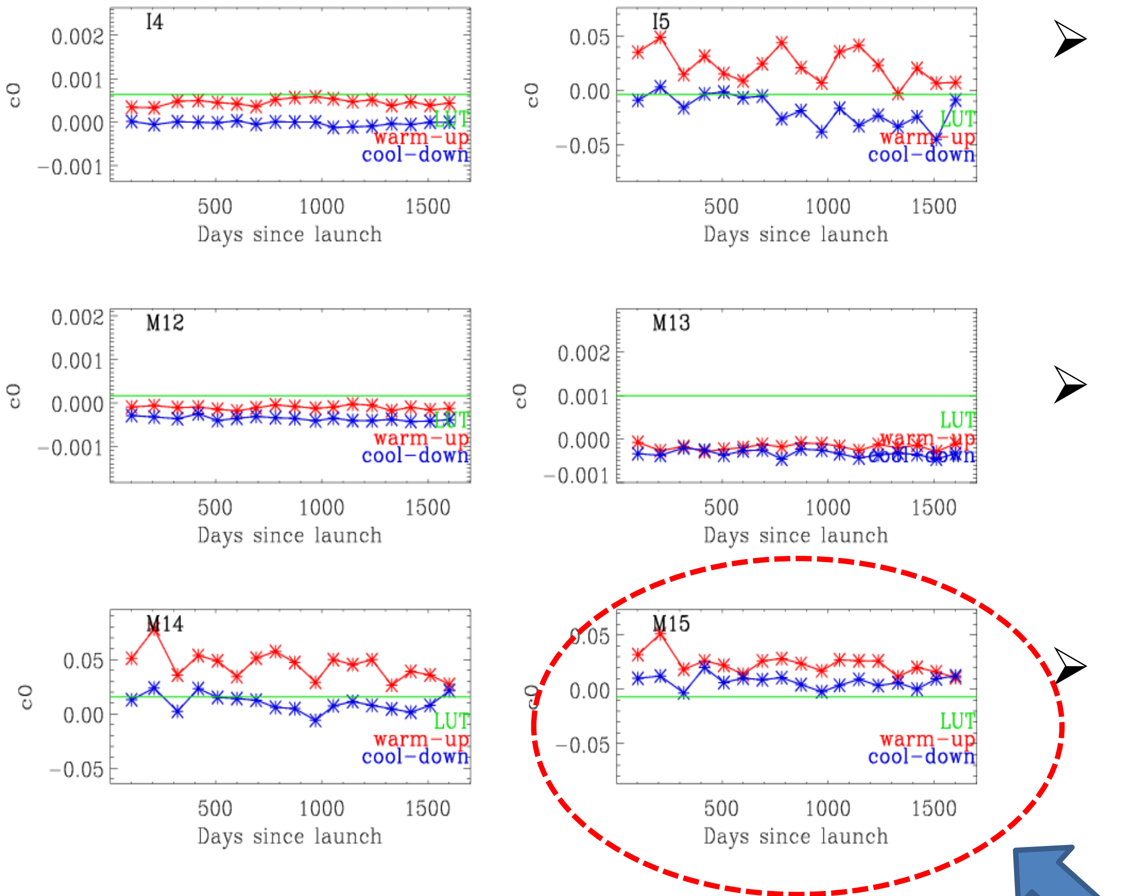

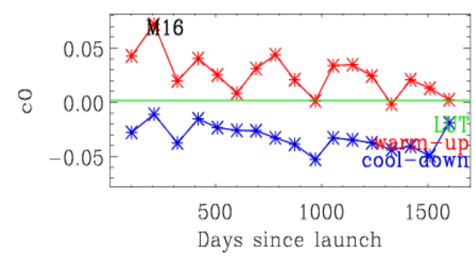

Courtesy of NASA VCST, June 2016 MODIS/VIIRS Science Team Meeting

- Prelaunch characterized C coefficients are currently used for operational SNPP VIIRS TEB SDR production;
- On orbit instrument environment may be different from prelaunch;
- Larger difference exist between prelaunch and WUCD derived C coefficients in some bands; e.g.

M15 WUCD derived c0s are consistently higher than the prelaunch values, and with opposite sign

Alternative Method to Improve TEB Calibration Modify C Coefficients

- An alternative method is to explore using WUCD derived C coefficients to address TEB calibration issues.
  - VCST WUCD C coefficients were used as references in this study;
  - One LUT (VIIRS-SDR-DELTA-C-LUT) needs to be modified;
  - Similar method was used for MODIS TEB.
- TEB calibration terms from typical granules with nominal (292.5K), warm (315 K), and cold (272.5 K) BB temperatures at nadir were exacted using ADL and used for:
  - further analyzing the sensitivity of different terms, including C coefficients, on WUCD F-factor anomaly and scene temperature biases;
  - Refining Tele and Tomm dependencies of C coefficients.
- The method was applied to M15 in this study:
  - Band averaged, Tomm dependent modifications were applied to c0, which show large differences between prelaunch and WUCD values;
  - Prelaunch c1 and c2 values are generally consistent those derived by WUCD, therefore unchanged;
  - c2 values are small (on the order of 1E-8), not sensitivity to WUCD anomalies.

M15 F-factors (HAM-A)

March 2016 WUCD | **June 2016 WUCD**

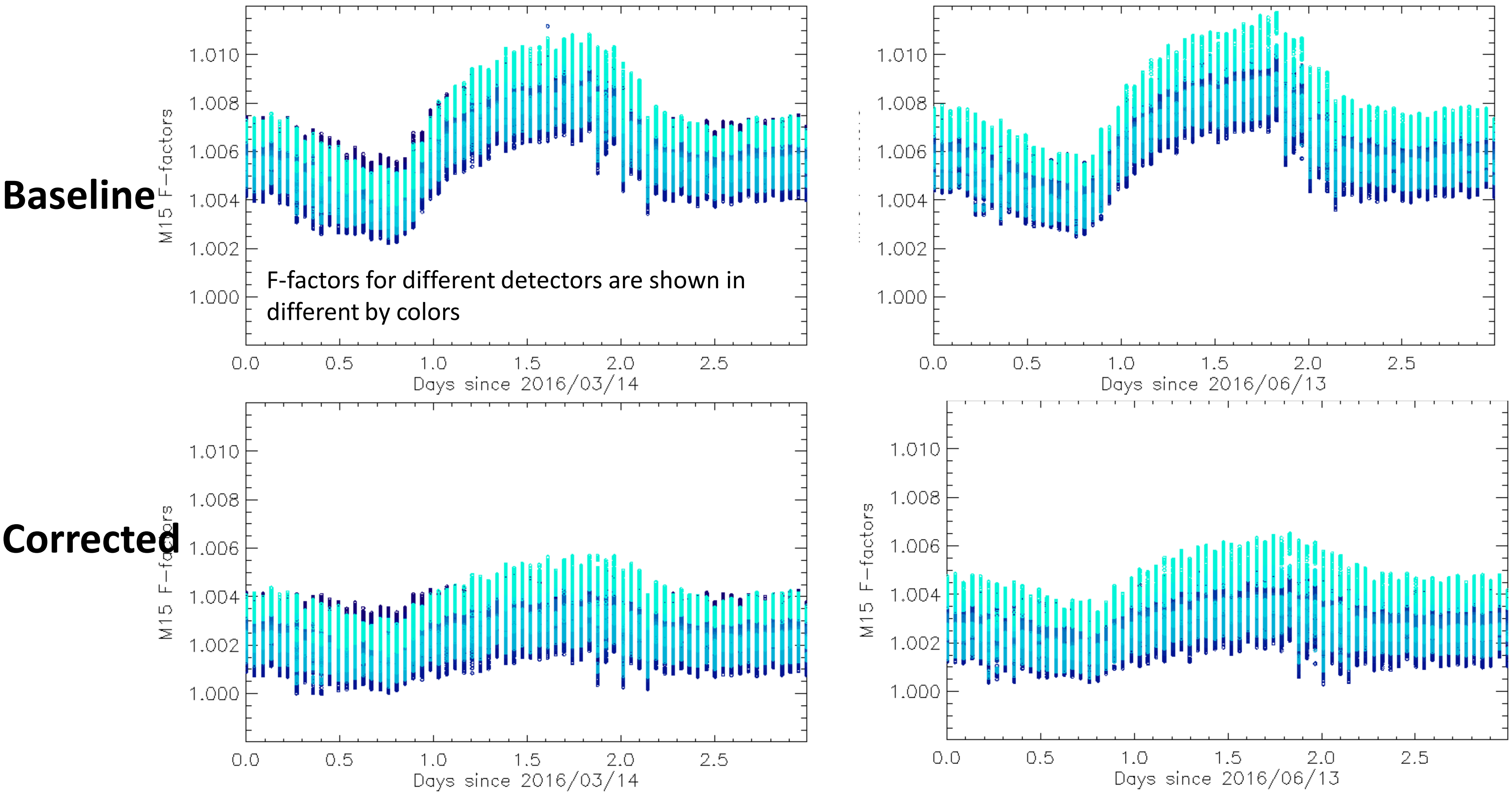

After correction, M15 F-factors become more consistent during normal, warm, and cold BB temperatures. HAM-B shows similar patterns.

Band-Averaged F-factor Time Series for M15 (November 2015 - June 2016)

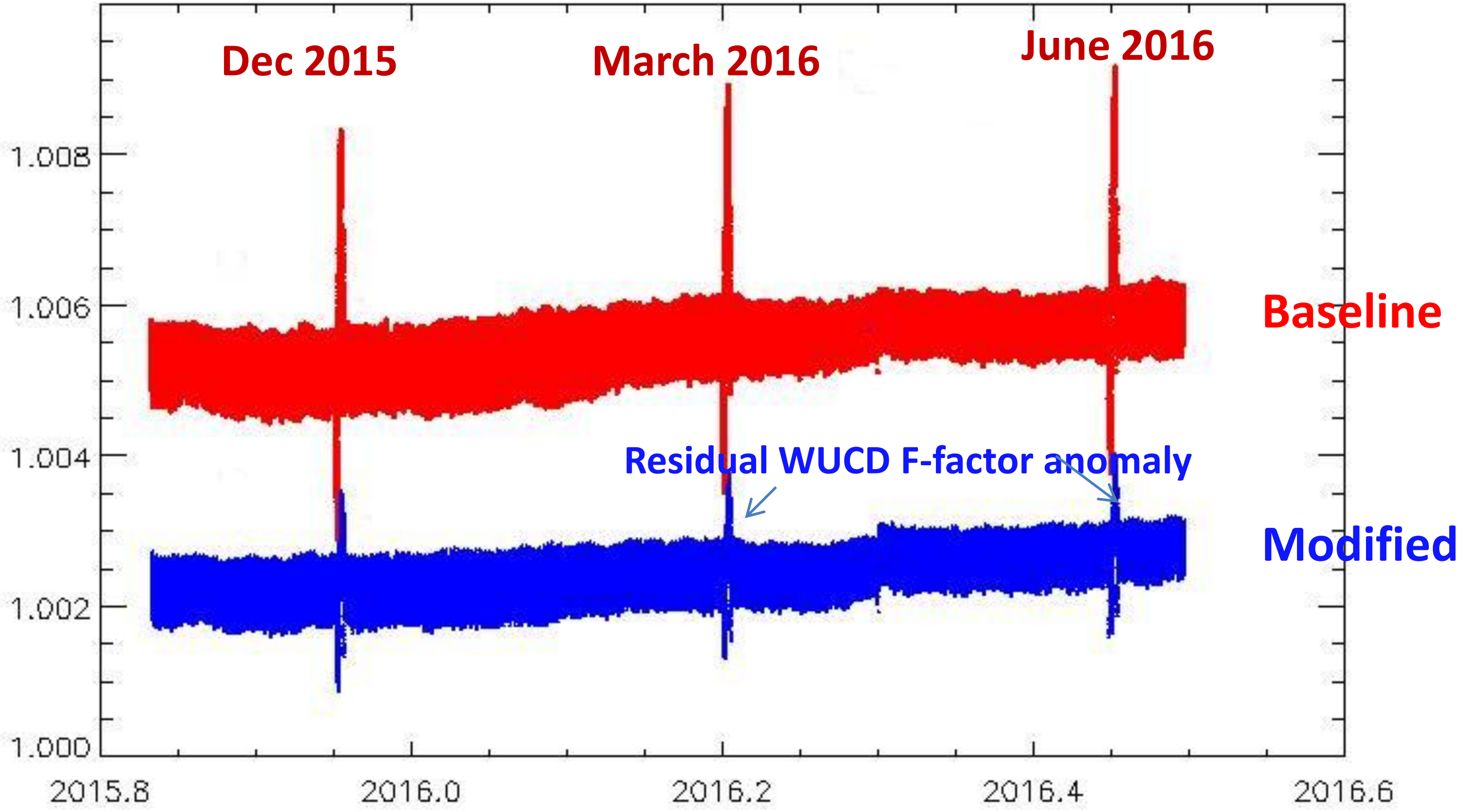

- WUCD F-factor anomalies are significantly reduced after applying the modified c0 values.
- c0 values, esp its Tomm dependency, can be refined to further reduce the anomalies.

Three Types of M15 BT biases Based on Comparisons with CrIS (Baseline)

1. **Cold scene bias**
   Larger bias under cold scene temperatures
2. **Constant bias**
   VIIRS M15 and CrIS BTs differ by ~0.2 K on average during nominal BB temperatures
3. **WUCD biases**
   1. Cold bias during warm up
   2. Warm bias during cool down

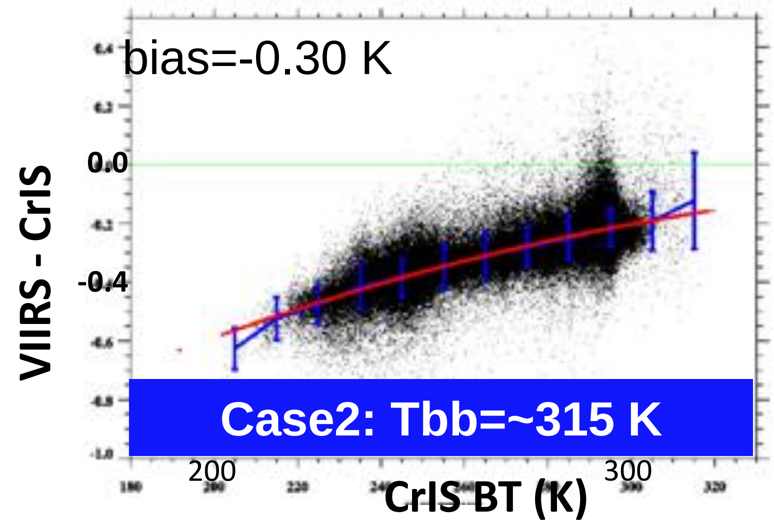

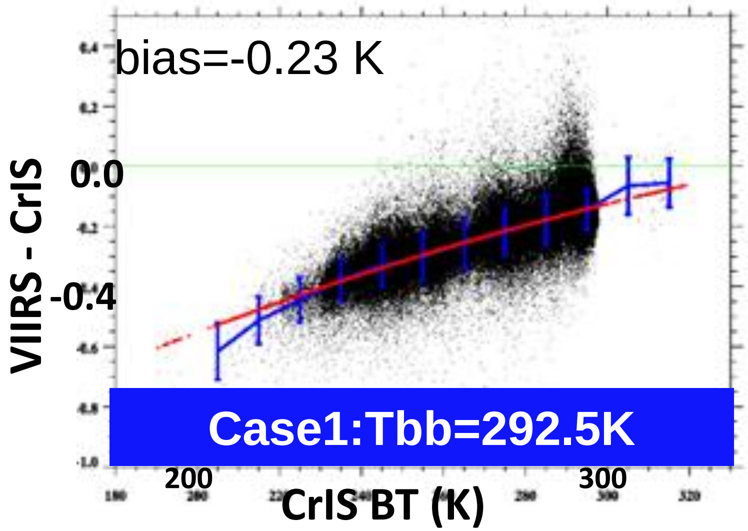

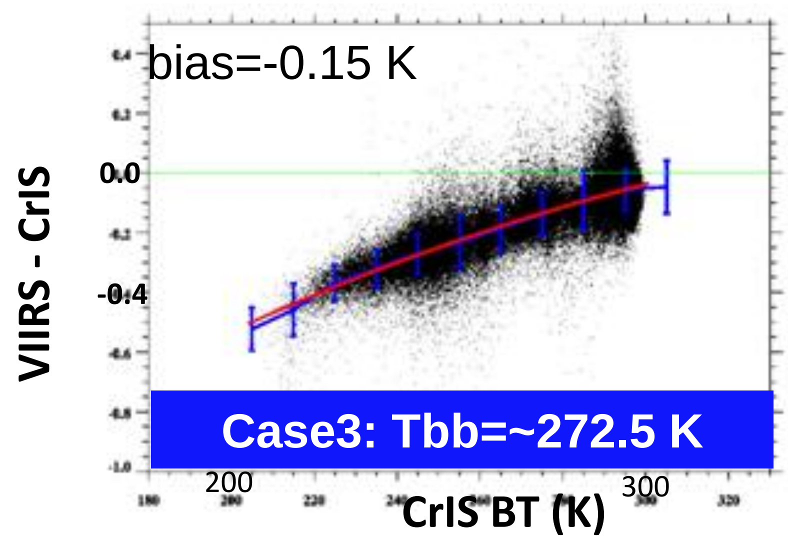

Courtesy of Likun Wang (STAR CrIS SDR Team), each plot was generated using 2 hours of data

Three Types of M15 BT biases Based on Comparisons with CrIS (Updated)

1. **Cold scene bias was almost removed;**
2. **Constant bias was reduced by ~0.1 K;**
3. **WUCD biases removed:**
   Remaining constant biases are close to each other under different BB temperature settings.

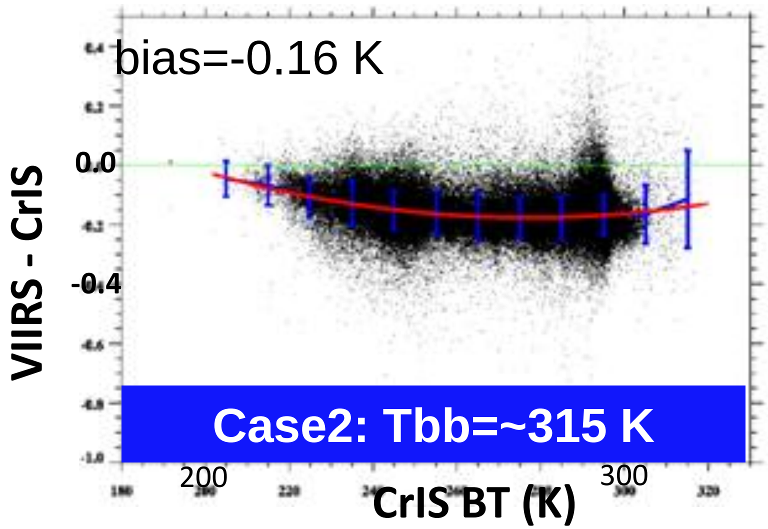

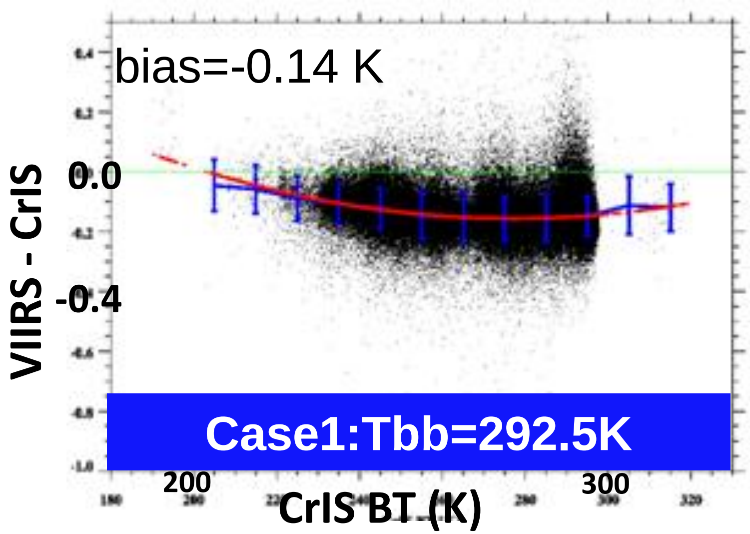

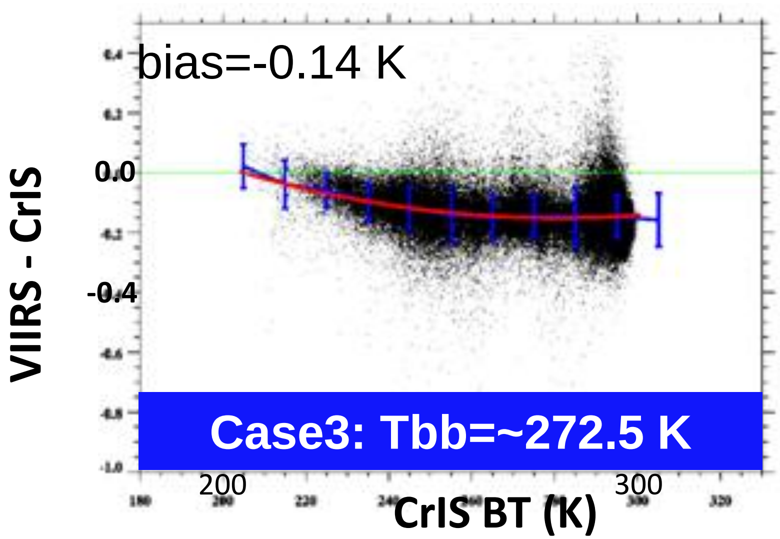

Courtesy of Likun Wang (STAR CrIS SDR Team)

Other Potential Improvement: TEB calibration Equation

- **Current VIIRS TEB Calibration Equations:**

$$F = \frac{\mathrm{RVS}(\theta_{obc})\cdot\left\{\left(1-\frac{1}{\mathrm{RVS}(\theta_{obc})}\right)\cdot\frac{\left\{\left(1-\overline{\rho_{rta}(\lambda)}\right)\cdot\overline{L(T_{rta},\lambda)}-\overline{L(T_{ham},\lambda)}\right\}}{\overline{\rho_{rta}(\lambda)}}+\overline{\varepsilon_{obc}(\lambda)}\cdot\overline{L(T_{obc},\lambda)}+\overline{L_{obc\_rfl}(T_{sh},T_{cav},T_{tele},\lambda)}\right\}}{\sum_{j=0}^{2} c_j\cdot dn_{obc}{}^{j}}$$

$$\overline{L_{ap}}(\theta,B) = \frac{F\cdot\sum_{i=0}^{2} c_i\cdot dn^i - (\mathrm{RVS}(\theta,B)-1)\cdot\frac{\left\{\left(1-\overline{\rho_{rta}(\lambda)}\right)\cdot\overline{L(T_{rta},\lambda)}-\overline{L(T_{ham},\lambda)}\right\}}{\overline{\rho_{rta}(\lambda)}}}{\mathrm{RVS}(\theta,B)}$$

F-factor scales c0,c1, c2 equally on orbit

- **MODIS-equivalent TEB Calibration Equations:**

$$c_1^{'} = \frac{RVS(\theta_{obc})\cdot\left\{\left(1-\frac{1}{\mathrm{RVS}(\theta_{obc})}\right)\cdot\frac{\left\{\left(1-\overline{\rho_{rta}(\lambda)}\right)\cdot\overline{L(T_{rta},\lambda)}-\overline{L(T_{ham},\lambda)}\right\}}{\overline{\rho_{rta}(\lambda)}}+\overline{\varepsilon_{obc}(\lambda)}\cdot\overline{L(T_{obc},\lambda)}+\overline{L_{obc\_rfl}(T_{sh},T_{cav},T_{tele},\lambda)}\right\}-c_0-c_2\cdot dn^2_{obc}}{dn_{obc}}$$

$$\overline{L_{ap}}(\theta,B) = \frac{c_0+c_1^{'}\cdot dn+c_2\cdot dn^2-(\mathrm{RVS}(\theta,B)-1)\cdot\frac{\left\{\left(1-\overline{\rho_{rta}(\lambda)}\right)\cdot\overline{L(T_{rta},\lambda)}-\overline{L(T_{ham},\lambda)}\right\}}{\overline{\rho_{rta}(\lambda)}}}{\mathrm{RVS}(\theta,B)}$$

Only c1 is derived for each scan on orbit, no scaling of c0 and c2
This requires further study

Summary

- The VIIRS SDR teams have been working diligently to address remaining issues in TEB calibration;
- The Aerospace's method was reviewed;
- An new method was proposed, preliminary results are promising:
  - Based on WUCD derived C coefficients and sensitivity analysis;
  - Only change one LUT, no other change is needed;
  - Effectively reducing 3 types of M15 scene BT biases:

    1)Cold scene bias; 2)Constant bias; 3) WUCD bias.
- Next step:
  - Further refine the new method and apply it to all TEB bands
  - Conduct more impact studies for all methods;
  - Continue to explore other potential solutions.

Backups

March 14-16 WUCD Event

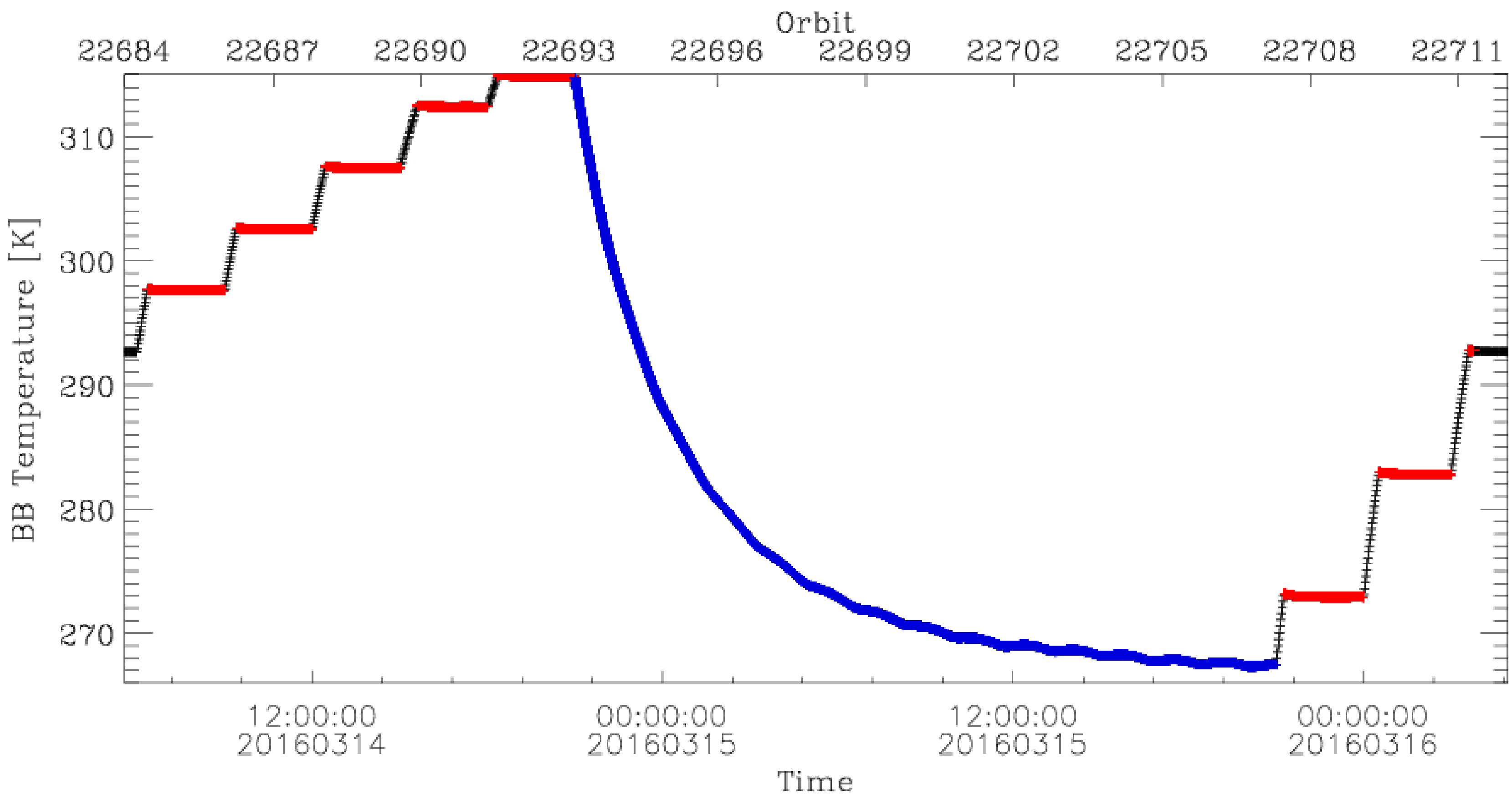

Courtesy of NASA VCST, June 2016 MODIS/VIIRS Science Team Meeting

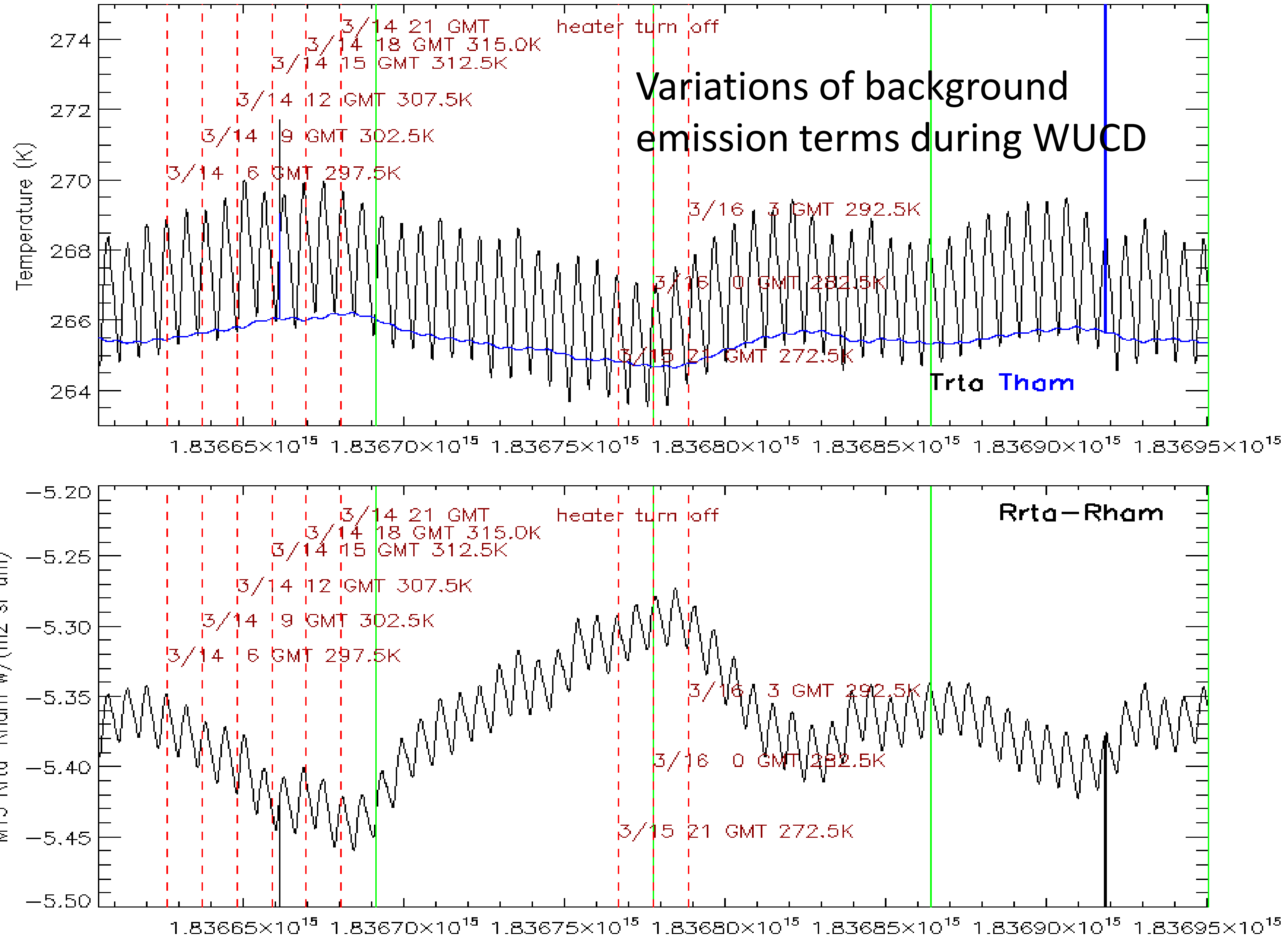
Variations of background emission terms during WUCD
Temperature (K)
274
272
270
268
266
264
3/14 21 GMT
heater turn off
3/14 18 GMT 315.0K
3/14 15 GMT 312.5K
3/14 12 GMT 307.5K
3/14 9 GMT 302.5K
3/14 6 GMT 297.5K
3/16 3 GMT 292.5K
3/16 0 GMT 282.5K
3/15 21 GMT 272.5K
Trta Tham
1.83665×10^15 1.83670×10^15 1.83675×10^15 1.83680×10^15 1.83685×10^15 1.83690×10^15 1.83695×10^15
−5.20
−5.25
−5.30
−5.35
−5.40
−5.45
−5.50
Rrta−Rham
3/14 21 GMT
heater turn off
3/14 18 GMT 315.0K
3/14 15 GMT 312.5K
3/14 12 GMT 307.5K
3/14 9 GMT 302.5K
3/14 6 GMT 297.5K
3/16 3 GMT 292.5K
3/16 0 GMT 282.5K
3/15 21 GMT 272.5K
1.83665×10^15 1.83670×10^15 1.83675×10^15 1.83680×10^15 1.83685×10^15 1.83690×10^15 1.83695×10^15

NASA VCST WUCD c1 and c2

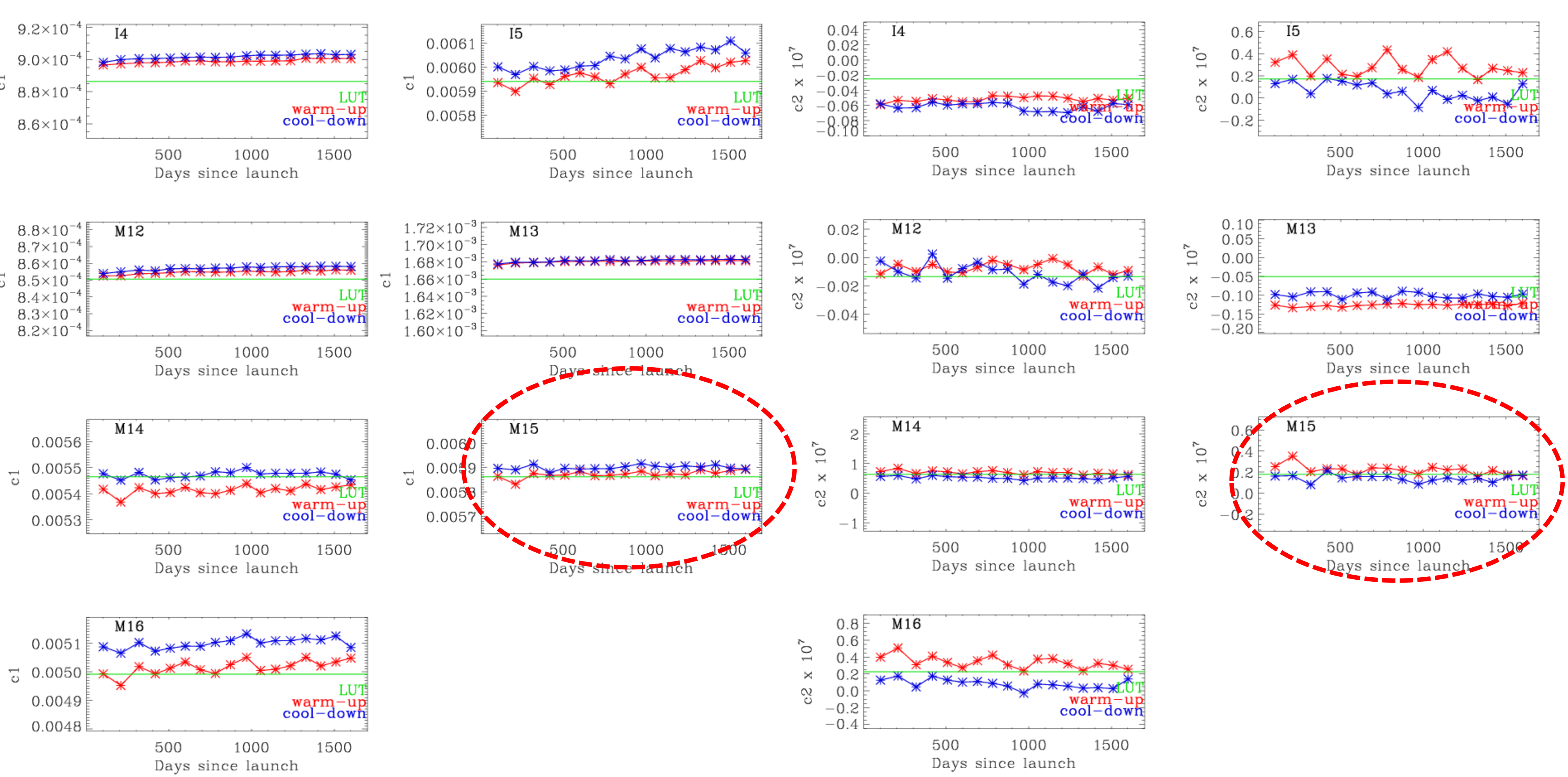

Courtesy of NASA VCST, June 2016 MODIS/VIIRS Science Team Meeting

S-NPP VIIRS DNB Calibration Reanalysis

08/09/2016

Sirish Uprety[a], Yalong Gu[b], Changyong Cao[c], Slawomir Blonski[b] and Xi Shao[d]
CIRA CSU[a], ERT[b], NOAA/NESDIS/STAR[c], UMD[d]

Outline

- Background
- S-NPP DNB major calibration updates
  - Cal. Coeff. Update using VROP
  - Modulated RSRs
  - Straylight correction
  - Terrain Corrected geo
- DNB On-Orbit Calibration
- Compare temporal trends of cal. coeffs.
  - Offset and gain ratio
- Summary

Background

- S-NPP VIIRS DNB has been providing quality nightime data.
- A number of calibration updates has been performed since early launch
  - aiming to improve the radiometric performance.
  - causes discontinuity in calibration time series.
- DNB calibration parameters (offsets and gain ratio) are determined either using the VROP based data or by using the onboard calibrator data
  - IDPS operational product uses VROP data (offset and gain ratio).
  - RSBAutoCal in IDPS and NASA LandSIPS uses OBC data (gain ratio and slope for offset change).
- This study is focused on reanalyzing the DNB calibration parameters.
- Reanalysing the DNB calibration and reprocessing with improved calibration is a key to generate radiometrically more accurate and consistent data archive.

DNB major calibration updates

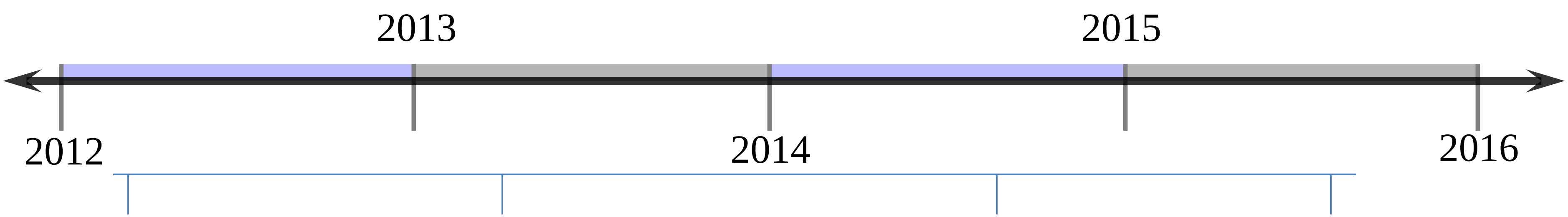

March 2012
1st calibration update using VROP

- *Updated both onboard and ground offset tables and gain ratio*
- *Improved the radiometric accuracy of esp. for HGS data.*

April 2013
DNB RSR LUT updated with modulated RSRs

- *Accounts for the RTA degradation impact on RSRs*
- *Improved the radiometric accuracy of all gain stages*

August 2014
Straylight correction implemented

- *Characterize and correct the straylight*
- *improves the data quality*

May 2015
DNB terrain correction implemented

- *Improves the geolocation accuracy (accuracy from few pixels (over high altitudes such as Tibet) to sub-pixel level)*

Cal. Coeff. Update using VROP

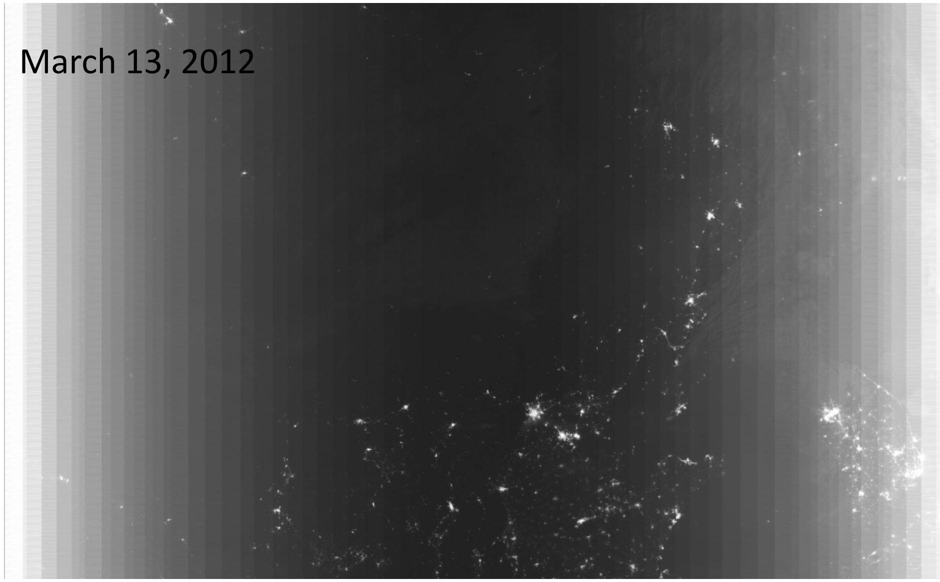

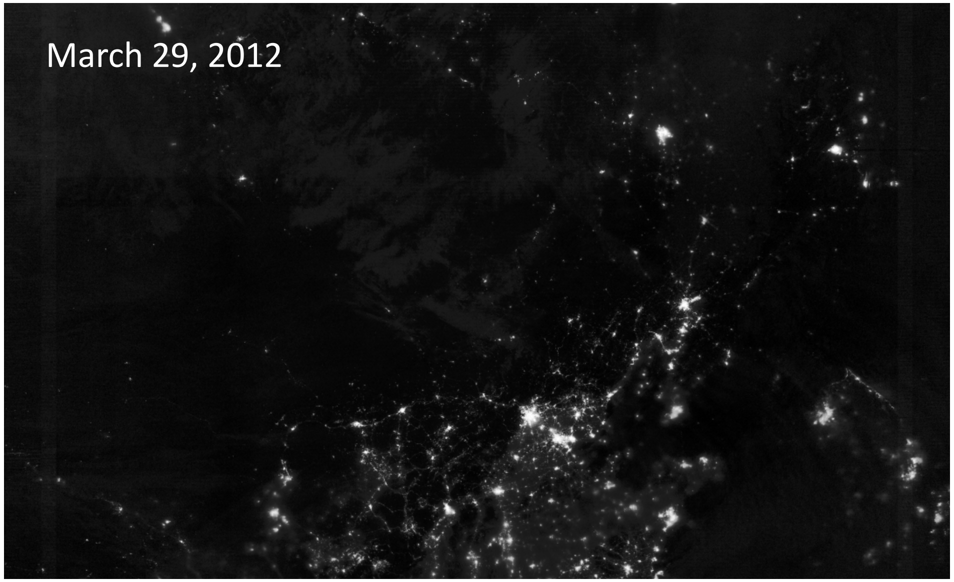

- Show DNB image over same location in earth after 16-day repeat cycle.
- Figure on right shows improvement in DNB calibration after updating offset table (onboard and ground offset) and gain ratio tables for the first time on March 22, 2012 based on VROP.

Time-Dependent RSR LUTs

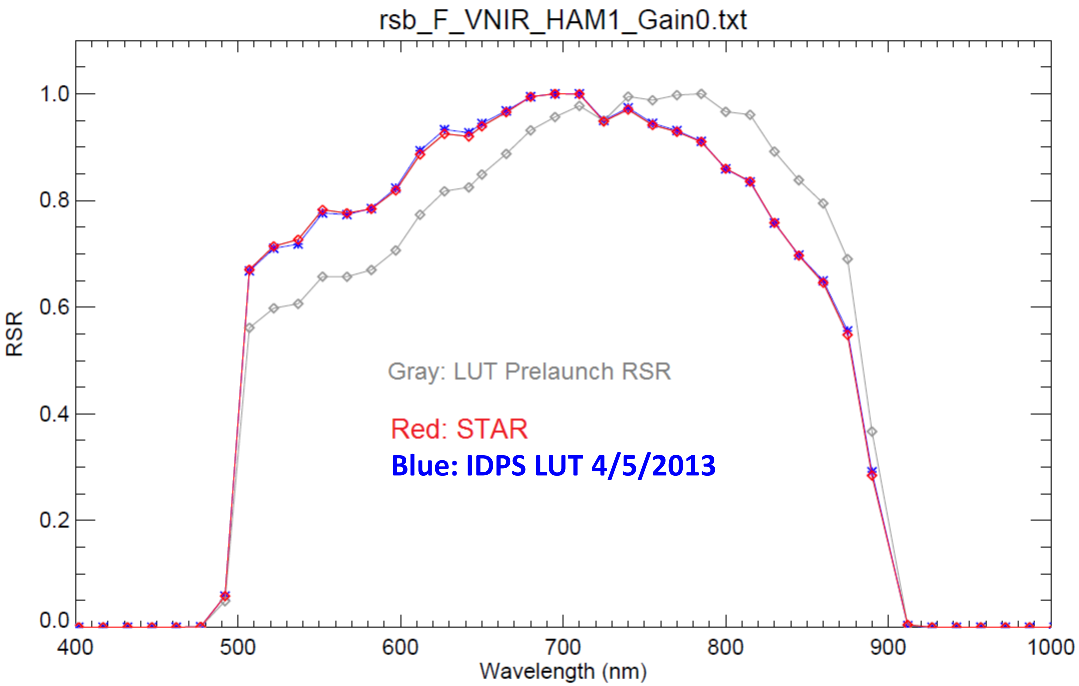

- VIIRS DNB RSRs modified by the telescope degradation
- Derived directly from the F factor changes for bands M4, M5, M6, and M7
- Without using a degradation model
- Agree well with the DNB “modulated” RSR from the IDPS LUT updated on April 5, 2013

- Approx. 50 time-dependent RSRs provide near-continues DNB E_{sun} changes with steps smaller than 0.1%

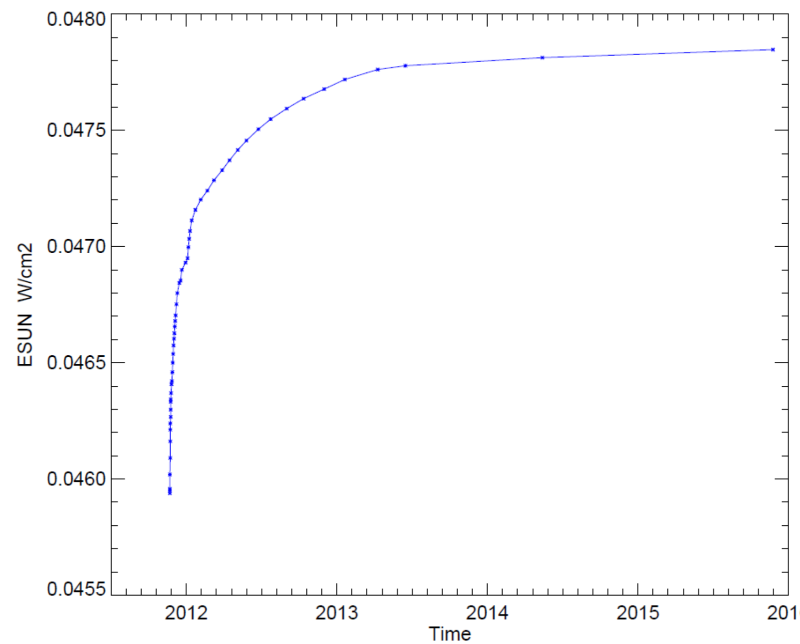

DNB LGS Gain Reprocessing for Aggregation Mode 1

RSBAutoCal w/o RHW filtering:

1. Using two RSR LUTs that were used in the operational production of the VIIRS SDRs

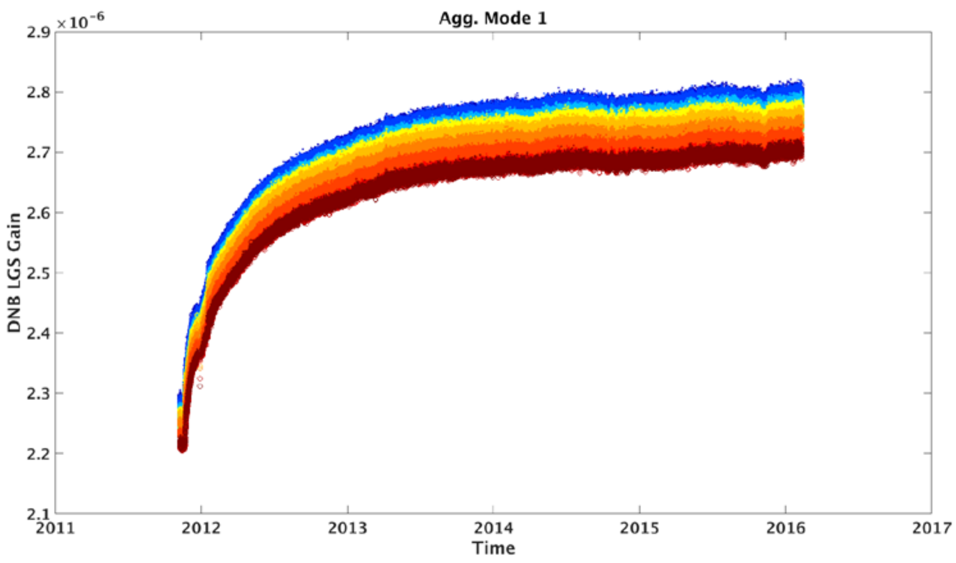

2. Using the additional, time-dependent RSR LUTs modified by the telescope throughput degradation

Similar results for all aggregation modes

SNPP DNB Stray Light Correction

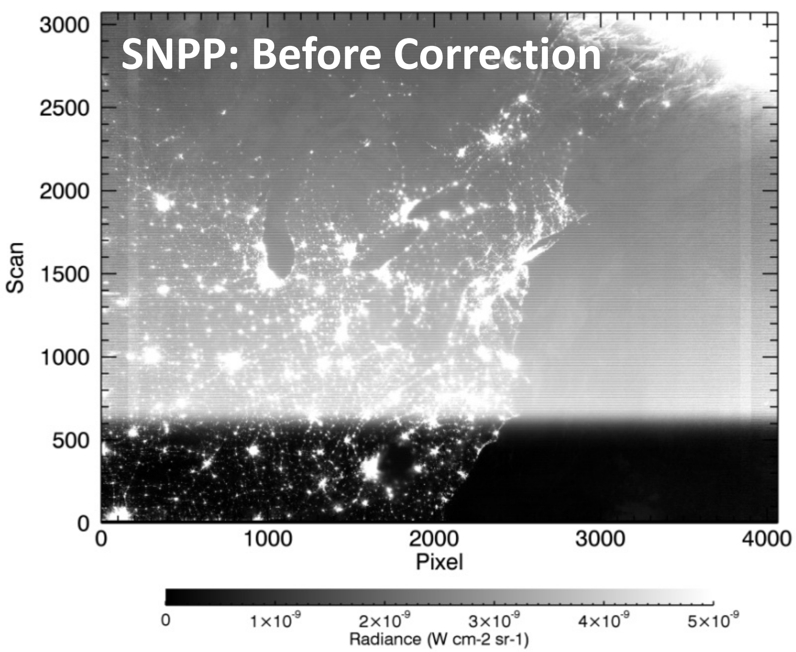

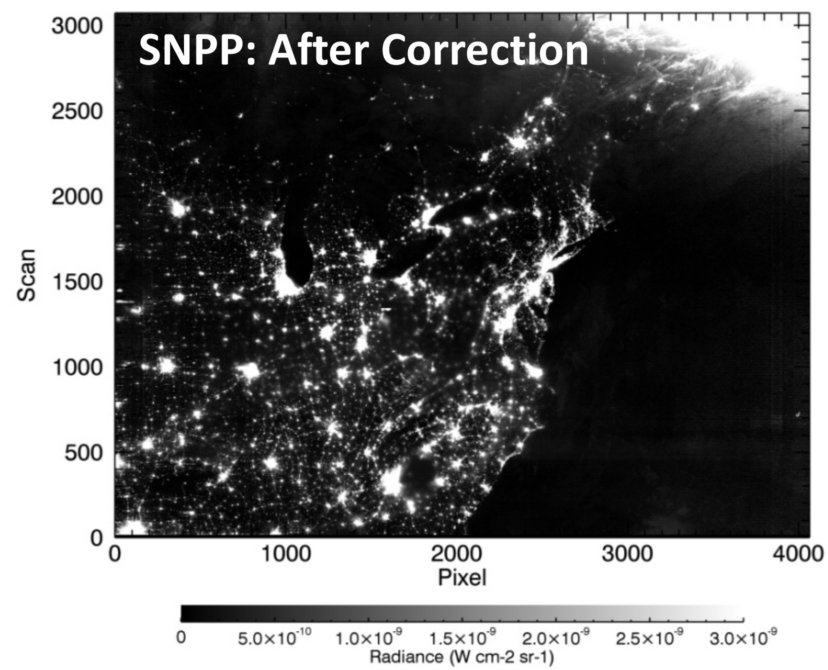

- SNPP DNB Stray Light correction transitioned from NG to STAR in 2014
- STAR supported the updates of operational stray light LUT for solar vector error correction.
- All 12 LUTs were updated by the end of 2015

(Courtesy, Wenhui Wang)

DNB On-Orbit Calibration

- LGS is calibrated using solar diffuser whereas MGS and HGS are calibrated through cross-calibration approach.
- Using VROP 702 and 705
  - performed every month during new moon.
  - Used by NOAA IDPS operational data
  - V702 used to estimate onboard offset table through observations over Pacific Ocean.
  - V705 used to estimate ground offset table (Pacific Ocean) and gain ratio (twilight region)
- Using onboard calibration data
  - NASA VCST *(Ref: Lee et al., 2014)*
    - Estimates gain ratio through cal sector data
    - Estimates ground offset using baseline reference from a) Pitch Maneuver data for HGS and b)VROP for MGS and LGS
    - Offset change over time is characterized through drift in dark measurements from BB
  - RSBAutoCal in IDPS
    - Not operational yet
    - Estimates gain ratio through cal sector data
    - Estimates ground offset using baseline reference from VROP 705
    - Offset change over time is characterized through drift in dark measurements from BB, SV and SD

Ground Offset Table Reanalysis

- Reanalysed VROP data from Feb. 2012 to April 2016 to estimate monthly offset and gain ratio.
- DN0 estimated at STAR using VROP agrees very well with that from LUT. However, starting early 2015, LUT based DN0 is smoothed out.
- Pitch maneuver data as an initial reference and estimated the drift through BB trend.
- Pitch maneuver based DN0 has larger discrepancies with VROP (10-15 DNs) for agg. zone 1. The difference is reduced at higher agg. zones.

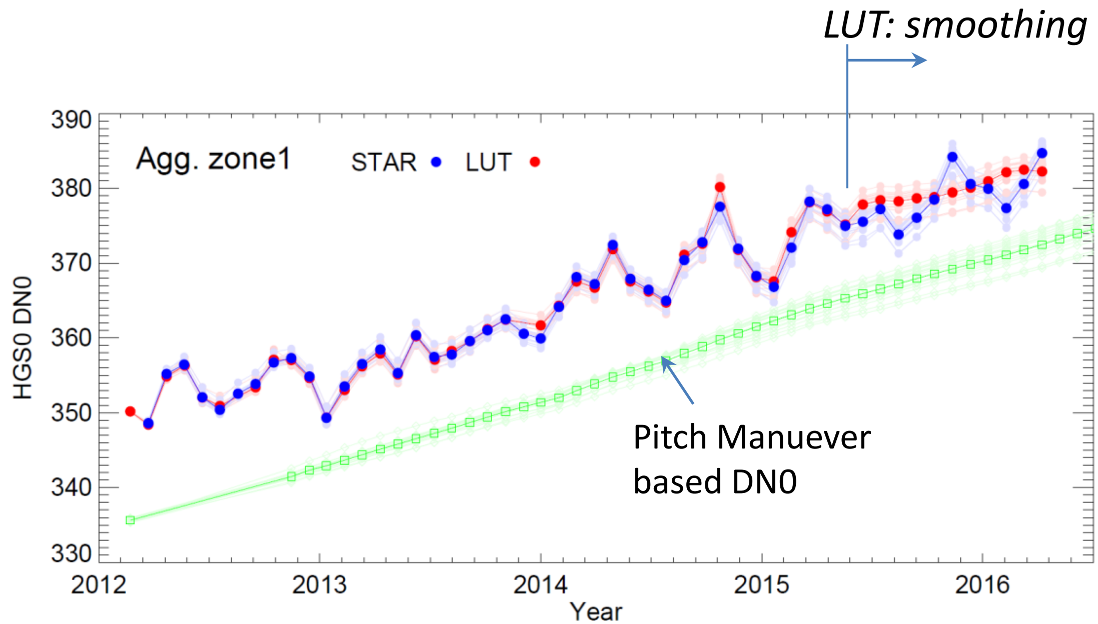

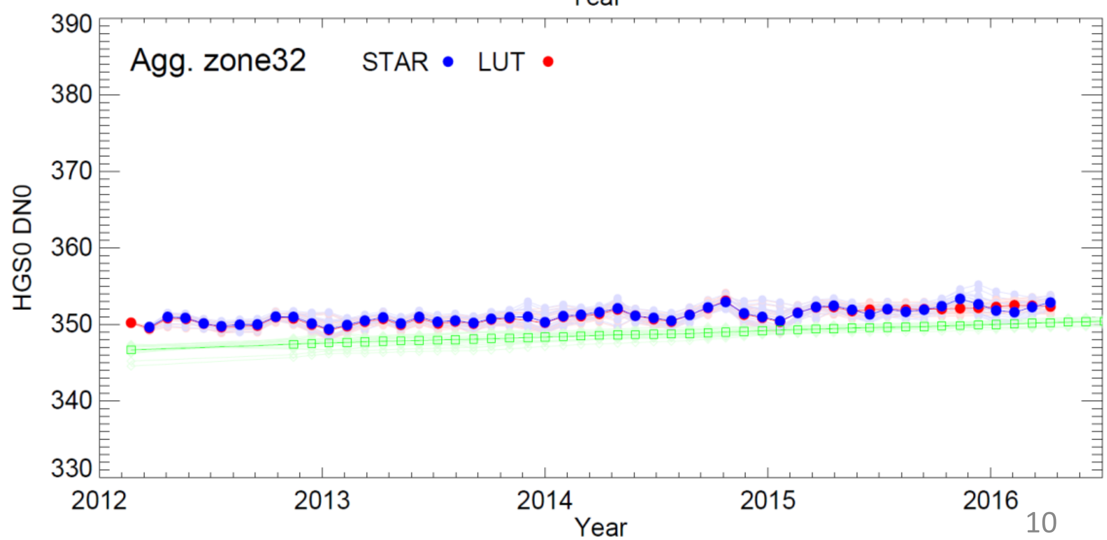

Compare HGS Drift

- Top: HGS rate of change fitted from 47 new moon days (02/21/2012 and 46 days between 11/13/2012 and 07/04/2016).
- Cal view data: follow the RSBAutoCal algorithm approach to determine DNB dark signal.
- Earth view data (VROP): DNB DN0 LUT (HGS)
- Middle: relative difference of the fitted change of rate (rate_CalView - rate_EarthView)/rate_EarthView.
- Bottom: zoomed in figure of the middle figure

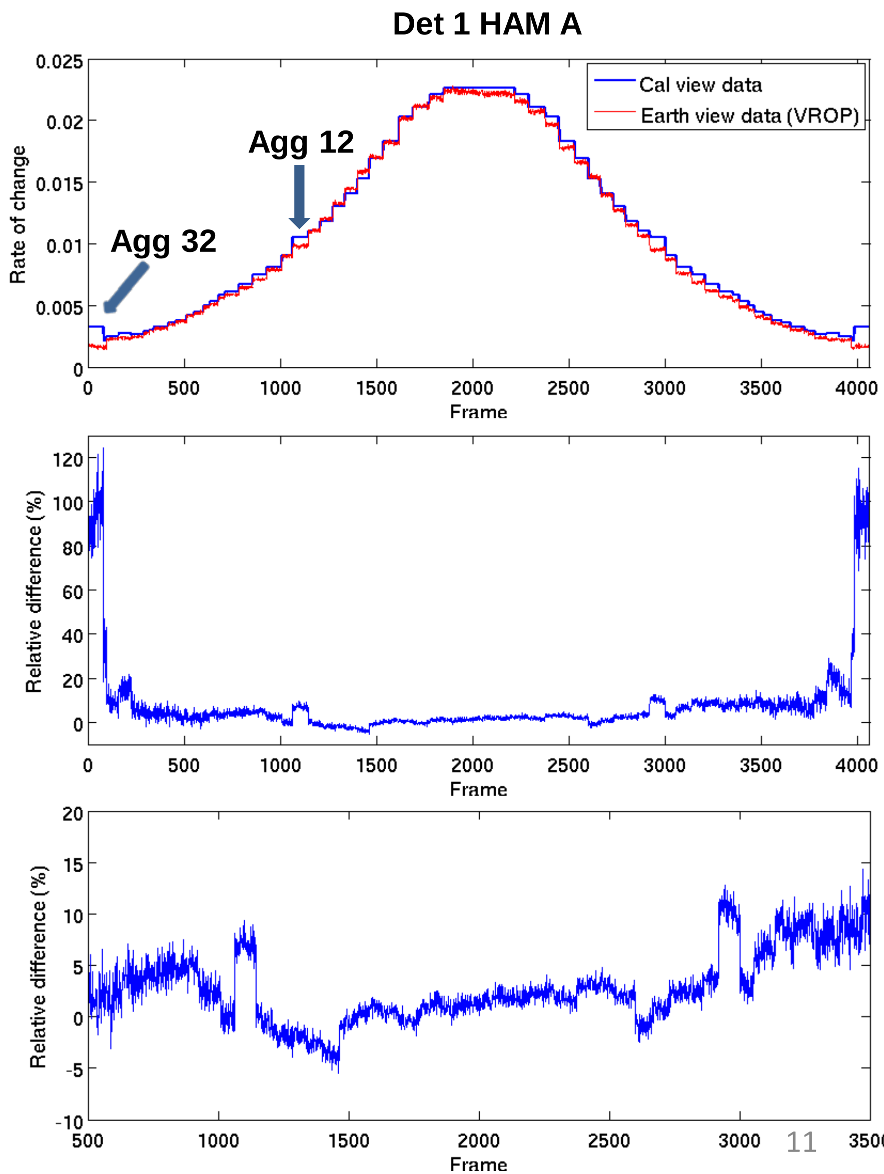

MGS Ground Offset (DN0)

- MGS drift ranges from nearly 2.2 to 3 DNs for 16 dets.
- There exists difference in drift computed by STAR and from LUT. The difference increases over time.
- Difference ~1.2 DNs over four years for agg. Zone 1.
- Drift difference decreases over higher agg. zones such that it is no more noticeable for agg. zone 25 and higher.
- Does it impact on gain ratio?

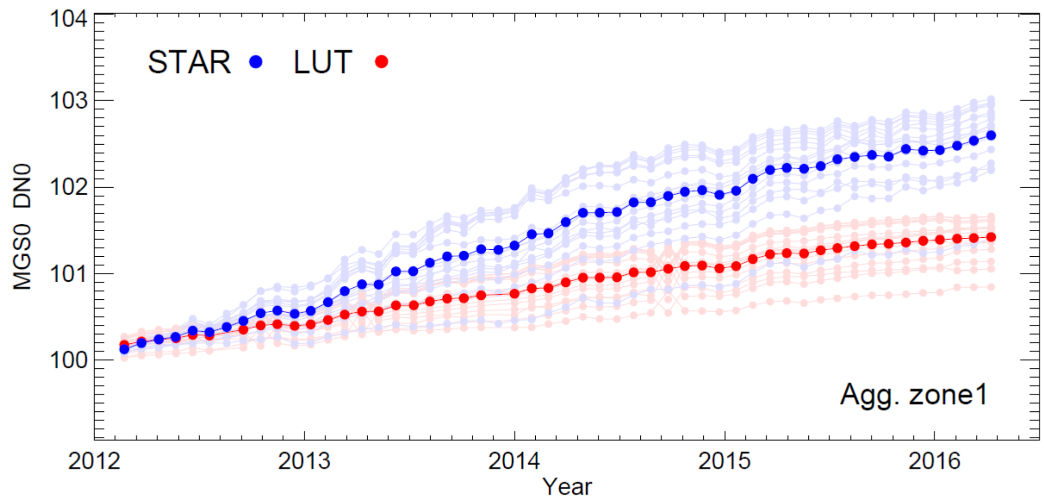

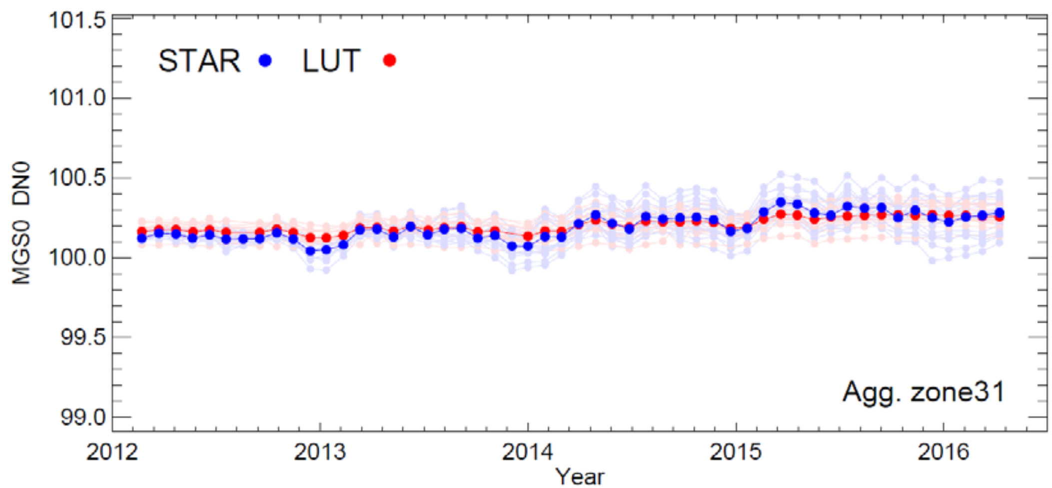

LGS DN0

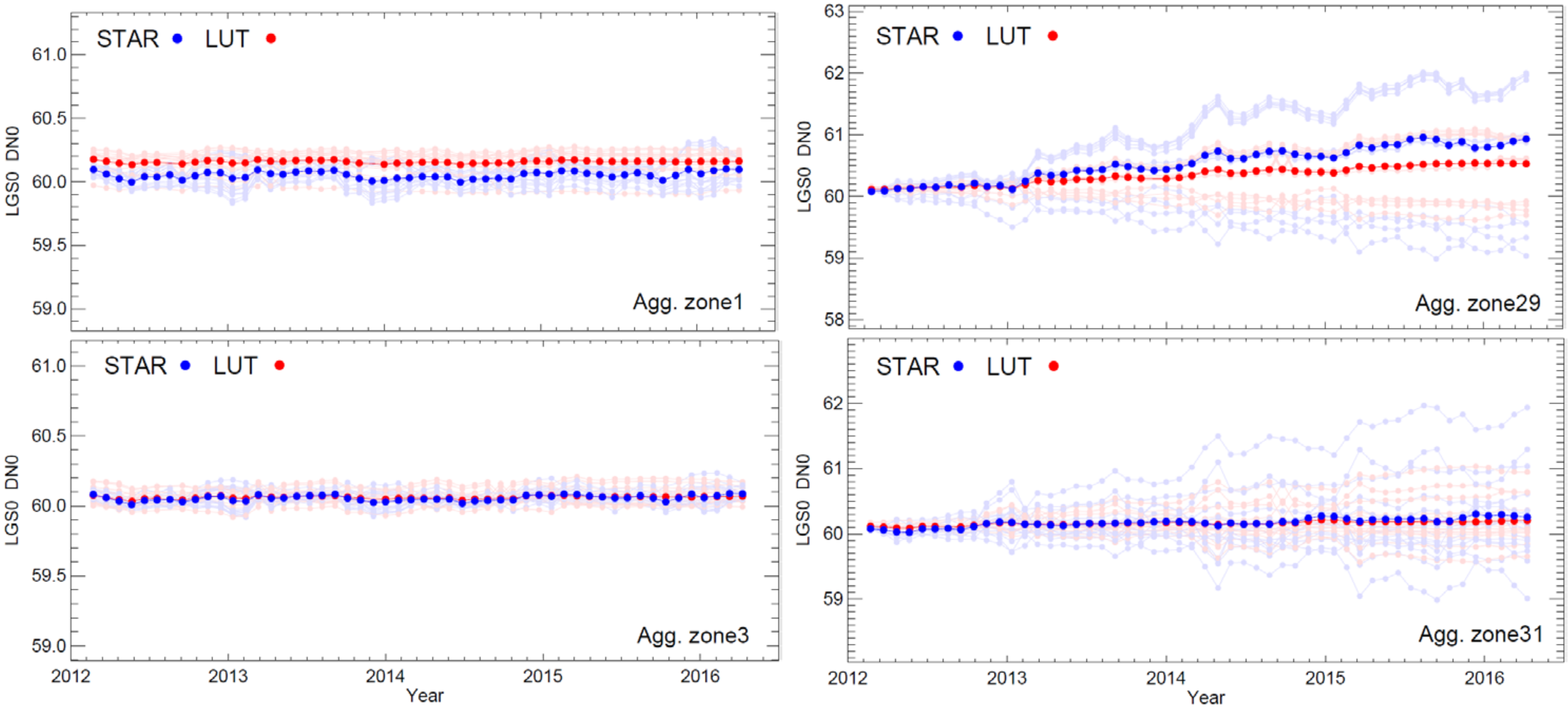

- Few agg. zones suggest ~0.05 to 0.1 DN difference in det. mean that is nearly consistent over time.
- Agg. zone 29-32 suggest large detector spread that is drifting in both upward and downward direction. More noticeable detector dependent spread after October 2012!

Gain Ratio over 32 Agg. Zones

- For LGS and MGS, total offset corresponding to V702 for the same VROP event is used.
- *By using total offset, even if the long term drift in dark offset (DN0) is not accounted properly, there is no impact on gain ratio.*
- For 04/07/2016: HGS/LGS shows upto ~8% difference between VROP and OBC based gain ratio for first few agg. Zones at nadir.
- $(C_{MGS})_{det,\ agg} = (C_{LGS})_{det,\ agg} \times G_{MGS/LGS}$
  $(C_{HGS})_{det,\ agg} = (C_{LGS})_{det,\ agg} \times G_{HGS/LGS}$

  where, $G_{HGS/LGS} = G_{MGS/LGS} \times G_{HGS/MGS}$

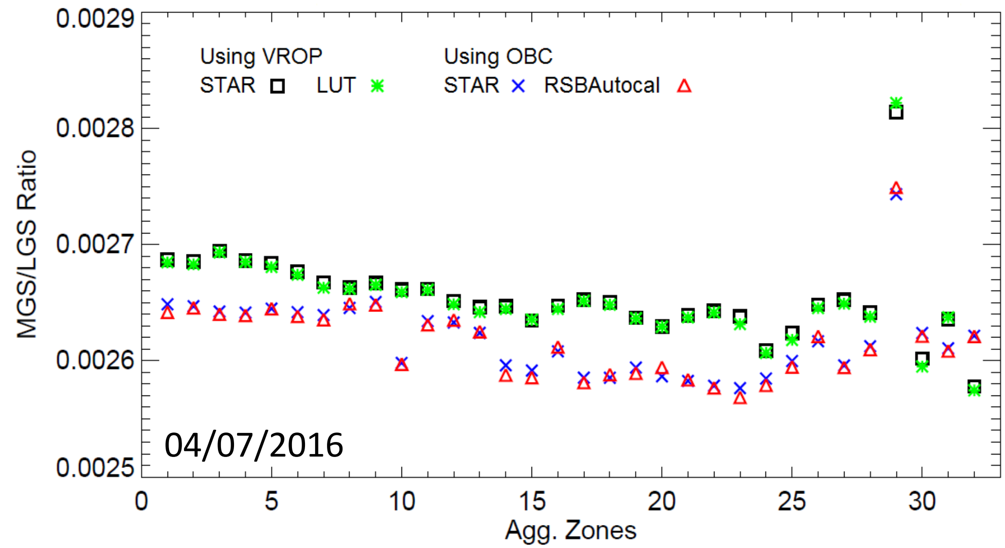

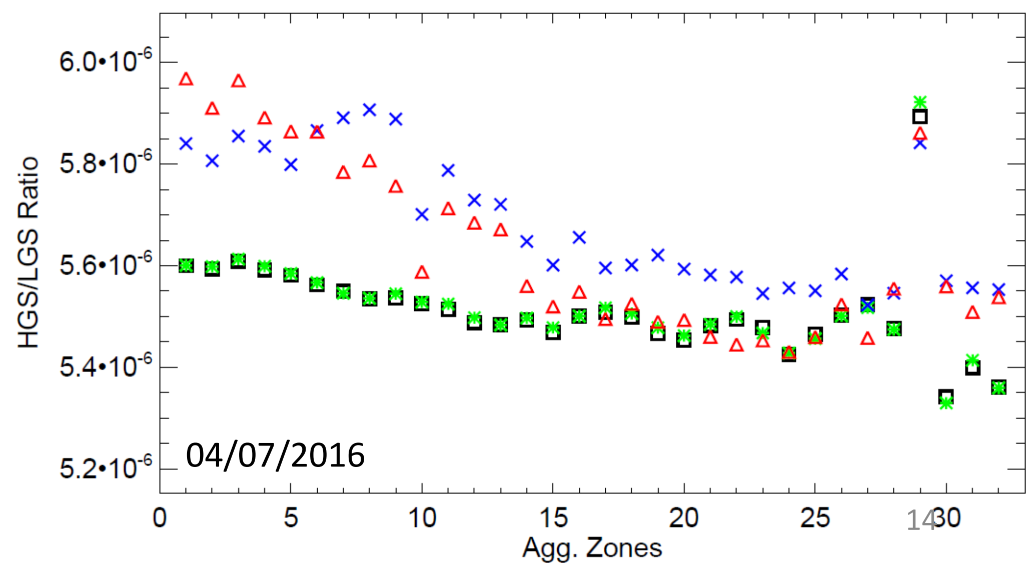

Compare Gain Ratio Trends

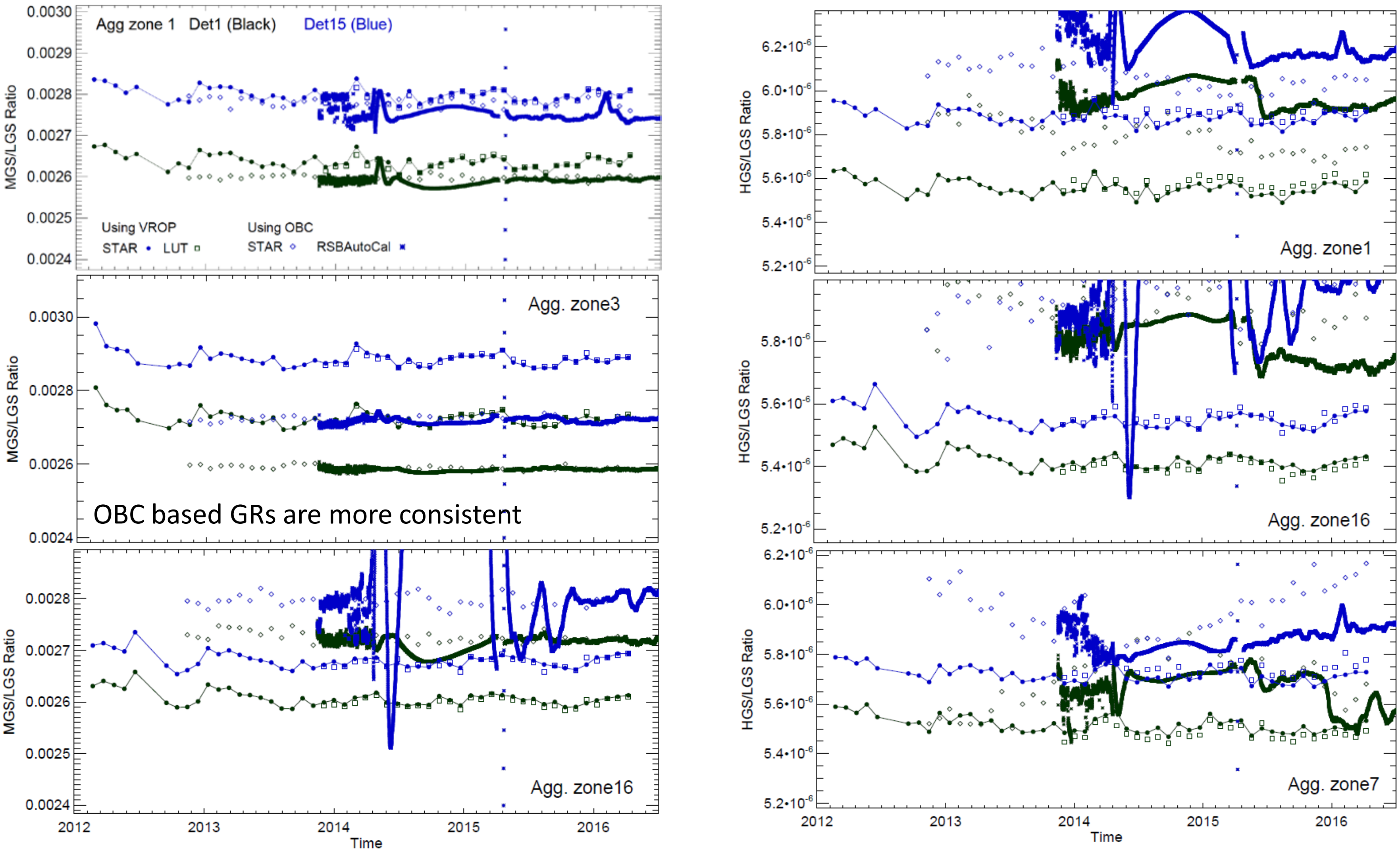

- OBC based gain ratios shows discrepancy among each other and with VROP based values .
- While RSBAutocal based gain ratios suggest to be in better agreement with STAR more recently, some agg. zones indicate much larger discrepancies.

Summary

- VIIRS DNB has gone through a number of improvements in calibration since launch.
- Temporal trends of ground offset using VROP agrees well with LUT for HGS and LGS. MGS suggests discrepancy of ~1.2 DN for agg. zone 1.
- Pitch Maneuver data based offset indicates difference of ~15-20 DN with VROP for agg. zone 1 which decreases over the higher agg. zones.
- OBC indicate large discrepancy in gain ratio with VROP, ~10% (HGS/LGS) for some agg. zones and needs further investigation.
- OBC suggests much larger spread in time series for HGS/LGS.
- RSBAutocal based gain ratio is more unstable esp. during 2014/2015 and indicates larger discrepancy with STAR computed values and needs further investigation.
- Request LUT from VCST and compare with both offset and gain trends to analyze the differences.

VIIRS DNB SDR Algorithm Improvements

Steve Mills
NOAA STAR/ERT
9 August 2016

Subtopics

1. Cal based gain ratios and stray light correction
2. DNB Offset & Noise Analysis from Cal Data
3. Determining offsets using Earth view—a statistical method using a parametric model with method of moments estimator

Part 1 –Cal based gain ratios and stray light correction

Cal Sector Data around Night to Day Transition

- **In theory the cal space-view (SV), blackbody (BB) calibration (cal) should always be dark throughout the orbit.**
  - Space has very little light except for stars and airglow in the ionosphere
  - The blackbody is black, meaning that it should not reflect any light
- **In fact, both the SV and the BB are affected by stray light**
  - They have strong signals during the day and around both terminator crossing.
  - This stray light is correlated with the stray light seen in the earth-view (EV)
- **The stray light has been shown to be dependent on satellite solar zenith angle (SSZA) and satellite solar azimuth angle (SSAA)**
  - during the night to day transition in the southern hemisphere the stray light is quite different from the northern hemisphere because of the SSAA is in the opposite direction.
  - There is a seasonal change in the SSAA over the orbit and so the stray light changes from month to month.
- **The solar diffuser (SD) cal sector data is almost always the strongest**
  - This is not surprising since the SD has almost 100% reflectance
  - Even when the sun is not directly illuminating the SD it apparently is being illuminated by earthshine throughout the twilight, daytime and even nighttime.

EV "Stray light" around night-to-day terminator crossing

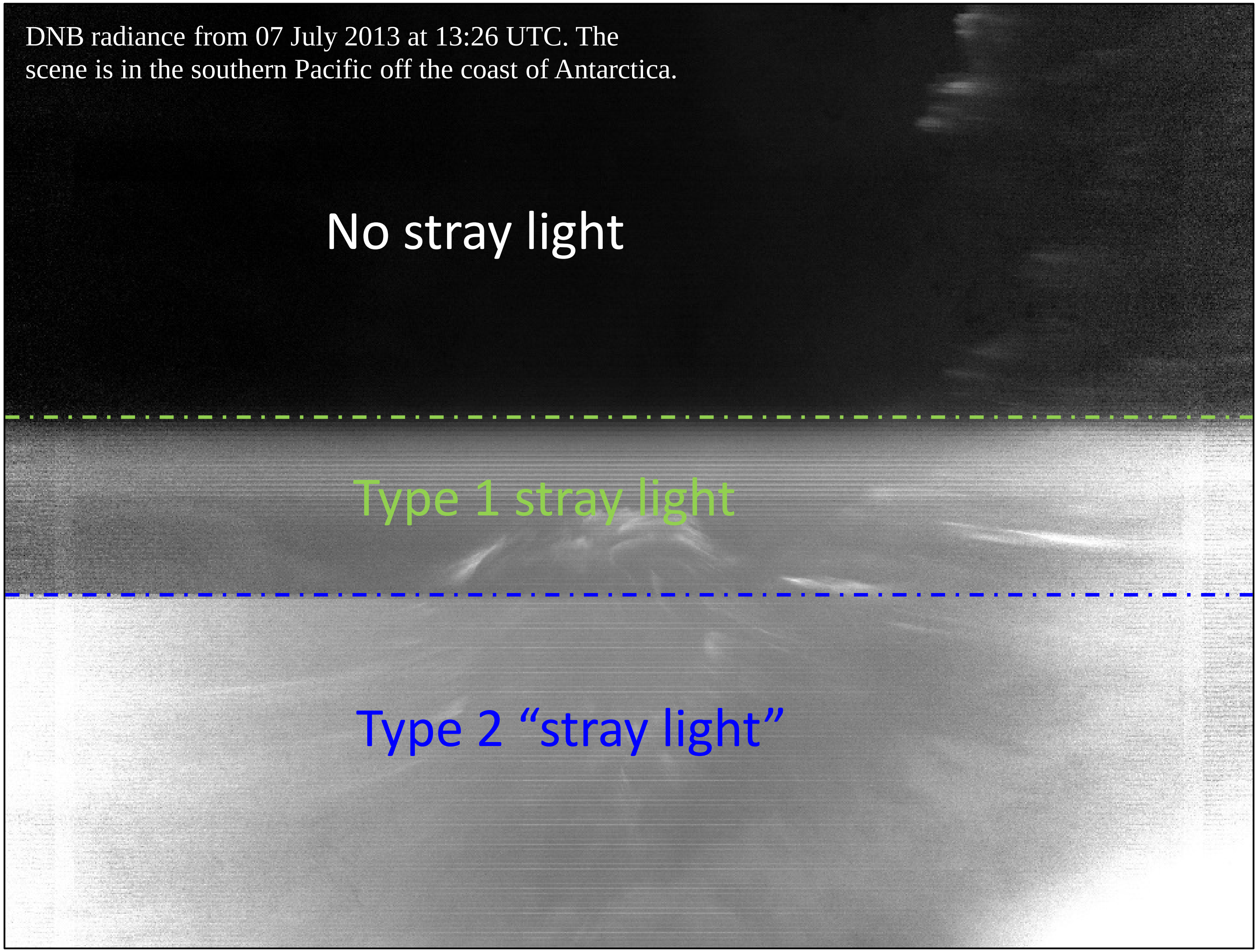

Comparing SD, SV and EV signals during night to day transition in southern hemisphere

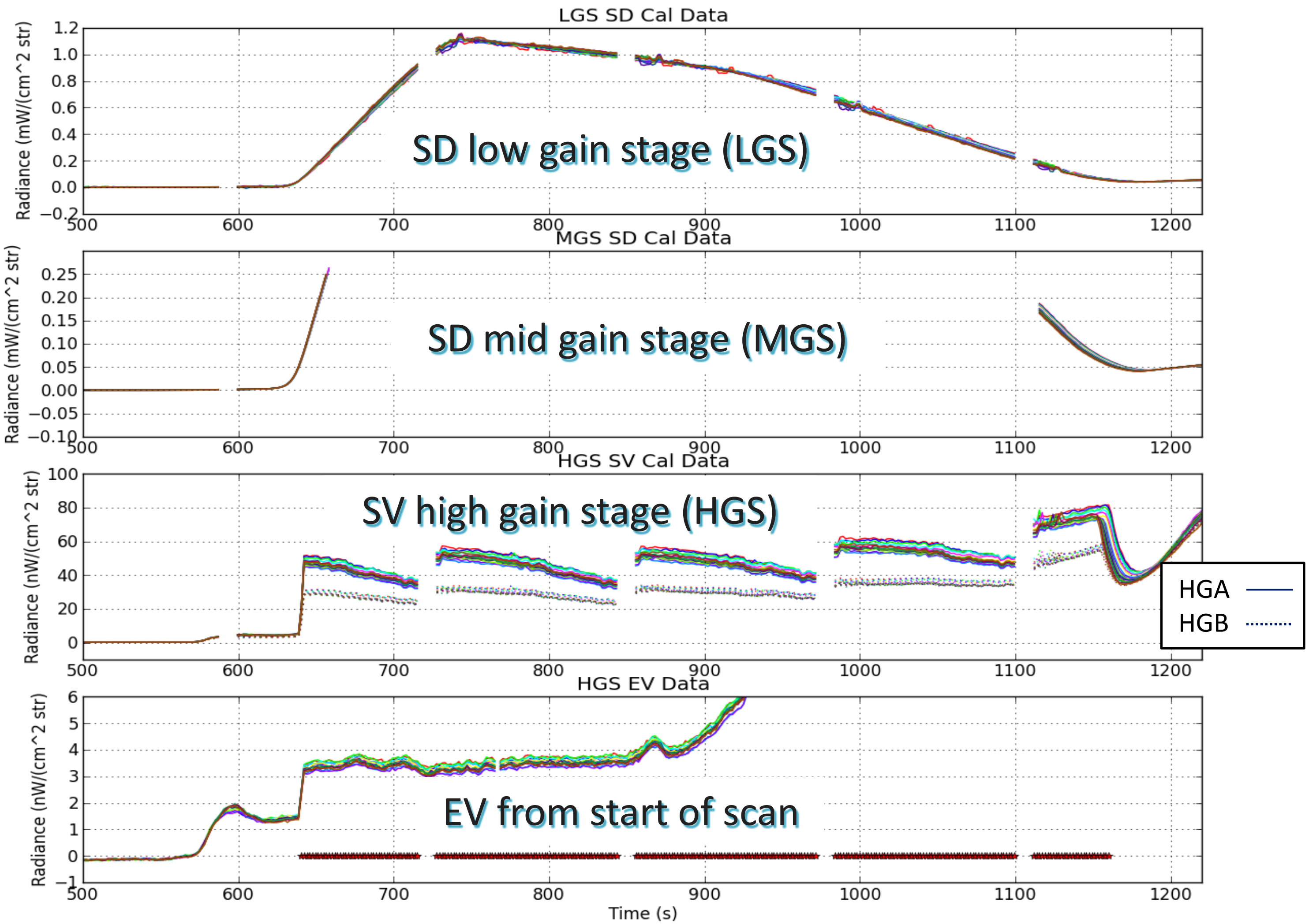

Comparing SD, SV and EV signals during southern hemisphere terminator crossing

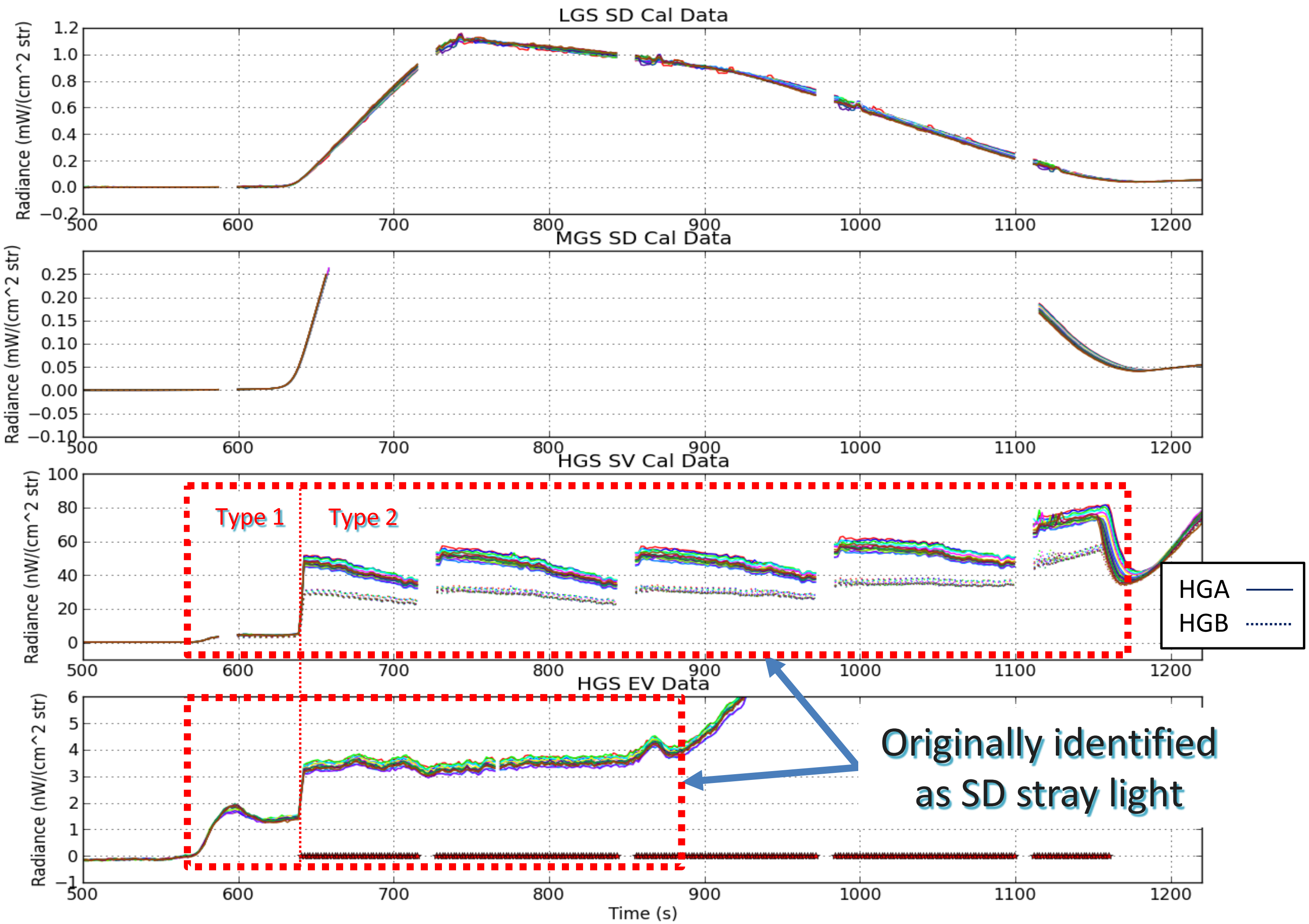

Comparing SD, SV and EV signals during southern hemisphere terminator crossing

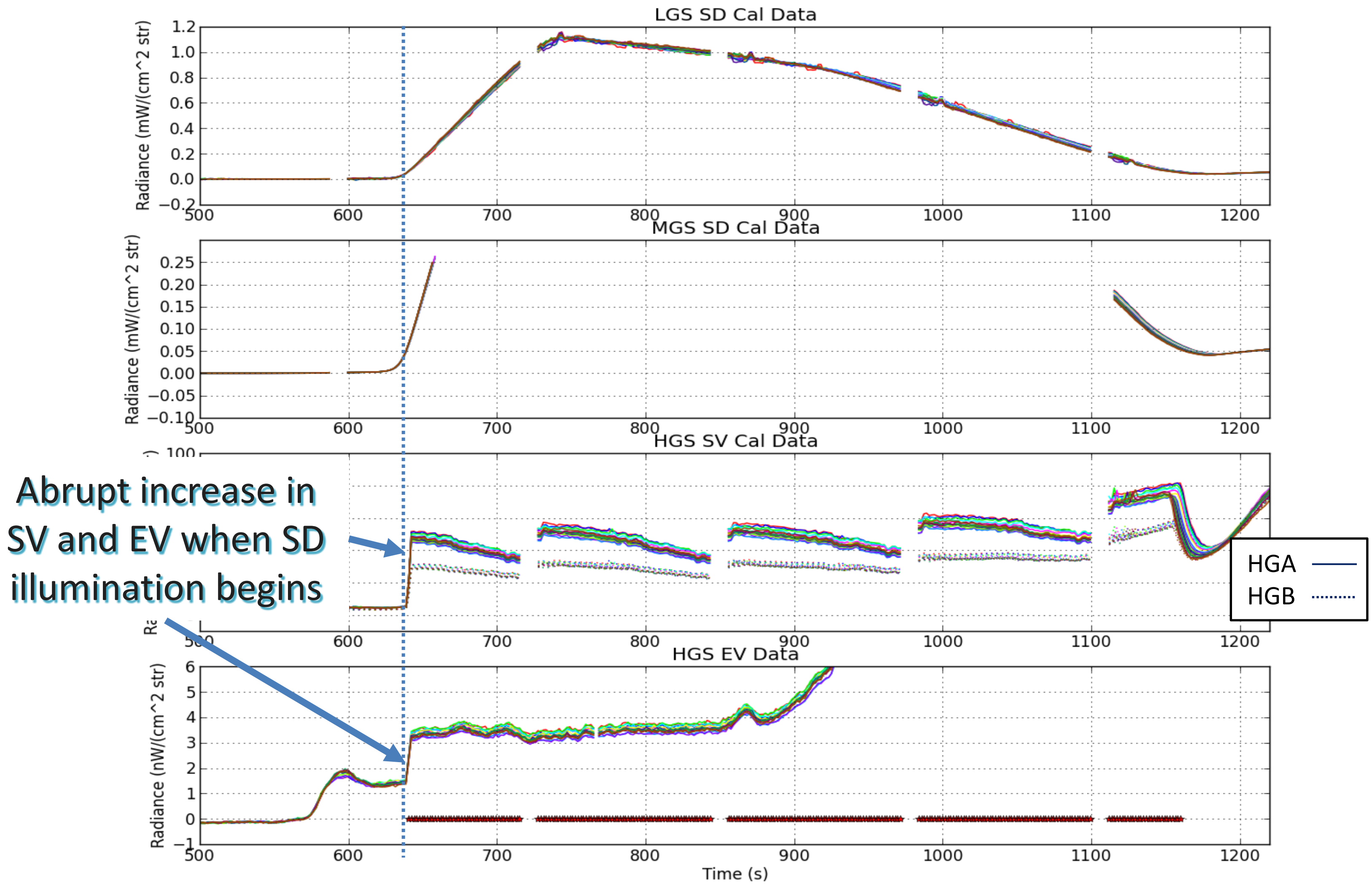

Comparing SD, SV and EV signals during southern hemisphere terminator crossing

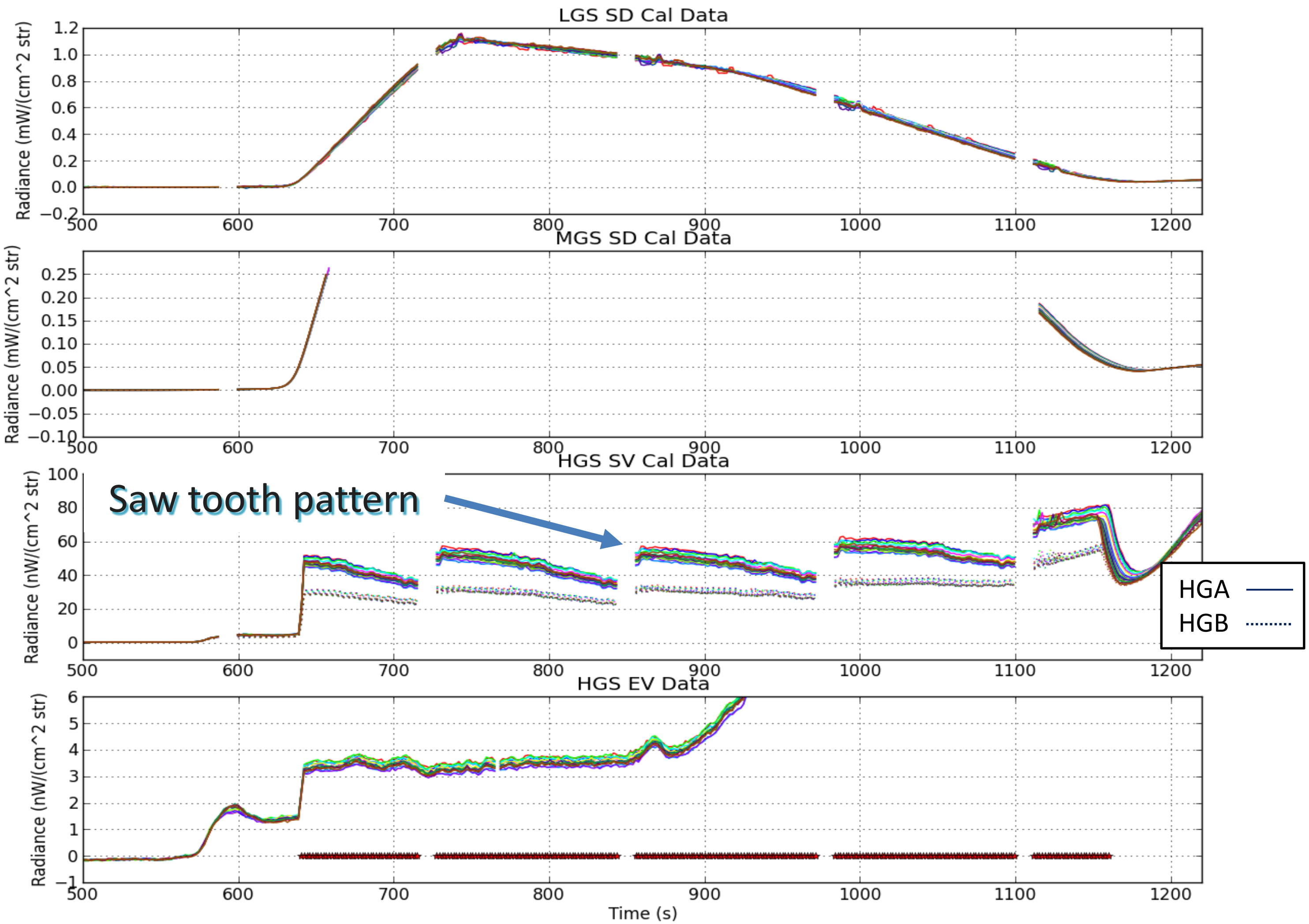

Comparing SD, SV and EV signals during southern hemisphere terminator crossing

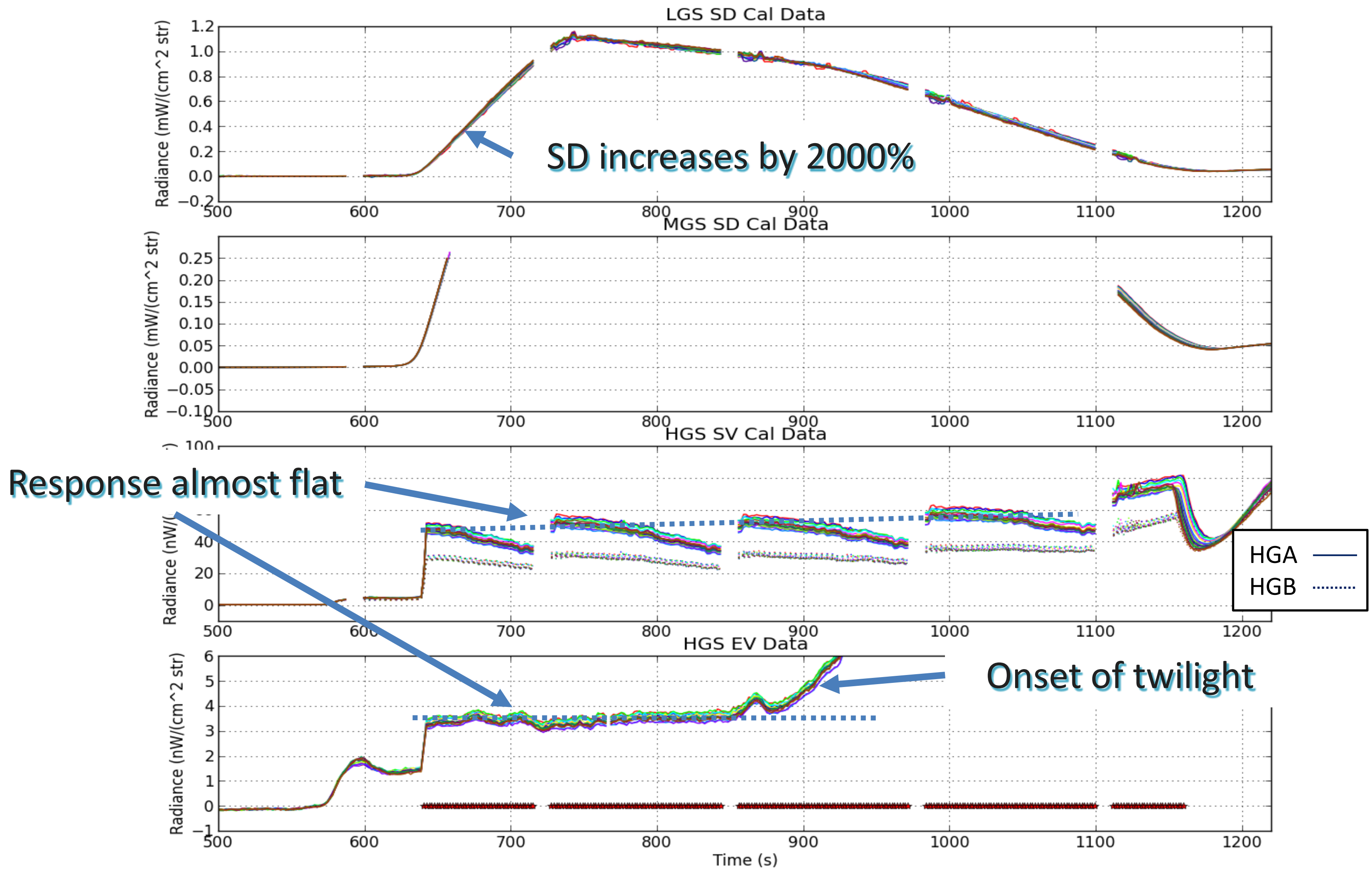

Comparing SD, SV and EV signals during southern hemisphere terminator crossing

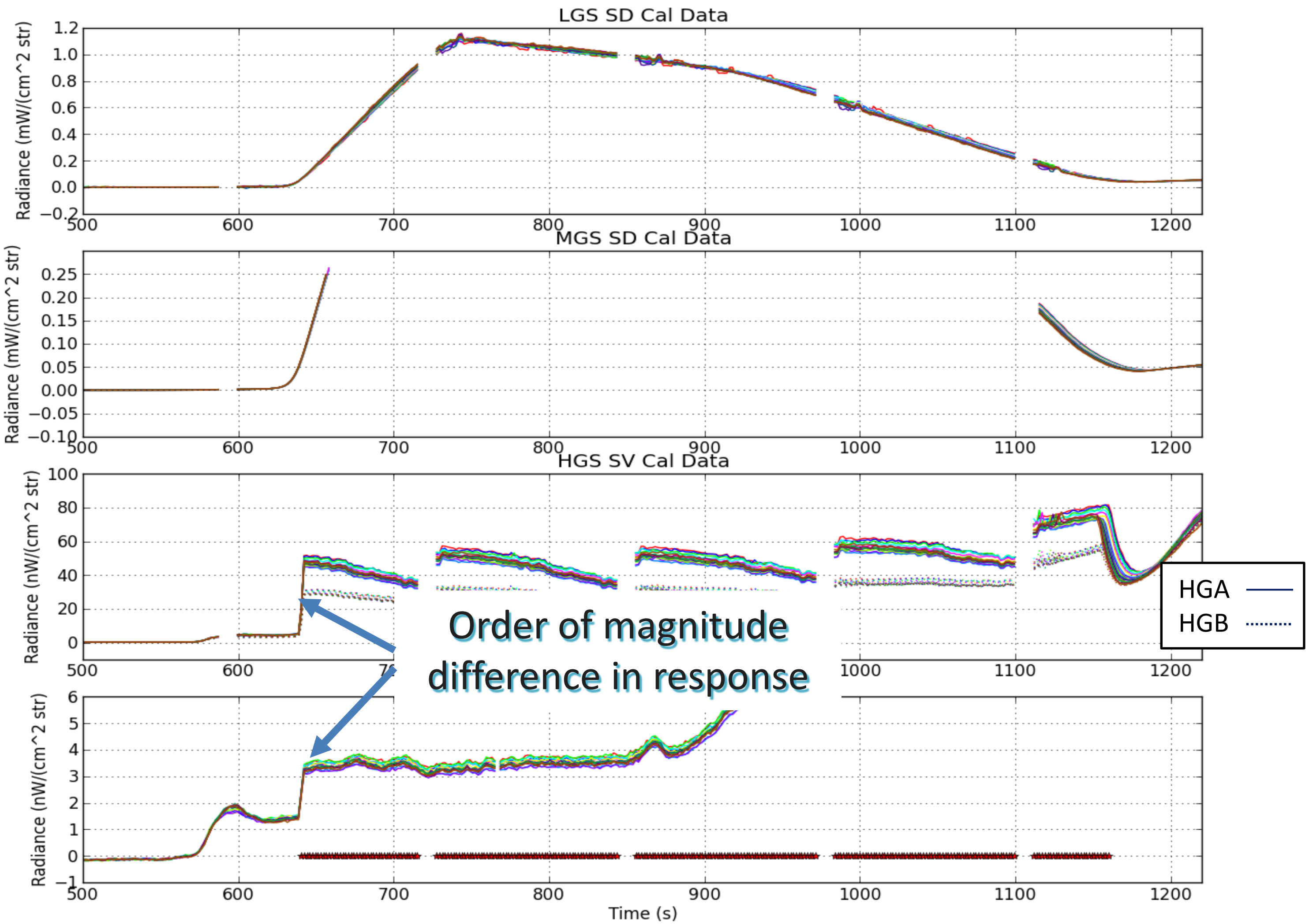

SV signal during this period

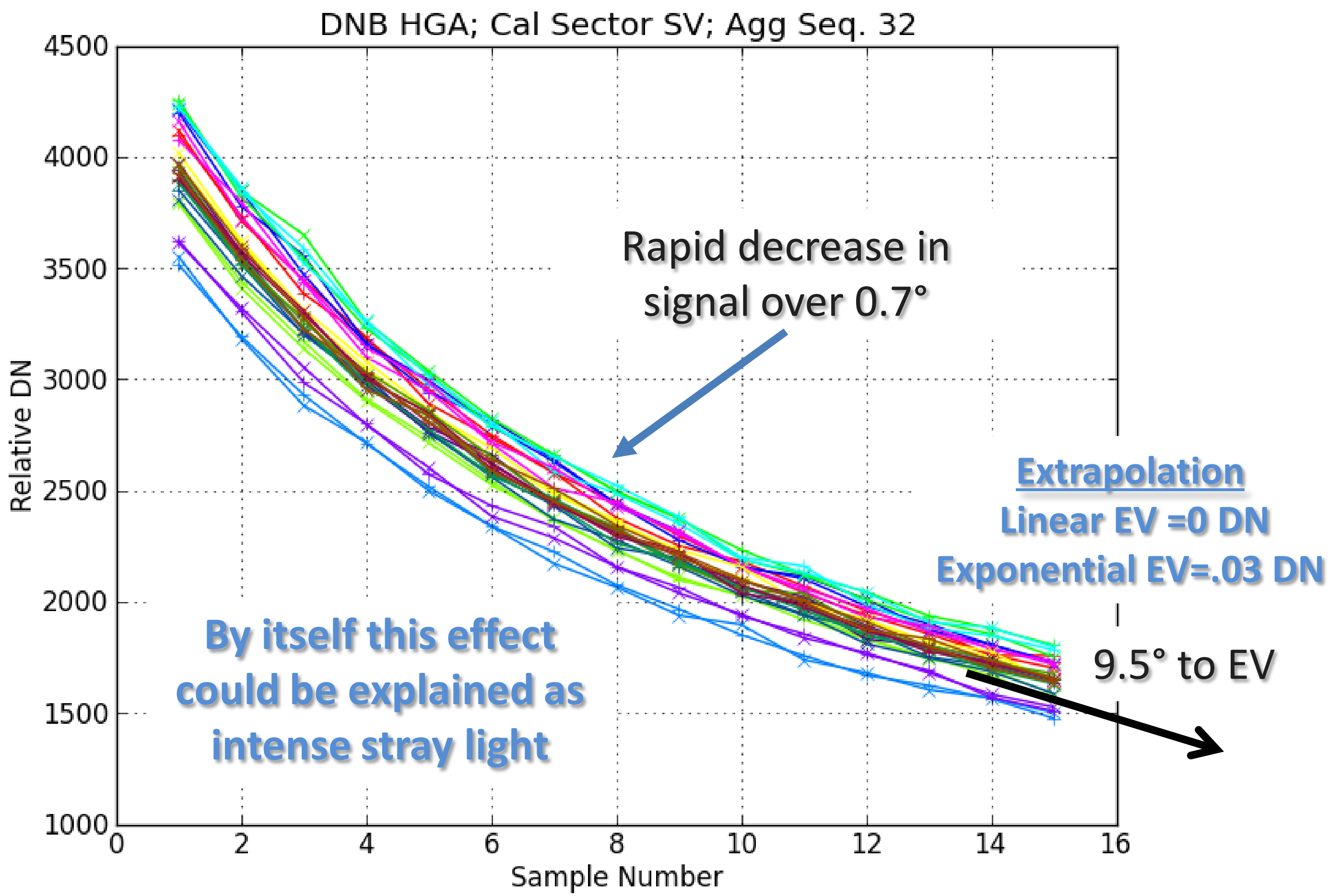

Inconsistencies with stray light hypothesis—What is really going on?

- **Alternative hypothesis**—hysteresis from intense SD signal
  - There are known to be problems with the S-NPP VIIRS DNB anti-blooming electronics
  - Other mechanisms are possible, e.g. some super-saturation effect in the HGS CCD
- **Fact 1:** HGS SV & EV signals abruptly start and end over the direct solar illumination of the SD
  - **Possible cause:** anti-blooming circuit abruptly triggered with rapid increase in SD radiance
- **Fact 2:** Saw tooth pattern on HGS SV related to aggregation mode
  - **Possible cause:** because the SV signal rapidly decreases & the with lower aggregation there is less time per sample, the overall decrease is less with less aggregation
- **Fact 3:** SV & EV HGS signals otherwise uncorrelated with SD signal but instead have a flat response
  - **Possible cause:** anti-blooming trigger causes an excess charge that is fixed and thus causing offsets
- **Fact 4:** EV signal is order of magnitude les than SV mean
  - **Possible cause:** Excess charge is rapidly discharged for every sample of SV and continues after the 16 samples that are transmitted

How does this effect “stray light” correction?

- The type 2 “stray light” offset correction works well over most of the area.
- In the current algorithm the onset of type 2 stray light uses the solar angle with respect to the satellite.

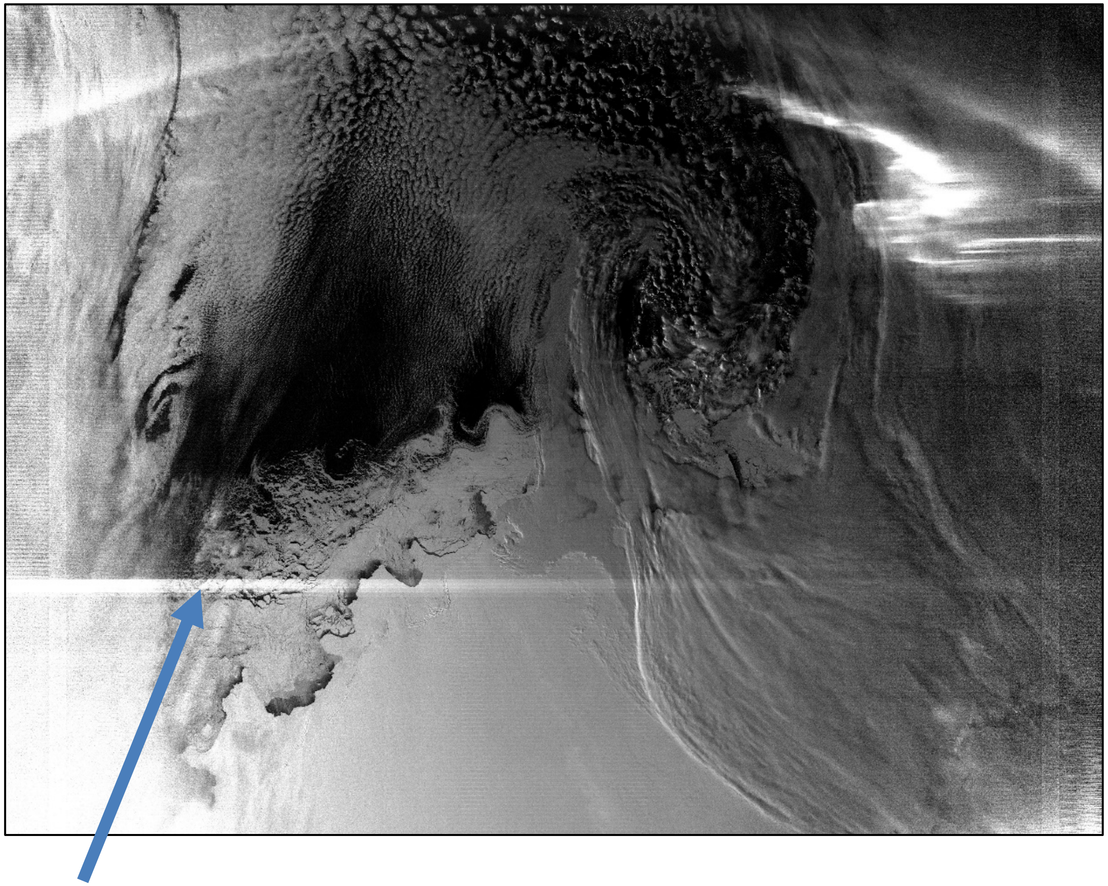

- The onset prediction often is off by up to 3 scans, leaving either a dark or light streak from under-correction or over-correction.
- A better predictor would be to use the SD signal with a threshold. The threshold of 0.06 mW cm^{-2} $steradian^{-1}$ was used to test this.

Using a SD threshold to predict the SV and EV onset

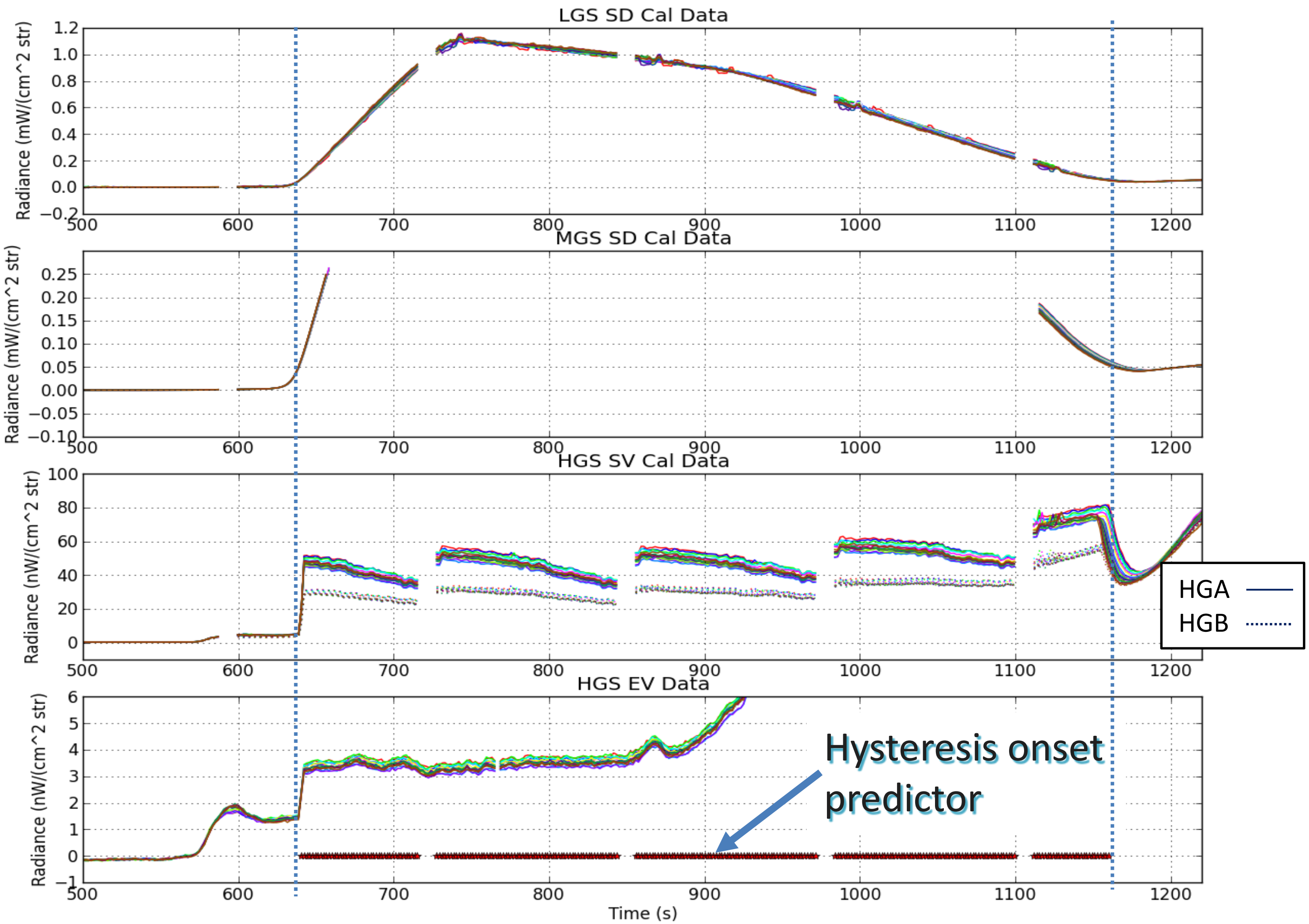

Hysteresis affect on gain ratios from SV or BB

- For the SD the HGA & HGB signals are almost always saturated and it is rare that MGS/HGS gain ratios can be produced (4 to 5 scans per orbit).
- Therefore RSBAutoCal currently uses MGS/HGS gain ratios from the SV and BB signal.
- Since the SV & BB should ideally have no signal, almost all the observed signal must be stray light or hysteresis.
- The validity of these gain ratios is based on the assumption that the stray light equally illuminates both MGS and HGS.
  - There is evidence that this is not true, even on average.
- During the daytime the EV signal is as strong as or stronger than the SD signal during solar illumination.
- The BB HGS signal is therefore likely to also be affected by hysteresis during daytime.
- If some of the BB or DV signal is hysteresis then it is not even optical, so this further invalidates using SV or BB for gain ratios.
- Therefore, the SV and BB signals should never be used for cross-calibration.
  - Automatic cross-calibration for MGS/HGS is therefore not possible.
  - Automatic cross-calibration using the SD for LGS/MGS gain ratios should still be effective

SV MGS/HGB cross-calibration

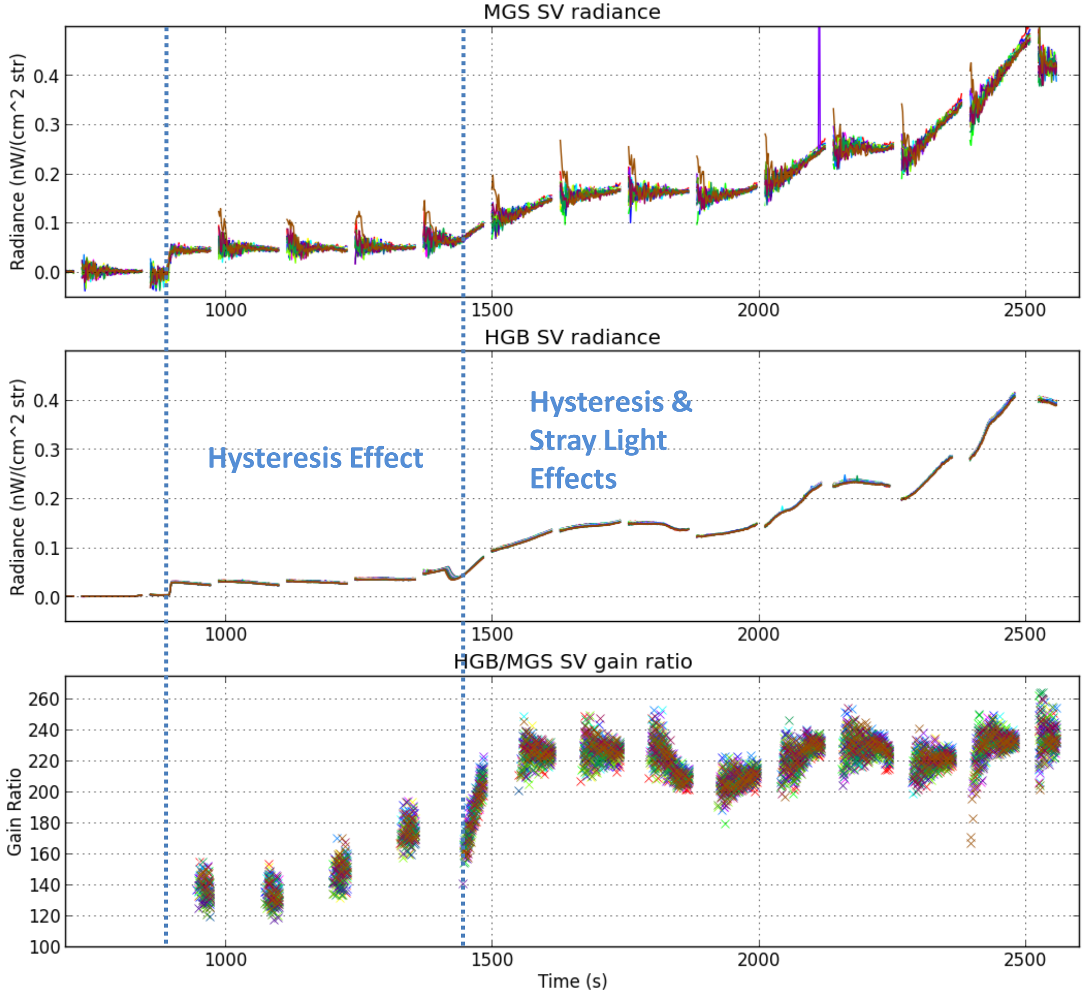

Gain ratio threshold
SNR(MGS)>15

BB MGS/HGB cross-calibration

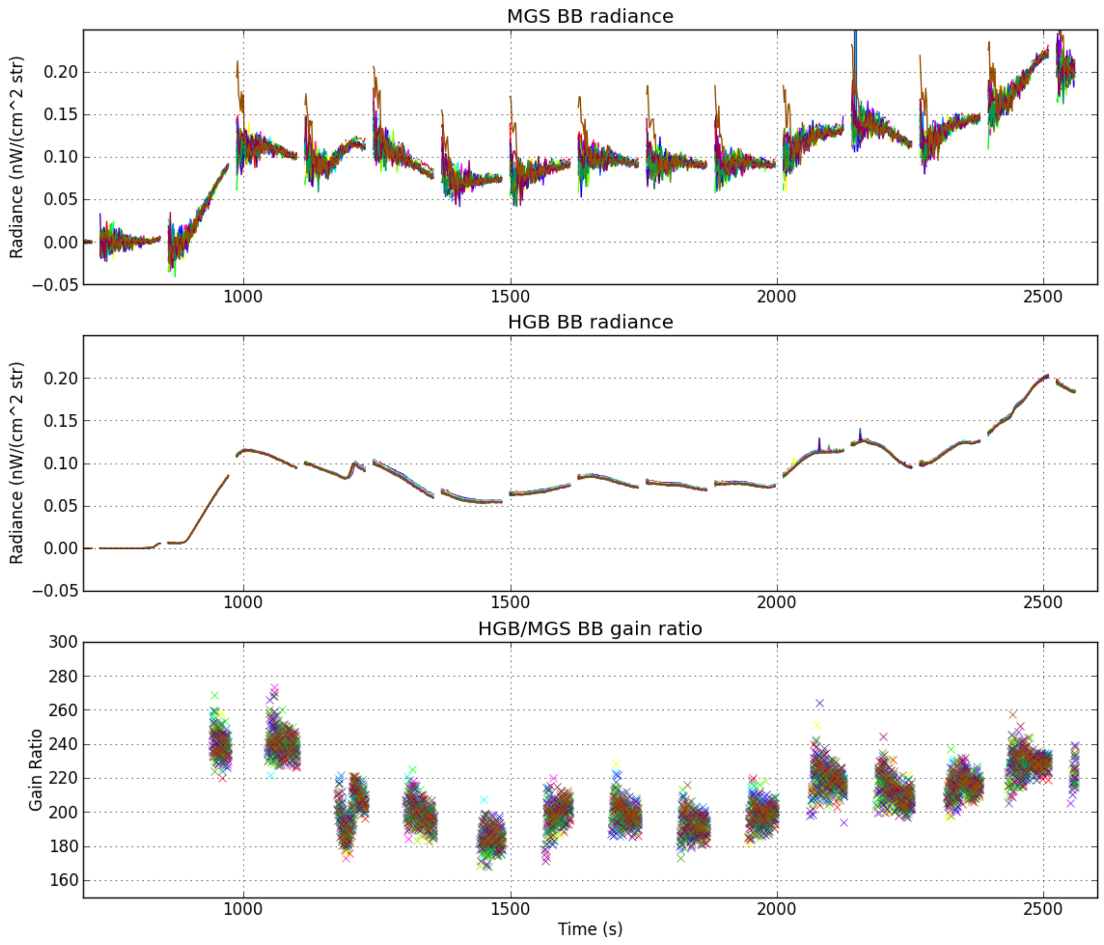

Gain ratio threshold
SNR(MGS)>15

SD MGS/HGA cross-calibration

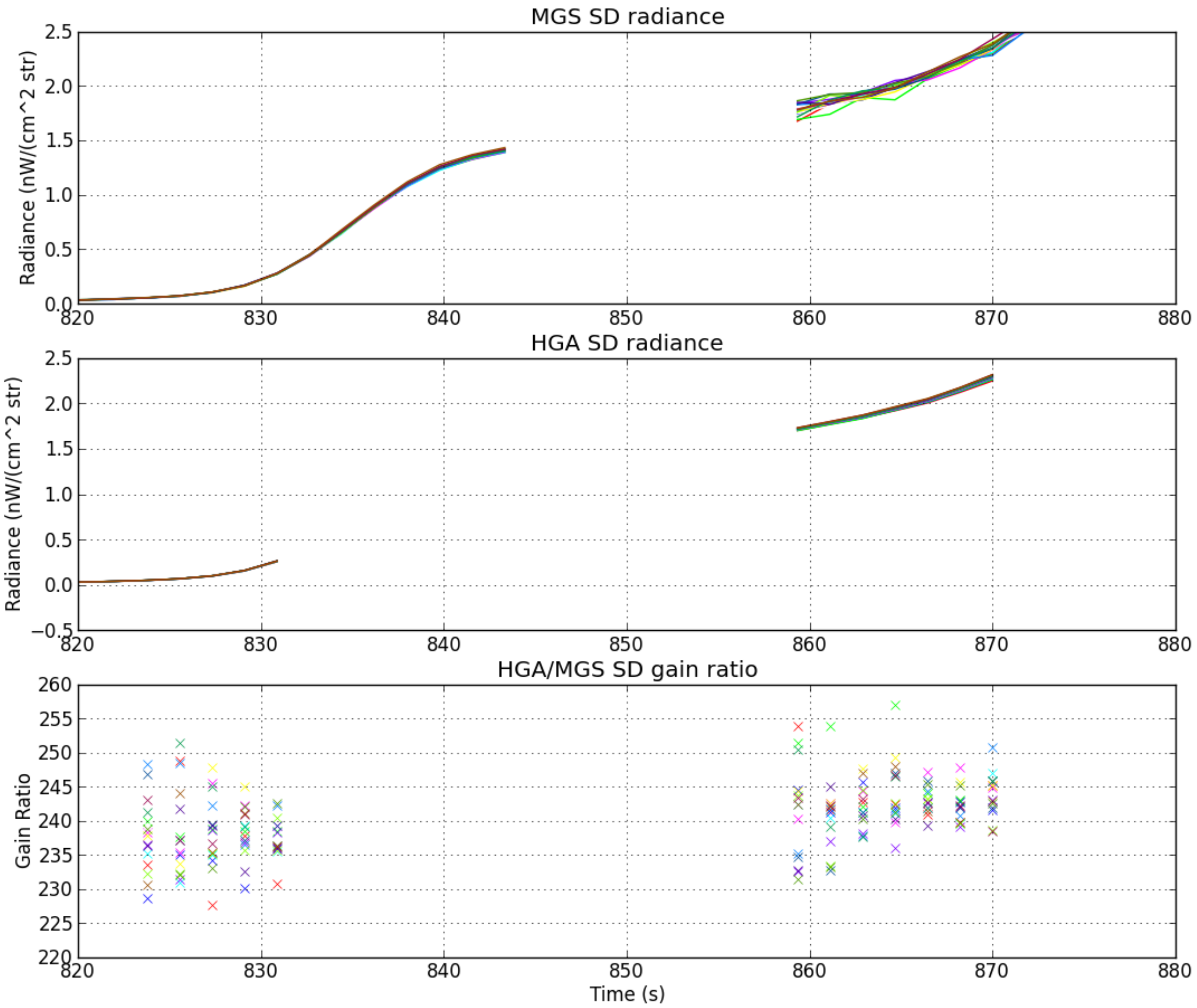

Gain ratio threshold
SNR(MGS)>15

SD LGS/MGS day-to-night cross-calibration

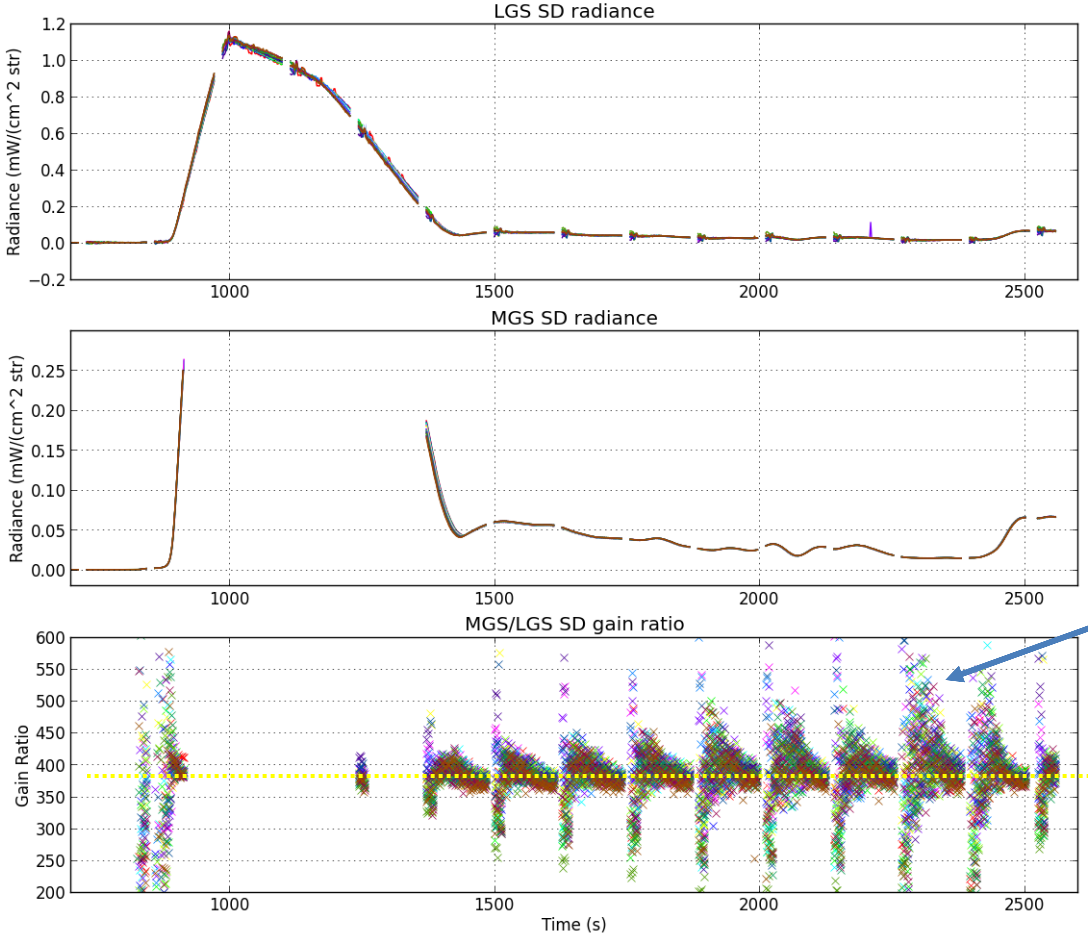

Spread due to noise & nonlinearity

Gain ratio threshold SNR(LGS)>15

Stable over orbit

Conclusions & Recommendations

- What was previously thought to be stray light from direct sunlight on the SD is actually a hysteresis effect
  - The cause is unknown but it may be related to anti-blooming in the HGS
- The hysteresis affects the SV cal signal about an order of magnitude more than the EV
  - It rapidly decreases over the 16 cal samples
  - The rapid decrease explains a saw tooth pattern in the SV that is associated with the 72 scan DNB cal cycle
- The onset of the effect for the SV and EV is abrupt after which it immediately goes to a flat response
- Prediction of the onset has always been a problem for the stray light correction, but using a simple threshold on the SD signal onset can be predicted to within one scan.
- It is likely that the BB cal signal is also impacted by hysteresis from the EV during the daytime.
- Hysteresis adversely affects gain ratios derived from the SV or BB.
  - Large uncertainties (>50%) are probably due to hysteresis and uneven stray light illumination.
- RSBAutoCal should not use the SV or BB to produce gain ratios
- Probably there is no reliable way to automatically produce MGS/HGS gain ratios

Part 1—Backup

SV MGS/HGA cross-calibration

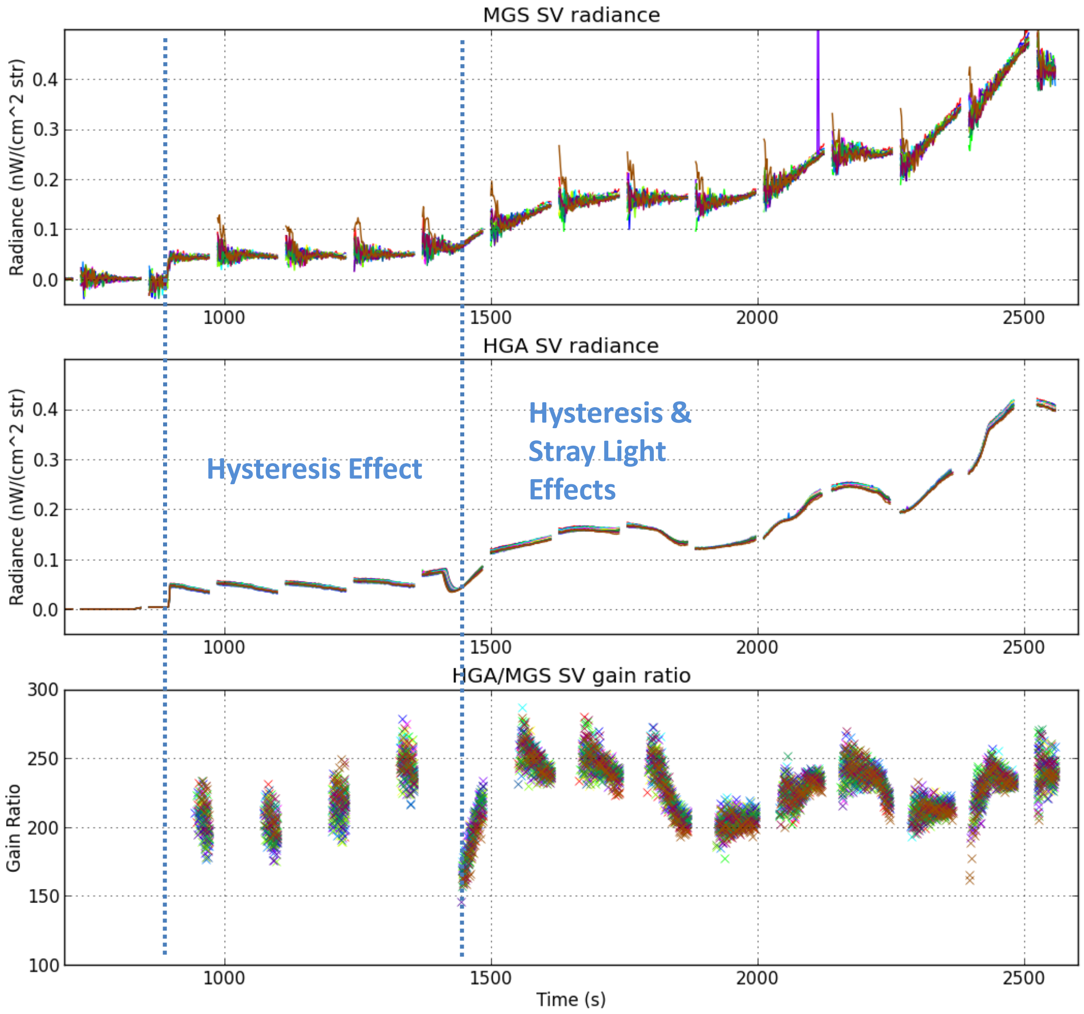

Gain ratio threshold
SNR(MGS)>15

BB MGS/HGA cross-calibration

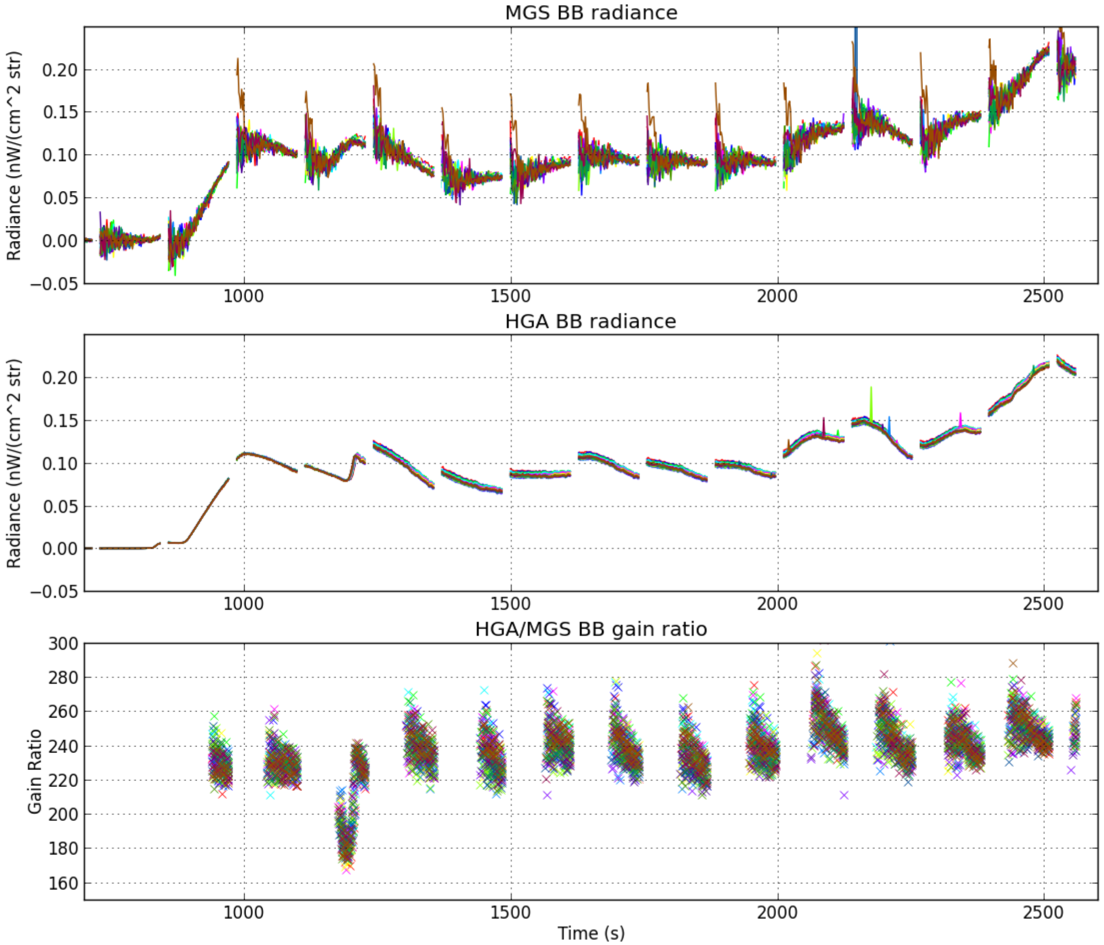

Gain ratio threshold
SNR(MGS)>15

SD MGS/HGB cross-calibration

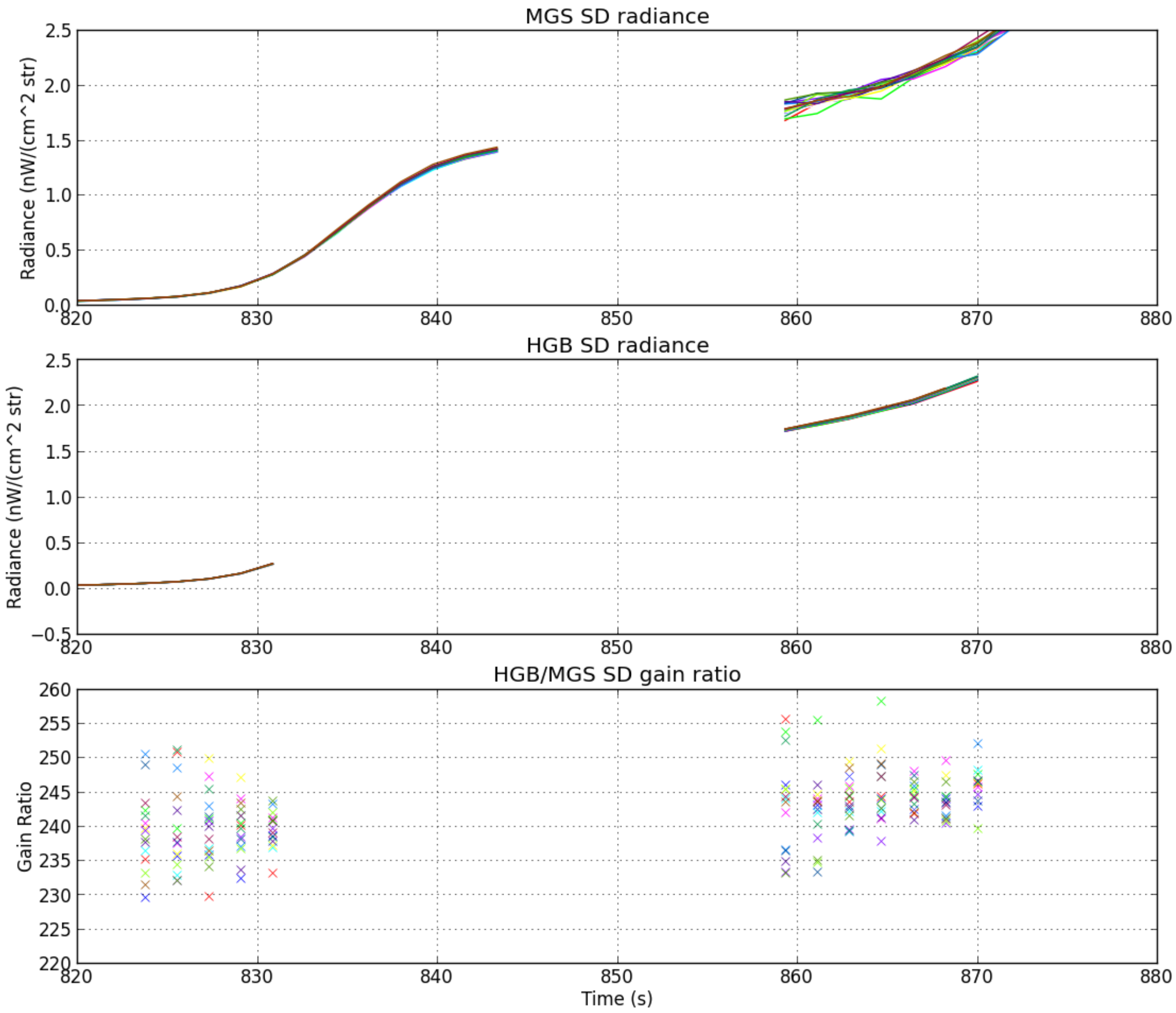

Gain ratio threshold
SNR(MGS)>15

Part 2—DNB Offset & Noise Analysis from Cal Data

DNB Offset using cal data

- Because of fixed pattern offsets in the EV, the cal sector data cannot be used to determine absolute offset
- It has been proposed that dark cal data can be used for tracking the relative change in dark offset
  - This has not been demonstrated to be true for all agg modes
- Rather than replicate what has already been done I try to develop a statistically rigorous method for determining these offset along with the dark noise
- In particular, evaluation of fixed pattern offset in the cal samples and method for outlier removal are considered

Will use a statistically rigorous methodology

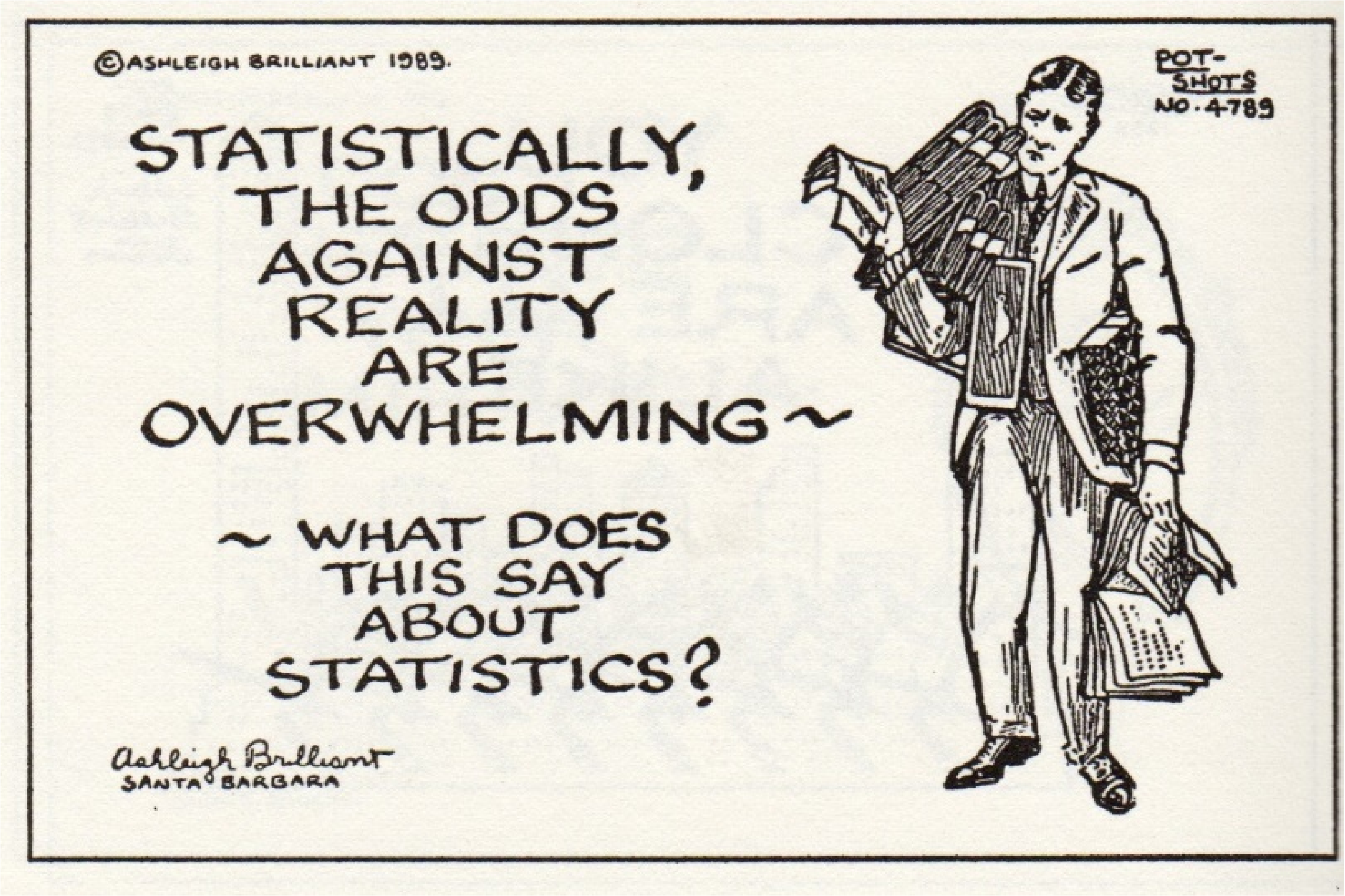

Fixed Pattern Offset (FPO) Dominates HGA Cal

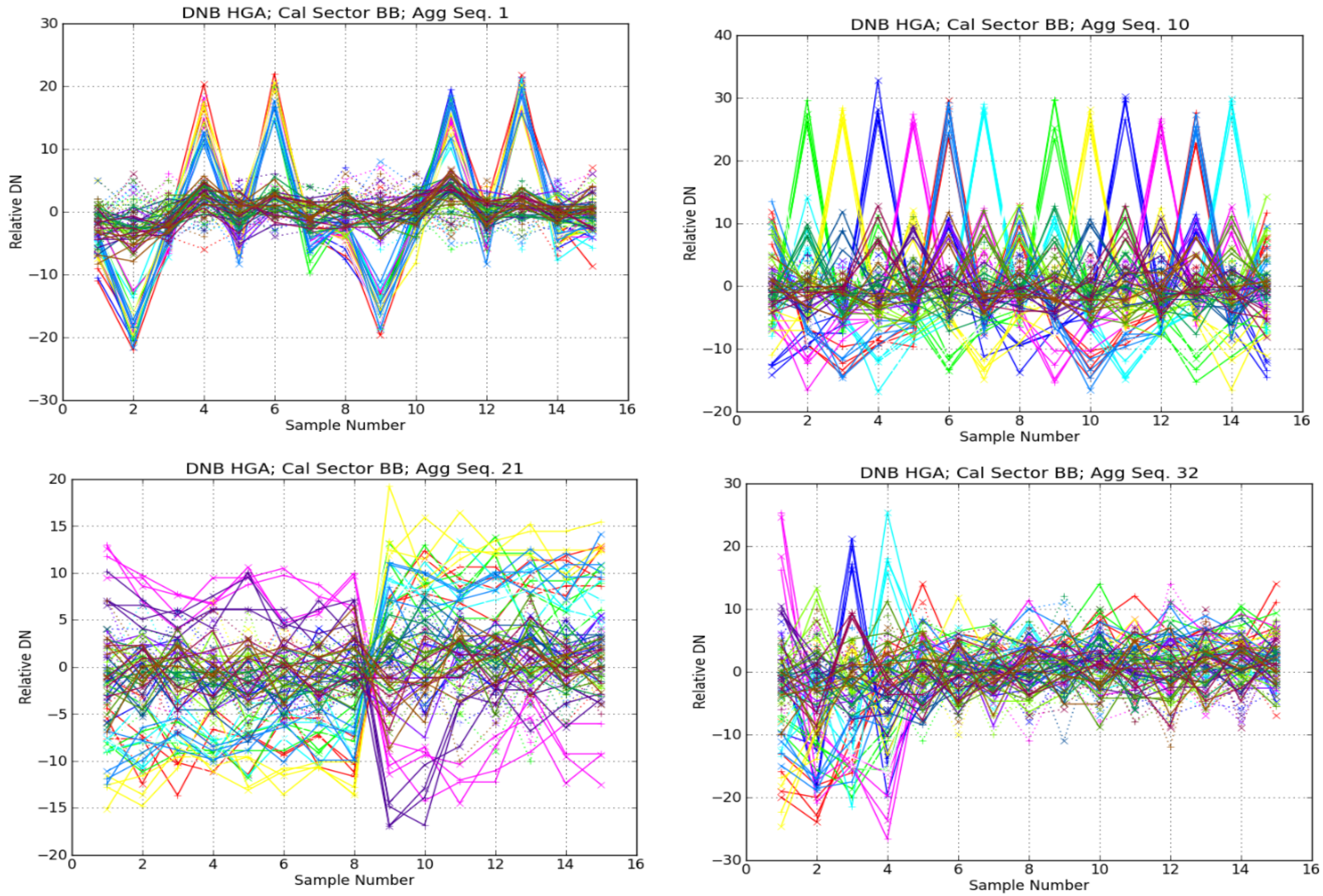

HGA Fixed Pattern Offsets for 4 aggregations. Solid lines are offsets, dotted lines are differences plotted to show noise level. Both HAM sides are plotted with "+" for side 0 and "x" for side 1. Color indicates detector number.

Fixed Pattern Offset Dominates MGS Cal

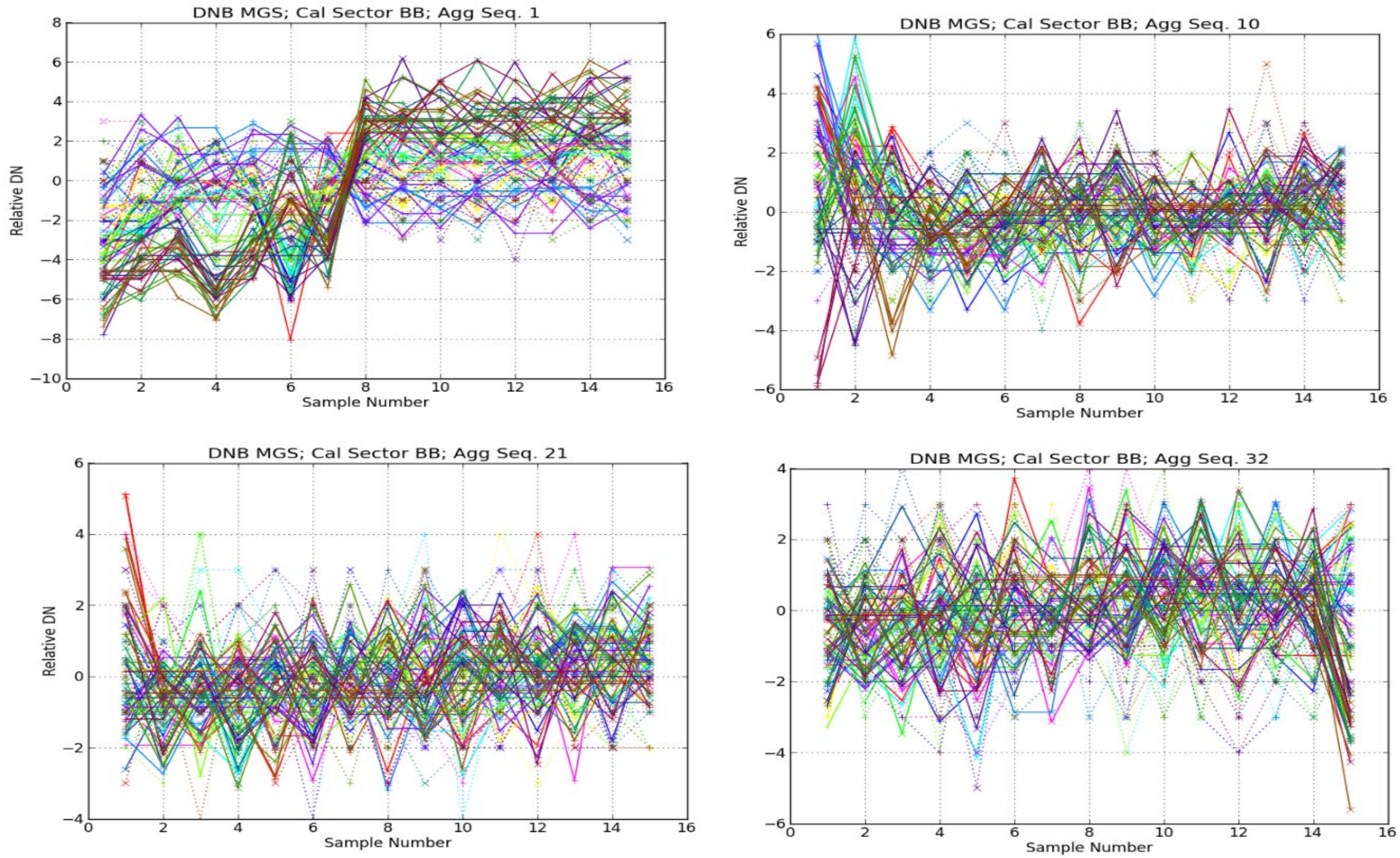

MGS Fixed Pattern Offsets for 4 aggregations. Solid lines are offsets, dotted lines are differences plotted to show noise level. Both HAM sides are plotted with "+" for side 0 and "x" for side 1. Color indicates detector number.

Fixed Pattern Offset Dominates LGS Cal

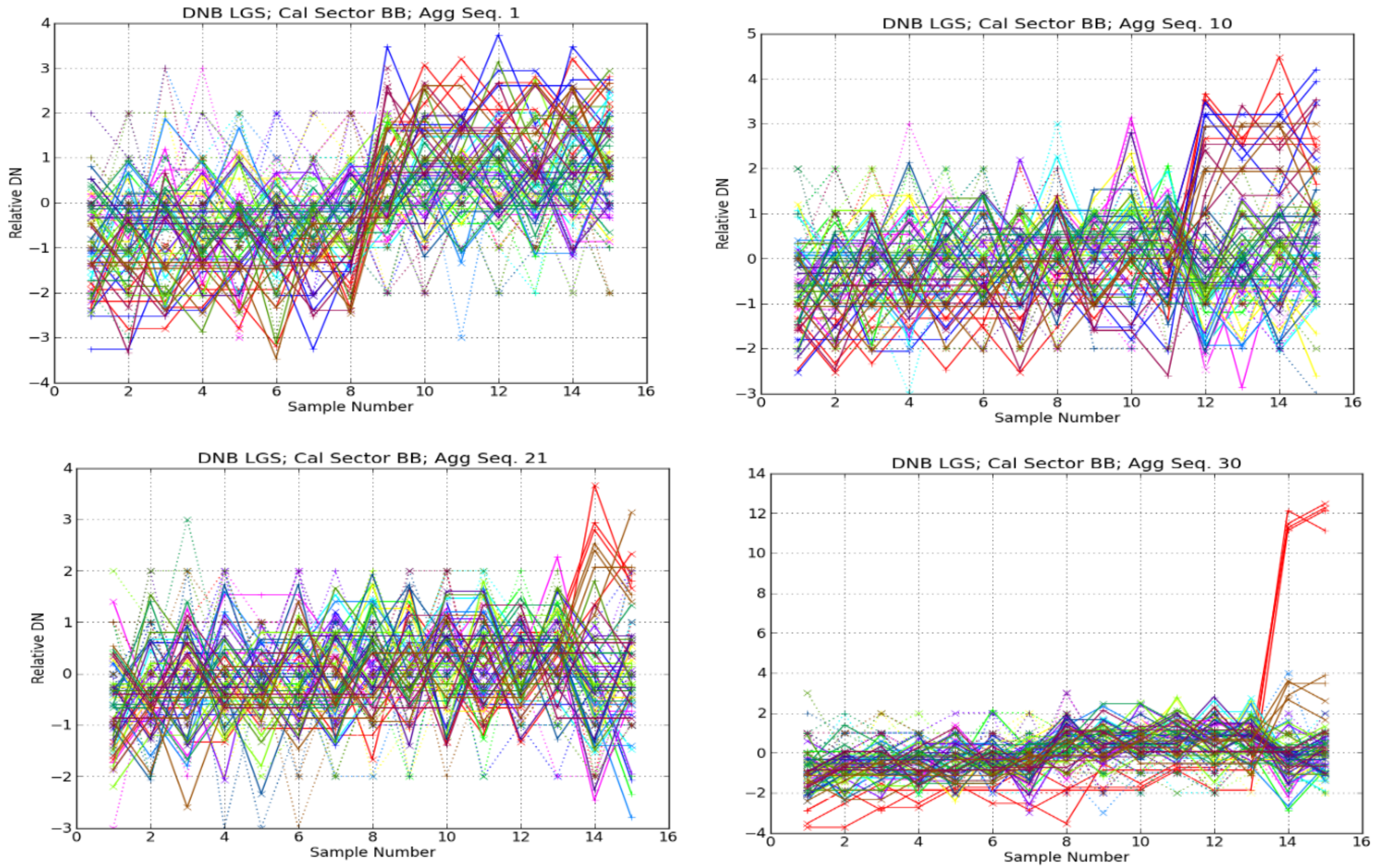

LGS Fixed Pattern Offsets for 4 aggregations. Solid lines are offsets, dotted lines are differences plotted to show noise level. Both HAM sides are plotted with "+" for side 0 and "x" for side 1. Color indicates detector number.

Difference in Means, HG SV-BB

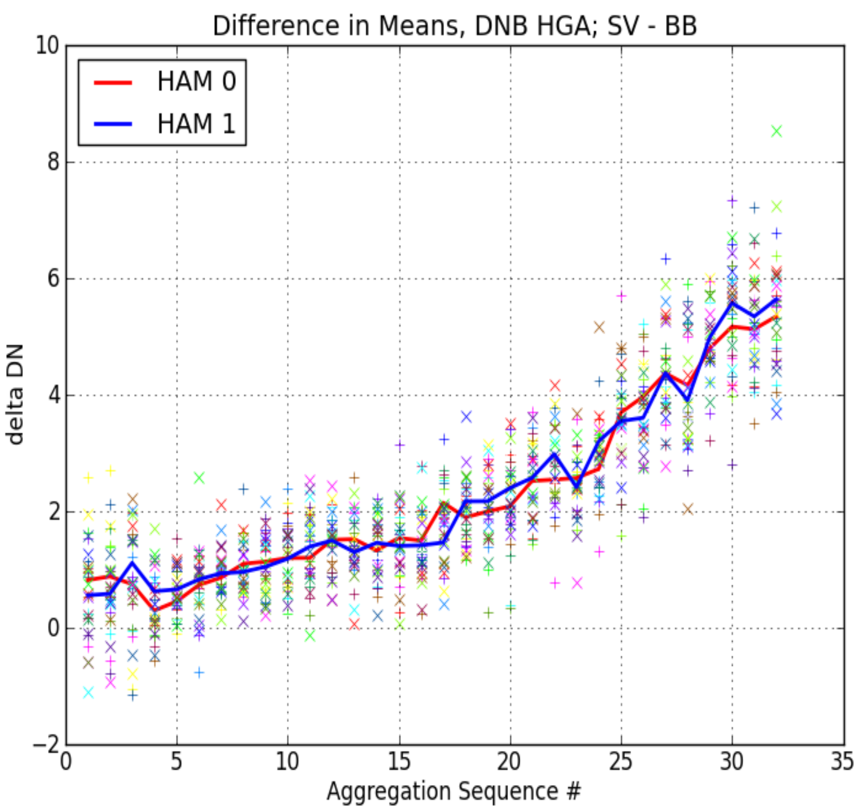

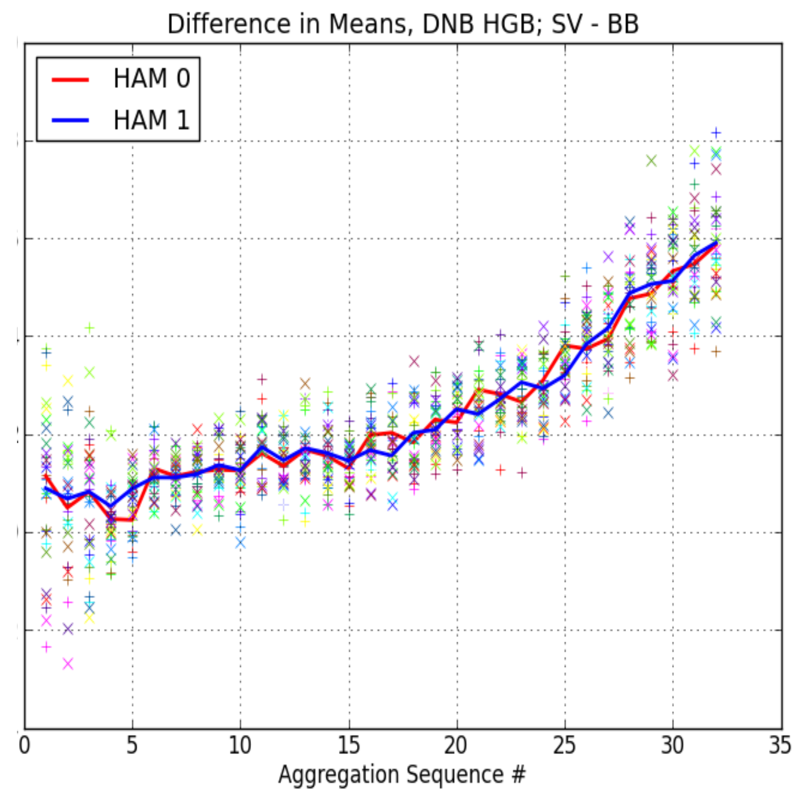

Increase due to airglow in ionosphere limb

Difference in Means, HG SD-BB

New Moon

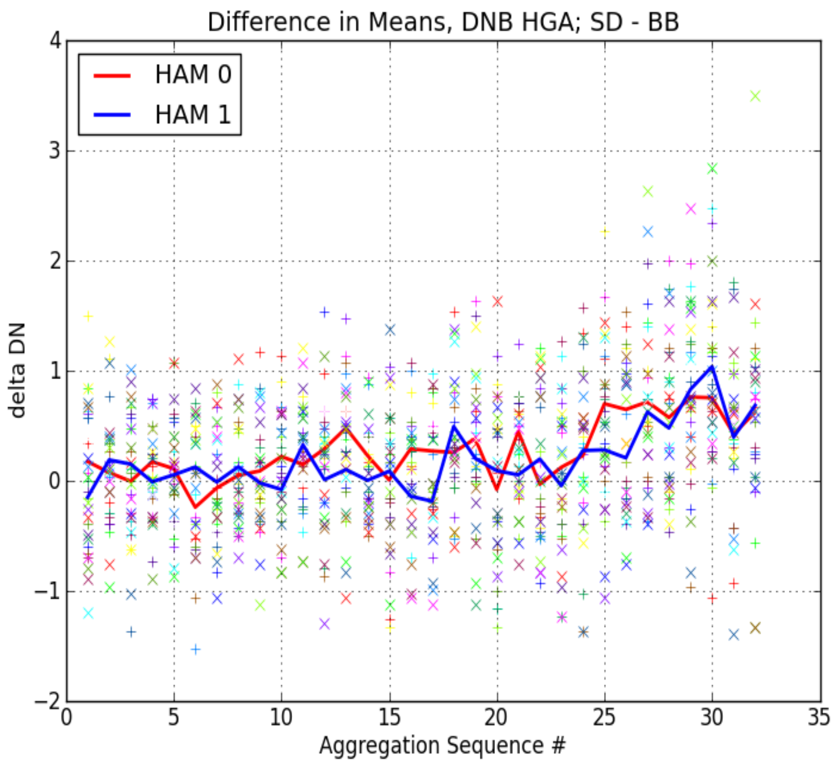

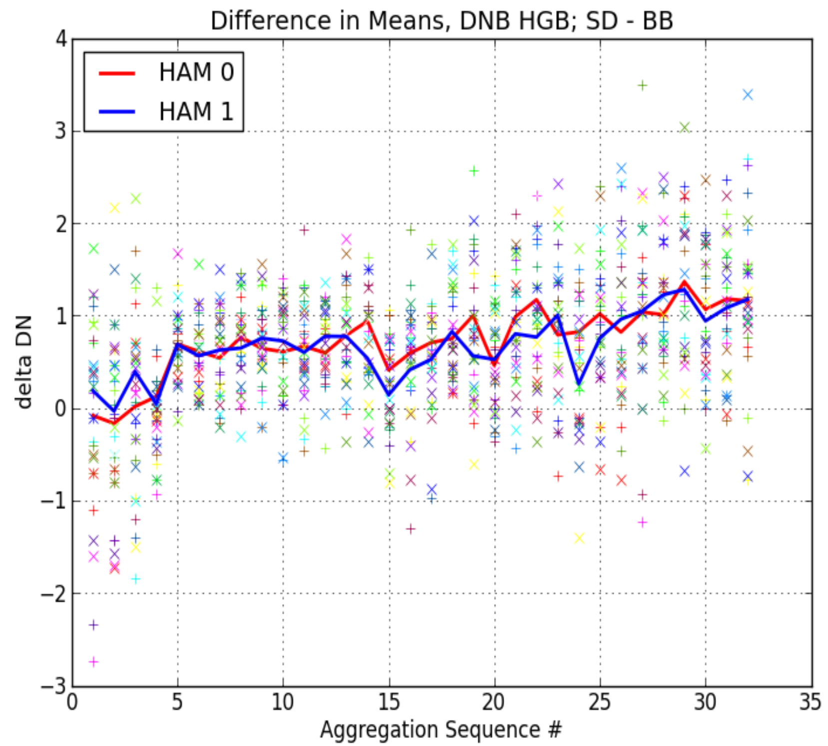

Small bias on SD due to faint light (e.g. airglow) from earth

Difference in Means, HG SD-BB

Full Moon

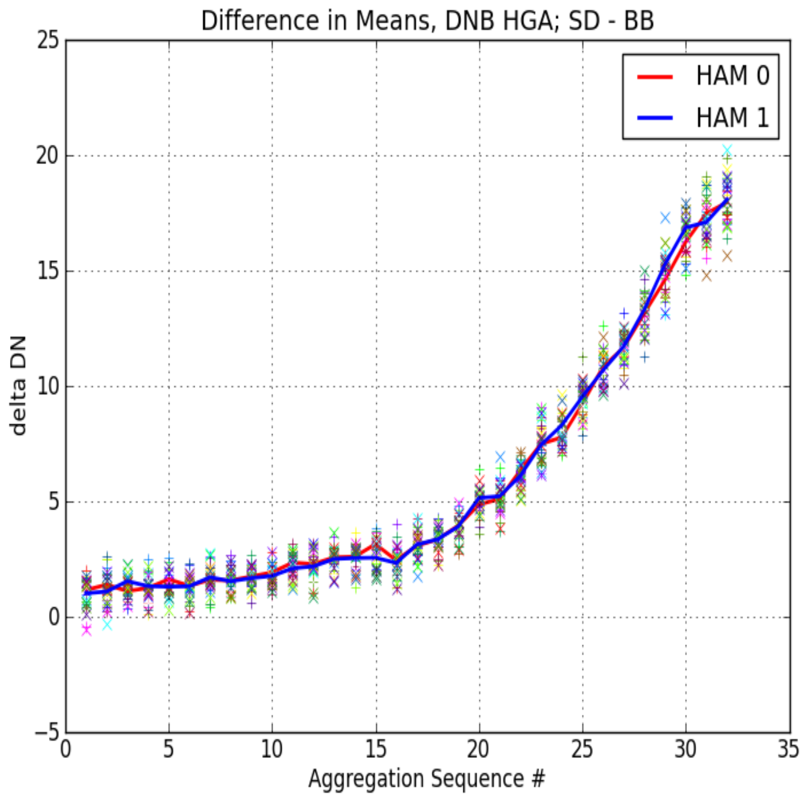

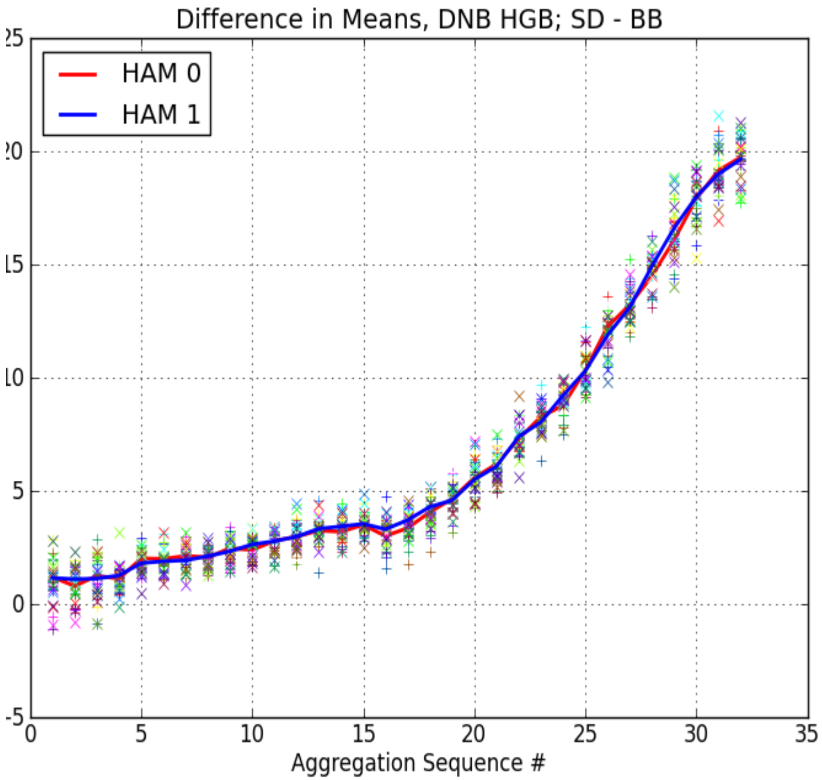

Large bias on SD due to moonlight from earth

Detector noise and FPO variation compared for HGA

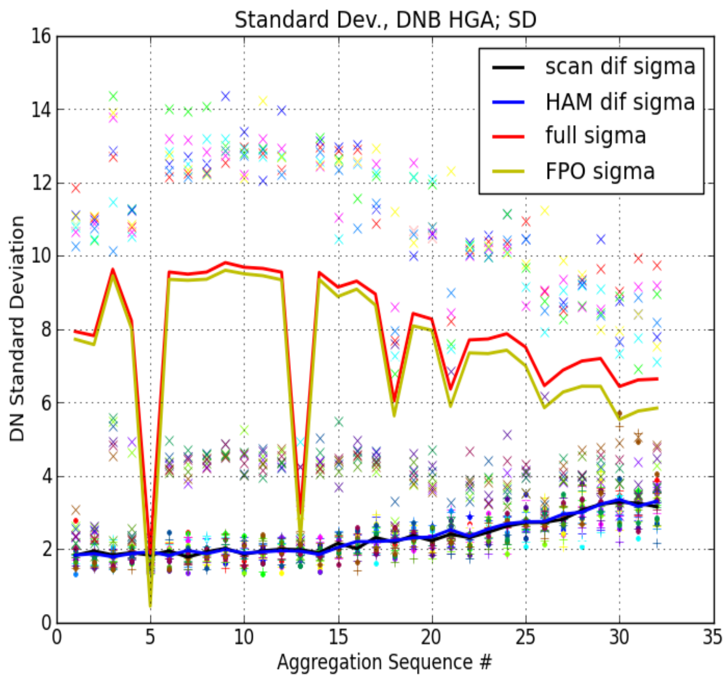

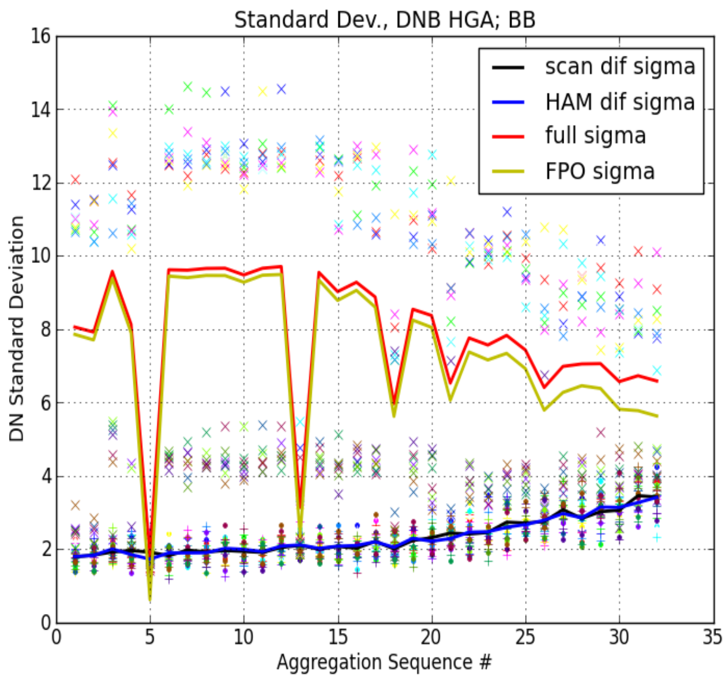

FPO variation dominates in the samples

Noise Equivalent Radiance (NER) by Aggregation

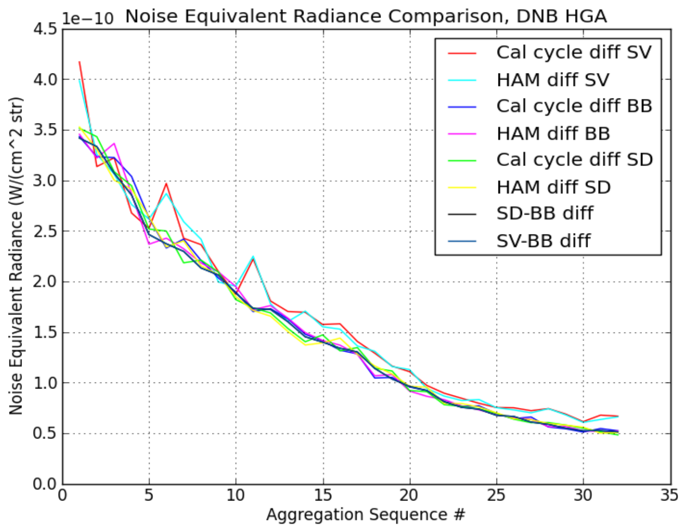

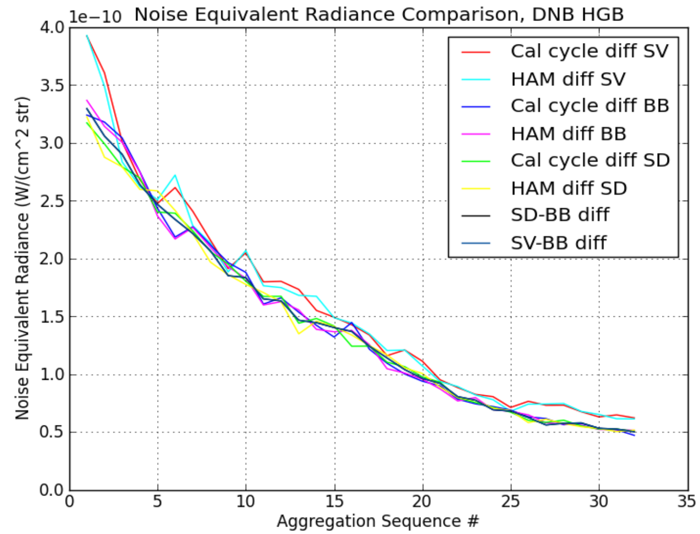

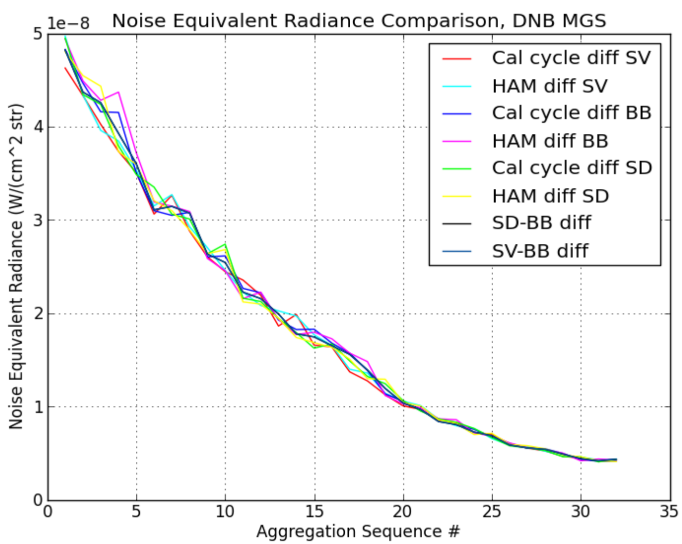

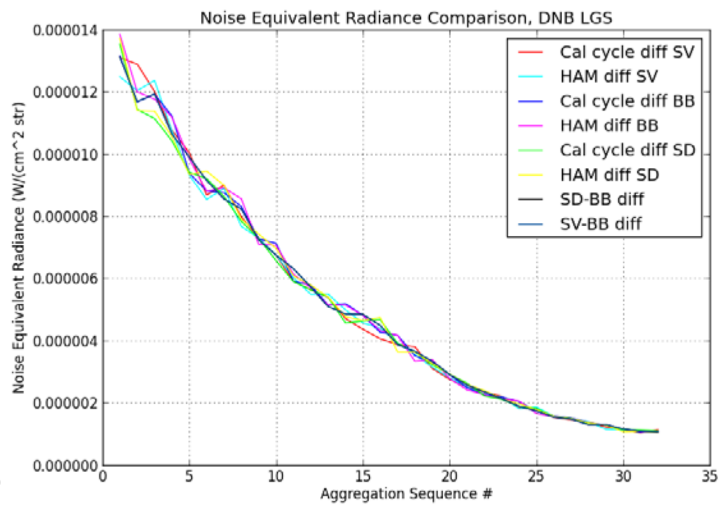

Methods of Outlier Mitigation (1 of 2)

- Winsorization –This method does not require taking the mean or the median and uses the entire ensemble to identify outliers.
  - It takes as parameters the maximum and minimum percentile of data outside of which are to be treated as outliers, for example, the lowest 2% and highest 2%.
  - Any data that is identified within the lowest range is replaced with the value exactly at the lowest cutoff point.
  - Likewise, data that is identified within the highest range is replaced with the value exactly at the highest cutoff point.
  - Because it replaces the data rather than remove it, the resulting ensemble has the same number of elements as the input ensemble.
- Trimming—This is similar to winsorization except that it removes, rather than replaces, the data below or above the percentile limits.
  - Like winsorization it takes as parameters the maximum and minimum percentile of data outside of which are to be treated as outliers,
  - but instead of replacing these values it trims these data elements from the ensemble.
  - The resulting ensemble has fewer elements than the input ensemble.

Methods of Outlier Mitigation (2 of 2)

- Multilayer Median Trimming (MMT)—
  - This method may be based on Peirce's Criterion which uses the median rather than the mean because outliers will always increase the standard deviation, and will shift the mean but will have very little effect on the median.
  - It is called multilayer because it repeats the trimming process multiple times with successively tighter trimming of outliers.
  - The process is to compute the median and σ, then trim values $> n\sigma$ or $< -n\sigma$ from the median.
  - This process is repeated multiple times with successively lower values of n.
  - This process is often applied with integer values of n, but this is not a necessary requirement.

Conclusions & Recommendations (1 of 3)

- The cal data may be useful in determining offset drift in the EV.
  - Because of the high uncertainty in the offsets derived from earth view data it is not certain whether in fact the drifts always correlate.
  - It has been shown that they approximately correlate for at least some detectors and Agg. Seq., but this has not been shown to be true in general.
- The BB is the best cal data to use for offset determination and for noise estimation because it is not strongly contaminated by indirect light from the earth or by airglow, unlike the SD and SV.
  - Even for the MGS, during a full moon there is sufficient light to produce a detectable offset in SD, and likewise for airglow contamination in the SV.
  - Also, including SV and SD only adds an unnecessary level of complexity to the analysis and at worst may reduce the accuracy.
- Because of FPO data ensemble averages should always be taken over the same sample over many scans
  - Per scan averages should never be taken
  - Outlier removal should be done on per sample ensembles, and never per scan

Conclusions & Recommendations (2 of 3)

- FPO is a function of sample number, detector number, Agg. Seq. and gain stage, but is not apparently a function of HAM side or cal source.
- To determine NEC without the effect of FPO, data with the same sample number, detector number, Agg. Seq. and gain stage can be subtracted, and the standard deviation taken.
- NEC determined in this way was found for:
  - HGA and HGB to go from 1.75 DN for Agg. Seq. 1 to 3.3 DN for Agg. Seq. 32.
  - MGS NEC = 1.01 DN for all Agg. Seq.
  - LGS NEC = 0.74 DN for all Agg. Seq.
- After eliminating data effected by solar stray light using the solar nadir angle, there are about 10,000 samples per day for each detector, HAM side, Agg Seq. and gain stage combination.
- This number of samples is sufficient to determine offset drift for for the daily mean
  - high-gain Agg. Seq. 32 to within a HGS uncertainty = 0.03 DN.
  - MGS and LGS the uncertainty = 0.01 DN.

Conclusions & Recommendations (3 of 3)

- The method used for outlier mitigation has a large impact on the uncertainty of the daily mean offset as well as the NEC.
  - Modeling showed that Winsorization had the least impact on uncertainty, and this is the process that is recommended here.
  - Trimming and Multilayer Median Trimming were also considered but did not perform as well.
- More important than the method used for outlier mitigation is the limits used.
  - These should not be arbitrarily set but should be set by first determining the probability of outliers that are mostly due to HEP hits.
  - It is recommended that this probability should be determined using either Peirce's criterion and/or Chauvenet's criterion to identify likely outliers.
- There may be sufficient indirect light during a full moon to produce a detectible signal in the daily mean offsets from BB.
  - These events should be studied and if necessary removed from the trending using a threshold lunar phase.
- Outlier processing should also be performed on the daily mean offsets after removing the impact of drift.
  - This may be need to remove anomalous events that occur over a period longer than a few seconds.

Part2—Backup

DNB Cal Data Form

- As with all the other bands on VIIRS, the DNB views the space view (SV), black body (BB) and solar diffuser (SD) calibration (cal) views one per scan. There are two differences regarding the DNB functionality compared with the other bands:
- It has 4 gain stages, HGA, HGB, MGS and LGS, compared with 1 or 2 stages compared with the other bands;
- It has 32 aggregation modes plus 4 diagnostic aggregation modes compared with 3 aggregation modes for the other bands.
- To accommodate these differences, the DNB cal data are acquired differently. The features of the data that are different are:
- There are only 16 samples per scan per gain stage for DNB (compared with 48 for Moderate Resolution bands and 96 for imagery bands).
- The aggregation modes cycle through every 72 scans with 2 scans for each mode (one for each HAM side).
- Aggregation modes are numbered from the center at 1 to the edge at 32
- Aggregation sequences are numbered from the <u>edge</u> at 1 to the center at 32

Rate of Offset Change Comparison

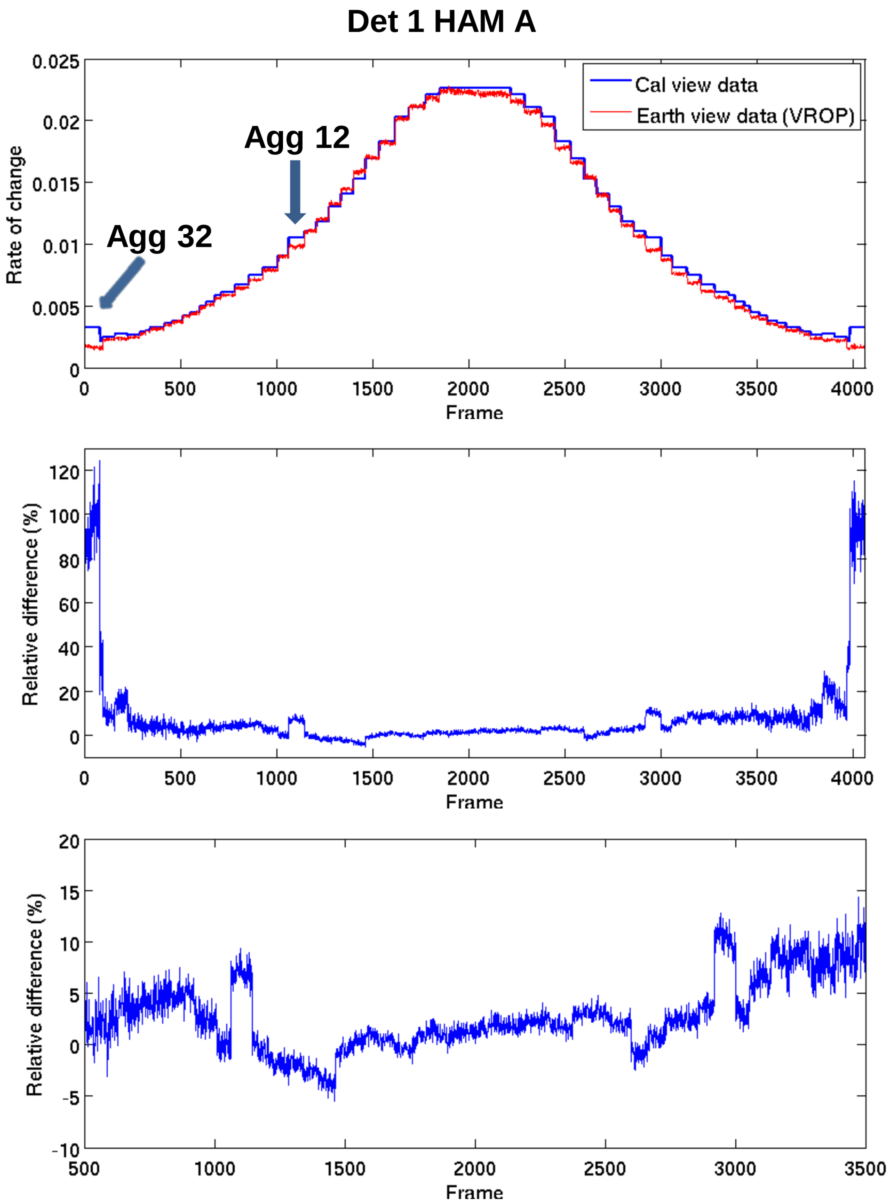

Top: HGS rate of change fitted from 47 new moon days (02/21/2012 and 46 days between 11/13/2012 and 07/04/2016).
Cal view data: follow the RSBAutoCal algorithm to determine DNB dark signal.
Earth view data (VROP): DNB DN0 LUT (HGS)

Middle: relative difference of the fitted change of rate (rate_CalView - rate_EarthView)/rate_EarthView.

Bottom: zoomed in figure of the middle figure

Fixed Pattern Offset Dominates HGB Cal

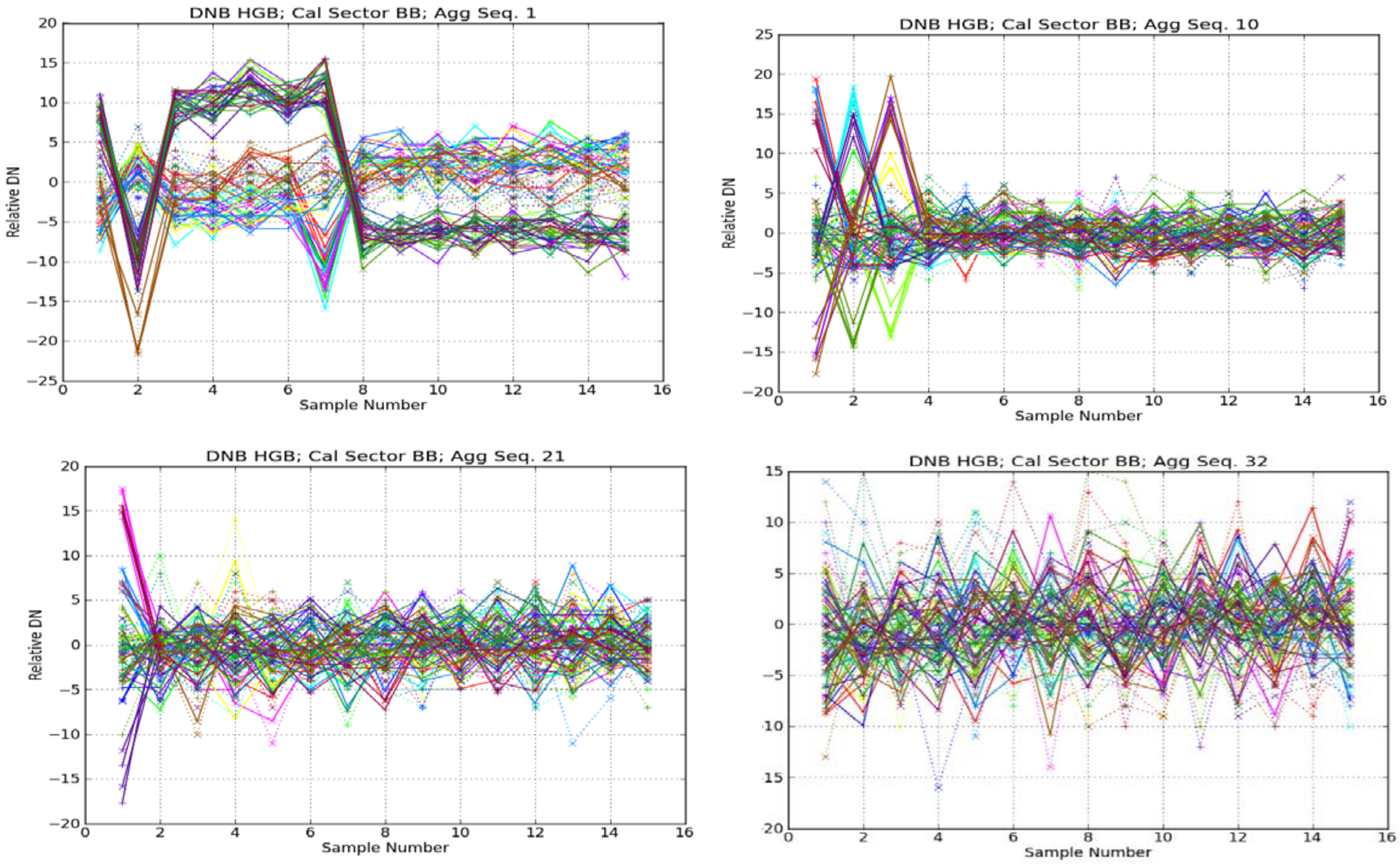

HGB Fixed Pattern Offsets for 4 aggregations. Solid lines are offsets, dotted lines are differences plotted to show noise level. Both HAM sides are plotted with "+" for side 0 and "x" for side 1. Color indicates detector number.

Detector noise and FPO variation compared for HGB

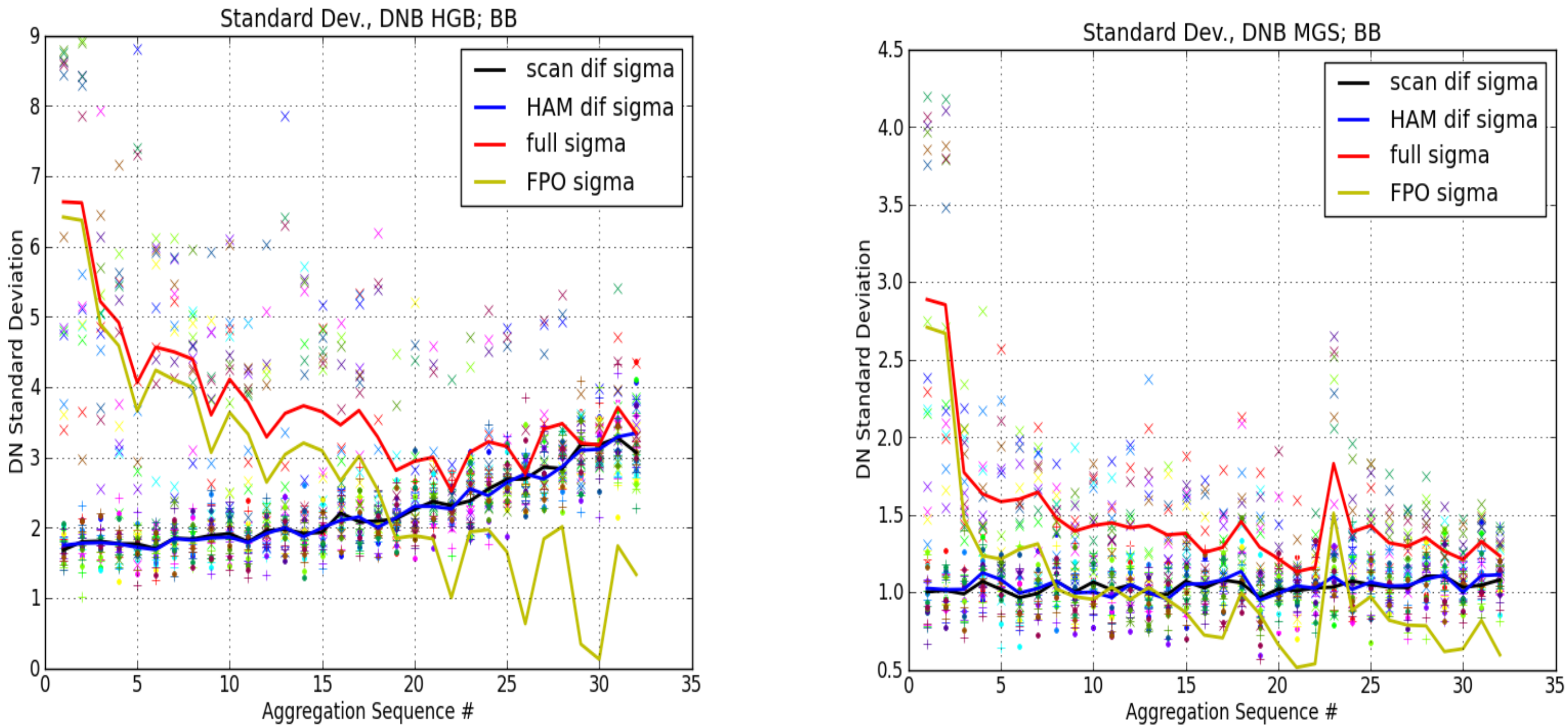

FPO variation for HGB is different from HGA, but it usually dominates for lower Aggregation Sequence Number

HGA & HGB Dark Noise Equivalent Counts (NEC) Computed 8 Ways

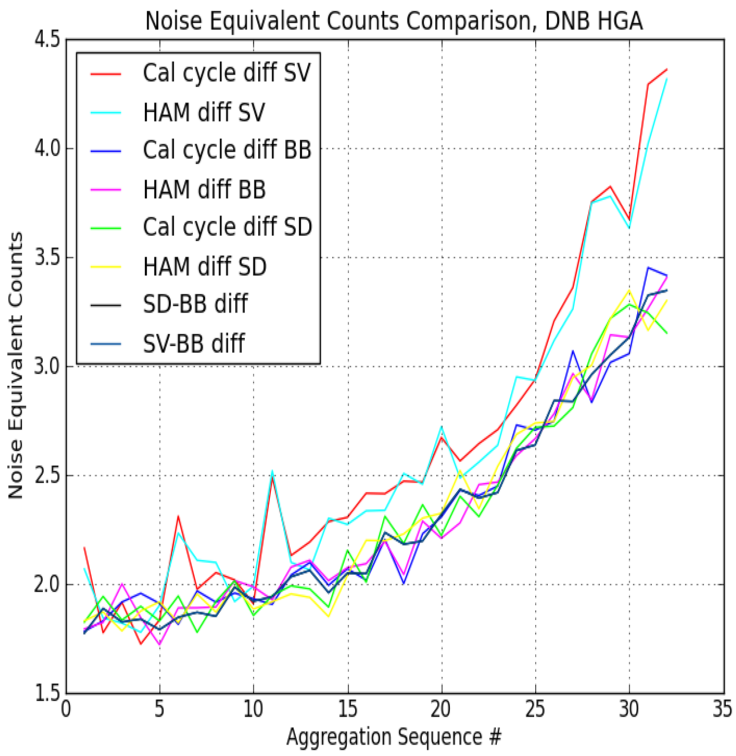

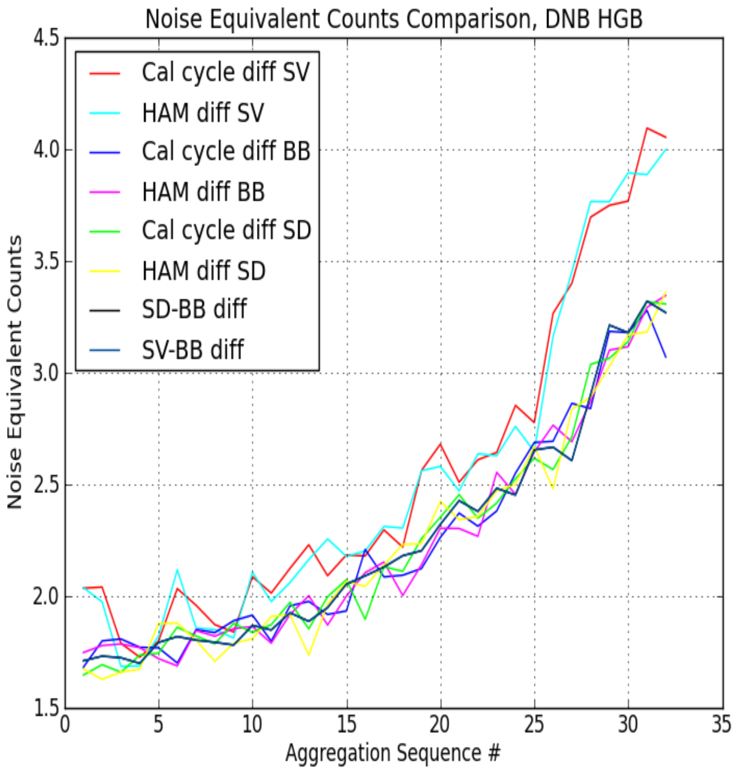

- Cal cycle SV difference is large due to airglow variation and long time span
- HAM SV likely has higher NEC due to airglow variation

Part 3—Determining offsets using Earth view—a statistical method using a parametric model with method of moments estimator

Summary of methodology

- The primary method for determining dark offset is to view the earth at night over the Pacific during a new moon
- but even without any lunar illumination, there is always some detectable light coming from the earth.
- This makes it difficult to use dark earth view data to determine offset tables that are not biased.
- What is proposed here is to use a statistical estimator and a parametric model of the natural illumination to determine the level of natural illumination and therefore correct for it.
- I considered for this are Maximum Likelihood Estimation (MLE) and the Method of Moments Estimation (MME).
- Here only MME will be considered, but it would be worthwhile to investigate MLE.

What data to use

- When determining the MGS and LGS offsets only the data from VROP 702 and 705 are available to be used, but for HGS this is not a restriction.
- The HGS offset data has always been taken over the Pacific Ocean on the day of the new moon, but is it really necessary to restrict the data to only these exact new moon dates?
- The reason for using the Pacific is because there is very few fixed lights, but this is just as true for the Indian Ocean or most of the Atlantic Ocean.
- Also there are places on land such as the Sahara Desert which are similarly deplete of fixed light.
- Because there are databases that provide data on persistent light over the entire earth, recommend that rather than restricting the data collection to certain regions, it is better to use all data and then filter out pixels where there are persistent lights based on the geolocation of the pixels.

Ocean With no lunar illumination

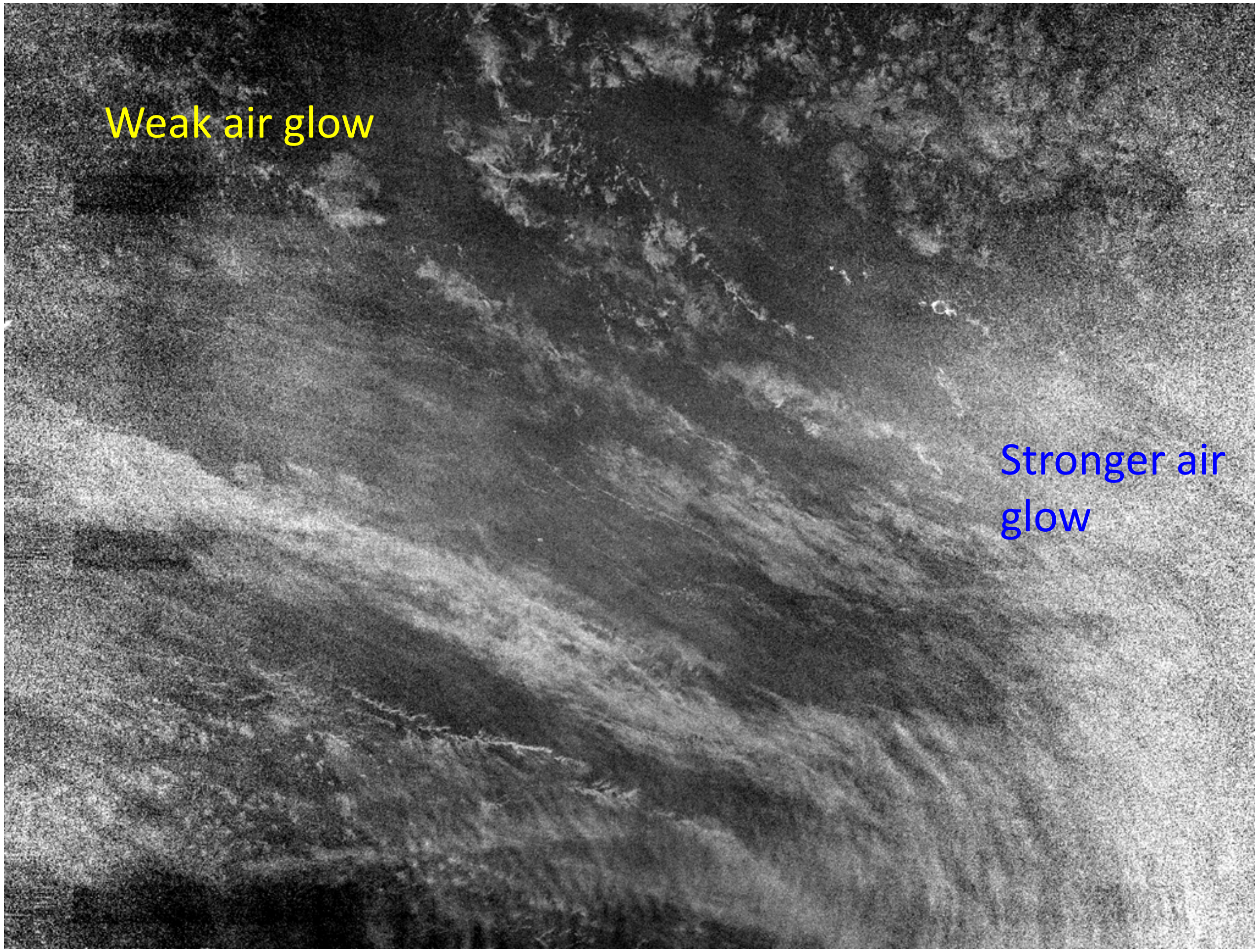

HGS granule taken on 22 Sep 2014 between 11:47:052 and 11:52:46 UTC, during a new moon in the region over the South Pacific Ocean. The plotting range from black to white is from -8.3×10^{-11} to 4.2×10^{-10} W cm^{-2} str^{-1}.

Distributions from new moon DNB scenes

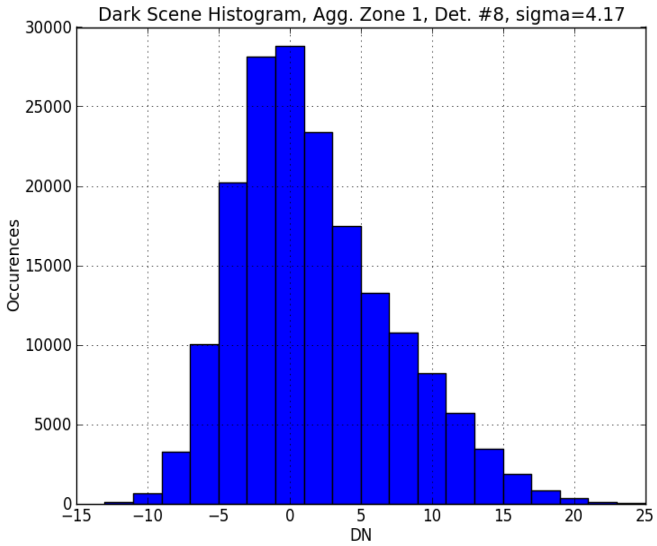

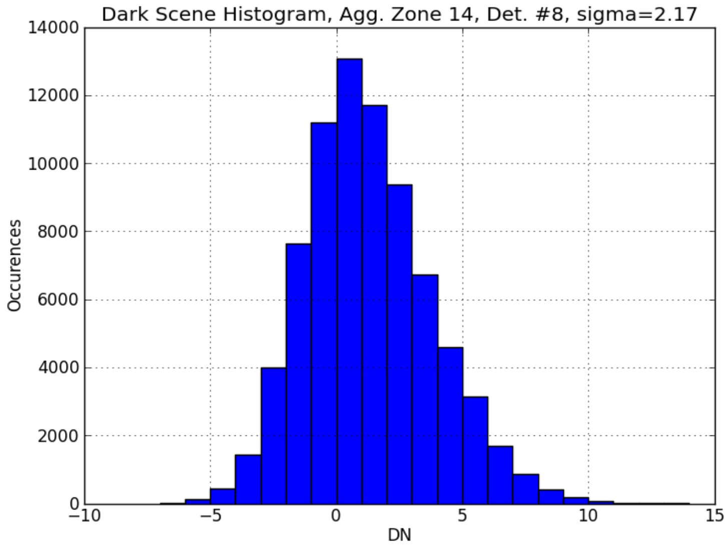

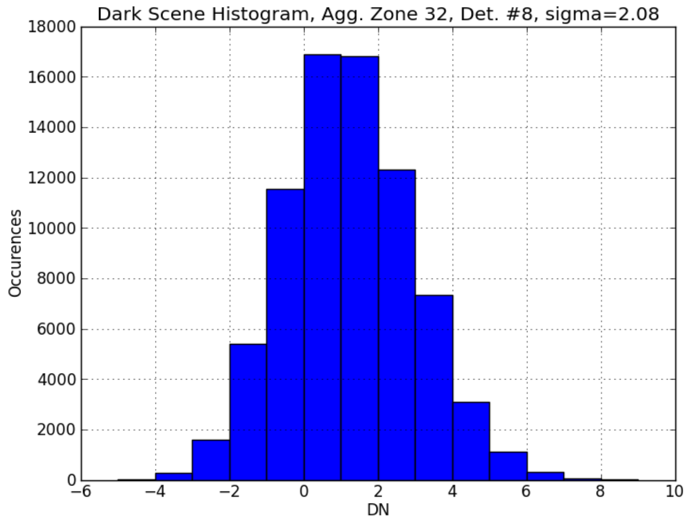

Distribution shape changes with aggregation zone. More skew near nadir.

Math model for scene radiance

Types of illumination:

- Unnatural nighttime illumination (UNI) includes electrical lights, gas flares and other anthropogenic fires.
- Natural Nighttime Illumination (NNI):
  - extraterrestrial nighttime illumination (ETI), including stars, zodiacal light and planets.
  - Airglow, both direct and reflected.
  - natural terrestrial sources other than airglow, including the Aurora Borealis, Aurora Australis, lightning, algae blooms and natural fires.

Remove through filtering

$$L_{all} = \xcancel{L_{UNI} + L_{terr}} + L_{ET} + L_{AG}\ ,$$

where: L_{UNI} = radiance of UNI; L_{terr} = radiance from natural terrestrial sources other than airglow; L_{ET} = reflected ETI radiance; L_{AG} = reflected and emitted airglow radiance

$$L_{NNI_n} = E_{ET}(d, t_{sol}, lat) \cdot \rho_n + (c_i \cdot \rho_n(\theta_i) + \sec\theta_i) L_{AG_{emis_n}}$$

$E_{ET}(d, t_{sol}, lat)$ = extraterrestrial irradiance as a function of date, solar time and latitude respectively; and ρ = surface reflectance, and *n* indicates the ensemble index. E_{AG} = downward airglow irradiance; ρ = surface reflectance in units of steradians^{-1}; θ =satellite zenith angle on the earth; and $L_{AG\ emiss}$ = upward total column airglow emission when θ =0

Equate sensor response to scene radiance model

$$DN_{LUT\,j,s,h,k} = DN'_{LUT\,j,s,h,k} - DN_{NNI\,j,s,h,k,m}$$

Where $DN_{LUT\,j,s,h,k}$ is the ideal offset LUT,

$DN'_{LUT\,j,s,h,k}$ is the offset LUT as it is currently produced from

$DN_{NNI\,j,s,h,k,m}$ is the NNI offset that we wish to determine.

indices j, k and m, referring to detector number, aggregation zone number and latitude bin respectively. The index n refers to a random sample of the ensemble, s refers to the sample within the aggregation zone and h refers to HAM side.

$$L'_{n,j,s,h,k,m} + L'_{NNI\,j,s,h,k,m} = E_{ET_m} \cdot \rho_{n,k,m} + \left(c_{k,m}\,\rho_{n,k,m} + \sec\theta_k\right) L_{AG_{emis}\,n,m} + L'_{noise\,n,j,k}$$

$$L'_{NNI\,j,s,h,k,m} = DN_{NNI\,j,s,h,k,m} / g_{j,k}\ ;$$

$$L'_{n,j,s,h,k,m} = \left(DN_{n,j,s,h,k,m} - DN'_{LUT\,j,s,h,k}\right) / g_{j,h,k}$$

$$L'_{noise\,n,j,k} = N_{n,j,k} / g_{j,k}\ ;$$

Where: $g_{j,k}$ =gain; $N_{n,j,k}$ =noise counts; $DN_{NNI\,j,s,h,k,m}$ =

$DN_{n,j,s,h,k,m}$ = measured counts

Ugly Math!

Produce simultaneous equations using 1st, 2nd & 3rd moments (mean, variance & skew)

we make the assumption that $L_{AG_{emis}}$ has a gamma distribution:

$$\langle L_{AG_{emis\,n,m}} \rangle_n = \int_{-\infty}^{\infty} L^{\alpha_m} / [\beta_m{}^{1+\alpha_m} \Gamma(1+\alpha_m)] e^{-L/\beta_m} \, dL = \beta_m (1-\alpha_m)$$

Mean:

$$\overline{L'_{NNI\,k,m}} = E_{ET\,m} \langle \rho_{n.m,k} \rangle_n + \beta_m (1-\alpha_m) \cdot \left[c_{k,m} \langle \rho_{n,m,k} \rangle_n + \sec\theta_k \right] - \langle L'_{n,k,m} \rangle_n$$

There are 4 unknowns here: $\overline{L'_{NNI\,k,m}}$, α_m, β_m and $c_{k,m}$

Variance:

$$\sigma^2 \left(L'_{n,k,m} \right)_n = \sigma^2 \left[E_{ET\,m} \cdot \rho_{n,k,m} + \left(c_{k,m}\, \rho_{n,k,m} + \sec\theta_k \right) L_{AG_{emis\,n,m}} + L'_{noise_{n,k}} \right]_n$$

Skewness:

$$\langle \left(L'_{n,k,m} + L'_{NNI\,k,m} \right)^3 \rangle_n = \langle \left[E_{ET\,m} \cdot \rho_{n,k,m} + \left(c_{k,m}\, \rho_{n,k,m} + sec\,\theta_k \right) L_{AG_{emis\,n,m}} + L'_{noise_{n,k}} \right]^3 \rangle_n$$

This gives 192 equations and 130 unknowns. Solve using Newton-Raphson method and regression

Uglier Math!

Conclusions

- Because of the statistical nature of the sensor noise and scene radiance, a statistical estimator seems to be the only way to solve this problem
- More work is needed to develop this methodology
- The math is complicated but it should not be difficult to program in a language such as Python or IDL.
- In addition to providing unbiased offsets, this method would also provide a mathematical model for understanding airglow distribution